

UC Berkeley

UC Berkeley Electronic Theses and Dissertations

Title

Conversion of Biomass into Chemicals

Permalink

<https://escholarship.org/uc/item/1vc3140q>

Author

Shiramizu, Mika

Publication Date

2013

Peer reviewed|Thesis/dissertation

Conversion of Biomass into Chemicals

by

Mika Shiramizu

A dissertation submitted in partial satisfaction of the

requirements for the degree of

Doctor of Philosophy

in

Chemistry

in the

Graduate Division

of the

University of California, Berkeley

Committee in charge:

Professor F. Dean Toste, Chair

Professor Robert G. Bergman

Professor Alexander Katz

Fall 2013

Conversion of Biomass into Chemicals

Copyright 2013

by Mika Shiramizu

Abstract

Conversion of Biomass into Chemicals

by

Mika Shiramizu

Doctor of Philosophy in Chemistry

University of California, Berkeley

Professor F. Dean Toste, Chair

In order to conserve finite fossil fuels and reduce green house gas emission, the development of sustainable energy is an inevitable challenge in the 21st century. Among the alternative energy sources, cellulosic biomass (e.g. energy grasses such as miscanthus or agricultural waste such as corn stover, bagasse, cereal straws, and wood chips) presents several unique advantages: (1) it can produce liquid fuels or chemicals that substitute the existing petroleum-derived ones without requiring significant modification of infrastructure, (2) it is renewable and potentially carbon-neutral in overall life cycle, and (3) it is inexpensive, ubiquitous and faces less land use competition with food compared to edible biomass (sugar, starch and oil). Aiming to contribute to the development of biomass conversion technology, my Ph.D. study was conducted at the Energy Biosciences Institute, a multidisciplinary joint initiative for biomass research between UC Berkeley, Lawrence Berkeley National Laboratory, University of Illinois at Urbana-Champaign, and BP. Specifically, my focus has been the downstream conversion of sugar/sugar derivatives into chemicals, as described below.

Chapter 1: Polyethylene terephthalate (PET) is a plastic in large demand worldwide, due to its utility in the manufacturing of a range of products from beverage containers to synthetic fibers. The key monomer of PET, terephthalic acid, is currently produced by oxidizing *p*-xylene from crude oil. In an effort to reduce our dependence on fossil fuel, we demonstrated a route to synthesize solely biomass-derived *p*-xylene as a drop-in replacement. Namely, we explored the feasibility of converting 2,5-dimethylfuran (derived from 5-(hydroxymethyl)furfural, a typical by-product of cellulose hydrolysis) and acrolein (produced from glycerol, a side-product of fatty acid methyl ester biodiesel production) into *p*-xylene. This synthesis consisted of a sequential Diels-Alder reaction, oxidation, dehydration, and decarboxylation. In particular, the pivotal first step, the Diels-Alder reaction to construct 7-oxabicyclo[2,2,1]hept-2-ene core structure, was studied in detail to provide useful kinetic and thermodynamic data. The concept was realized and the bio-derived *p*-xylene was obtained in 34 % overall yield over four steps.

Chapter 2: The deoxygenation reaction of sugar moieties is essential for the conversion of cellulosic biomass to chemicals and fuels. While numerous reports focus on the pyrolysis, hydrogenolysis and acid-catalyzed dehydration reaction of biomass, one much less developed deoxygenation pathway is the deoxydehydration (DODH) reaction, which removes two adjacent hydroxyl groups from vicinal diols to afford alkenes. We have developed an oxorhenium-catalyzed DODH reaction using a sacrificial alcohol (e.g. 1-butanol, 3-pentanol) as a recyclable and environmentally friendly solvent/reductant, and successfully applied it to sugars, sugar acids and sugar alcohols. When combined with the alcohol reductant, oxorhenium compounds, namely methyltrioxorhenium (MTO) and perrhenic acid (HReO_4), showed much higher activity than other precedented DODH systems and enabled the unstable polyol substrates to undergo clean DODH reactions. Linear polyene products and aromatic compounds were obtained with remarkable selectivity. Mechanistic insights were acquired by studying the isolated Re(V) species as well as by examining the unprecedented modes of DODH on 2-ene-1,4-diol and 2,4-diene-1,6-diol moieties.

Table of Contents

Prelude Oxorhenium-Catalyzed Hydrolysis of Cellulose under Hydrogen

Introduction	1
Hypothesis	2
Results and Discussion	3
Conclusion	7
References and Notes	8

Chapter 1 On the Diels-Alder Approach to Solely Biomass-Derived Polyethylene Terephthalate (PET): Conversion of 2,5-Dimethylfuran and Acrolein to p-Xylene

Introduction	10
Condition Optimization for Diels-Alder Reaction	13
Thermodynamics of Diels-Alder Reaction	17
Retro Diels-Alder Reaction	21
Conversion of Compound 1 to p-Xylene	26
Conclusion	28
Experimental	29
References and Notes	38

Chapter 2 Oxorhenium-Catalyzed Deoxydehydration of Polyols Using Alcohol Solvent as a Reductant

Introduction	41
Optimization of Reaction Conditions	43
Sugar Alcohols	46
Inositols	48
Reaction Mechanism	50
1,4- and 1,6-DODH	53
Sugar Acids	56
Sugars	63
Conclusion	66
Appendix	67
Experimental	75
References and Notes	141

Acknowledgments

I sincerely thank my research advisor, Prof. F. Dean Toste, for his tremendous support and guidance over the past five years. I knew nothing about Energy Biosciences Institute (EBI) when I was applying to UC Berkeley. When you suggested I become the first one from the Toste group to join this project at our first meeting in August 2008, you opened a door to the whole new world for me. I admit I struggled a lot in my first year—learning about biomass, and understanding what is cool and what is not cool to study in this field. It was not straightforward to come up with a research topic which is practical (at least potentially) and at the same time interesting chemistry-wise! However, at the end, I am now so happy that I chose to work on biomass chemistry. I truly enjoyed the unique, interdisciplinary work environment I had. I learned a lot about sustainability as a whole, and I feel I have grown to a “second-generation” chemist who can integrate many different ideas. Thank you, Dean, for this opportunity.

Along these lines, I would like to thank EBI directors Prof. Chris Somerville, Dr. Paul Willems and Prof. Isaac Cann for creating this great environment. In the EBI retreat 2013, Prof. Somerville mentioned that he wants EBI to be an “intellectual chaos”, where he believes good ideas come from, given good people. I totally agree EBI is working well that way. And this freedom to explore ideas is not something to be taken for granted (consider \$\$\$ involved). It has been my privilege to conduct Ph.D. study at this institute.

I am thankful to BP technological advisors residing at EBI (past and present), Dr. Joseph Binder, Dr. Amit Gokhale, Dr. Martin Carrera, Dr. Craig Vaughn and Dr. Stephen Pietsch. It was a great experience to work with you face to face, learning the industrial perspectives hands-on. Especially, Joe—I cannot thank you enough for all the discussion, suggestions and encouragement in my initial years.

I also appreciate all the help I received from the Toste group members. While EBI taught me about sustainability, it is this group of excellent talents who taught me chemistry. Particularly, I would like to acknowledge Dr. Gregory Hamilton and Dr. Robert Phipps, two of the smartest people I ever know. Also, my fellow 2008 entering class graduate student labmates, Dr. Jeffrey Wu, Dr. Aaron Lackner and Dr. Yiming Wang. You guys are awesome easy-going hard-workers. I respect you all.

My special, special thanks goes to my fiancé Dr. James Long. You are the one who made my graduate school life so colorful. From weekday dinner at home to vacation trip in Hawaii, I cherish all the moments. Life is great with you, James. Thank you so much for your love and support.

Lastly, I am very grateful to my family in Japan, especially my parents. It was probably not an easy thing to send off a daughter to another country. However, you always trust my decision and let me pursue whatever dream of mine. I always appreciate how lucky I am to have such an understanding family. ありがとう。

August 2013
Mika Shiramizu

Prelude

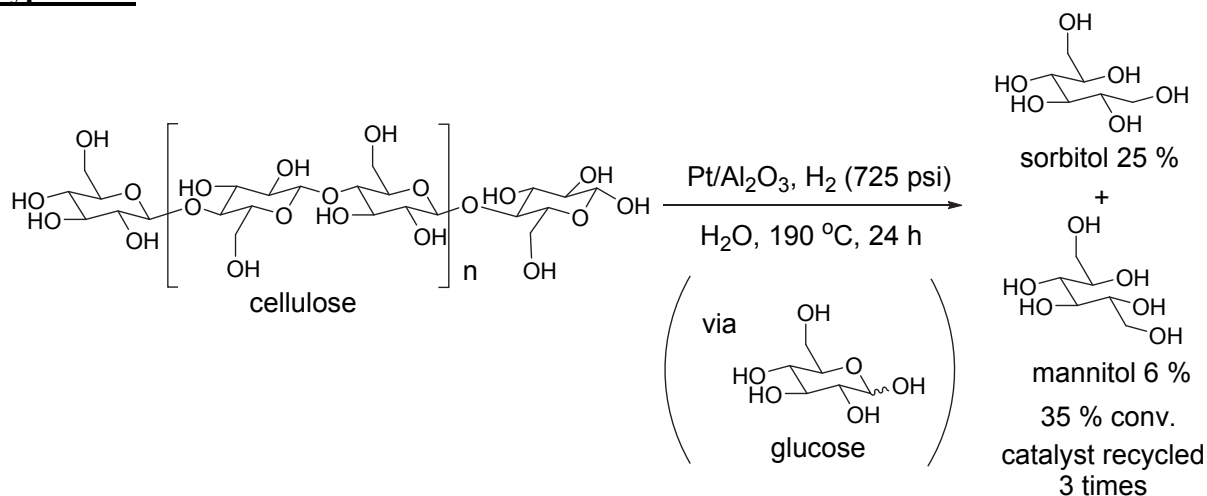
Oxorhenium-Catalyzed Hydrolysis of Cellulose under Hydrogen

Introduction

The United States has been one of the world's largest producers of biofuels since the oil crises of the 1970s, supported by various federal and state policies such as Energy Tax Act in 1978 and Renewable Fuel Standard in 2005.^[1] The key driving forces for the US alternative energy development have been (1) conservation of finite fossil fuels, (2) energy security (necessity to secure domestic oil supply) and (3) need for reducing the greenhouse gas emission. The first-generation biofuels (until 1990s) mainly consisted of ethanol fermented from corn or sugar cane (for gasoline engine) and fatty acid methyl esters trans-esterified from vegetable oils (for diesel engine). In 2000s, however, the limitations of the fuels from edible sources were becoming apparent; in addition to the criticism of food-fuel land use competition, various analyses found their economic and environmental benefits to be questionable.^[1] Lignocellulosic biomass (e.g. energy grasses such as miscanthus, or agricultural waste such as corn stover, bagasse, cereal straws and wood chips) thus started to attract attention as an inexpensive and ubiquitous alternative energy source. The main components of lignocellulosics are cellulose (polymer of glucose, 40-60 dry wt%), hemicellulose (oligomer of glucose, xylose and other sugars, 20-40 dry wt%) and lignin (highly cross-linked aromatic polymer consisting of syringyl and sinapyl units, 10-25 dry wt%).^[2] Given the established sugar fermentation technology, much of the earlier research on cellulosic biofuels (second-generation biofuels) aimed at the substitution of sugar/starch feedstocks with cellulose/hemicellulose-derived sugars to produce cellulosic ethanol.

In the process of cellulosic bioethanol production, one of the biggest challenges is the cellulose hydrolysis. While starch is a polymer of glucose with $\alpha(1\rightarrow4)$ linkages, cellulose is a polymer of glucose with $\beta(1\rightarrow4)$ linkages. This structural difference makes cellulose much more recalcitrant than starch due to the 3-D network of hydrogen bonding.^[3] While the enzymatic hydrolysis is mild, high-yielding (up to 95 %) and selective, it could be costly and generally requires a long time (days) for completion.^[2b, 3] Therefore, mineral acids (e.g. H_2SO_4) are more commonly used in large scale processing to provide glucose (up to 90 %) in a relatively short reaction time (minutes to several hours).^[2b, 3] The concerns with this method are (1) corrosiveness to the reactors, (2) difficulty in recovery of the acid catalyst, and (3) the waste (salts, water) accumulation from the neutralization of the acid stream if the catalyst recovery is impractical. Extensive research has been done in the development of recyclable solid acid catalysts to address these issues.^[3-4] However, many face a fundamental problem that cellulose is insoluble in most solvents and solid-solid interaction is limited. Therefore, such an approach often requires an extensive pretreatment of cellulose such as ball-milling.

Hypothesis



Scheme 1 The conversion of cellulose into hexitols by one-pot hydrolysis and hydrogenation.^[5]

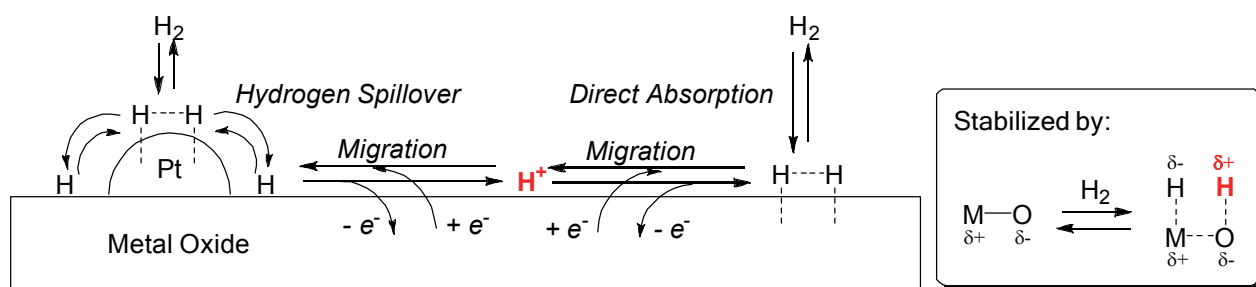


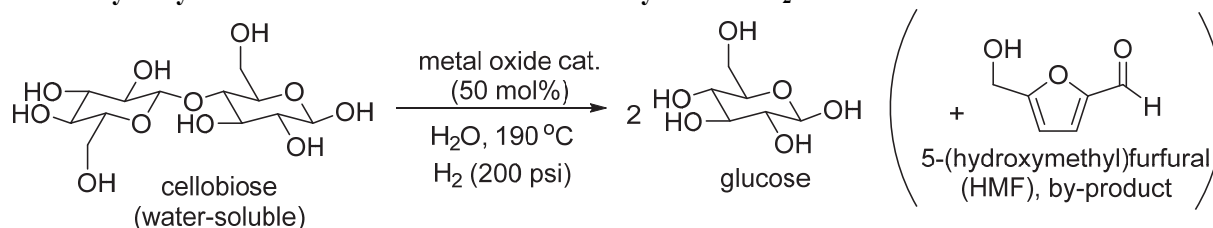
Figure 1 The proposed mechanisms of protonic sites generation on metal oxides from molecular hydrogen.^[6]

With this background, my first project at Berkeley in 2008 was the development of a “switchable” H₂ pressure-controlled acid catalyst for cellulose hydrolysis (i.e. acidic under H₂ pressure, neutral when H₂ gas is released). The inspiration came from the report by Fukuoka and Dhepe in 2006,^[5, 7] in which cellulose was converted into C6 sugar alcohols over Pt/Al₂O₃ catalyst under H₂ (Scheme 1). They argued that H₂ undergoes heterolytic cleavage to produce hydride-type hydrogen and proton-type hydrogen stabilized on the surface of the metal oxide (Al₂O₃) either by direct absorption or by hydrogen spillover on the Pt surface^[6] (Figure 1); The observation that glucose was produced only in <4 % yield when Al₂O₃ was used alone potentially implied that the support metal oxide itself is not particularly acidic. They hypothesized that such a “H⁺” generated reversibly in-situ from H₂ is responsible for hydrolysis of cellulose to glucose, the necessary step before the Pt-catalyzed fast hydrogenation occurs. Although Hattori et al. has presented compelling evidence for the generation of H₂-originated protonic sites for other metal oxides such as Pt/SO₄²⁻-ZrO₂ and demonstrated their use in Brønsted acid-catalyzed reactions such as cumene cracking^[6], it must be noted that there was no direct experimental evidence for this hypothesis by Fukuoka group. Because glucose is much

less thermally stable than sugar alcohols, the low glucose yield in the presence of Al_2O_3 alone does not exclude the possibility of glucose decomposition under the harsh conditions employed. In fact, more recent relevant studies seem to indicate that such a mechanism is unlikely and the cellulose hydrolysis occurs either thermally or on the intrinsic acidic sites of Al_2O_3 at the elevated temperature.^[8] Wang et al. measured the FT-IR of pyridine adsorbed on $\text{Ru}/\text{Al}_2\text{O}_3$ and observed no generation of Brønsted acidic sites under H_2 pressure.^[6b, 9] Essayem et al. reported hydrothermal cellulose dissolution in the absence of catalyst, which was enhanced by $\text{Pt}/\text{Al}_2\text{O}_3$.^[10] Also, as circumstantial evidences, Pt ,^[11] Ru ^[12] and Ni ^[13] catalysts on support materials other than metal oxides (e.g. carbon black) have been reported to function in a similar manner. Adding an external acid was found beneficial to promote hydrolysis in several cases (e.g. Ru/C with heteropolyacids).^[14] Nonetheless, the concept of using H^+ formed from H_2 in the cellulose hydrolysis was new and intrigued us because it would address the recycling/neutralization problems of conventional mineral acids if H_2 cleavage is reversible and controllable by temperature and H_2 pressure. Furthermore, assuming the metal oxide catalyst is insoluble in water after the reaction, it would be easily recovered and reused. We wondered if metal oxides other than Al_2O_3 could indeed catalyze the cellulose hydrolysis by such a unique mechanism. We therefore set out to explore the metal oxide-catalyzed hydrolysis of cellulose to glucose under H_2 , because glucose is challengingly thermally unstable but more valuable than hexitols as a feedstock for fermentative bioethanol production.

Results and Discussion

Table 1 Hydrolysis of cellobiose with metal oxide catalyst under H_2 .



entry	cat.	time (h)	glucose yield (%)	HMF yield (%)	conv. (%)
1	Al_2O_3 (Acidic)	8	67	5	88
2	Al_2O_3 (Basic)	8	71	10	78
3	CuO	8	69	5	79
4	Ti_2O_3	8	56	6	75
5	CeAlO_3	8	47	11	100
6	Sc_2O_3	8	62	5	100
7	ZrO_2	8	51	9	71
8	HfO_2	8	55	4	73
9	ReO_3	8	66	4	100
10	ReO_3	1	90	0	100
11	WO_3	8	49	2	96
12	none	6	28	0	41

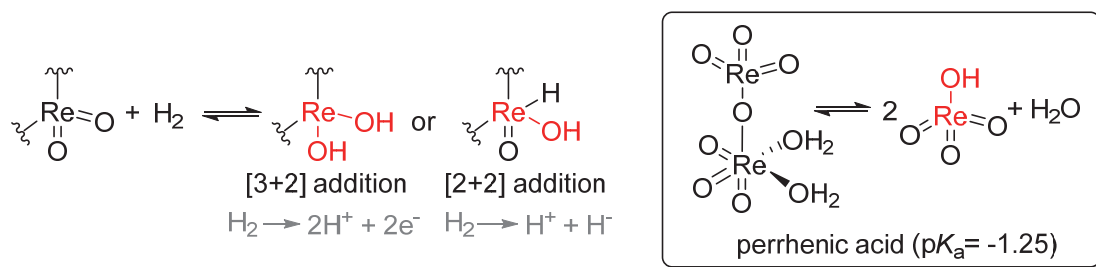


Figure 2 The proposed formation of protonic sites from H_2 on oxorhenium species.

A set of metal oxide catalysts was first screened under H_2 pressure for the hydrolysis of cellobiose (yield and conversion were determined by HPLC using a calibration curve prepared with authentic samples). Cellobiose, the water-soluble glucose dimer with a $\beta(1 \rightarrow 4)$ linkage, is commonly accepted as a model substrate for cellulose. It was soon realized that finding a general optimum condition for this reaction is not trivial because the glucose yield was fairly time- and temperature-sensitive. Nonetheless, several metal oxides gave significantly higher glucose yield than no-catalyst conditions (Table 1). Among the catalysts which gave $>60\%$ glucose yields in 8 hours (Al_2O_3 , CuO , Sc_2O_3 , ReO_3), ReO_3 particularly interested us because $\text{ReO}_2 \cdot 2.5\text{H}_2\text{O}$ ^[15] as well as monomeric oxorhenium species such as CH_3ReO_3 (methyltrioxorhenium, MTO) and $\text{ReI}_2\text{O}_2(\text{PPh}_3)_2$ ^[16] were known to activate molecular hydrogen and catalyze the hydrogenation reactions of alkenes, sulfoxides, and carbonyl, nitro and carboxyl moieties. It is not understood whether H_2 is activated by [3+2] addition^[17] or by [2+2] addition^[16] on rhenium-oxo compounds, but in either case we expected a resulting Re-OH bond to be highly acidic, in an analogy to the strong ($\text{p}K_{\text{a}} = -1.25$) Brønsted acid perrhenic acid HReO_4 (Figure 2).

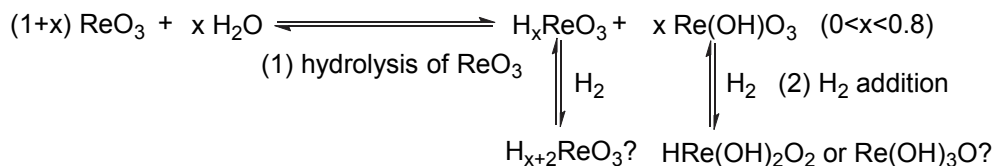
Table 2 Comparison of hydrogen and inert gas for oxorhenium compounds.

cellobiose		cat. (20 mol%)		glucose	
		$\xrightarrow{\text{H}_2\text{O, gas (200 psi), 190 }^\circ\text{C, 1 h}}$			
		<hr/>			
		H_2		Ar	
		<hr/>		<hr/>	
entry	cat.	yield (%) ^[a]	yield (%) ^[a]		
<hr/>	<hr/>	<hr/>	<hr/>	<hr/>	<hr/>
1	ReO_3	62	40		
2	HReO_4	71	58 ^[b]		
3	CH_3ReO_3	54 ^[c]	13		
4	none	–	<1		
		<hr/>			

^[a]The cellobiose conversion was correspondent to the glucose yield in all cases. ^[b]85 % Glucose yield after 4 h. ^[c]95 % Glucose yield after 4 h.

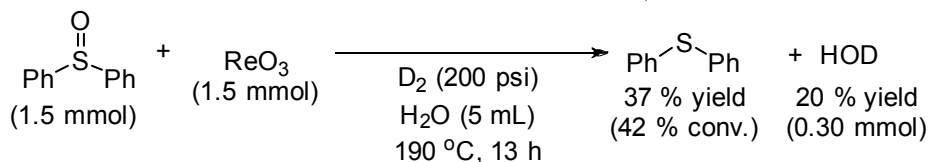
To clarify if there was indeed any enhancement of the acidity of ReO_3 due to H_2 , we conducted the cellobiose hydrolysis under Ar and compared it with the results under H_2 (Table 2, entry 1). HReO_4 and MTO were also tested to examine whether an effect was observed for

homogeneous oxorhenium species (entries 2 and 3); MTO was known to catalyze reduction reactions under H₂,^[16] and we suspected HReO₄ might be formed from MTO under aqueous reaction conditions. Although the system was clearly much more acidic in the presence of ReO₃ (entry 1) compared with the no-catalyst conditions (entry 4), the results were somewhat confusing as to what was responsible for the generated acidity. While there appeared to be a difference between H₂ and Ar, the glucose yield was significant even under Ar. We therefore hypothesized that Brønsted acidic Re-OH bond is produced from ReO₃ not only from H₂ addition but also from H₂O addition, as reported by Kimizuka et al.^[18] Furthermore, the undefined species H_xReO₃ may also interact with H₂, to make the system more complex (Scheme 2).



Scheme 2 Addition of H₂O and H₂ to ReO₃.

In order to investigate the plausibility of the activation of H₂ on ReO₃ in a more direct manner than by measuring glucose yield from cellobiose hydrolysis, we tested the reduction of diphenyl sulfoxide with a stoichiometric amount of ReO₃ and obtained diphenyl sulfide in 37 % yield (Scheme 3). No reaction was observed in the absence of ReO₃. A peak of HOD was also detected in ²H NMR after the reaction^[19], while in the absence of sulfoxide there was virtually no difference in the amount of HOD with or without ReO₃ (Table 3). This result hinted that ReO₃ may indeed interact with H₂. (However, later in 2012, Fernandes et al. reported the ReOCl₃(PPh₃)₂^[20]-catalyzed reduction of sulfoxides to sulfides without adding any reductant.^[21] Thus retrospectively, it is possible that such a reaction played a role in our observation of ReO₃-mediated sulfoxide reduction shown in Scheme 3.)

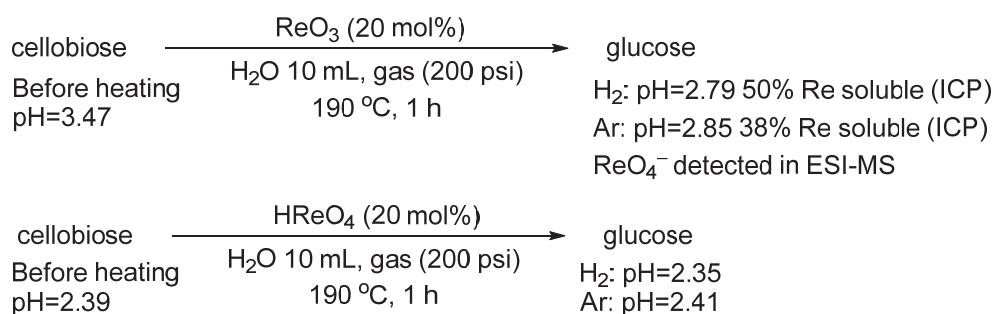


Scheme 3 Reduction of diphenyl sulfoxide to diphenyl sulfide.

Table 3 HOD formation without diphenyl sulfoxide.

		H ₂ O 5 mL (278 mmol)	+ ReO ₃ (x mmol)	gas (200 psi) 190 °C, 4 h	HOD
entry	x			gas	HOD (mmol)
1	1.5			D ₂	0.055
2	0			D ₂	0.048
3	0			H ₂	0.041

However, we next studied the interaction of ReO_3 with H_2O (Scheme 4) and found to our disappointment that ReO_3 was irreversibly transformed into a different homogeneous acidic species. After the reaction, the system stayed acidic (by pH measurement) under both H_2 and Ar atmospheres, breaking the foremost promise of “reversible H^+ generation from H_2 ”. When the reaction mixture was filtered, ICP analysis of the filtrate indicated that nearly half of ReO_3 remained dissolved in water. ESI-MS indicated that this homogeneous Re species was predominantly ReO_4^- ion. However, some black material was also left in the solution and could be recovered by filtration. According to Scheme 2, we suspected that it is a mixture of remaining ReO_3 and the reduced Re species H_xReO_3 . However, it was difficult for us to characterize this compound. Powder X-ray diffraction data taken on this recovered material did not show any significant change from ReO_3 (standard, blue line) as reported for $\text{H}_{0.57}\text{ReO}_3$ by Majid et al.^[22] (Figure 3).



Scheme 4 The irreversible change occurred of ReO_3 under reaction conditions.

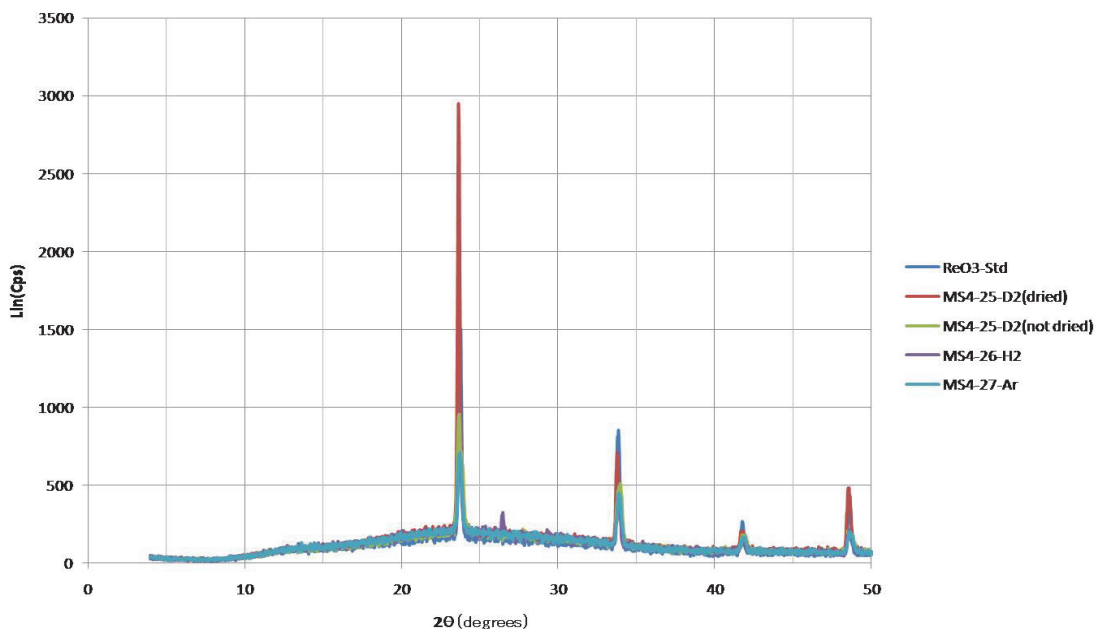


Figure 3 Powder X-ray diffraction of the solid material recovered from the aqueous cellobiose hydrolysis reaction by ReO_3 under H_2 , Ar or D_2 (according to Scheme 4).

Conclusion

While the exact nature of the transformation occurring on ReO_3 under the high-temperature aqueous reaction conditions remained unclear due to the complexity of the system, our results indicated that ReO_3 could not provide the desired catalysis based on H_2 -controlled, reversibly generated protonic sites as envisioned. We therefore decided to pursue a different project theme. Herein, it is worth specific mention that the price of gasoline dropped dramatically from late 2008 to early 2009 (US\$4.0/gallon in June-July 2008 to US\$1.7-1.8/gallon in January 2009).^[23] The biomass research community was significantly affected by this change and the target products from biomass conversion rapidly became more diverse. Not only cellulosic ethanol for gasoline-blending^[24] but also bio-derived chemicals/materials and unconventional fuel candidate molecules, such as furfural and 5-(hydroxymethyl)furfural derivatives, began to attract much attention as premium-priced products. Reflecting this trend, we started to investigate the synthesis of biomass-derived terephthalic acid from 2,5-dimethylfuran using the Diels-Alder reaction approach, which is described in Chapter 1. Nonetheless, we remained interested in the diphenyl sulfoxide reduction (Scheme 3), because it showed some promise of the water-insensitive H_2 activation by ReO_3 or by in situ-generated HReO_4 . Therefore, in parallel to the work on terephthalic acid project, we were seeking an application of the reductive reactivity of oxorhenium catalysts in the context of biomass chemistry. It was at this time in October 2009 that the Abu-Omar group reported the MTO-catalyzed deoxydehydration (DODH) of diols to alkenes using H_2 as a reductant.^[25] While the first DODH reaction was described by Cook and Andrews in 1996 using phosphine as a reductant,^[26] this was the first of the modern development of DODH chemistry with a focus on practical application. We were inspired to develop this reaction further because the DODH reactivity was relevant to our observation. Specifically, because the substrate scope in Abu-Omar's initial report was limited to simple diols (only 1,2-hexanediol, *cis*-1,2-cyclohexanediol and 1,4-anhydroerythritol were investigated), we envisioned the expansion of this methodology to polyol deoxygenation, which would be much more relevant to the biomass deoxygenation. This is how we started to explore the oxorhenium-catalyzed deoxydehydration of polyols, which is described in Chapter 2.

References and Notes

- [1] B. D. Solomon, J. R. Barnes, K. E. Halvorsen, *Biomass Bioenergy* **2007**, *31*, 416-425.
- [2] a) L. Petrus, M. A. Noordermeer, *Green Chem.* **2006**, *8*, 861-867; b) C. N. Hamelinck, G. v. Hooijdonk, A. P. C. Faaij, *Biomass Bioenergy* **2005**, *28*, 384-410.
- [3] R. Rinaldi, F. Schüth, *ChemSusChem* **2009**, *2*, 1096-1107.
- [4] R. Rinaldi, F. Schuth, *Energy Environ. Sci.* **2009**, *2*, 610-626.
- [5] P. L. Dhepe, A. Fukuoka, *ChemSusChem* **2008**, *1*, 969-975.
- [6] a) H. Hattori, T. Shishido, *Catal. Surv. Asia* **1997**, *1*, 205-213; b) H. Hattori, *Top. Catal.* **2010**, *53*, 432-438; c) H. Hattori, in *Studies in Surface Science and Catalysis, Vol. Volume 138* (Eds.: A. Guerrero-Ruiz, I. Rodriguez-Ramos), Elsevier, **2001**, pp. 3-12.
- [7] A. Fukuoka, P. L. Dhepe, *Angew. Chem. Int. Ed.* **2006**, *45*, 5161-5163.
- [8] S. Van de Vyver, J. Geboers, P. A. Jacobs, B. F. Sels, *ChemCatChem* **2011**, *3*, 82-94.
- [9] M. Liu, W. Deng, Q. Zhang, Y. Wang, Y. Wang, *Chem. Commun.* **2011**, *47*, 9717-9719.
- [10] a) V. Jollet, F. Chambon, F. Rataboul, A. Cabiac, C. Pinel, E. Guillon, N. Essayem, *Green Chem.* **2009**, *11*, 2052-2060; b) V. Jollet, F. Chambon, F. Rataboul, A. Cabiac, C. Pinel, E. Guillon, N. Essayem, *Top. Catal.* **2010**, *53*, 1254-1257.
- [11] H. Kobayashi, Y. Ito, T. Komanoya, Y. Hosaka, P. L. Dhepe, K. Kasai, K. Hara, A. Fukuoka, *Green Chem.* **2011**, *13*, 326-333.
- [12] a) W. Deng, M. Liu, X. Tan, Q. Zhang, Y. Wang, *J. Catal.* **2010**, *271*, 22-32; b) W. Deng, X. Tan, W. Fang, Q. Zhang, Y. Wang, *Catal. Lett.* **2009**, *133*, 167-174; c) C. Luo, S. Wang, H. Liu, *Angew. Chem. Int. Ed.* **2007**, *46*, 7636-7639; d) N. Yan, C. Zhao, C. Luo, P. J. Dyson, H. Liu, Y. Kou, *J. Am. Chem. Soc.* **2006**, *128*, 8714-8715.
- [13] a) N. Ji, T. Zhang, M. Zheng, A. Wang, H. Wang, X. Wang, J. G. Chen, *Angew. Chem. Int. Ed.* **2008**, *47*, 8510-8513; b) L.-N. Ding, A.-Q. Wang, M.-Y. Zheng, T. Zhang, *ChemSusChem* **2010**, *3*, 818-821; c) S. Van de Vyver, J. Geboers, M. Dusselier, H. Schepers, T. Vosch, L. Zhang, G. Van Tendeloo, P. A. Jacobs, B. F. Sels, *ChemSusChem* **2010**, *3*, 698-701.
- [14] a) R. Palkovits, K. Tajvidi, A. M. Ruppert, J. Procelewska, *Chem. Commun.* **2011**, *47*, 576-578; b) J. Geboers, S. Van de Vyver, K. Carpentier, P. Jacobs, B. Sels, *Green Chem.* **2011**, *13*, 2167-2174; c) J. Geboers, S. Van de Vyver, K. Carpentier, K. de Blohouse, P. Jacobs, B. Sels, *Chem. Commun.* **2010**, *46*, 3577-3579.
- [15] H. S. Broadbent, T. G. Selin, *J. Org. Chem.* **1963**, *28*, 2343-2345.
- [16] P. M. Reis, P. J. Costa, C. C. Romão, J. A. Fernandes, M. J. Calhorda, B. Royo, *Dalton Trans.* **2008**, 1727-1733.
- [17] K. Valliant-Saunders, E. Gunn, G. R. Shelton, D. A. Hrovat, W. T. Borden, J. M. Mayer, *Inorg. Chem.* **2007**, *46*, 5212-5219.
- [18] a) S. Horiuchi, N. Kimizuka, A. Yamamoto, *Nature* **1979**, *279*, 226-227; b) N. Kimizuka, T. Akahane, S. Matsumoto, K. Yukino, *Inorg. Chem.* **1976**, *15*, 3178-3179; c) M. Castriota, E. Cazzanelli, G. Das, R. Kalendarev, A. Kuzmin, S. Marino, G. Mariotto, J. Purans, N. Scaramuzza, *Mol. Cryst. Liq. Cryst.* **2007**, *474*, 1-15.
- [19] The produced amount was calibrated by subtracting the naturally existing HOD in standard sample of water of the same volume.
- [20] The authors reorted that HReO₄, Re₂O₇ were ineffective.
- [21] S. C. A. Sousa, J. R. Bernardo, C. C. Romão, A. C. Fernandes, *Tetrahedron* **2012**, *68*, 8194-8197.
- [22] C. A. Majid, M. A. Hussain, *J. Phys. Chem. Solids* **1995**, *56*, 255-259.

- [23] Weekly U.S. regular conventional retail gasoline prices, published by U.S. Energy Information Administration. <http://www.eia.gov/petroleum/gasdiesel/>
- [24] This direction (production of bio-derived gasoline) further started to face a competition with hybrid electric vehicles as they became more affordable. See: J. Ohlrogge, D. Allen, B. Berguson, D. DellaPenna, Y. Shachar-Hill, S. Stymne, *Science* **2009**, *324*, 1019-1020.
- [25] J. E. Ziegler, M. J. Zdilla, A. J. Evans, M. M. Abu-Omar, *Inorg. Chem.* **2009**, *48*, 9998-10000.
- [26] G. K. Cook, M. A. Andrews, *J. Am. Chem. Soc.* **1996**, *118*, 9448-9449.

Chapter 1

On the Diels-Alder Approach to Solely Biomass-Derived Polyethylene Terephthalate(PET): Conversion of 2,5-Dimethylfuran and Acrolein to *p*-Xylene

Portions of the work in this chapter have been published:

M. Shiramizu, F. D. Toste, Chem. Eur. J. 2011, 17, 12452-12457.

Introduction

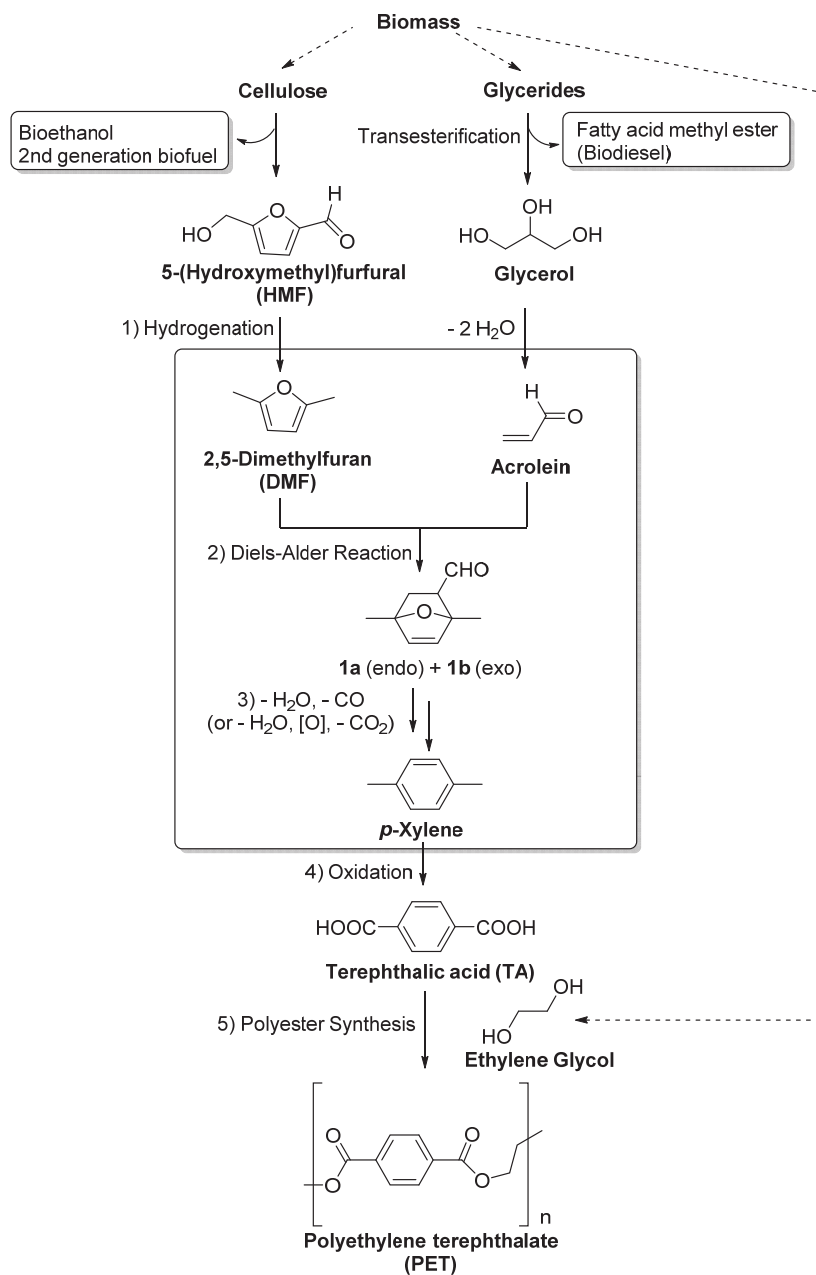
In response to the increasingly urgent issue of sustainability, lignocellulosic biomass has attracted attention as a renewable and carbon-neutral energy source. However, the selective acidic hydrolysis of cellulose to glucose, the feedstock for fermentative bioethanol production, is difficult due to the recalcitrant crystalline structure of cellulose^[1] and the instability of product sugars.^[2] Instead, 5-(hydroxymethyl)furfural (HMF), a dehydrated aromatic form of glucose or fructose, is typically obtained as a major byproduct under harsh conditions^[3] or even as the predominant product in the presence of designed catalysts.^[4]

The utility of HMF warrants further exploration. Due to its low energy density and instability, HMF is not a promising candidate as a liquid fuel, but rather it is a potential intermediate for renewable chemicals.^[4c] One often proposed approach is the oxidation of HMF to 2,5-furandicarboxylic acid (FDCA).^[5] FDCA has been suggested as a potential replacement for terephthalic acid (TA).^[6] TA is an important raw material for the production of polyethylene terephthalate (PET), a high-demand plastic with wide utility ranging from beverage containers to synthetic fibers (total PET consumption in US: 5.01 million metric tons in 2007).^[7] Although the direct substitution of FDCA for TA in polymer synthesis has been known since the 1970s,^[8] it has not been successfully commercialized to date. This can be attributed not only to the difference in chemical properties between FDCA and TA but also to the difficulty of introducing new chemicals to an existing market.^[9]

Based on the background above, it is desirable to develop a novel route to convert HMF to an established commodity chemical such as TA.^[10] The envisioned transformation of HMF to TA requires the addition of a building block of at least two carbons, which ideally would also come from renewable sources. When we started our HMF conversion project in 2009, the most relevant work in this context was the conversion of 2,5-dimethylfuran (DMF), the hydrogenated form of HMF, and ethylene gas to *p*-xylene via a one-pot Diels-Alder reaction and thermal dehydrative aromatization. It was described by two individually published patents,^[11] which were followed by several publications in more recent years.^[12] This strategy is attractive because it is atom-economical, the claimed *p*-xylene yield is high (up to 92 %) and ethylene can be produced from bio-ethanol dehydration.^{[13] [14]} Nonetheless, the process requires high pressure of ethylene (claimed 1-105 atm) as well as high reaction temperature (claimed 100-300 °C). More

importantly, the product is inherently limited to *p*-xylene and there is no opportunity in the synthetic pathway to diverge the end products. We thus wondered if other biomass-derived dienophiles can be also utilized in this DMF Diels-Alder approach to bio-aromatics. In this regard, acrolein caught our attention as the most attractive target.^[15] Acrolein can be efficiently prepared from the dehydration of glycerol,^{[16][17]} which is currently overproduced and rapidly decreasing its price as a side-product of growing biodiesel production.^[18] There is an urgent need for developing the routes to convert glycerol/glycerol derivatives into bulk chemicals in order to enhance the value of bio-refinery while decreasing the waste output. In addition, acrolein has one excess carbon as an aldehyde, which can be easily removed as CO^[19] (or as CO₂ after oxidation^[20]) to produce *p*-xylene once aromatized. We also envisioned that this carbon could provide access to other products such as trimellitic acid (for plastics and trimellitate plasticizers) or various substituted aromatic compounds via decarbonylative^[21] or decarboxylative^[22] coupling (for speciality chemicals applications). It is already well established that ethylene glycol, the ester condensation partner in the final polyester synthesis step, can be produced from sugar-based feedstocks^[23] or from cellulose^[24] via hydrogenolysis. Therefore, this approach of DMF-acrolein Diels-Alder reaction could provide a glycerol (biofuel waste product)-based alternative route to a fully renewable, solely biomass-derived PET.

To realize this concept, our strategy consisted of the following five steps (Scheme 1): 1) hydrogenation of HMF to DMF, 2) Diels-Alder reaction with acrolein to construct the 7-oxabicyclo[2,2,1]hept-2-ene core structure **1**, 3) aromatization and removal of aldehyde carbon to obtain *p*-xylene, 4) oxidation of *p*-xylene to TA, and 5) condensation of TA and ethylene glycol to furnish PET. Currently, PET is mass-produced by steps 4 and 5 using *p*-xylene obtained from crude oil. Therefore, its replacement with bio-derived *p*-xylene would be easily implementable because little change is required in the downstream infrastructure and operation. As step 1 is preceded, ^[25] this work focuses on the conversion of DMF and acrolein to *p*-xylene (steps 2 and 3).

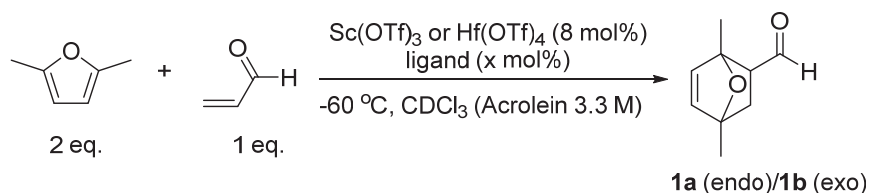


Scheme 1 Proposed PET synthesis using biomass-derived carbon feedstocks.

Condition Optimization for Diels-Alder Reaction

When we started our investigation, there were only two reports on the Diels-Alder reaction between DMF and acrolein.^[26] Burrell et al. used very high pressure (15 kbar)^[27] while Laszlo et al. used an Fe^{III}-doped K-10 bentonite clay catalyst.^[28] Although we initially expected that the Diels-Alder reaction would proceed more smoothly for DMF and acrolein than for DMF and ethylene based on the electron deficient nature of acrolein, reported yields were rather moderate (ca. 40 %) in both methods. We thus decided to seek a more efficient simple Lewis acid catalyst capable of mediating this transformation. However, the difficulty soon became apparent: the initial screening of common Lewis acids such as AlCl₃, Et₂AlCl, TiCl₄, SnCl₂, BF₃•Et₂O, ZnCl₂ and ZnI₂ at temperatures between 25 °C and -78 °C (1-3 eq. DMF) in various solvents showed no promise, mainly due to the instability of acrolein. In most cases, we observed either no reaction or immediate and complete decomposition of acrolein. Nonetheless, when we specifically focused on group 3 and 4 metal (Sc, Y, Zr, Hf) species inspired by a reported HfCl₄-catalyzed Diels-Alder reaction of DMF and benzyl acrylate,^[29] we finally observed a trace amount of **1** by ¹H NMR using 8 mol% Sc(OTf)₃ (-60 °C, 2 eq. DMF, CDCl₃).^[30]

Table 1 Sc(OTf)₃ and Hf(OTf)₃ -catalyzed Diels-Alder reaction of DMF and acrolein with bidentate ligands.



entry	cat.	ligand (mol%)	drying agent	time (h)	yield 1a+1b (%)
1	Sc(OTf)₃	Phen (20)	MS4Å powder	96	76
2	Sc(OTf) ₃	Phen (15)	MS4Å powder	20.5	46
3	Sc(OTf) ₃	Phen (10)	MS4Å powder	20	12 ^a
4	ScCl ₃	Phen (20)	MS4Å powder	20	N.R.
5	Hf(OTf) ₄	Phen (30)	MS4Å powder	66	45
6	Hf(OTf)₄	Phen (20)	MS4Å powder	69	82
7	Hf(OTf) ₄	Phen (20)	Na ₂ SO ₄	90.5	59
8	Hf(OTf) ₄	Phen (20)	MgSO ₄	90.5	46
9	Hf(OTf) ₄	Phen (20)	none	24	10 ^a
10	Hf(OTf) ₄	Phen (10)	MS4Å powder	1	N.D. ^b
11	Hf(OTf) ₄	Phen (0)	MS4Å powder	1	N.D. ^b
12	HfCl ₄	Phen (20)	MS4Å powder	20	12
13	Sc(OTf) ₃	Bipy (20)	MS4Å powder	7.5	N.R.
14	Sc(OTf) ₃	Bipy (10)	MS4Å powder	18.5	15 ^a
15	Hf(OTf) ₄	Bipy (20)	MS4Å powder	7.5	N.R.

^aSignificant decomposition of acrolein. DMF remained. ^bImmediate decomposition of acrolein. DMF remained.

We then started to optimize the reaction conditions. In this study, the yield of **1** was determined by ^1H NMR using an internal standard (SiEt_4). Because high concentrations are generally preferable for Diels-Alder reactions due to its negative reaction entropy, DMF was used as a co-solvent: As a representative example, for 6 mmol of acrolein, 1.3 mL (12 mmol) of DMF and 1.8 mL of CDCl_3 was used (the reaction shown in Table 1). In all cases, the product **1** was obtained as a mixture of **1a** (endo product) and **1b** (exo product) with a d.r. of **1a/1b** = 1.0 to 1.4. However, envisioning the formation of the same product from both stereoisomers after the subsequent aromatization step (see Scheme 1), we were not concerned with the low diastereoselectivity. We first tried using a combination of $\text{Sc}(\text{OTf})_3$ or $\text{Hf}(\text{OTf})_4$ and a phenanthroline or bipyridine ligand, hoping that the ligand pocket would facilitate the preferential coordination of Lewis acid to the sterically accessible acrolein (dienophile) carbonyl instead of DMF. To our delight, the addition of phenanthroline ligand dramatically increased the yield, at a specific catalyst to ligand ratio (catalyst:Phen= 8 mol%:20 mol%; Table 1, entries 1 and 6). The use of drying agent, namely MS4\AA powder, was found beneficial (entries 6-9). Chloride salts were less effective than triflate salts (entries 4 and 12).

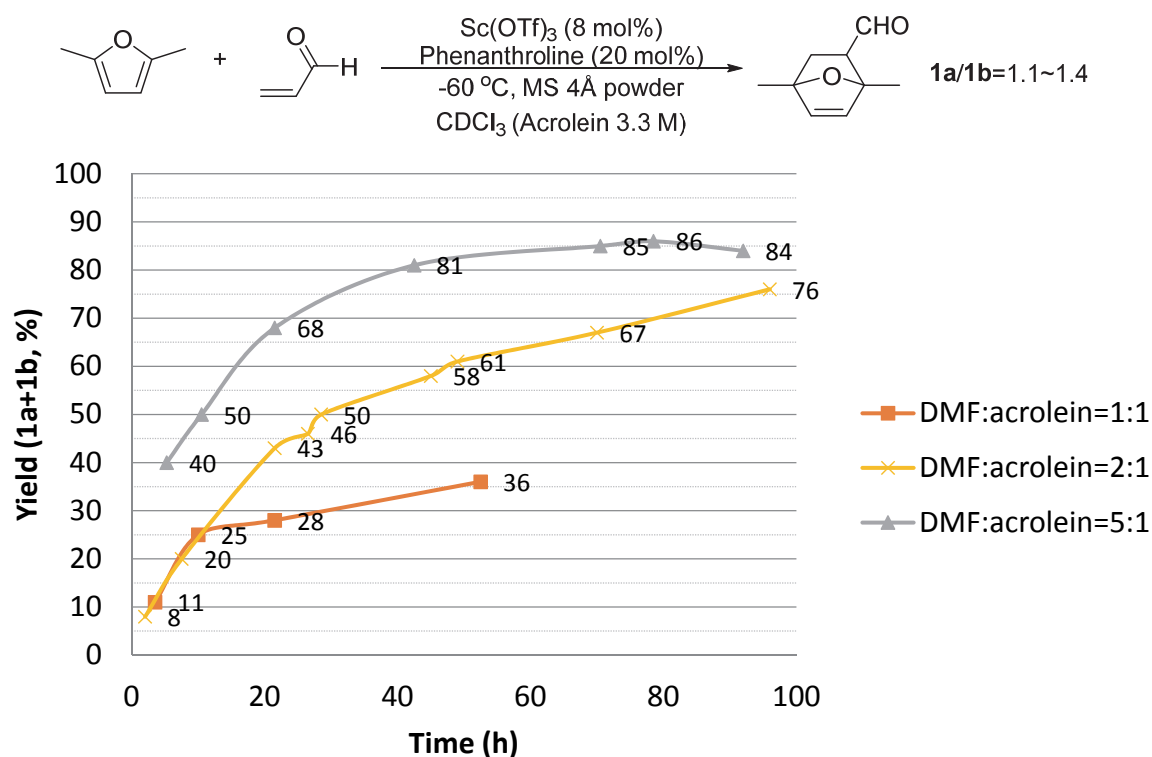
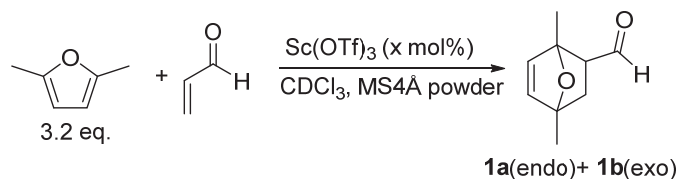


Figure 1 Diels-Alder reaction reaction profile comparison at different DMF:acrolein molar ratio.

We next examined the DMF/acrolein molar ratio using $\text{Sc}(\text{OTf})_3$ (Figure 1). Decreasing the DMF:acrolein ratio from 2:1 to 1:1 led to a partial decomposition of acrolein and low overall yield. Increasing the ratio to 5:1, on the other hand, enhanced the reaction rate but the final yields reached after 4 days were comparable. DMF/acrolein molar ratio could not be increased much further from 5:1 because neat DMF starts to freeze at c.a. $-60\text{ }^\circ\text{C}$ (DMF m.p. $-62\text{ }^\circ\text{C}$). In contrast, ca. 1:1 (v/v) mixture of DMF and chloroform (m.p. $-64\text{ }^\circ\text{C}$) did not freeze even at $-78\text{ }^\circ\text{C}$ due to the freezing-point depression of the mixture. Therefore, we concluded that DMF:acrolein ratio of

2:1 to 5:1 provided a good balance for a practical reaction and the concentration of 3.2 eq. DMF and 3.3 M acrolein in CDCl_3 , which composed $\text{DMF}:\text{CDCl}_3$ =ca. 1:1 (v/v), was employed as the standard conditions to allow the investigation of lower temperature reactions.

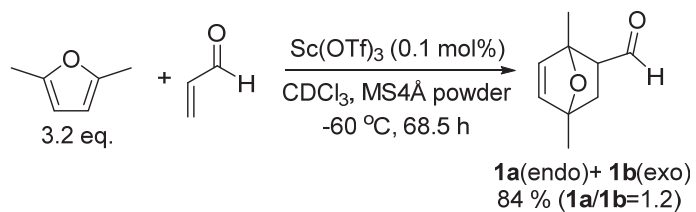
Table 2 Effect of $\text{Sc}(\text{OTf})_3$ loading.



entry	temp. [$^{\circ}\text{C}$]	x [mol%]	time [h]	yield [%]	conversion [%]	d.r. (1a/1b)
1	-60	1	6.5	18	58	1.1
2	-60	0.5	24	11	70	1.2
3	-60	0.1	24	70	75	1.1
			44	80	80	1.2
			68.5	83	84	1.2
4	-60	0.05	44	50	52	1.2
5	-60	0	44	0	0	—
6	0	0.1	24	22	22	1.2
7	0	0	5	0	0	—
8	25	0.1	24	6	17	1.0
9	25	0	5	4	6	1.2
			24	7	7	1.1
10	-78	0.1	8	23	23	1.0

As described above, we identified conditions (Table 1, entries 1 and 6) which afforded **1** in good yields using phenanthroline ligand. However, the sharp sensitivity of the reaction to the amount of phenanthroline led us to speculate that the catalysis was happening with the small amount of ligand-free Sc or Hf catalyst, instead of the ligand-bound Lewis acid with a specific steric environment as we originally envisioned. In other words, because the low ligand to metal ratio caused the immediate decomposition of acrolein (Table 1, entries 3, 10 and 11), we suspected that the ligand might have simply poisoned a certain portion of the Lewis acid catalyst, thereby providing an optimum amount of Lewis acidity. In fact, when we examined the ligand-free conditions using a much decreased loading of $\text{Sc}(\text{OTf})_3$, we found 0.1 mol% $\text{Sc}(\text{OTf})_3$ catalyzed the reaction as efficiently as the previously optimized $\text{Sc}(\text{OTf})_3$ 8 mol%-phenanthroline 20 mol% system (Table 2, entry 3). The major problem with this reaction was that it required a long time (in the order of a few days) to achieve a good total yield (up to 84 %). However, it was difficult to accelerate it while retaining the high selectivity/cleanliness of the system. Increasing the catalyst loading led to the decomposition of acrolein (entries 1 and 2) and increasing the temperature led to the significant decrease in yield (entries 6 and 8) while the reaction was too slow at -78°C (entry 10). In the absence of catalyst, no reaction occurred at $\leq 0^{\circ}\text{C}$ at least on a reasonable time scale (entries 5 and 7), but a thermal Diels-Alder reaction was

observable at 25 °C (entry 9). To summarize, our optimized conditions (Table 2, entry 3) are shown in Scheme 2.



Scheme 2 Optimized conditions for the Diels-Alder reaction of DMF and acrolein.

Thermodynamics of Diels-Alder Reaction

The significant temperature dependence of yield observed in the optimization process implied that this Diels-Alder reaction was under thermodynamic control rather than kinetic control. We thought that a more thorough understanding of the reaction mechanism and thermodynamics could offer insights that might lead to further improvements in the yield and efficiency of the reaction. To investigate, the reaction profile was compared at different temperatures using the conditions in Scheme 2 (Figure 2). The diastereomeric ratio mostly stayed constant ($\mathbf{1a}/\mathbf{1b}=1.1-1.2$). At a higher temperature, the reaction proceeded faster but the yield plateaued at a lower level (e.g. 84 % in 3 days at $-60\text{ }^{\circ}\text{C}$ vs. 75 % in less than 24 h at $-55\text{ }^{\circ}\text{C}$). When the equilibrium constant $K_{eq(\mathbf{1a})}=[\mathbf{1a}]/[\text{DMF}][\text{acrolein}]$ and $K_{eq(\mathbf{1b})}=[\mathbf{1b}]/[\text{DMF}][\text{acrolein}]$ was calculated using the converged values at each temperature ($-60\text{ }^{\circ}\text{C}$ to $25\text{ }^{\circ}\text{C}$) and $\ln K_{eq}$ was plotted against $1/T$ (T =temperature in K), a clear linear relationship was obtained (Figure 3). It indicated that this reaction was indeed under thermodynamic control (i.e. the thermodynamic equilibrium had been reached when it reached the yield plateau in Figure 2). Using the slope and intercept values of Figure 2, based on the equation

$$\ln K_{eq} = \frac{-\Delta G^{\circ}}{RT} = -\frac{\Delta H^{\circ}}{RT} + \frac{\Delta S^{\circ}}{R}$$

where R (ideal gas constant) $=1.986\times 10^{-3}$ [kcal/K•mol], the standard enthalpy(ΔH°) and entropy (ΔS°) for this reaction were experimentally determined to be $\Delta H^{\circ}=-6.41$ [kcal/mol], $\Delta S^{\circ}=-0.0304$ [kcal/K•mol] for $\mathbf{1a}$ and $\Delta H^{\circ}=-6.39$ [kcal/mol], $\Delta S^{\circ}=-0.0307$ [kcal/K•mol] for $\mathbf{1b}$.

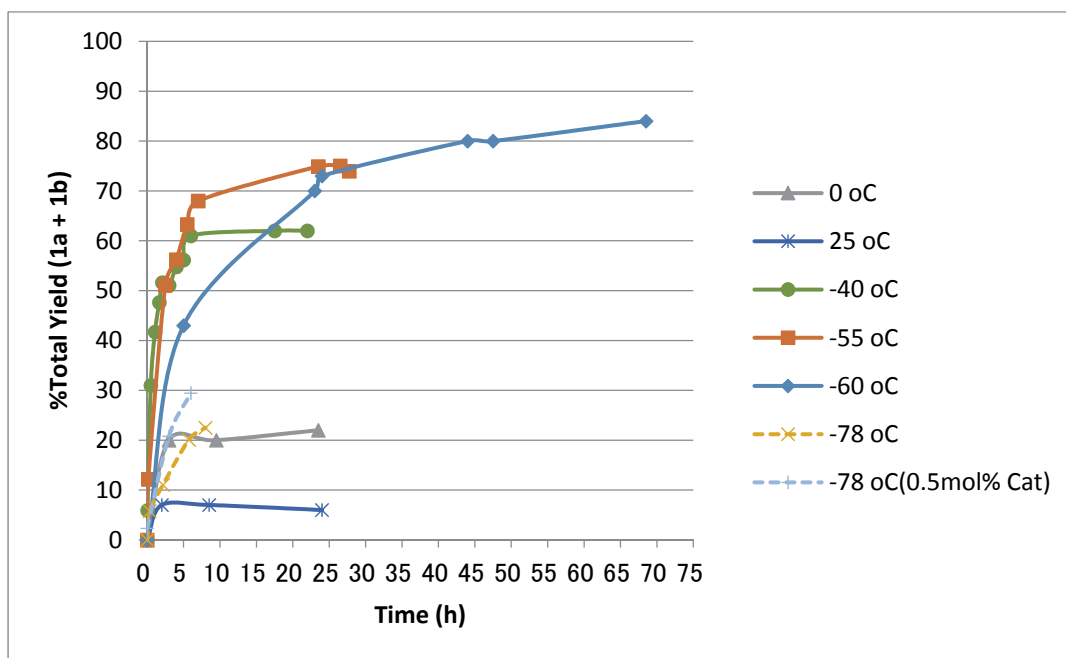


Figure 2 Temperature dependence of DMF-acrolein Diels-Alder reaction.

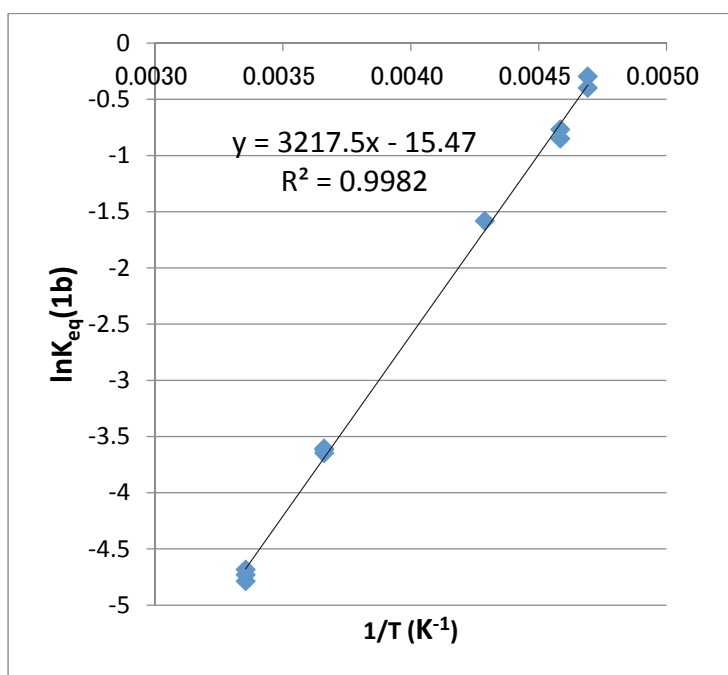
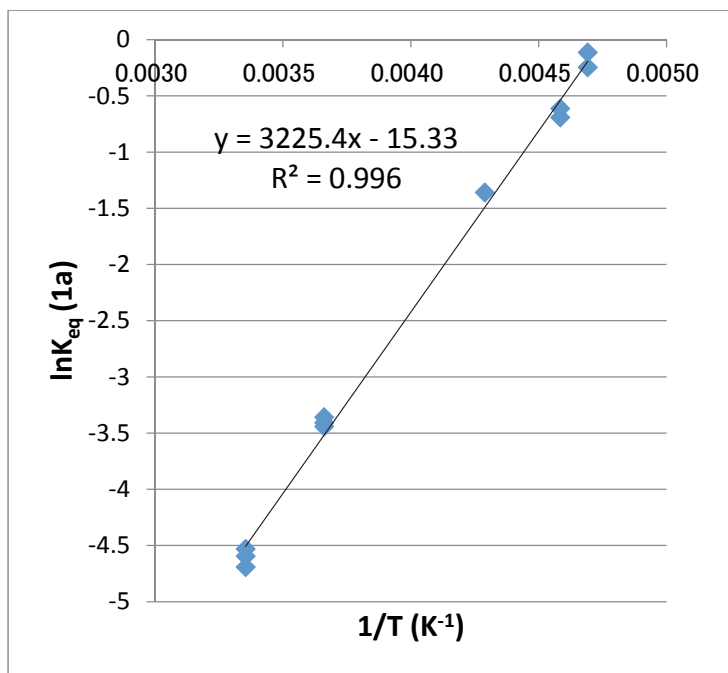
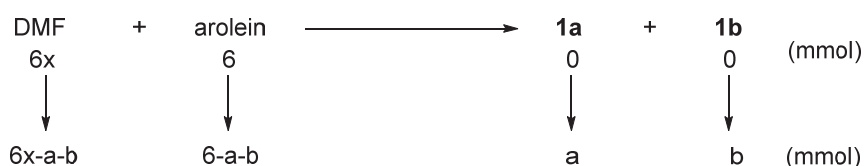


Figure 3 Linear relationship between $\ln K_{eq}$ and $1/T$ (obtained from the data shown in Figure 2).

We were aware that it is more desirable if this Diels-Alder reaction could be performed at ambient temperature because cooling is a cost- and energy-intensive operation. Unfortunately, the ΔH° and ΔS° values indicated that the low temperature is inherently required regardless of the catalysis conditions. Typically, when a Diels-Alder reaction is under thermodynamic control, a method to increase the equilibrium yield without changing the temperature is to increase the concentration of starting materials. In our case, this means increasing the amount of DMF

because DMF is used as a co-solvent in near-heat condition (DMF:CDCl₃=ca. 1:1 (v/v)). However, as shown in Figure 4, a model calculation indicated that it is impossible to go above ca. 16 % yield at 25 °C (for x>0, y<16). A similar calculation for -55 °C likewise suggested that it is impossible to obtain >90 % yield with a reasonable amount of DMF as long as it is governed by thermodynamics. This is in agreement with our empirical finding from the condition optimization process that the yield was enhanced significantly when the DMF:acrolein ratio is increased from 1:1 to 2:1, but not from 2:1 to 5:1 (Figure 1). Therefore, the approach to increase the equilibrium yield was unfortunately found rather impractical and not pursued further. The only possible method to obtain a high yield of **1** at room temperature would be to shift the reaction mechanism to kinetic control, for example by constantly derivatizing **1** into another compound. However, due to the system complexity, such an idea was left for future investigation.

x eq. of DMF, 6 mmol scale as an example



total volume=(0.64x+2.31)mL

0.64 x: DMF volume based on the density and molecular weight.
 2.31 mL: a total volume of acrolein 6 mmol (0.4 mL), CHCl₃ (1.8 mL) and internal standard SiEt₄ (114 μL).

For 25 °C,

$$K_{eq}(1a, 25C) = \frac{\frac{a}{(0.64x + 2.31)}}{(6x - a - b) \cdot \frac{(6 - a - b)}{(0.64x + 2.31)}} = 0.0110$$

$$K_{eq}(1b, 25C) = \frac{\frac{b}{(0.64x + 2.31)}}{(6x - a - b) \cdot \frac{(6 - a - b)}{(0.64x + 2.31)}} = 0.00934$$

$$\frac{K_{eq}(1a, 25C)}{K_{eq}(1b, 25C)} = \frac{a}{b} = 1.18 \therefore a = 1.18b$$

$$y = \text{Theoretical Yield}[\%] = \frac{a+b}{6} \times 100$$

$$b = 0.0263y, a + b = 0.060y$$

$$\frac{0.0263y(0.64x + 2.31)}{(6x - 0.06y)(6 - 0.06y)} = 0.00934, \therefore x = \frac{0.00167y^2 - 3.18y}{y - 16.7}$$

Likewise for -55 °C,

$$K_{eq}(1a, -55C) = \frac{\frac{a}{(0.64x + 2.31)}}{\frac{(6x - a - b)}{(0.64x + 2.31)} \cdot \frac{(6 - a - b)}{(0.64x + 2.31)}} = 0.586$$

$$K_{eq}(1b, -55C) = \frac{\frac{b}{(0.64x + 2.31)}}{\frac{(6x - a - b)}{(0.64x + 2.31)} \cdot \frac{(6 - a - b)}{(0.64x + 2.31)}} = 0.491$$

$$\frac{K_{eq}(1a, 25C)}{K_{eq}(1b, 25C)} = \frac{a}{b} = 1.19 \therefore a = 1.19b$$

$$y = \text{Theoretical Yield}[\%] = \frac{a + b}{6} \times 100$$

$$b = 0.0274y, a + b = 0.060y$$

$$\frac{0.0274y(0.64x + 2.31)}{(6x - 0.06y)(6 - 0.06y)} = 0.491, \therefore x = \frac{0.00909y^2 - 1.24y}{y - 90.9}$$

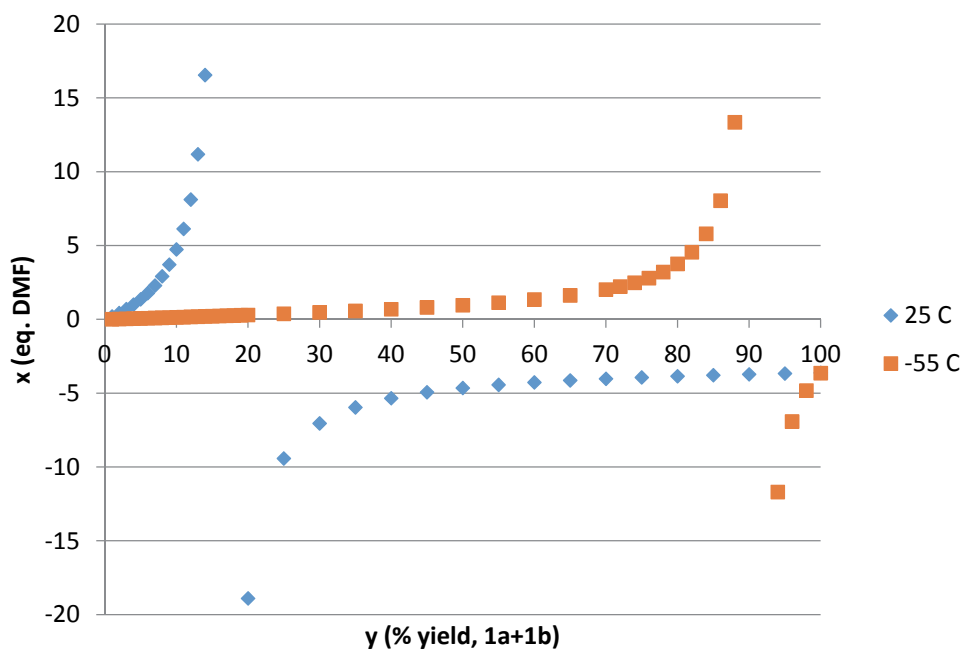


Figure 4 Calculated relationship between the equivalent of DMF and yield.

Retro Diels-Alder Reaction

Although the low temperature required for the Diels-Alder reaction step presented an economical concern for scale-up, given the good yield and product selectivity achieved, we decided to proceed to the downstream conversion of **1** to aromatics (namely, *p*-xylene: Scheme 1, Step 3). While all optimization and thermodynamics studies in the previous sections were carried out using ^1H NMR analysis, we started investigating the isolation of **1**. It was not trivial because **1** was highly subjective to the retro Diels-Alder reaction, as the measured ΔH° and ΔS° values suggest. Most importantly, to retain a good yield of **1**, it was essential to quench the catalyst at low temperature after the completion of the forward Diels-Alder reaction. When $\text{Sc}(\text{OTf})_3$ was unquenched, **1** underwent a retro Diels-Alder reaction extremely rapidly when allowed to warm. In Figure 5, after achieving the equilibrium yield (83 %) at -60°C in the forward $\text{Sc}(\text{OTf})_3$ -catalyzed Diels-Alder reaction, the reaction mixture was as is brought to 0°C (yellow) or 25°C (blue) at time=0 h. The new equilibrium states (20 % yield at 0°C and 8 % yield at 25°C), which were identical to the states obtained from the forward Diels-Alder reaction at those temperatures (see Figure 2), were reached by $\text{Sc}(\text{OTf})_3$ -catalyzed retro Diels-Alder reaction in less than 10 min.

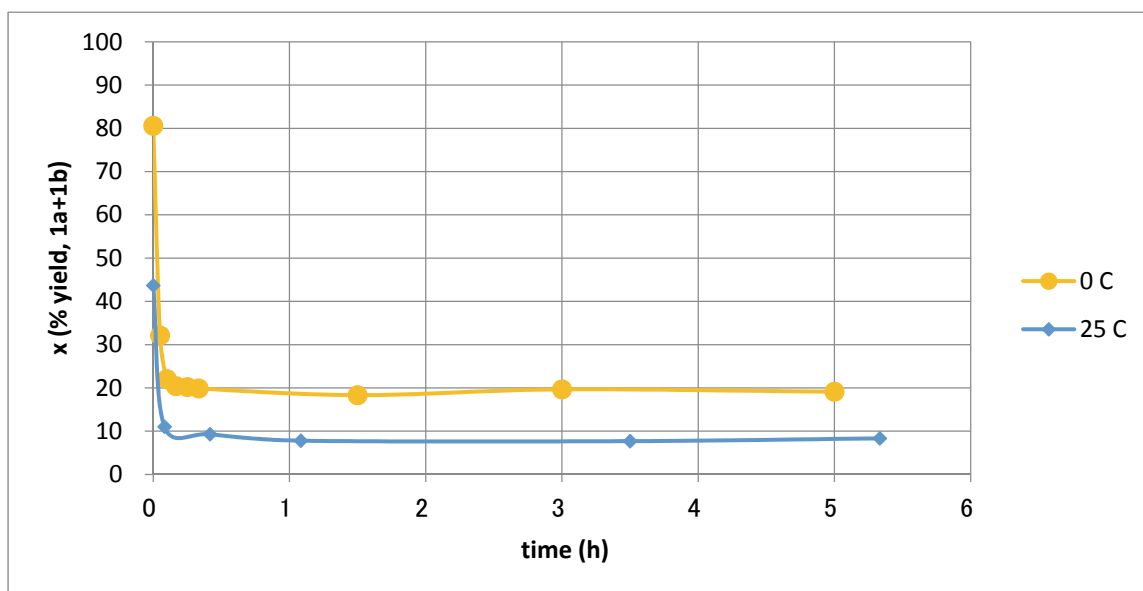
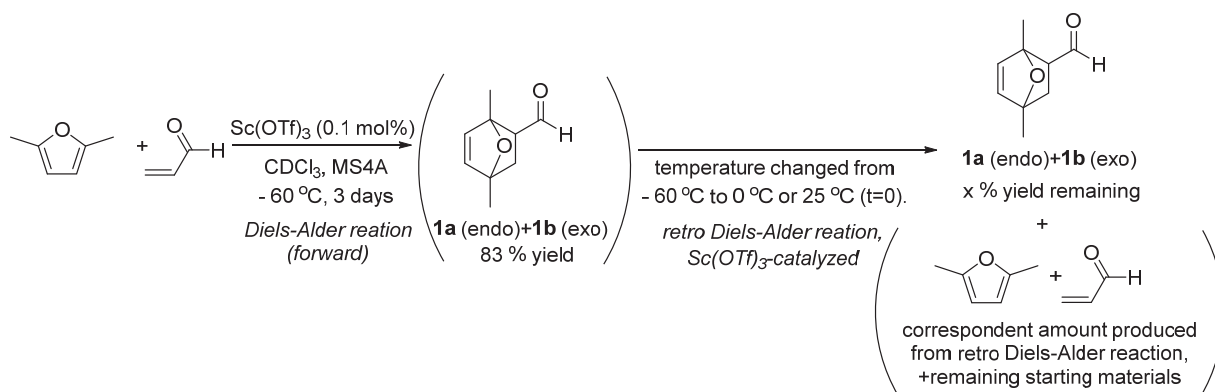


Figure 5 Retro Diels-Alder reaction in the presence of unquenched $\text{Sc}(\text{OTf})_3$ catalyst.

Moreover, at 25 °C, the retro Diels-Alder reaction of **1** was fast even after quenching the catalyst.^[31] This raised a fundamental technical problem because the common isolation/purification techniques could not be applied to **1** at room temperature. As shown in Figure 6, after the catalyst was quenched by 100-fold dilution at – 60 °C (method A, blue), retro Diels-Alder reaction at 25 °C was still very significant, although it was much slower with half-life ($t_{1/2}$) of more than 2 hours (Figure 6, method A) when compared with the unquenched conditions ($t_{1/2}$ <10 min in the presence of 0.1 mol% Sc(OTf)₃, Figure 5). To ascertain that there was no residual Sc(OTf)₃ catalyzing this retro Diels-Alder reaction, another portion of the diluted solution was washed with a weak aqueous base (NaHCO₃ saturated solution) (Figure 6, method B, orange) and then the decay of **1** was monitored by ¹H NMR (25 °C). No significant difference in the half-life was observed between two methods, confirming that the 100-fold dilution was enough to quench the catalyst. The exponential decay of Figure 6 indicated that the retro Diels-Alder reaction was in first-order to [**1**], as logically expected. Therefore, we plotted ln(**1**) (mmol) against time (h) and obtained a linear relationship (Figure 7, quenching method B was used). Different solvents were also examined for dilution in hopes of retarding the retro Diels-Alder reaction by changing the polarity, but only minor effects were observed. The slope of this linear plot represents the rate constant k . Following the equation

$$\ln[1a] = -kt + \ln[1a]_{initial}, \ln[1b] = -kt + \ln[1b]_{initial} \quad (t=\text{time})$$

Because the volume was constant (the same NMR sample was monitored at different time points), the concentration factors of [**1a**] and [**1b**] can be rewritten as

$$\ln(1a, \text{mmol}) = -kt + \text{const.}, \ln(1b, \text{mmol}) = -kt + \text{const.} \quad (t=\text{time})$$

Using the k values, based on the Eyring equation (k_B =Boltzman constant, h =Plank constant, T =temperature)

$$k = \frac{k_B T}{h} \exp\left(-\frac{\Delta G^\ddagger}{RT}\right)$$

as well as the half-life definition

$$t_{1/2} = \frac{\ln 2}{k} = \frac{0.693}{k}$$

Gibbs free energy of activation (ΔG^\ddagger) and half-life ($t_{1/2}$) for this thermal retro Diels-Alder reaction at 25 °C were experimentally determined as in Table 3. Combining the ΔG^\ddagger value with ΔH° and ΔS° values determined in the previous section, the experimentally determined energy diagram for the thermal Diels-Alder reaction of DMF and acrolein is shown in Figure 8.

The ΔG^\ddagger values provided ample information. In particular, they suggested that thermal retro Diels-Alder reaction of **1**, which was problematic at 25 °C, could be prevented at ≤ 0 °C. Based on the general expression $\Delta G^\ddagger = \Delta H^\ddagger - T\Delta S^\ddagger$, because ΔS^\ddagger is positive for retro Diels-Alder reaction, ΔG^\ddagger value increases as the temperature decreases. When $\Delta G^\ddagger_{25\text{C}}$ values in Table 3 were used, the half-lives ($t_{1/2}$) for **1a** and **1b** at 0 °C in chloroform were calculated to be 85 h and 95 h, respectively. Because the actual $t_{1/2}$ at 0 °C must be longer than these values given $\Delta G^\ddagger_{0\text{C}} > \Delta G^\ddagger_{25\text{C}}$, it suggested that **1** was stable toward a retro Diels-Alder reaction at ≤ 0 °C in the laboratory time scale. Indeed, when the solution of **1** was monitored by ¹H NMR at 0 °C after catalyst quench (i.e.

in the experiment shown in Figure 6, temperature was brought to 0 °C and monitored by ¹H NMR at 0 °C instead of 25 °C), essentially no reaction was observed over a period of 10 h in CDCl₃, CD₂Cl₂, CD₃CN, or toluene-d₈. Therefore, this kinetic study of the retro Diels-Alder reaction overall told us that in order to isolate the maximum yield of **1**, it is necessary to a) after conducting the Lewis acid-catalyzed Diels-Alder reaction at low temperature, quench the catalyst at the same low temperature avoiding warming as much as possible, and b) handle **1** at ≤ 0 °C, not at room temperature.

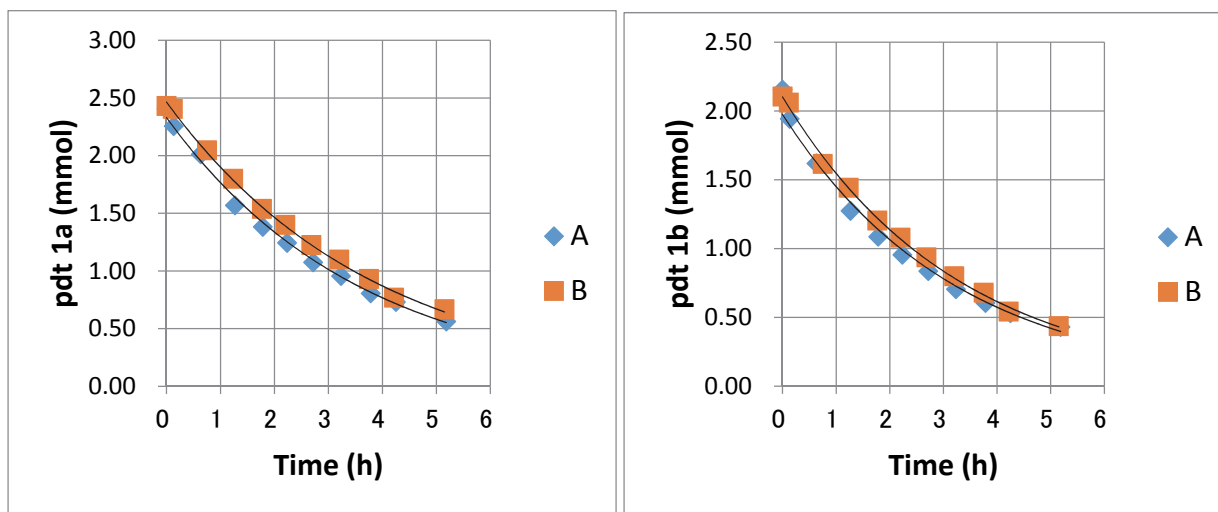
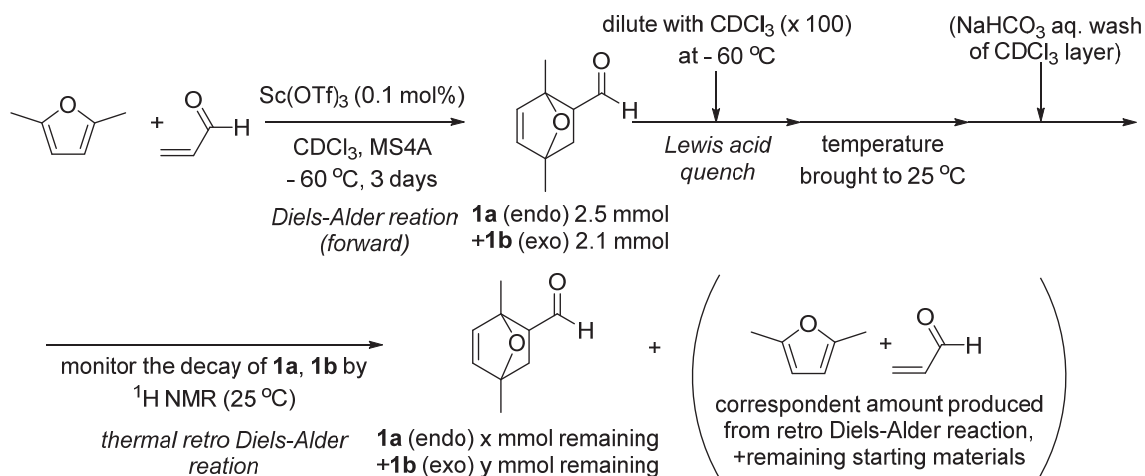
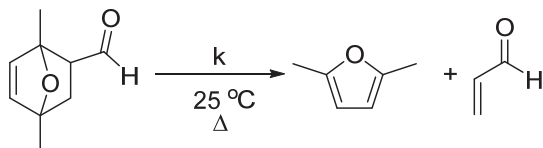


Figure 6 Retro Diels-Alder reaction at 25 °C after quenching Sc(OTf)₃ catalyst. (Quenching method A (blue): aliquot of reaction mixture was diluted with CDCl₃ (×100) at -60 °C. Quenching method B (orange): aliquot of reaction mixture was diluted with CDCl₃ (×100) at -60 °C, and further washed with sat. NaHCO₃ aq. for aqueous basic quench.)



1a (endo), 1b (exo)

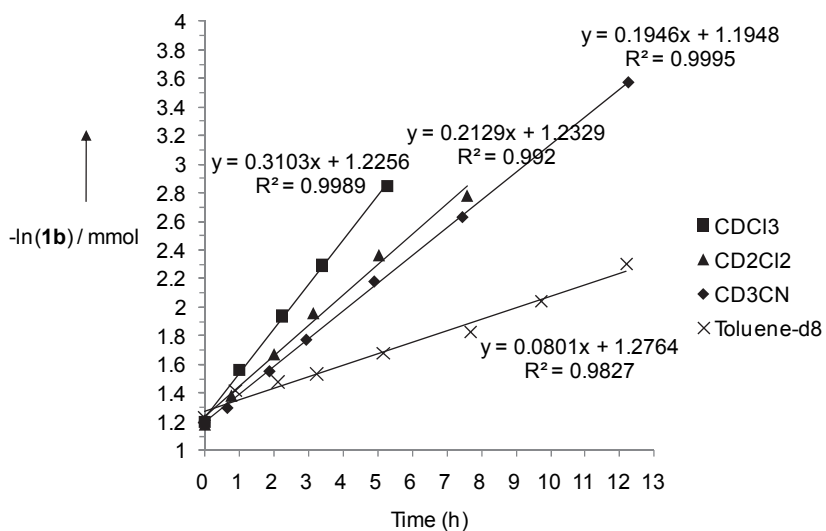
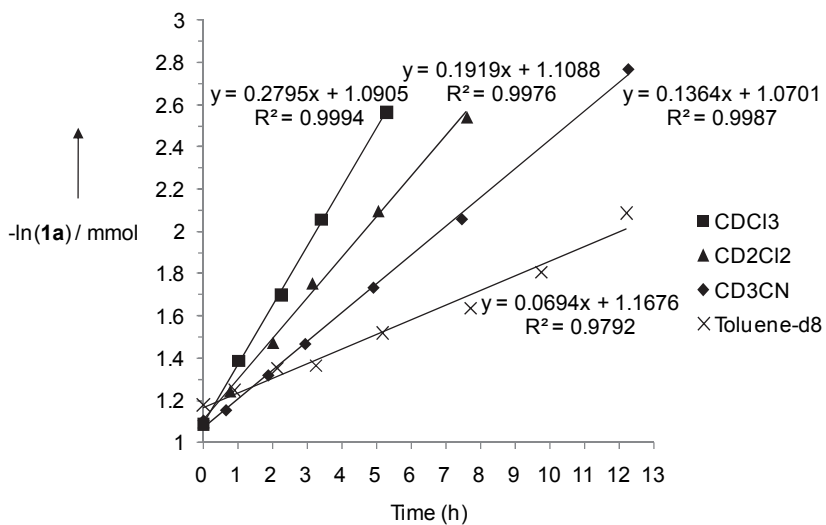


Figure 7 Kinetics of thermal retro Diels-Alder reaction at 25 °C.

Table 3 Thermal retro Diels-Alder reaction at 25 °C.

Solvent	1a (endo)			1b (exo)		
	k [h ⁻¹]	ΔG [‡] [kcal/mol]	t _{1/2} [h]	k [h ⁻¹]	ΔG [‡] [kcal/mol]	t _{1/2} [h]
CDCl ₃	0.2795	23.04	2.48	0.3103	22.98	2.23
CD ₂ Cl ₂	0.1919	23.27	3.61	0.2129	23.21	3.26
CD ₃ CN	0.1364	23.47	5.08	0.1946	23.26	3.56
Toluene-d ₈	0.0594	23.87	9.99	0.0801	23.78	8.65

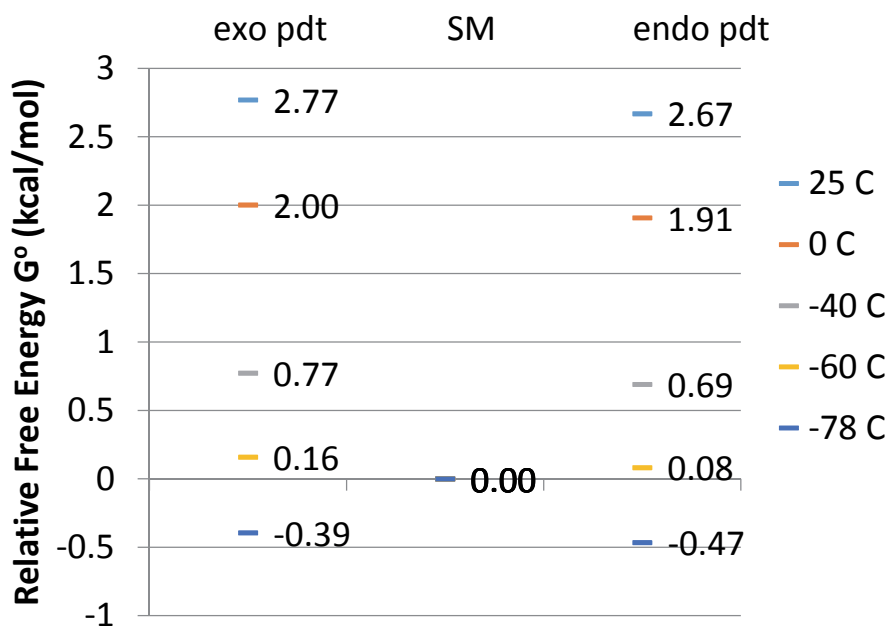
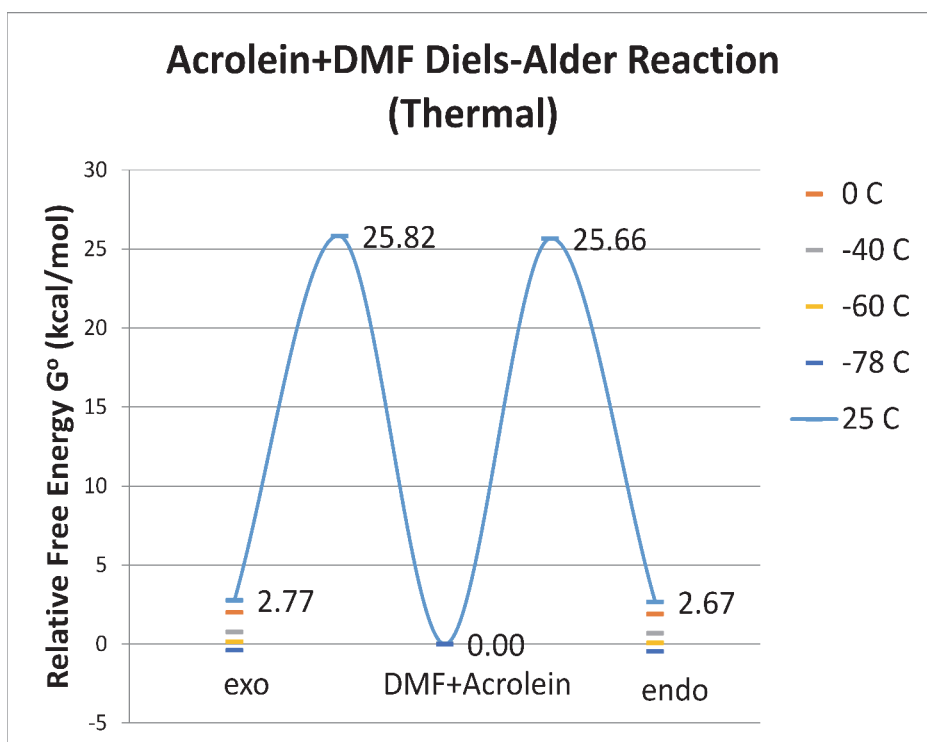
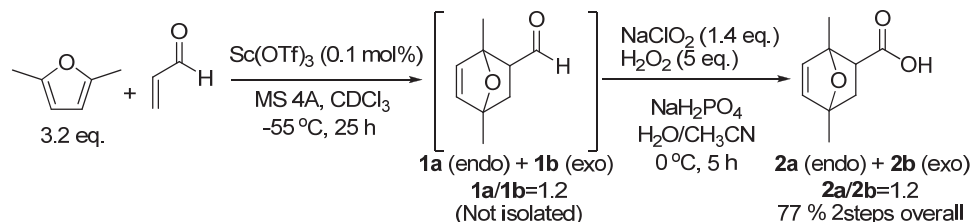


Figure 8 Energy diagram for the thermal Diels-Alder reaction of DMF and acrolein (top) and a close-up of the starting material/product thermodynamics (bottom) in chloroform.

Conversion of Compound 1 to *p*-Xylene

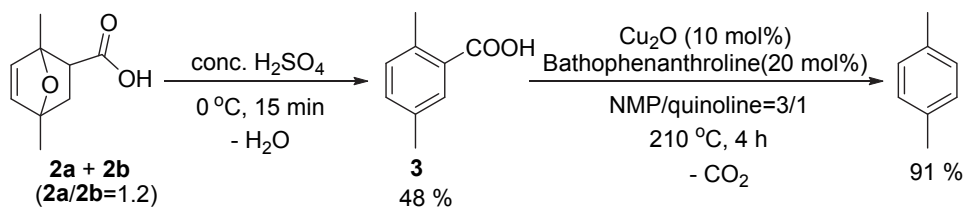
Based on the knowledge garnered from the mechanistic investigation, the best approach to isolate the Diels-Alder product **1** appeared to be a three-step sequence consisting of a Diels-Alder reaction at -60 to -55 °C, quenching the catalyst at the same low temperature, and derivatization of **1** to a more stable compound at ≤ 0 °C. Regarding the derivatization methods, initially we investigated two approaches to straightforwardly advance toward the desired end-product *p*-xylene: a) Rh-catalyzed decarbonylation,^[19] and b) base or acid-catalyzed aromatization of **1** to **2**, 5-dimethyl-benzaldehyde. However, in our hands these reactions were not directly applicable to **1** because **1** was subject to rapid retro Diels-Alder reaction and decomposition upon any harsh treatment. Therefore, we sought to first derivatize **1** to a more stable compound under mild conditions. The oxidation of aldehyde **1** to the carboxylic acid **2** appeared to be suitable for this purpose. In particular, we chose Pinnick oxidation using H₂O₂ as a mild, green and economical oxidant^[32] and successfully devised an operationally straightforward, one-pot Diels-Alder/Pinnick oxidation protocol (Scheme 3).^[33] After confirming ca. 75 % conversion of acrolein to **1** by ¹H NMR, the catalyst was quenched by adding an aq. NaH₂PO₄/CH₃CN mixture at -55 °C. The reaction mixture was allowed to warm to 0 °C, and H₂O₂ and NaClO₂ were added. The oxidation was complete in 5 hours, giving **2** in good yield (near-quantitative yield for oxidation step, 77 % from DMF and acrolein). Notably, the excess reagents and byproducts are all removed by simple aqueous workup and evaporation under reduced pressure, leaving **2** in nearly pure form without further purification. Carboxylic acid **2** was much less prone to a retro Diels-Alder reaction than **1** and could be stored for a few hours at RT and for several months at -20 °C.^[34]



Scheme 3 One-pot Diels-Alder/Pinnick oxidation sequence.

With isolated **2** in hand, we studied its conversion to *p*-xylene. Although **2** was much more stable than **1**, it still underwent decomposition when heated. Because decarboxylation generally required high temperature conditions,^[20] we needed to proceed in the order of aromatization followed by decarboxylation. The reported dehydrative aromatization reactions of similar 7-oxabicyclo[2,2,1]hept-2-ene structures mostly used strongly acidic conditions.^[35] Among the various acids tested, the highest yield (48 %) of 2,5-dimethyl benzoic acid (**3**) was obtained when we treated the crude **2a/2b** mixture with conc. H₂SO₄ (Scheme 4, first step). Base-catalyzed dehydration using KHMDS or other reagents^[36] was unsuccessful, presumably due to the unprotected COOH group. Direct pyrolysis^[37] also led only to decomposition. We are currently seeking a more efficient aromatization method. The Cu₂O-catalyzed protodecarboxylation of aromatic carboxylic acids has been reported by Gooßen et al.^[20] When **3** was subjected to this system, *p*-xylene was obtained in 91 % yield without optimization (Scheme 4, second step). Combined with the two steps described in Scheme 3, this route from DMF and

acrolein to *p*-xylene gave 34 % overall yield over four steps, thereby realizing the concept of biomass-derived PET synthesis (Scheme 1).



Scheme 4 Conversion of 2 to *p*-xylene.

Conclusion

In conclusion, we have developed a route to convert DMF and acrolein into *p*-xylene for bio-renewable PET production, with an aim to produce a renewable biomass-derived drop-in replacement for currently fossil fuel-derived commodity chemicals. One particular feature of our strategy is that both raw materials (DMF, acrolein) are derived from waste products (HMF, glycerol) of biofuel production. Our scheme consists of a Diels-Alder reaction, oxidation, dehydrative aromatization and decarboxylation. It was designed to achieve high atom-economy and avoid toxic by-products. Unfortunately, the immediate practicality of the process shown in this study is limited due to the low temperature conditions in the Diels-Alder reaction step and the moderate yield in the aromatization step. However, the detailed thermodynamic and kinetic studies of the pivotal Diels-Alder reaction step provided ample information about the mechanistic nature of this reaction, and the data obtained in this work would contribute to the development of other analogous reactions. We believe our solely bio-renewable *p*-xylene synthesis, 34 % overall yield over 4 steps, serves as a valuable demonstration of sustainable chemistry in the field of biomass utilization.

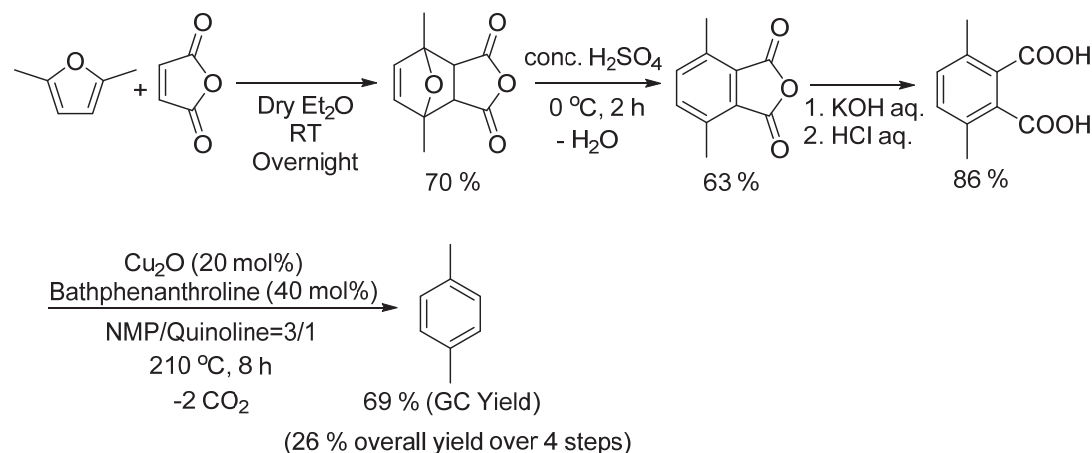
Experimental

1. General

Commercial materials and solvents were reagent grade and used as received. ^1H , ^{13}C NMR spectra were recorded with Bruker AVB-400, AVQ-400, DRX-500, and AV-600 spectrometers; chemical shifts are reported in ppm. HRMS data were obtained *via* the Micro-Mass/Analytical Facility operated by the College of Chemistry, University of California, Berkeley. LCMS analysis was carried out using a Agilent 1200 series liquid chromatograph coupled to Thermo LTQ XL ion trap mass spectrometer. GC analysis was carried out using a Varian CP-3800 gas chromatograph equipped with a flame ionization detector coupled to a Varian 320-MS mass spectrometer using a FectoFour capillary column (VF-5 ms, 30 m length, 0.25 mm diameter) coated with a 0.25 mm thick stationary phase (5% phenyl and 95% dimethylpolysiloxane). Thin-layer chromatography (TLC) analysis was performed using Merck silica gel 60 F254 TLC plates, and visualized by staining with phosphomolybdic acid or bromocresol green. Flash column chromatography was carried out on Merck 60 silica gel (32–63 μm).

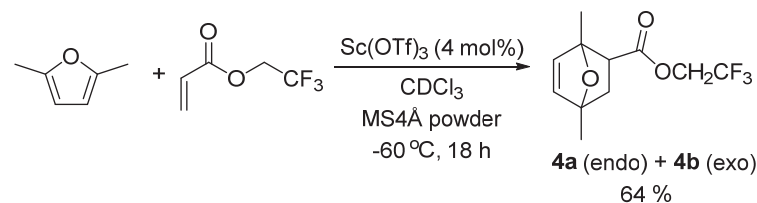
2. Conversion of DMF and maleic anhydride to *p*-xylene

The first 3 steps were conducted according to the literature procedures and the yields reasonably matched the reported values.^[35a, 38] The 4th step, copper-catalyzed protodecarboxylation of 3,6-dimethylphthalic acid, followed the procedure used for 2,5-dimethylbenzoic acid (**3**) based on the report by Gooßen et al.^[20] See Experimental Section 4-g).



3. Conversion of DMF and 2,2,2-trifluoroethyl acrylate to *p*-xylene.

a) Diels-Alder reaction of DMF and 2,2,2-trifluoroethyl acrylate.



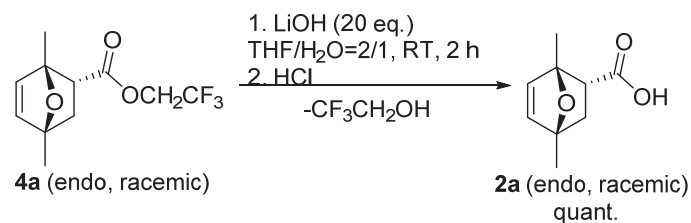
A flame-dried 50 mL flask was charged with Sc(OTf)₃ (196 mg, 0.398 mmol), activated powdered 4Å molecular sieves (250 mg) and a magnetic stir bar. The flask was purged with nitrogen by vacuum/N₂ cycles (4 times). CHCl₃ (1.5 mL) was added and the mixture was cooled to -60 °C. DMF (961 mg, 10.0 mmol) and 2,2,2-trifluoroethyl acrylate (1.54 g, 10.0 mmol) were added and the mixture was stirred at the same temperature for 20 h. Water (5 mL) was added and the reaction mixture was kept in contact with the frozen layer for 10 min at -60 °C, then allowed to warm to RT. The mixture was extracted with CHCl₃ (3 × 60 mL) and the combined organic phase was washed with brine (60 mL), dried over Na₂SO₄, filtered, and concentrated *in vacuo*. 1,4-dimethyl-7-oxa-bicyclo[2.2.1]hept-5-ene-2-carboxylic acid 2,2,2-trifluoroethyl ester (**4**) was obtained as a mixture of diastereomers (2.61 g, **4a**(endo)/**4b**(exo)=6.1). Diastereoselectivity (endo-exo ratio) was determined by ¹H NMR analysis : δ3.00 (dd, *J*= 9.0, 3.9 Hz, 1 H, **4a**, endo major), 2.65 (dd, *J*=7.8, 4.2 Hz, 1 H, **4b**, exo minor). The residue was purified by flash column chromatography on silica gel (CH₂Cl₂ 100 %) to give **4a** (colorless oil, 1.21 g, 4.84 mmol, 48 %) as the first to elute (TLC: R_f=0.35, 100 % CH₂Cl₂) and **4b** (colorless oil, 84.2 mg, 0.337 mmol, 3 %) as the second to elute (TLC: R_f=0.25, 100 % CH₂Cl₂). 328 mg (1.31 mmol, 13 %) of **4a/4b** mixture (colorless oil, **4a/4b**=0.96) was also collected between those fractions.

Following the same procedure, when HfCl₄ and ZrCl₄ (4 mol%) were used instead of Sc(OTf)₃, similar yields were obtained with somewhat lower diastereoselectivity (**4a/4b**=4.3 and 4.7 in crude mixture, respectively).

4a: ¹H NMR and ¹³C NMR spectra of **4a** were correspondent to those reported in the literature.^[39] ¹H NMR (300 MHz, CDCl₃) δ 6.27(d, *J*= 5.7 Hz), 1 H), 6.04(d, *J*= 5.7 Hz, 1 H), 4.56(dq, *J*= 12.6, 8.4 Hz, 1 H), 4.31(dq, *J*= 12.6, 8.4 Hz, 1 H), 3.00 (dd, *J*= 9.0, 3.9 Hz, 1 H), 2.01(dd, *J*= 11.7, 9.0 Hz, 1 H), 1.86(dd, *J*= 11.7, 3.9 Hz, 1 H), 1.74(s, 3 H), 1.60(s, 3 H); ¹³C NMR(125 MHz, CDCl₃) δ 170.7, 140.6, 136.0, 122.8(q, 1C, *J*= 277 Hz), 87.4, 86.2, 60.1(q, 1C, *J*= 37 Hz), 50.9, 38.2, 18.6, 18.5.

4b: ¹H NMR (600 MHz, CDCl₃) δ 6.24(d, *J*= 5.4 Hz, 1 H), 6.16(d, *J*= 5.4 Hz, 1 H), 4.60(dq, *J*= 12.6, 8.4 Hz, 1 H), 4.41(dq, *J*= 12.6, 8.4 Hz, 1 H), 2.65 (dd, *J*=7.8, 4.2 Hz, 1 H), 2.03(dd, *J*= 11.4, 4.2 Hz, 1 H), 1.75(dd, *J*= 11.4, 7.8 Hz, 1 H), 1.66(s, 3 H), 1.55(s, 3 H); ¹³C NMR(150 MHz, CDCl₃) δ 172.0, 140.9, 138.8, 123.0(q, 1C, *J*= 277 Hz), 88.2, 85.9, 60.3(q, 1C, *J*= 36 Hz), 49.3, 38.7, 18.3, 16.2. HRMS (ESI) calc for [C₁₁H₁₃O₃F₃²³Na]⁺: *m/z* 273.0709, found 273.0709.

b) Hydrolysis of **4a** to **2a**.



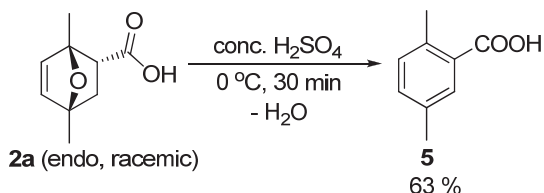
To a solution of LiOH (954 mg, 40.0 mmol) in THF (3.2 mL) and H₂O (1.6 mL), **4a** (505 mg, 2.02 mmol) was added and stirred at RT for 2 h. The mixture was washed with Et₂O (30 mL),

then the aqueous layer was acidified with 1 N HCl aq. to pH=2 and extracted with EtOAc (3 × 40 mL). The combined EtOAc layers were dried over Na₂SO₄, filtered, and concentrated *in vacuo*. 1,4-dimethyl-7-oxabicyclo[2.2.1]hept-5-ene-2-carboxylic acid (endo) **2a** was obtained as white powder (339 mg, 2.02 mmol, >99 %).

2a: ¹H NMR (500 MHz, CDCl₃) δ 10-12.5 (br, 1H), 6.30(d, *J*= 5.5 Hz), 1 H), 6.16(d, *J*= 5.5 Hz, 1 H), 2.99 (dd, *J*= 9.5, 3.5 Hz, 1 H), 2.03(dd, *J*=11.5, 9.5 Hz, 1 H), 1.86(dd, *J*=11.5, 3.5 Hz, 1 H), 1.79(s, 3 H), 1.63(s, 3 H); ¹³C NMR(125 MHz, CDCl₃) δ 178.5, 140.4, 136.3, 87.3, 86.2, 51.1, 38.1, 18.7, 18.5. HRMS (ESI) calc for [C₉H₁₁O₃]⁻: *m/z* 167.0714, found 167.0714.

When **4a/4b** mixture was subjected to the same conditions, **2a/2b** mixture was obtained with the retention of diastereomeric ratio. Diastereoselectivity (endo-exo ratio) was determined by ¹H NMR analysis using the peaks at δ3.00 (dd, *J*= 9.0, 3.5 Hz, 1 H, **2a**, endo), 2.62 (dd, *J*=8.0, 3.5 Hz, 1 H, **2b**, exo). LCMS found two peaks for [C₉H₁₁O₃]⁻ (endo and exo): *m/z* calc. 167.1, found 167.1.

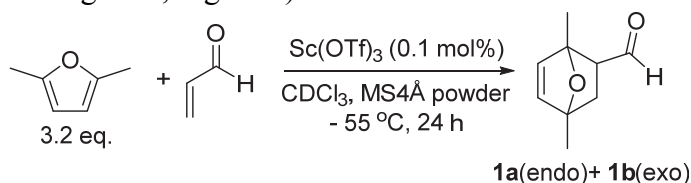
c) Aromatization of **2a** to 2,5-dimethylbenzoic acid (**5**).



To conc. H₂SO₄ (1 mL), **2a** (76.4 mg, 0.454 mmol) was added at 0 °C. The resultant thick brown mixture was stirred at the same temperature for 30 min, then poured onto ice. 10 N KOH was added to basify the mixture to pH=12, and aqueous layer was washed with Et₂O (3 × 50 mL). The aqueous layer was then acidified to pH=2 with 5N HCl and extracted with EtOAc (3 × 50 mL). The combined EtOAc layers were washed with brine (50 mL), dried over Na₂SO₄, filtered, and concentrated *in vacuo* to yield **5** (42.7 mg, 0.284 mmol, 63 %). The ¹H and ¹³C NMR spectra of **5** corresponded to those of an authentic sample.

4. Conversion of DMF and acrolein to *p*-xylene.

a) A representative procedure for Diels-Alder reaction of DMF and acrolein (Table 1, Table 2, Figure 1, Figure 2).

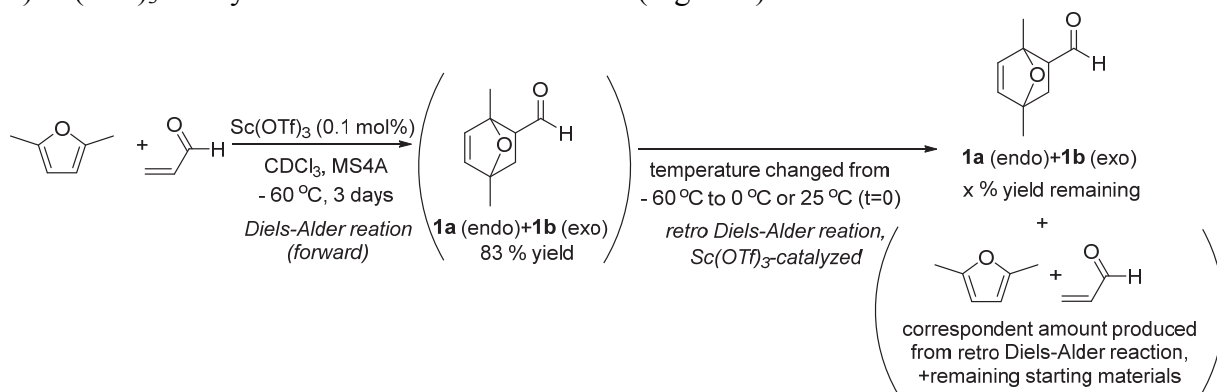


A 20 mL vial fitted with a PTFE septum screw cap was charged with a magnetic stirbar, Sc(OTf)₃ (3.0 mg, 0.0060 mmol) and activated molecular sieves 4Å powder (300 mg) and purged with nitrogen by vacuum/N₂ cycle (4 times). Tetraethylsilane (115 μL, 90.9 mg, 0.630 mmol) and CDCl₃ (1.8 mL) were added and the mixture was cooled to -55 °C. DMF (1.93 mL, 19.0 mmol) and acrolein (400 μL, 5.90 mmol) were subsequently added over a few minutes. The initial reaction mixture was analyzed to determine the amount of DMF and acrolein originally present in the system, before Diels-Alder reaction proceeded to the significant extent. After

stirring at $-55\text{ }^{\circ}\text{C}$ for 24 h, 75 % ^1H NMR yield (against SiEt_4 internal standard) of **1** (**1a**=2.4 mmol, **1b**=2.0 mmol, **1a/1b**=1.2) was obtained (remaining DMF=13 mmol, acrolein=1.4 mmol).

Sampling/yield determination procedure (catalyst quench by simple dilution): A small aliquot (ca. 10 μL) of the reaction mixture was taken by syringe and immediately diluted in CDCl_3 (ca. 1.0 mL) pre-cooled to $-55\text{ }^{\circ}\text{C}$. The sample was quickly filtered through a Pasteur pipette filled with Na_2SO_4 to a NMR tube and ^1H NMR spectrum was corrected at RT. Thus prepared NMR sample was kept frozen at $-78\text{ }^{\circ}\text{C}$ (acetone/dry ice bath) when immediate ^1H NMR analysis was not possible. The yield and conversion were determined using the peak of tetraethylsilane as an internal standard. The peaks used for yield/conversion calculation were as follows: tetraethylsilane δ 0.51 (q, $J=8.0$ Hz, 8H), DMF δ 5.86 (s, 2H), acrolein δ 6.52 (dd, $J=9.5, 1.0$ Hz, 1H) or 9.59 (d, 7.2 Hz, 1H), **1a** δ 6.12 (d, $J=5.6$ Hz, 2H) or 9.36 (d, $J=3.2$ Hz, 1H), **1b** δ 6.16 (d, $J=5.6$ Hz, 2H) or 9.55 (d, $J=5.6$ Hz, 1H). Relative stereochemistry of **1a** and **1b** were determined using δ 2.84-2.88 (m, 1H) and δ 2.39-2.34 (m, 1H). Because the exo-hydrogen of **2a**, **4a** has a more downfield resonance than the endo-hydrogen of **2b**, **4b**, analogously the former was assigned as **1a** (endo, major) and the latter was assigned as **1b** (exo, minor).

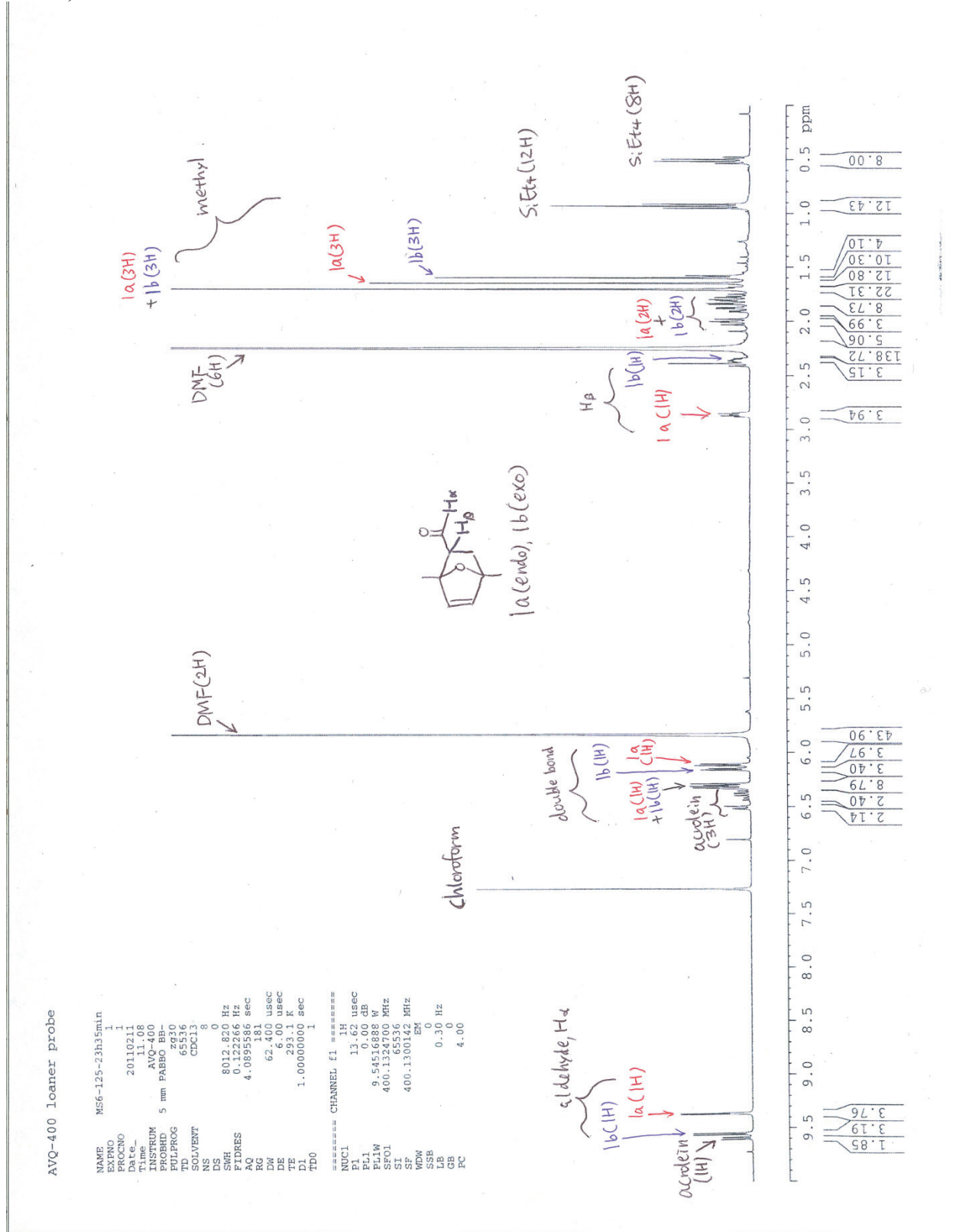
b) $\text{Sc}(\text{OTf})_3$ -catalyzed retro Diels-Alder reaction (Figure 5).



Diels-Alder reaction was conducted following the procedure described in 4-a). A 20 mL vial fitted with a PTFE septum screw cap was charged with a magnetic stirbar, $\text{Sc}(\text{OTf})_3$ (3.0 mg, 0.0060 mmol) and activated molecular sieves 4 \AA powder (298 mg) and purged with nitrogen by vacuum/ N_2 cycle (4 times). Tetraethylsilane (114 μL , 90.2 mg, 0.625 mmol) and CDCl_3 (1.8 mL) were added and the mixture was cooled to $-60\text{ }^{\circ}\text{C}$. DMF (1.96 mL, 17.6 mmol) and acrolein (400 μL , 5.40 mmol) were subsequently added over a few minutes. After stirring at $-60\text{ }^{\circ}\text{C}$ for 24 h, 83 % ^1H NMR yield (against SiEt_4 internal standard) of **1** (**1a**=2.5 mmol, **1b**=2.0 mmol, **1a/1b**=1.2) was obtained (remaining DMF=13 mmol, acrolein=0.87 mmol).

The retro Diels-Alder reaction in the presence of $\text{Sc}(\text{OTf})_3$ was monitored as follows: A portion (0.5 mL) of the reaction mixture above (containing **1a** 2.5 mmol and **1b** 2.0 mmol, kept at $-60\text{ }^{\circ}\text{C}$) was drawn and quickly transferred to another vial at $25\text{ }^{\circ}\text{C}$ and left at this temperature with stirring. After a given time (10 min to 6 h), an aliquot (10 μL) was taken from this warmed mixture and diluted with CDCl_3 (1 mL, $25\text{ }^{\circ}\text{C}$) and immediately analyzed by ^1H NMR to calculate the remaining amount of **1a** and **1b** (x , %yield) against SiEt_4 internal standard. The plot of Figure 5 ($25\text{ }^{\circ}\text{C}$) was thus obtained. For retro Diels-Alder reaction at $0\text{ }^{\circ}\text{C}$, similarly, another portion (0.5 mL) of the same reaction mixture (containing **1a** 2.5 mmol and **1b** 2.0 mmol, kept at

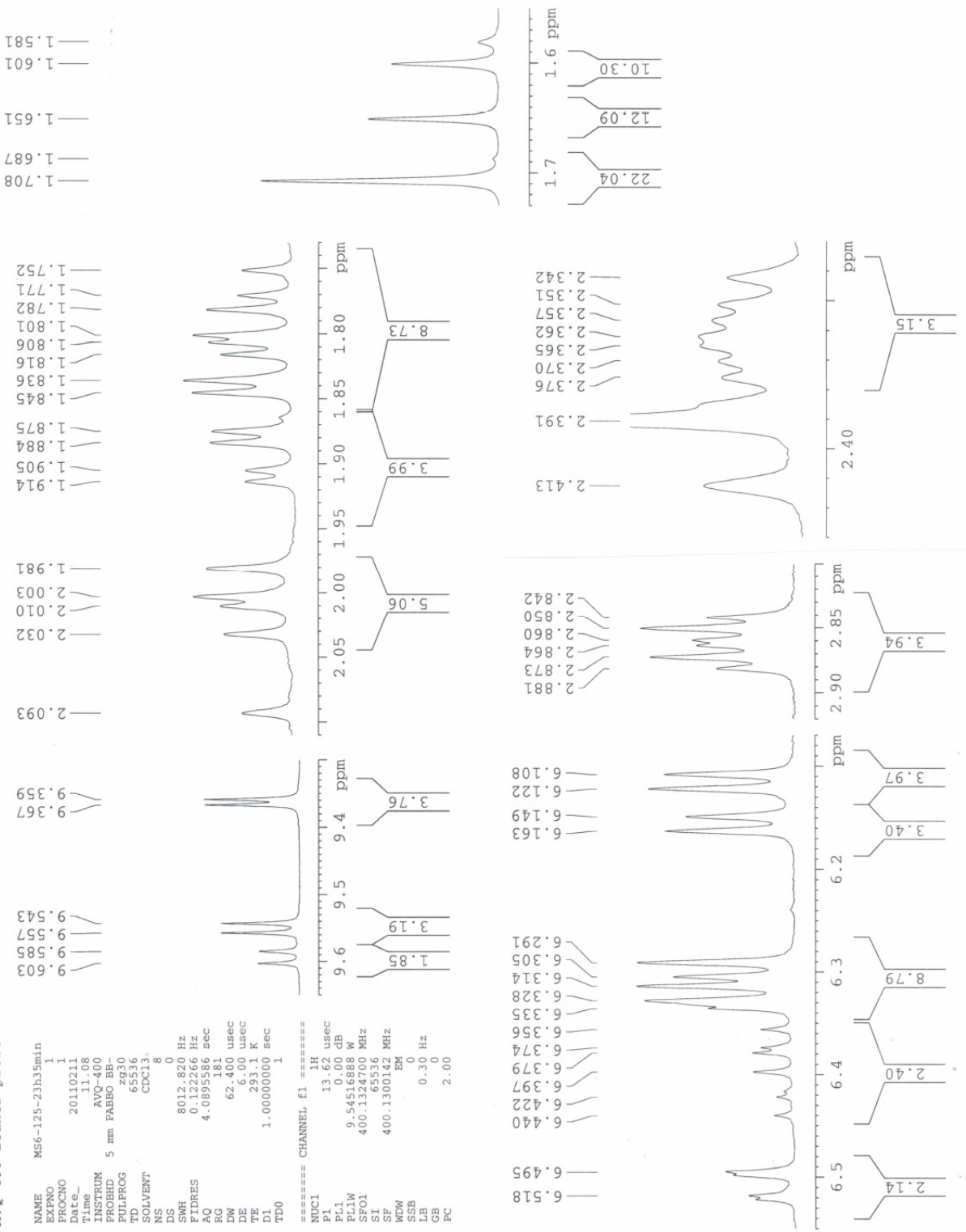
d) Representative ^1H NMR spectra of crude reaction mixture (DMF, acrolein, **1a**, **1b**, SiEt_4 in CDCl_3).



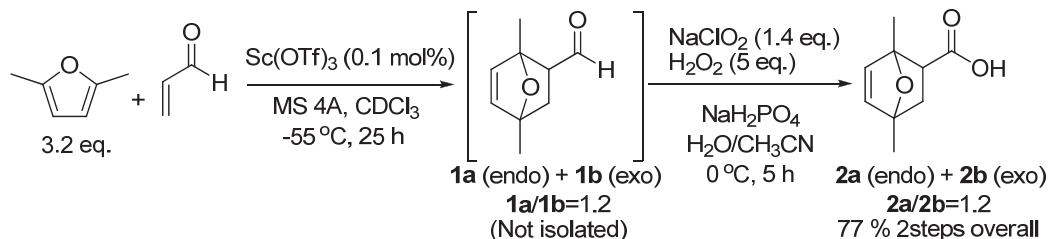
AVQ-400 loaner probe

```

NAME MS6-125-23h35min
EXPNO 1
PROCNO 1
Date_ 20110211
Time_ 11.08
INSTRUM AVQ-400
PROBHD 5 mm PABBO BB-
PULPROG zg30
TD 65536
SOLVENT CDCl3
NS 0
DS 0
SWH 8012.820 Hz
FIDRES 0.122266 Hz
AQ 4.0895586 sec
RG 181
DW 62.400 usec
DE 6.00 usec
TE 293.1 K
D1 1.00000000 sec
TDO 1
===== CHANNEL f1 =====
NUC1 1H
P1 13.62 usec
PL1 0.00 dB
PL1W 9.54516888 W
SFO1 400.1324700 MHz
SI 65536
SF 400.1300142 MHz
WDW EM
SSB 0
LB 0.30 Hz
GB 0
PC 2.00
  
```

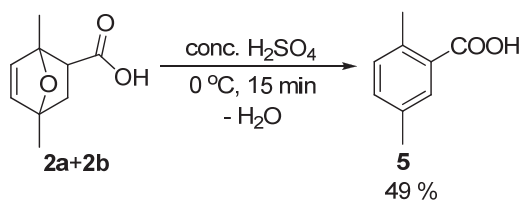


e) One-pot Pinnick oxidation of **1** to **2**



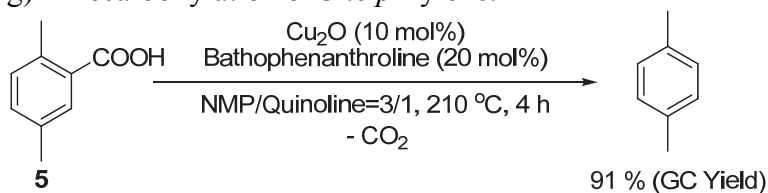
Following the procedure described in 4-a), a Diels-Alder reaction of DMF and acrolein was conducted in a septum-capped 100 mL flask in 14.3 mmol scale ($-55\text{ }^{\circ}\text{C}$). After 25 h, a mixture of CH₃CN (14 mL), NaH₂PO₄•H₂O (1.11 g, 8.00 mmol) and H₂O (6 mL) pre-cooled to $0\text{ }^{\circ}\text{C}$ was slowly added to this mixture at $-55\text{ }^{\circ}\text{C}$. The mixture became frozen and it was kept at $-55\text{ }^{\circ}\text{C}$ for 10 min, then 34 % H₂O₂ aq. (7.0 mL, 70 mmol, pre-cooled to $0\text{ }^{\circ}\text{C}$) was added. The mixture was allowed to warm to $0\text{ }^{\circ}\text{C}$, and 80 % NaClO₂ (1.77 g, 20.0 mmol) in H₂O (20 mL, pre-cooled to $0\text{ }^{\circ}\text{C}$) was added in small portions over 3 h. The reaction progress was monitored by ¹H NMR (sampling procedure is described in 4-a)) and TLC. Upon complete consumption of **1** in additional 5 h, the molecular sieves were filtered off and organic solvents were removed *in vacuo* without heating. The mixture was extracted with CH₂Cl₂ (3 × 40 mL), dried over MgSO₄, filtered, and concentrated *in vacuo* (crude 1). The aqueous layer was then acidified with 0.1 N HCl aq. to pH=3 and extracted with CH₂Cl₂ (3 × 40 mL), dried over MgSO₄, filtered, and concentrated *in vacuo* (crude 2). Both crude products gave sufficiently pure **2a/2b** mixture. Diastereoselectivity (endo-exo ratio) was determined by ¹H NMR analysis: δ3.00 (dd, J= 9.0, 3.5 Hz, 1 H, **2a**, endo major), 2.62 (dd, J=8.0, 3.5 Hz, 1 H, **2b**, exo minor). Crude 1: thick pale-yellow oil, 1.62 g (9.70 mmol, **2a/2b**=1.2), crude 2: thick colorless oil, 0.238 g (1.40 mmol, **2a/2b**=1.5), Overall: 1.86 g (11.1 mmol, **2a/2b**=1.2), 77 % yield over 2 steps from DMF and acrolein. LCMS found two peaks for [C₉H₁₁O₃]⁻ (endo and exo): *m/z* calc. 167.1, found 167.1. Retention times matched with those obtained from a Diels-Alder reaction of DMF and 2,2,2-trifluoroethyl acrylate followed by hydrolysis (see 3-b)).

f) Aromatization of **2** to 2,5-dimethylbenzoic acid (**5**).



Aromatization of **2a/2b** mixture in conc. H₂SO₄ was conducted following the procedure described in 3-c).

g) Decarboxylation of **5** to *p*-xylene.



Decarboxylation of 2,5-dimethylbenzoic acid (**5**) was conducted following the procedure reported by Goßen et al.^[20] as follows: **5** (authentic material, 300 mg, 2.00 mmol), Cu_2O (28.9 mg, 0.200 mmol), bathophenanthroline (133 mg, 0.400 mmol), degassed solvents (NMP 3.0 mL/quinoline 1.0 mL) and a stirring bar were added to a stainless steel pressure vessel. The vessel was purged with N_2 and the mixture was stirred at 210 °C for 4 h. After cooling to RT, the mixture was transferred to a flask, and the vessel was washed with Et_2O and combined. The resultant organic phase was washed with 5 N HCl aq (3×20 mL) and brine (20 mL), then dried over Na_2SO_4 . Tetraethylsilane (66.4 mg, 0.460 mmol) was added as a GC internal standard, thoroughly mixed and the aliquot of sample was diluted with Et_2O and analyzed by GC. The retention time and GC-MS spectra of the product matched with those of an authentic sample. Yield of *p*-xylene calculated by GC-FID using a separately prepared calibration curve : 91 %.

References and Notes

- [1] R. Rinaldi, F. Schüth, *ChemSusChem* **2009**, *2*, 1096-1107.
- [2] Q. Xiang, Y. Lee, R. Torget, *Appl. Biochem. Biotechnol.* **2004**, *115*, 1127-1138.
- [3] a) G. W. Huber, S. Iborra, A. Corma, *Chem. Rev.* **2006**, *106*, 4044-4098; b) J. N. Chheda, Y. Román-Leshkov, J. A. Dumesic, *Green Chem.* **2007**, *9*, 342-350.
- [4] a) J. B. Binder, R. T. Raines, *J. Am. Chem. Soc.* **2009**, *131*, 1979-1985; b) C. Li, Z. Zhang, Z. K. Zhao, *Tetrahedron Lett.* **2009**, *50*, 5403-5405; c) R.-J. van Putten, J. C. van der Waal, E. de Jong, C. B. Rasrendra, H. J. Heeres, J. G. de Vries, *Chem. Rev.* **2013**, *113*, 1499-1597.
- [5] a) P. Verdeguer, N. Merat, A. Gaset, *J. Mol. Catal.* **1993**, *85*, 327-344; b) Y. Y. Gorbanev, S. K. Klitgaard, J. M. Woodley, C. H. Christensen, A. Riisager, *ChemSusChem* **2009**, *2*, 672-675; c) O. Casanova, S. Iborra, A. Corma, *ChemSusChem* **2009**, *2*, 1138-1144.
- [6] a) T. A. Werpy, J. E. Holladay, J. F. White, Pacific Northwest National Laboratory (PNNL), Richland, WA (US), **2004**; b) J. J. Bozell, G. R. Petersen, *Green Chem.* **2010**, *12*, 539-554.
- [7] B. Kuczynski, R. Geyer, *Resour. Conserv. Recy.* **2010**, *54*, 1161-1169.
- [8] A. Gandini, in *Polymer Chemistry, Vol. 25*, Springer Berlin Heidelberg, **1977**, pp. 47-96.
- [9] A. Gandini, A. J. Silvestre, C. P. Neto, A. F. Sousa, M. Gomes, *J. Polym. Sci., Part A: Polym. Chem.* **2009**, *47*, 295-298.
- [10] Z. Lin, M. Ierapetritou, V. Nikolakis, *AIChE J.* **2013**, *59*, 2079-2087.
- [11] a) K. Takahashi, S. Sone, WO 2009110402 A1. b) T. Brandvold, WO 2010151346A1. Another related patent was published in 2013: c) WO2013040514 A1.
- [12] a) C. L. Williams, C.-C. Chang, P. Do, N. Nikbin, S. Caratzoulas, D. G. Vlachos, R. F. Lobo, W. Fan, P. J. Dauenhauer, *ACS Catal.* **2012**, *2*, 935-939; b) P. T. M. Do, J. R. McAtee, D. A. Watson, R. F. Lobo, *ACS Catal.* **2012**, *3*, 41-46; c) D. Wang, C. M. Osmundsen, E. Taarning, J. A. Dumesic, *ChemCatChem* **2013**, *5*, 2044-2050.
- [13] For examples of ethylene production from ethanol, see: a) U. Tsao, H. B. Zasloff, US4134926 A. b) J. M. Jacobs, P. A. Jacobs, J. B. Uytterhoeven, US4670620 A. c) T. Aida, Y. Asami, M. Kojima, US4302357 A.
- [14] I. Takahara, M. Saito, M. Inaba, K. Murata, *Catal. Lett.* **2005**, *105*, 249-252.
- [15] In the course of our study, we also studied maleic anhydride and 2,2,2-trifluoroethyl acetate as alternative raw materials. *p*-Xylene was obtained in both cases in moderate overall yields. See experimental section.
- [16] a) Y. Magatani, K. Okumura, US2011/112330 A1, 2011. b) J.-L. Dubois, DUBOIS, Y. Magatani, K. Okumura, EP2265565 B1, 2012. c) H. Redlingshofer, C. Weckbecker, K. Huthmacher, A. Dorflein, US2008/183019 A1, 2008. d) Y. Arita, H. Kasuga, M. Kirishiki, H. Tsuneki, EP2103590 A1, 2009.
- [17] a) B. Katryniok, S. Paul, M. Capron, C. Lancelot, V. Belliere-Baca, P. Rey, F. Dumeignil, *Green Chem.* **2010**, *12*, 1922-1925; b) J. Deleplanque, J. L. Dubois, J. F. Devaux, W. Ueda, *Catal. Today* **2010**, *157*, 351-358.
- [18] B. Katryniok, S. Paul, V. Bellière-Baca, P. Rey, F. Dumeignil, *Green Chem.* **2010**, *12*, 2079-2098.
- [19] a) K. Ohno, J. Tsuji, *J. Am. Chem. Soc.* **1968**, *90*, 99-107; b) C. M. Beck, S. E. Rathmill, Y. J. Park, J. Chen, R. H. Crabtree, L. M. Liable-Sands, A. L. Rheingold,

- Organometallics* **1999**, *18*, 5311-5317; c) D. H. Dougherty, L. H. Pignolet, *J. Am. Chem. Soc.* **1978**, *100*, 7083-7085.
- [20] L. J. Gooßen, W. R. Thiel, N. Rodríguez, C. Linder, B. Melzer, *Adv. Synth. Catal.* **2007**, *349*, 2241-2246.
- [21] a) X. Guo, J. Wang, C.-J. Li, *J. Am. Chem. Soc.* **2009**, *131*, 15092-15093; b) X. Guo, J. Wang, C.-J. Li, *Org. Lett.* **2010**, *12*, 3176-3178; c) Q. Shuai, L. Yang, X. Guo, O. Baslé, C.-J. Li, *J. Am. Chem. Soc.* **2010**, *132*, 12212-12213; d) L. Yang, X. Guo, C.-J. Li, *Adv. Synth. Catal.* **2010**, *352*, 2899-2904.
- [22] L. J. Gooßen, G. Deng, L. M. Levy, *Science* **2006**, *313*, 662-664.
- [23] a) T. P. Binder, P. D. Bloom, G. B. Poppe, US Patent 20080103340A1, 2008; b) S. P. Chopade, D. J. Miller, J. E. Jackson, T. A. Werpy, J. G. Frye, A. H. Zacher, US Patent 6291725B1, 2001.
- [24] a) M. Y. Zheng, A. Q. Wang, N. Ji, J. F. Pang, X. D. Wang, T. Zhang, *ChemSusChem* **2010**, *3*, 63-66; b) N. Ji, T. Zhang, M. Zheng, A. Wang, H. Wang, X. Wang, J. G. Chen, *Angew. Chem.* **2008**, *120*, 8638-8641; c) Y. Zhang, A. Wang, T. Zhang, *Chem. Commun.* **2010**, *46*, 862-864; d) N. Ji, T. Zhang, M. Zheng, A. Wang, H. Wang, X. Wang, Y. Shu, A. L. Stottlemeyer, J. G. Chen, *Catal. Today* **2009**, *147*, 77-85; e) Y. Liu, C. Luo, H. Liu, *Angew. Chem.* **2012**, *124*, 3303-3307; f) S. Van de Vyver, J. Geboers, P. A. Jacobs, B. F. Sels, *ChemCatChem* **2011**, *3*, 82-94.
- [25] a) Y. Román-Leshkov, C. J. Barrett, Z. Y. Liu, J. A. Dumesic, *Nature* **2007**, *447*, 982-985; b) M. Chidambaram, A. T. Bell, *Green Chem.* **2010**, *12*, 1253-1262; c) G. C. Luijckx, N. P. Huck, F. van Rantwijk, L. Maat, H. van Bekkum, *Heterocycles* **2009**, *77*, 1037-1044.
- [26] For aromatization of DMF via a Diels-Alder reaction with other dienophiles, see: a) A. de la Hoz, A. Diaz-Ortiz, J. M. Fraile, M. V. Gomez, J. A. Mayoral, A. Moreno, A. Saiz, E. Vazquez, *Synlett* **2001**, *6*, 753-756; b) J. Fraile, J. Garca, M. A. Gmez, A. de la Hoz, J. Mayoral, A. Moreno, P. Prieto, L. Salvatella, E. Vzquez, *Eur. J. Org. Chem.* **2001**, *15*, 2891-2899; c) K. Takanishi, S. Sone, WO2009110402, 2009.
- [27] W. G. Dauben, H. O. Krabbenhoft, *J. Am. Chem. Soc.* **1976**, *98*, 1992-1993.
- [28] P. Laszlo, J. Lucchetti, *Tetrahedron Lett.* **1984**, *25*, 4387-4388.
- [29] Y. Hayashi, M. Nakamura, S. Nakao, T. Inoue, M. Shoji, *Angew. Chem. Int. Ed.* **2002**, *41*, 4079-4082.
- [30] Polymer-bound Sc(OTf)₃ catalyst (Sigma, product # 590312, macroporous, 30-60 mesh, extent of labeling: 0.5-1.5 mmol/g loading) could be also used in lieu of Sc(OTf)₃.
- [31] At 25 °C, the equilibrium yield (7-8 %) was also reached in the forward direction with no catalyst. See Table 2, entry 9.
- [32] a) A. Raach, O. Reiser, *J. Prakt. Chem.* **2000**, *342*, 605-608; b) E. Dalcanale, F. Montanari, *J. Org. Chem.* **1986**, *51*, 567-569; c) F. E. Ziegler, Y. Wang, *J. Org. Chem.* **1998**, *63*, 7920-7930.
- [33] PDC oxidation in DMF was also tried but tis method was unsuccessful.
- [34] Acrylic acid and decomposition products were observed when left at RT for a few days.
- [35] a) T.-L. Chan, T. C. Mak, C.-D. Poon, H. N. Wong, J. H. Jia, L. L. Wang, *Tetrahedron* **1986**, *42*, 655-661; b) G. P. Jana, B. K. Ghorai, *Tetrahedron* **2007**, *63*, 12015-12025; c) F. I. Zubkov, E. V. Boltukhina, K. F. Turchin, A. V. Varlamov, *Tetrahedron* **2004**, *60*, 8455-8463; d) A. D. Mance, B. Borovička, B. Karaman, K. Jakopčić, *J. Heterocycl. Chem.* **1999**, *36*, 1337-1341.

- [36] a) F. Brion, *Tetrahedron Lett.* **1982**, 23, 5299-5302; b) M. E. Bunnage, T. Ganesh, I. B. Masesane, D. Orton, P. G. Steel, *Org. Lett.* **2003**, 5, 239-242.
- [37] W. A. Yarnall, E. S. Wallis, *J. Org. Chem.* **1939**, 4, 270-283.
- [38] L. Ebersson, *Acta Chem. Scand.* **1964**, 18, 2015-2021.
- [39] a) D. Liu, E. Canales, E. J. Corey, *J. Am. Chem. Soc.* **2007**, 129, 1498-1499; b) J. Y. Sim, G.-S. Hwang, K. H. Kim, E. M. Ko, D. H. Ryu, *Chem. Commun.* **2007**, 5064-5065.

Chapter 2

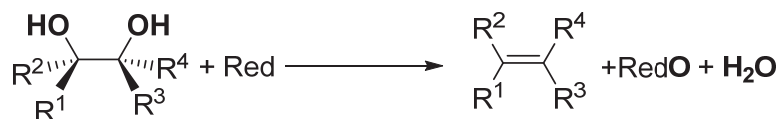
Oxorhenium-Catalyzed Deoxydehydration of Polyols Using Alcohol Solvent as a Reductant

Portions of the work in this chapter have been published:

*M. Shiramizu, F. D. Toste, *Angew. Chem. Int. Ed.* **2012**, *51*, 8082-8086.*

Introduction

With the growing demand for sustainability, cellulosic biomass has attracted much attention as a renewable, carbon-neutral and inexpensive feedstock for chemicals and fuels. However, the conversion of biomass faces a fundamental challenge that saccharides and their polyol derivatives, the most basic platform chemicals accessible from cellulose, are too oxygen-rich to be compatible with the current petroleum-based infrastructure. Current biomass deoxygenation methods are dominated by high-temperature pyrolysis,^[1] acid-catalyzed dehydration^[2] and hydrogenolysis reactions^[3] but they often suffer from poor product selectivity and the loss of carbon as humin or CO₂. In search of a more efficient process, interest is rapidly growing in the catalytic deoxydehydration (DODH) reaction to remove two adjacent hydroxyl groups from vicinal diols to afford alkenes^[4] (Scheme 1).



Scheme 1 A general scheme for DODH reaction.

While preliminary studies on ruthenium,^[5] vanadium^[6] and molybdenum catalysts^[7] have been reported, most precedents on DODH employ high-valent oxorhenium catalysts in conjunction with various reductants such as phosphines^[8], H₂^[9] and NaSO₃^[10]. The Nicholas and Jentoft groups recently reported carbon-supported perrhenate as the first heterogeneous DODH catalyst.^[11] Fernandes et al. reported the oxorhenium-catalyzed reductant-free deoxygenation of aromatic epoxides to alkenes,^[12] but this reaction does not seem applicable to aliphatic diols (see Appendix). In 2010, the Bergman and Ellman groups demonstrated a hydrogen transfer-type DODH reaction catalyzed by Re₂(CO)₁₀ and BrRe(CO)₅, using 5-nonanol, 3-octanol and 2-octanol as solvent/reductant.^[13] As noted by many groups, one particular feature of the DODH reaction is that the vicinal diol needs to accommodate the *cis*-diol structure: For example, while *cis*-1,2-cyclohexanediol is reactive, *trans*-1,2-cyclohexanediol is not. The stereospecificity is

also depicted in Scheme 1. This is explained by the metal diolate intermediate, analogous to the reverse reaction of OsO₄-catalyzed *cis*-dihydroxylation of olefins.^[14]

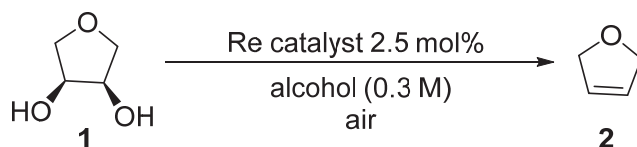
Although these methods are effective for simple vicinal diols and appear to lay solid foundations in the context of biomass deoxygenation, as of 2011, no DODH system had been reported to have a general efficiency on biomass-derived polyol substrates. Most reactions were developed based on model substrates (e.g. styrenediol, 1,2-octanediol) which are generally more hydrophobic (soluble in common organic solvents) and thermally stable. The only polyol example described was erythritol (C4 sugar alcohol) and product yields were moderate (21-62 %) after long reaction times (12-100 h).^[10b, 10c, 13] There was no report of DODH reaction of higher carbon number polyols such as C5-C6 sugar alcohols, which can be readily obtained by hydrogenation of naturally abundant sugars (e.g. xylose and arabinose, the major components of hemicellulose, and glucose, the component of cellulose). The substrate scope of DODH was also largely unexplored: no substrates bearing functionality other than hydroxyl and ether groups had been investigated, while sugar acids (carboxylic acids), obtained by mere oxidation of sugars, comprise another important group of saccharide derivatives. Moreover, the direct DODH reaction of saccharides was unprecedented, although they are clearly the most direct potential polyol feedstock from biomass.

Based on this background, we sought an efficient DODH protocol applicable to the challenging polyol substrates and developed a sacrificial alcohol (reductant/solvent)-based DODH reaction catalyzed by oxorhenium species^[15] instead of rhenium carbonyl compounds. This particular catalyst-reductant combination showed remarkably higher efficiency than any other precedents and smoothly converted sugar alcohols, sugar acids and sugars into linear alkene products and aromatics with high product selectivity. We demonstrated the application of DODH in commodity chemicals syntheses, shed light on the reaction mechanism by isolating the potential intermediate Re^V species and discovering novel modes of DODH reaction on 2-ene-1,4-diols and 2,4-diene-1,6-diols. Other research groups followed this study with DFT calculations^[16] as well as kinetic experiments,^[17] although the mechanistic details still remain the topic of active discussion. As the variants of this alcohol transfer hydrogenation-type strategy, Abu-Omar et al. independently reported the MTO-catalyzed deoxygenation of glycerol to a mixture of volatile compounds using neat glycerol itself as a reductant^[18] and the Nicholas group more recently reported the use of only one equivalent of benzyl alcohol as a reductant in aromatic solvents.^[19] We believe this work constitutes a significant contribution in broadening the range of value-added chemicals accessible from renewable biomass.

Optimization of Reaction Conditions

We embarked on the development of oxorhenium-catalyzed, sacrificial alcohol-driven DODH reaction intrigued by the work of Bergman and Ellman using rhenium carbonyl compounds ($\text{Re}_2(\text{CO})_{10}$, $\text{BrRe}(\text{CO})_5$) as catalyst and alcohol (5-nonanol, 3-octanol, 2-octanol) as reductant.^[13] The use of alcohol reductant was attractive to us in that the oxidized reductant (ketone) is experimentally easily traceable (unlike H_2 or NaSO_3), in addition to the fact that it can be easily hydrogenated if the reductant recycling is necessary (unlike PR_3). While the reported DODH results were promising, we thought there was room for significant improvement as we noted that those catalysts required air and high temperature for activation. We postulated that the actual active catalyst may be an oxidized rhenium species, and consequently oxorhenium compounds could constitute superior catalysts for this reaction. In addition to the precedented examples of oxorhenium-catalyzed DODH using different reductants,^[8a, 9, 10b, 10c] our group had previously developed silane-based reduction reactions using oxorhenium catalysts.^[20] With that expertise and a library of Re catalyst candidate compounds in hand, we were confident that we could identify an active oxorhenium catalyst capable of the alcohol-driven DODH. Furthermore, we also noticed that only large secondary alcohols have been investigated as DODH reductants in the original report. Thus as a secondary goal, we were interested in examining the use of other inexpensive/bio-derived alcohols including primary alcohols to make the process more practical and greener.

Table 1. Comparison of rhenium catalysts.

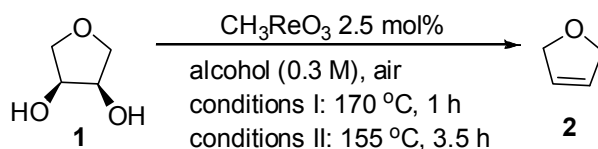


entry	catalyst	temp. (°C)	time (h)	alcohol	yield (%)	conv. (%)
1	$\text{Re}_2(\text{CO})_{10}$	170	1.5	3-octanol	91	100
2	CH_3ReO_3	170	1.5	3-octanol	92	100
3	$\text{Re}_2(\text{CO})_{10}$	155	3.5	3-octanol	>99	100
4	CH_3ReO_3	155	3.5	3-octanol	97	100
5	$\text{Re}_2(\text{CO})_{10}$	125	5.5	3-octanol	0	0
6	CH_3ReO_3	125	5.5	3-octanol	21	29
7	$\text{Re}_2(\text{CO})_{10}$	170	1.5	1-butanol	0	0
8	CH_3ReO_3	170	1	1-butanol	70	100
9	$\text{ReIO}_2(\text{PPh}_3)_2$	170	1	1-butanol	68	100
10	HReO_4	170	1	1-butanol	66	100
11	$\text{ReO}(\text{PPh}_3)_2\text{Cl}_3$	170	1.5	1-butanol	20	54
12	NH_4ReO_4	170	1.5	1-butanol	25	62

In the initial experiments evaluating the viability of oxorhenium compounds, 1,4-anhydroerythritol (**1**) was used as a model substrate (Table 1). With 2.5 mol% $\text{Re}_2(\text{CO})_{10}$, 2,5-dihydrofuran (**2**) was obtained in 91 % yield in 3-octanol at 170 °C (entry 1). Using these

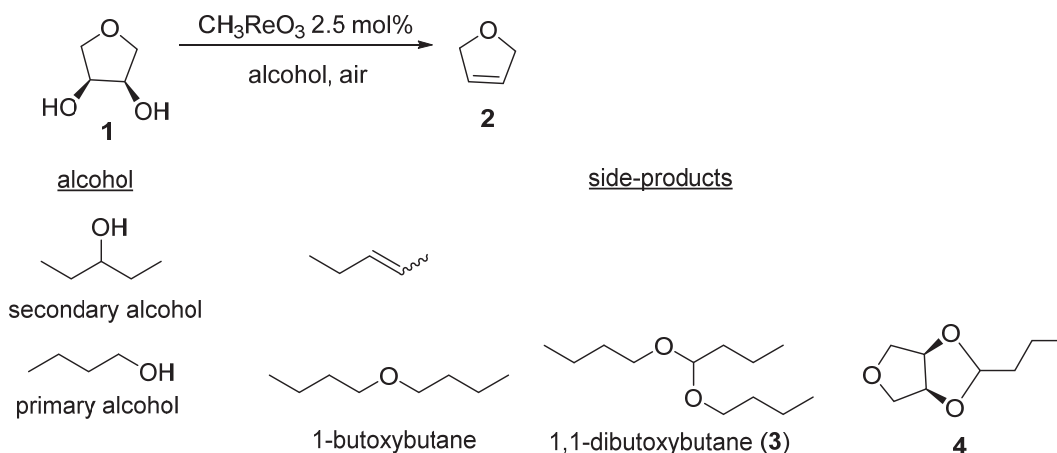
conditions, we screened a variety of oxorhenium catalysts and soon found that the rather simple, commercially available CH_3ReO_3 (methyltrioxorhenium, MTO) furnished **2** in excellent yield (entry 2). Both $\text{Re}_2(\text{CO})_{10}$ and MTO catalyzed the reaction efficiently at a temperature as low as ca. 155 °C (entries 3 and 4), but not at a temperature significantly lower than this threshold. The higher activity of MTO compared with $\text{Re}_2(\text{CO})_{10}$ was notable at 125 °C (entries 5 and 6), but it became even clearer when the alcohol was changed to 1-butanol, a typical biomass-derived alcohol.^[21] At 170 °C, while no reaction was observed with $\text{Re}_2(\text{CO})_{10}$ (entry 7), MTO delivered **2** in 70 % yield (entry 8). After the more extensive re-screening of oxorhenium catalysts using 1-butanol, $\text{ReIO}_2(\text{PPh}_3)_2$ and perrhenic acid HReO_4 were also found to be promising, affording **2** in similar yields (ca. 70 %, entries 9 and 10) while $\text{ReO}(\text{PPh}_3)_2\text{Cl}_3$ and NH_4ReO_4 showed moderate reactivity (entries 11, 12). We thus selected MTO as our first catalyst of choice at this point based on its ligand-free simple structure and its ease of handling as a crystalline solid, as opposed to the aqueous solution, the commercial form of HReO_4 .

Table 2. The effect of alcohols on MTO-catalyzed DODH reaction.



entry	alcohol	conditions	yield (%)	conv.(%)
1	ethanol	I	0	0
2	1-propanol	I	28	N.D.
3	2-propanol	I	0	0
4 ^[a]	1-butanol	I	70	100
5	2-butanol	I	0	0
6	1-butanol	II	trace	16
7	1-pentanol	II	51	100
8	isopentanol	II	61	100
9	2-methyl-1-butanol	II	57	100
10	2,2-dimethyl-1-propanol	II	42	89
11	3-pentanol	II	91	100
12	2-pentanol	II	78	100
13	3-methyl-2-butanol	II	62	85
14	2,4-dimethyl-3-pentanol	II	>99	100
15^[a]	3-octanol	II	97	100

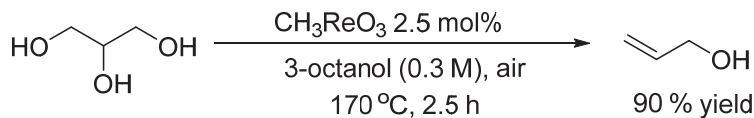
[a] Duplicate entry from Table 1.



Scheme 2 Side-products from the alcohol-driven DODH reaction.

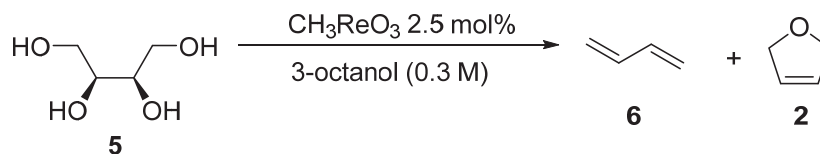
The difference among various alcohols was further evaluated using MTO (Table 2), including ethanol (entry 1) and amyl alcohols (entries 6-12) which can be produced by fermentation of glucose.^[22] The reactivity was dependent on both size and structure of the alcohol. For size, unfortunately small alcohols such as ethanol and propanols were ineffective even at high temperature (entries 1-3). In contrast, various larger (carbon number ≥ 5) alcohols could be used, affording **2** in ≥ 40 % yield without condition optimization in all cases (entries 7-15). This may be because the less hindered alcohols have stronger coordination ability and prevent the substrate diol binding to the catalyst, or because the smaller alcohols have poorer reducing ability.^[16] Because the use of anhydrous ethanol under N_2 gave the same results as in entry 1, it is unlikely that the water contaminant in the more hydrophilic small alcohols is the main cause of this dramatic difference.^[23] For structure, secondary alcohols generally gave better yields of **2** than primary alcohols. One reason might be the difference in dehydrated side-products formed along with the direct reaction products (**2** and aldehyde or ketone), as shown in Scheme 2. Dehydration could be somewhat suppressed when (1) reaction temperature was lower, (2) reaction time was shorter, or (3) the alcohol was sterically hindered, but never totally eliminated. From secondary alcohols, alkenes were formed from solvent^[24] but they did not seem to interfere with the desired DODH reaction. In contrast, from primary alcohols, besides the alcohol dimerization and acetalization of aldehyde (e.g. 1,1-dibutoxybutane **3**) the more concerning masked diol (e.g. **4**) was detected. Therefore, while the use of bio-derived alcohol (1-butanol) was demonstrated, we concluded that large (carbon number ≥ 5) secondary alcohols such as 3-pentanol, 2,4-dimethyl-3-pentanol and 3-octanol (entries 11, 14 and 15) are generally more favorable than primary alcohols for MTO, and mainly used them for further investigations.

Sugar Alcohols



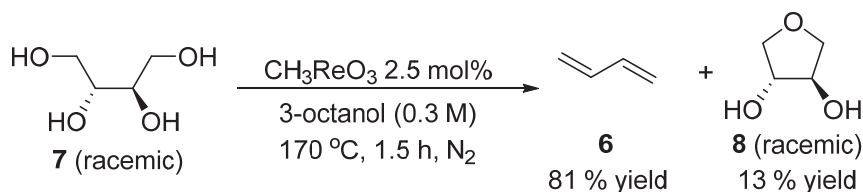
Scheme 3 DODH reaction of glycerol.

Table 3. DODH reaction of erythritol.



entry	atmosphere	temp(°C)	time(h)	yield 6 (%)	yield 2 (%)
1	N₂	170	1.5	89	11
2	air	170	1.5	72	15
3	N ₂	155	2.5	79	6
4 ^[a]	N ₂	155	5.5	73	7

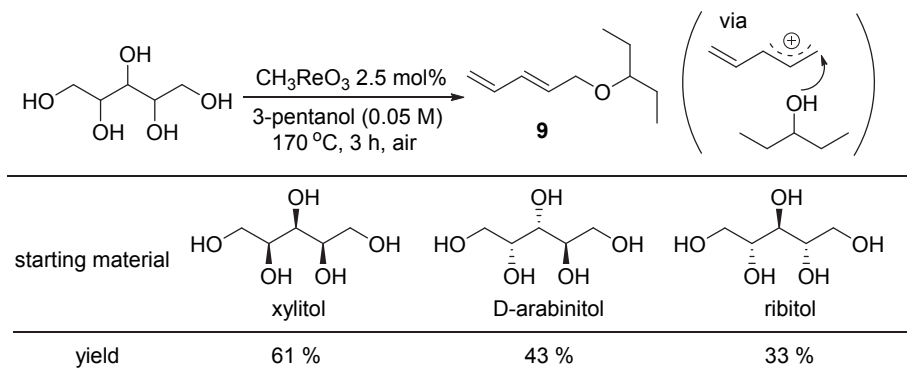
[a] HReO_4 (77 % solution in water) was used instead of MTO.



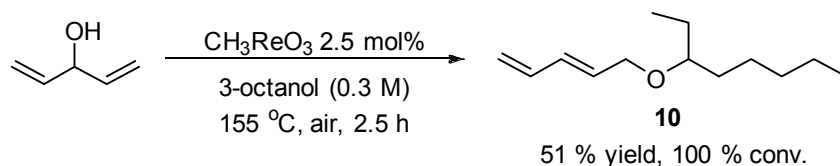
Scheme 4 DODH reaction of DL-threitol.

We began our investigation of polyol DODH by applying the MTO-alcohol system to glycerol, which is a by-product of biodiesel (fatty acid methyl esters) production from oil-based feedstocks and considered an important platform chemical for bio-based materials.^[25] To our delight, allyl alcohol was obtained in excellent yield (Scheme 3). Encouraged by this result, we then tested erythritol (**5**), a C4 sugar alcohol which can be obtained by the fermentation of glucose^[26] or by the decarbonylation of pentoses^[27] (Table 3). 1,3-Butadiene (**6**), an industrially important rubber precursor, was obtained in 89 % yield, with 2,5-dihydrofuran (**2**) as a minor product (11 %) under N₂ (entry 1). The reaction could be conducted in air, albeit producing **6** in slightly lower yield (entry 2). A higher temperature (170 °C) and shorter reaction time was preferred over lower temperature (155 °C) and longer reaction time, due to the decomposition of **6** (entry 3). We also tested HReO_4 as a catalyst to examine whether Brønsted acidity increased the yield of **2**,^[13] but it behaved in the same manner as MTO (entry 4). When DL-threitol (**7**) was subjected to the conditions identical to entry 1, **6** was obtained in a similar yield (81 %) and the

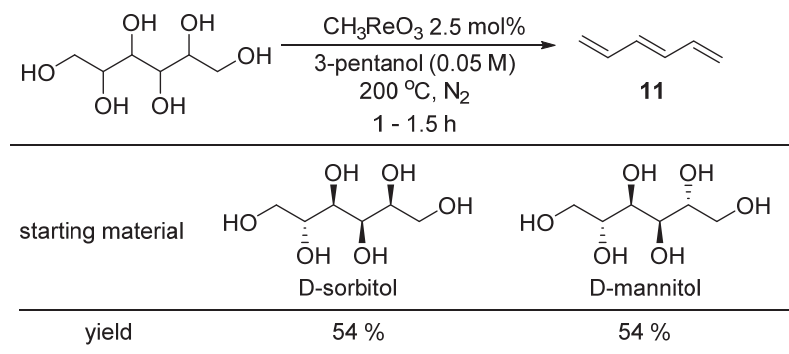
minor product (13 %) was 1,4-anhydrothreitol (**8**) instead of **2** (Scheme 4), suggesting that the diol substrate needs to accommodate the *cis*-conformation (assuming **2** is produced via **1**) to undergo DODH.



Scheme 5 DODH reaction of C5 sugar alcohols.



Scheme 6 Formation of (*E*)-3-(penta-2,4-dienyloxy)octane from penta-1,4-dien-3-ol.

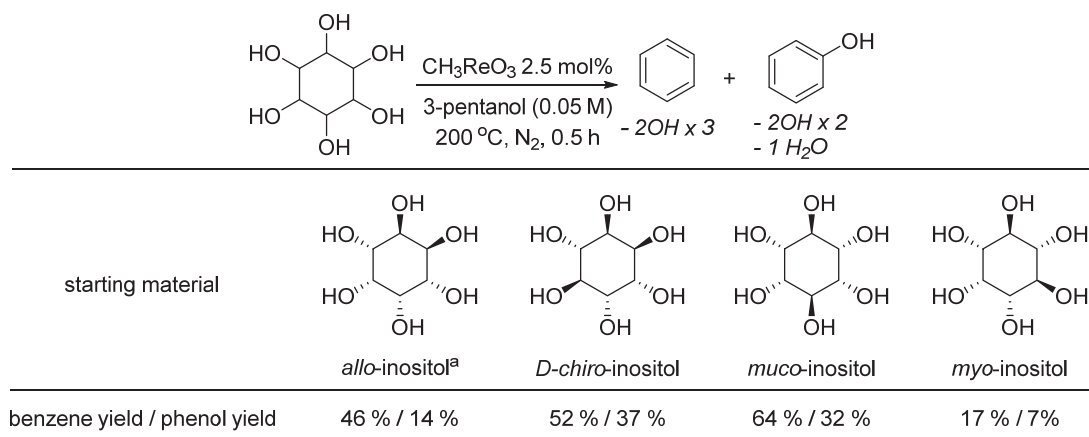


Scheme 7 DODH reaction of C6 sugar alcohols.

We were then able to demonstrate the first DODH reaction of C5 and C6 polyols. When we investigated xylitol, we initially struggled to obtain high yields: under previously employed conditions, (*E*)-5-penta-1,3-diene ethers (e.g. **9** with 3-pentanol; 3-octanol and 2,4-dimethyl-3-pentanol gave similar results) were obtained in 10-20 % yields. These ether products were isolated by flash column chromatography for characterization (see Experimental Section). Although the high boiling solvents (3-octanol and 2,4-dimethyl-3-pentanol) were difficult to remove by a standard laboratory measure (rotary evaporator), because the polarity of the product

was much lower than that of alcohol, the crude mixture was separable on small scale without concentration. Considering that three equivalents of alcohol are required for this transformation, lowering the concentration of xylitol significantly improved the yield to 61% (Scheme 5). Interestingly, D-arabinitol and ribitol also gave the same (*E*)-isomer **9** in respectable yields. The presumed *cis*-diol stereochemical requirement of the DODH reaction suggests that an *E-Z* isomerization process is involved. We propose the Lewis acid-catalyzed formation of a pentadienyl cation and its trapping by solvent alcohol, favoring the more stable (*E*)-conformation. When penta-1,4-dien-3-ol was heated in 3-octanol with 2.5 mol% MTO, (*E*)-3-(penta-2,4-dienyloxy)octane (**10**) was indeed obtained, supporting this hypothesis (Scheme 6). Gratifyingly, D-sorbitol and D-mannitol, C6 sugar alcohols derived from glucose and fructose, also underwent clean DODH reaction. (*E*)-hexatriene (**11**), an interesting polymer precursor,^[28] was obtained in 54 % ¹H NMR yield from both substrates when high temperature-short reaction time conditions were employed (Scheme 7). (*E*)-hexatriene was isolated for characterization by conducting the DODH reaction at 155 °C in 3-octanol (b.p. 175 °C) and constantly distilling the product as it forms (see Experimental Section).

Inositols



[a] 3-octanol was used instead of 3-pentanol.

Scheme 8 Deoxygenation of inositols to aromatics.

To further diversify the scope of biomass-derived chemicals accessible via DODH, we applied our reaction to inositols, a class of natural carbohydrate. On one hand, one can imagine the formation of benzene by three consecutive DODH reactions, given the appropriate stereochemistry or fast isomerization. On the other hand, based on the knowledge garnered from xylitol DODH reactions, a cationic species may readily form after two DODH events. Driven by aromatization, the net loss of water would yield a phenol moiety.^[29] As both benzene and phenol are stable, high-volume chemicals conventionally produced only from petroleum source, their bio-derived alternatives would be highly attractive. When different inositol isomers were examined, benzene and phenol were indeed obtained as a mixture, in the total yields of 24-96 % (Scheme 8).^[30] High yields of benzene were obtained not only from *allo*-inositol but also from *D-chiro*-inositol and *muco*-inositol. In contrast, *myo*-inositol, bearing only one *cis*-diol group,

gave low yields for both benzene and phenol. This implies that there is an efficient isomerization process to afford a *cis*-1,2-diol intermediate at the third DODH step, which could proceed via an oxygen transfer from oxorhenium catalyst (Figure 1) or via the rhenium-catalyzed 1,3-OH shift of allylic alcohol^[31] or simply via the isomerization of pentadienol under the Lewis acidic conditions.

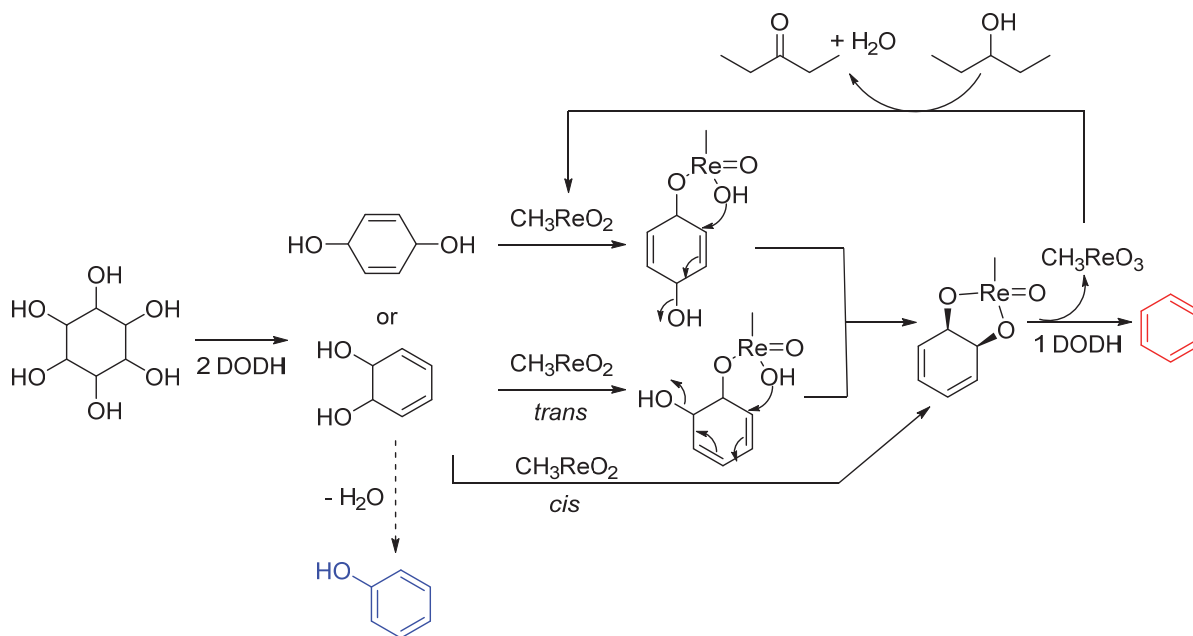


Figure 1 A proposed mechanism for diol isomerization of inositols.

Reaction Mechanism

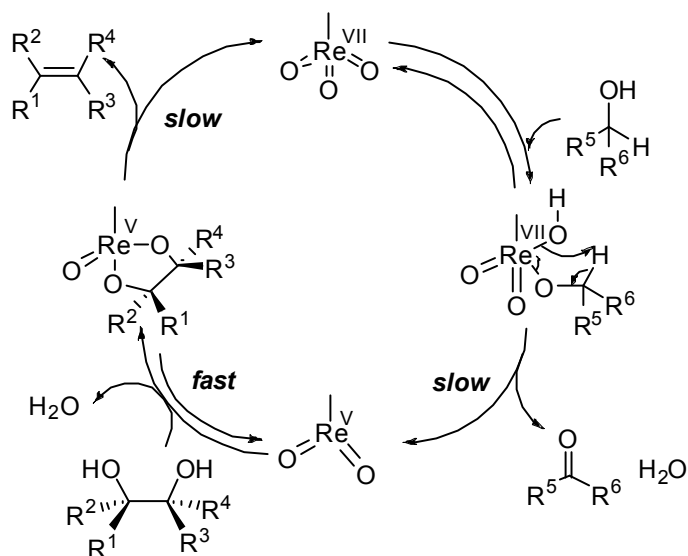
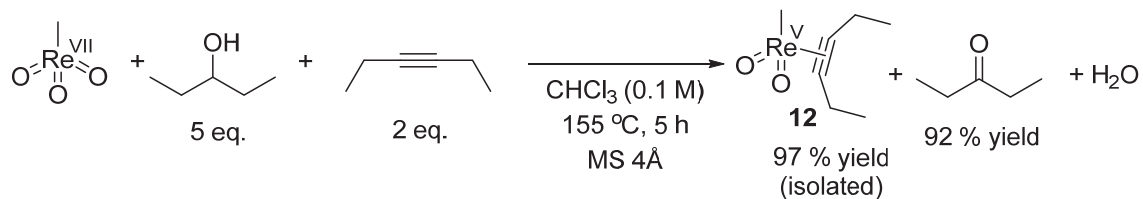
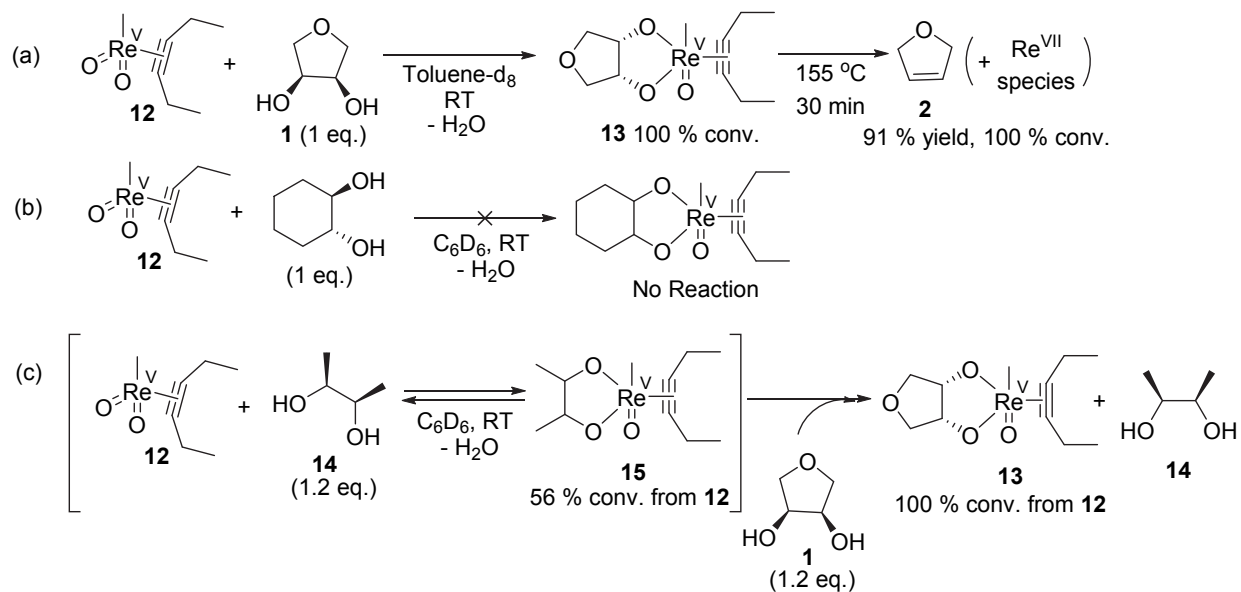


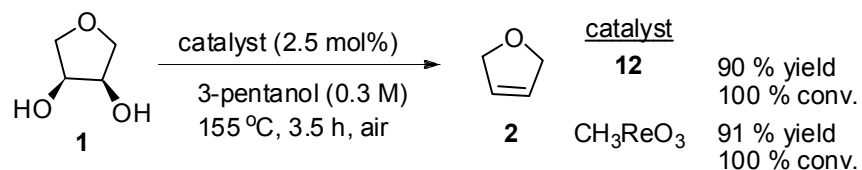
Figure 2 A proposed catalytic cycle for MTO-catalyzed alcohol-driven DODH reaction.



Scheme 9 The reduction of MTO by 3-pentanol.



Scheme 10 The diol binding to **12**.



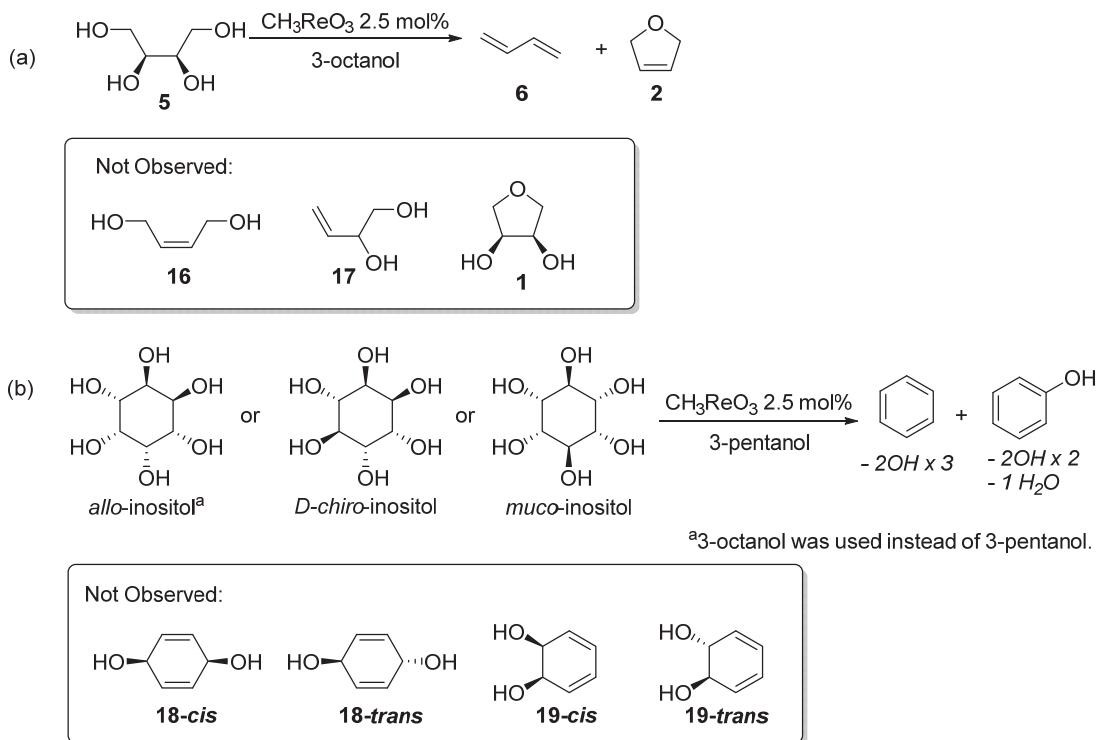
Scheme 11 Rhenium complex **12** as a DODH catalyst.

A plausible catalytic cycle for our DODH reaction is shown in Figure 2. Although the kinetic studies of Abu-Omar et al. suggested that Re diolate exists in equilibrium with its dinuclear form,^[17] we depicted only the monomer for the sake of simplicity. We propose it consists of (1) the reduction of Re^{VII} to Re^{V} by alcohol, (2) diol coordination to Re^{V} and (3) olefin extrusion (cycloreversion), based on the Cp^*ReO_3 and Tp^*ReO_3 system previously studied by Gable et al.^[32] The works of Gable focused on the cycloreversion mechanism (concerted [3+2] vs. stepwise [2+2]) and concluded it as “significantly asynchronous but concerted transition state” after rigorous mechanistic studies and calculations. We aimed to obtain more direct evidence for our particular system in each step of the catalytic cycle. We thus combined the reductant alcohol (3-pentanol), MTO and 3-hexyne ligand (Scheme 9). A known, stable Re^{V} compound **12**^[33] along with 3-pentanone was obtained after heating at 155 °C for 5 hours, ensuring that 3-pentanol is capable of reducing Re^{VII} to Re^{V} . Notably, this reduction appears too slow to be appreciable at lower temperature (cf. Table 1, entries 2, 4 and 6): Only a trace amount of **12** (5 % yield) was obtained at 125 °C after 1 h and no reaction was observed at room temperature. Also, the use of excess 3-pentanol was essential to facilitate the reaction: When only 1 eq. of 3-pentanol and 1 eq. of 3-hexyne was used, the conversion after 5 h was 51 %. 3-Hexyne was needed because the ligand-free methyldioxorhenium is unstable. A black insoluble material (presumably the oligomer of methyldioxorhenium^[34]) resulted when MTO and 3-pentanol alone were heated at 155 °C in the absence of 3-hexyne, leaving 3-pentanone in the organic phase (¹H and ¹³C NMR analysis).

The binding of diol **1** to **12** occurred immediately at RT to afford Re^{V} complex **13**, indicating it is a facile step in the catalytic cycle (Scheme 10a, first step). Although our efforts to obtain a crystal of **13** to carry out an X-ray diffraction study were unsuccessful, NMR analysis provided ample information about the structure of this compound, including that **13** is asymmetric (see Experimental Section). On the other hand, extrusion of olefin **2** from **13** required heating at 155 °C for 0.5 h (Scheme 10a, second step) and no reaction was observed in VT-NMR between RT and 100 °C.^[35] Although the effect of the 3-hexyne ligand cannot be ignored, our results implied that the alkene extrusion is another relatively slow step. The extent of diol binding to **12** varied depending on the diol structure. While *trans*-hexanediol showed no evidence of binding (Scheme 10b), as shown in Scheme 10c, combining *meso*-2,3-butanediol **14** (1.2 eq.) and **12** in C_6D_6 at RT produced **15** but only in 56 % conversion (i.e. the mixture of mol ratio **12** : **14** : **15** = 0.8 : 1.1 : 1.0 resulted). When the amount of **14** was increased (up to 6 eq.) in a separate experiment, the conversion (i.e. ratio of **15/12**) increased, but not to the extent of complete conversion. However, when **1** (1.2 eq.) was subsequently added to the above-mentioned mixture of **12** : **14** : **15** = 0.8 : 1.1 : 1.0, all rhenium compounds (**12** and **15**) were exclusively converted into **13**,

resulting in a solution of **13**, **14** and the excess **1** (observed mol ratio **13** : **14** : **1** = 1.0 : 1.2 : 0.2). The diol exchange from **15** to **13** indicates that this binding is reversible and that diol and Re diolate are in the fast equilibrium. Moreover, rhenium complex **12** exhibited the DODH catalytic activity virtually identical to MTO (Scheme 11), overall supporting that methyldioxorhenium(V) is the catalytically viable species. To summarize, although this work did not investigate the alternative catalytic cycle based on $\text{Re}^{\text{III}}\text{-Re}^{\text{V}}$ recently proposed by Abu-Omar et al.,^[36] the plausibility of each step of the catalytic cycle (Figure 2) was confirmed. We postulate that the rate-determining step is either the reduction of Re or the alkene extrusion (the recent DFT study by Z.-X. Wang et al. supports that the former is the rate-determining step^[16]) and the product selectivity is dictated by the difference in coordination ability of each diol.

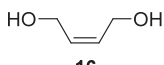
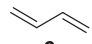
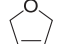
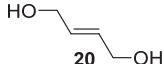
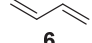
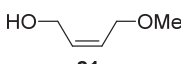
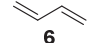
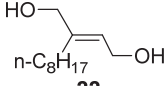
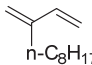
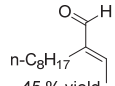
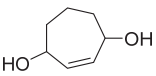
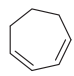
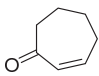
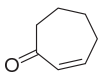
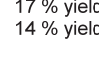
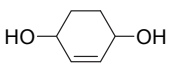
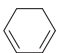
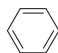
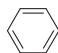
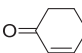
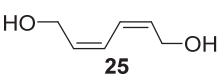
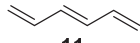
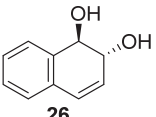
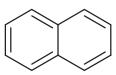
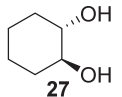
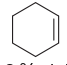
1,4- and 1,6-DODH



Scheme 12 The product selectivity toward complete DODH over partial DODH (See Table 3 and Scheme 8 for full reaction details).

As described in the previous section, we generally observed only the complete DODH products and not the partial DODH products in the MTO-catalyzed DODH of sugar alcohols. This made us interested in elucidating the mechanistic basis of polyol DODH. The reactions of erythritol (**5**) and inositols are shown in Scheme 12 as representative examples. The complete DODH products butadiene (**6**) and benzene were obtained in good yields and partially deoxygenated diol intermediates **1**, **16**, **17**, **18**, **19** were not observed. Although it is likely that the DODH reaction occurs too rapidly to observe **1**, **17** and **19-cis** on this timescale, all other intermediates must remain as the final products if DODH is possible only on *cis*-vicinal diols. In the case of erythritol, while four OH groups are seemingly similar, it is possible that the terminal primary OH groups have higher reactivity than internal ones and **1** and **17** are formed preferentially over **16**. However, in the case of *D-chiro*- and *muco*-inositols bearing only two sets of *cis*-diol, the formation of **18** or **19-trans** appears inevitable according to the present mechanistic hypothesis. Nonetheless, they showed as high benzene yield as *allo*-inositol, which bears three sets of *cis*-diol. This led us to speculate that not only *cis*-vicinal diols (**1**, **17** and **19-cis**), which are capable of direct coordination to Re catalyst, but also moieties such as **16**, **18** and **19-trans** are reactive toward DODH by oxorhenium-catalyzed isomerization of allylic alcohol.^[31]

Table 4. DODH reactions of 2-ene-1,4-diol and 2,4-diene-1,6-diol moieties.

		$\xrightarrow[\text{3-pentanol}]{\text{CH}_3\text{ReO}_3 \text{ 2.5 mol\%}}$ 170 °C, N ₂ , 0.5 h			
diol		deoxygenated product		dehydration product	
entry	diol	DODH product		dehydration product	
1 ^[a]	 16	 6 70 % yield		 2 6 % yield	
2 ^[a]	 20	 6 70 % yield			
3 ^[a]	 21	 6 0 % yield decomposition			
4	 22	 6 18 % yield		 23 45 % yield	
5 ^[b]	 23a: cis-diol 23b: trans-diol (racemic)	 23a: 36 % yield		 23b: 58 % yield	 17 % yield  14 % yield
6 ^[c]	 24a: cis-diol 24b: trans-diol (racemic)	 24a: 35 % yield	 24b: 23 % yield	 5 % yield	 trace 12 % yield
7 ^{[d][e]}	 25	 11 31 % yield			
8 ^[e]	 26	 9 % yield		1-naphthol 73 % yield + 2-naphthol 10 % yield	
9 ^[e]	 27	 0 % yield no reaction			

[a] 3-octanol was used instead of 3-pentanol. [b] 5 mol% catalyst loading. [c] It was not determined whether benzene was formed via dehydration of substrate or via oxidation of 1,3-cyclohexadiene. [d] Reaction temperature was 200 °C. [e] Reaction time was 1 h.

In order to examine this hypothesis and gain insights on the origin of the observed exquisite selectivity in polyol DODH reactions, we tested a series of 2-ene-1,4-diol (analogous to **16**, **18**) and 2,4-diene-1,6-diol (analogous to **19-trans**) substrates and indeed observed the unprecedented

“1,4-DODH” and “1,6-DODH” (Table 4). Both *cis*- and *trans*- 2-butene-1,4-diol (**16** and **20**) were reactive, excluding the possibility of the direct coordination of 1,4-diols to Re forming a 7-membered ring Re diolate (entries 1 and 2). Because no butadiene (**6**) was produced from (*Z*)-4-methoxy 2-buten-1-ol (**21**) under the same conditions, it appears that two OH groups are necessary (entry 3). Tri-substituted alkene **22** preferred a dehydration pathway rather than DODH, possibly because the electron-donating alkyl group stabilizes the allylic carbocation intermediate (entry 4). No significant reactivity difference was observed between *cis*- and *trans*-cyclic diols (entries 5 and 6), suggesting that either 1,3-OH shift is in a fast equilibrium or the shift of C-O bond position and Re diolate formation occur in one consecutive step (see Figure 1). Furthermore, DODH reaction was also applicable to *cis*, *cis*-muconic alcohol **25** to afford (*E*)-hexatriene (entry 7). Although aromatization to naphthols was inevitable, a small amount of naphthalene was also obtained from **26** (entry 8), in marked contrast to the non-conjugated *trans*-diol **27** which produced no trace of cyclohexene (entry 9).

Based on these observations, a plausible catalytic cycle of polyol DODH is shown in Figure 3, depicting erythritol (**5**) as a representative substrate. Note that the order of diol isomerization, Re diolate formation and reduction of Re has not been conclusively clarified. We assume that the 1,4- and 1,6-DODH reactions still ultimately proceed via a five-membered ring Re^V diolate intermediate before the olefin extrusion, identical to the last step of 1,2-DODH from *cis*-vicinal diols. This indicates that the DODH reaction is particularly useful for total deoxygenation of polyols by merging the several different intermediates into one product and thereby increasing the final product selectivity. We believe it also shows that our approach of using alcohol solvent as reductant is exceptionally suited for polyol DODH compared to other reductant systems^[8b] not merely because the substrates have better solubility but because the enhanced proton transfer^[16] maximizes this benefit of auto-selectivity increase.

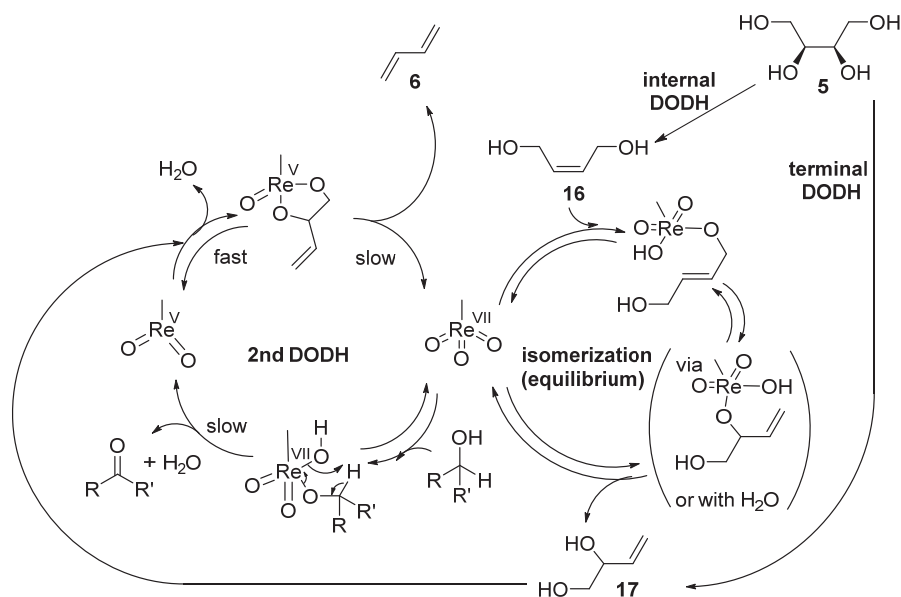
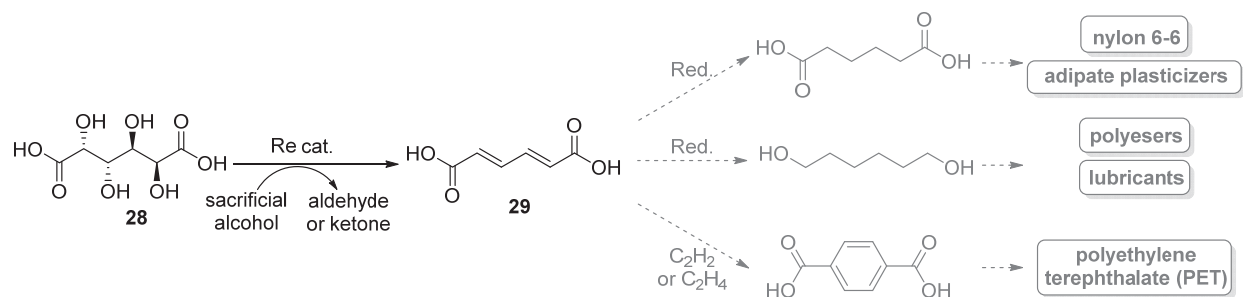
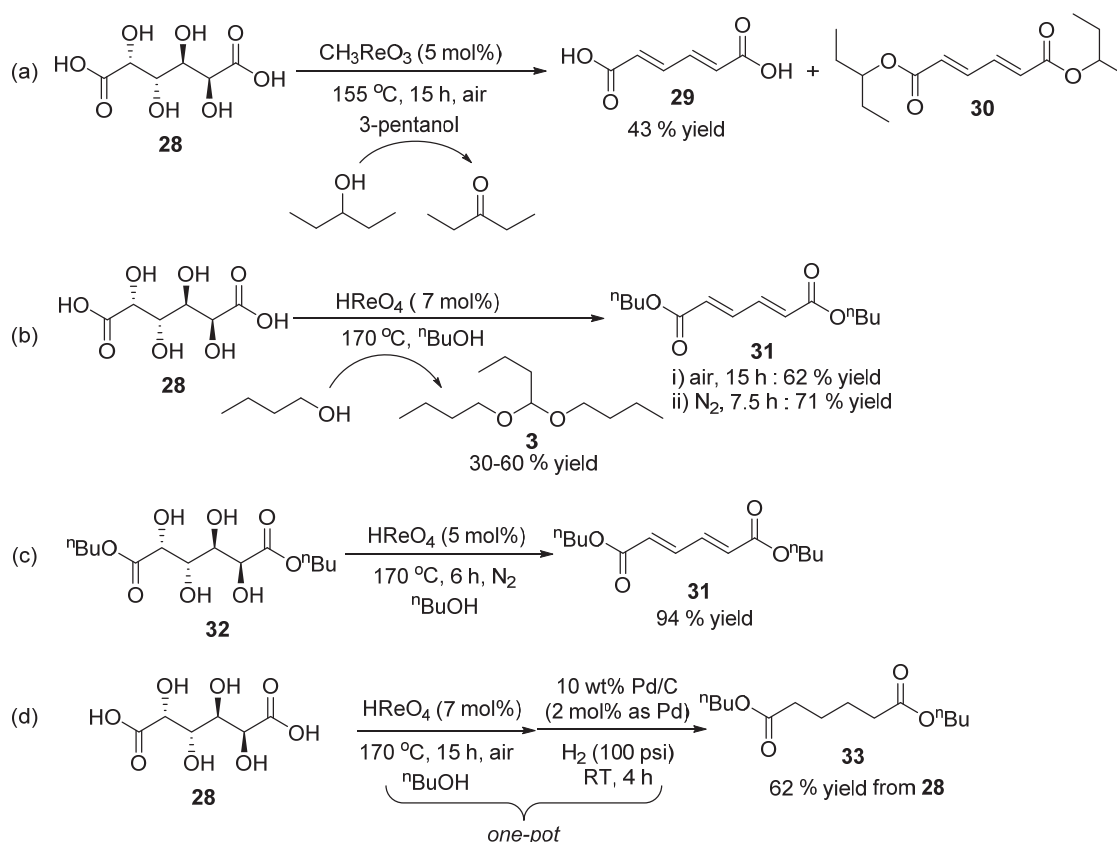


Figure 3 A proposed catalytic cycle for DODH reaction of polyols.

Sugar Acids



Scheme 13 Mucic acid to muconic acid: an example of sugar acid conversion towards commodity chemicals.



Scheme 14 DODH of mucic acid (**28**) and mucic acid dibutyl ester (**32**).

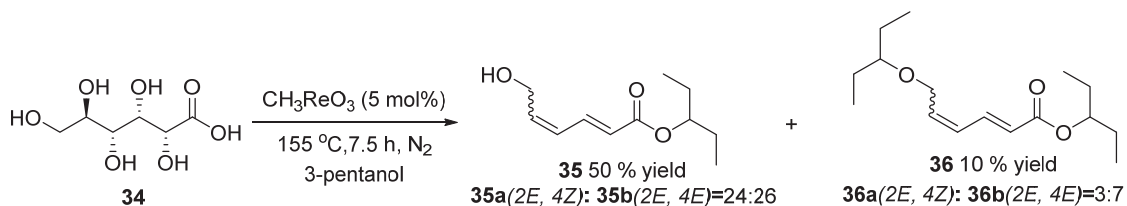
Ensuring the efficiency of polyol DODH reaction, we then turned to applying our system to the production of commodity chemicals from biomass. Realizing that carboxylic acids, esters and amides are prevalent in the chemical industry, sugar acids caught our attention in this regard. Particularly, C6 aldaric acids, obtained by the oxidation of C6 sugars, appeared an exciting target because the expected product muconic acid (*trans, trans*-muconic acid is shown as **29**) has wide utility as a precursor to adipic acid (for nylon 6-6 and adipate plasticizers),^[37] terephthalic acid (for polyethylene terephthalate)^[38] and 1,6-hexanediol (for polyesters^[39] and lubricants^[40]). While the biocatalytic route to produce *cis, cis*-muconic acid from glucose has been reported,^[41]

the chemical conversion would have a significant advantage for scale-up. C6 aldaric acids have four internal hydroxyl groups, but based on our finding of 1,4-DODH, we anticipated muconic acid as a single final product regardless of whether the first DODH takes place at the α,β -position or at the β,γ -position. In addition, as we noted that dehydration is a major competing reaction (see Table 4), which may account for the loss of mass balance in some sugar alcohol reactions (dehydrative decomposition of polyol), we thought the electron withdrawing carboxylic acid group might suppress this pathway by disfavoring the formation of allylic carbocation intermediate.

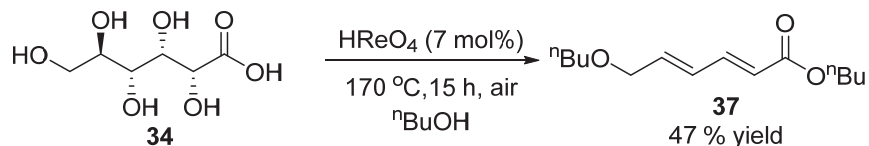
We therefore tested mucic acid (**28**), the oxidized form of galactose, because the stable *trans,trans*-stereochemistry of the product (**29**) was expected both from β,γ -/ α,δ - DODH (sterics) and from α,β -/ γ,δ - DODH (based on the *cis*-diol stereospecificity of DODH reaction). In the initial experiment using MTO and 3-pentanol (reductant/solvent), we obtained **29** in 43 % yield, exclusively in *trans,trans*-stereochemistry (Scheme 14a). However, because MTO is Lewis acidic and the sacrificial alcohol was used in large excess, the diester **30** (14 % yield) was also produced.^[42] Since **30** was easier to manipulate and purify than **29**, which has low solubility in common organic solvents as well as in neutral water, we sought to shift the selectivity toward the ester product. We thus envisioned replacing MTO with perrhenic acid (HReO₄). Previously, we identified HReO₄ as a promising DODH catalyst (see Table 1) but did not fully investigate this species because the reactivity was virtually identical to MTO for sugar alcohol substrates (see Table 3). For sugar acids, however, we thought the Brønsted acidity of HReO₄ may conveniently catalyze both DODH and the *in situ* acid-catalyzed esterification reaction. Gratifyingly, by using a slightly higher temperature and the sterically accessible primary alcohol 1-butanol instead of a secondary alcohol, we indeed obtained *trans,trans*-dibutyl muconate **31** in 62 % yield under air and in 71 % yield under an inert atmosphere (Scheme 14 b).^[43] The DODH reactivity of HReO₄-1-butanol appeared higher than MTO-1-butanol: While the combination of MTO-1-butanol was totally ineffective at 155 °C (cf. Table 2 entry 6), when the reaction shown in Scheme 14b was carried out at 155 °C under air for 15 h, **31** was obtained in 28 % yield. This could be because the majority of the oxidized alcohol (1-butanol) was trapped as acetal (1,1,-dibutoxybutane, **3**) under these conditions, masking the reactive aldehyde species (cf. Scheme 2). The marked difference between MTO and HReO₄ also indicated that they are two distinct species, and it is unlikely that MTO is converted to HReO₄ by water *in situ* to the significant extent. When mucic acid was pre-esterified in refluxing 1-butanol/HCl, thus prepared mucic acid dibutyl ester **32** was converted to **31** in near-quantitative yield, confirming the efficiency of DODH reaction step (Scheme 14 c). In order to emphasize the utility of **29** and **31** in commodity chemical synthesis, we also demonstrated the one-pot two-step conversion of **28** to dibutyl adipate **33**, confirming there is no interference from the Re catalyst during the Pd/C-catalyzed hydrogenation step (Scheme 14d).

Despite our best efforts, we were not able to convert **32** into **31** or **33** using H₂ as the sole reductant in the absence of alcohol, according to the system developed by Abu-Omar et al.^[9] This could be either because the reducing ability of H₂ was lower than alcohols, or because the competing hydrogenation eliminated the 1,4-DODH pathway, or because oligomerization / polymerization took place via Re-catalyzed ether cleavage (e.g. THF ring opening) and its nucleophilic attack to carboxylic acid / ester^[44] in cases where ethereal solvents (described as

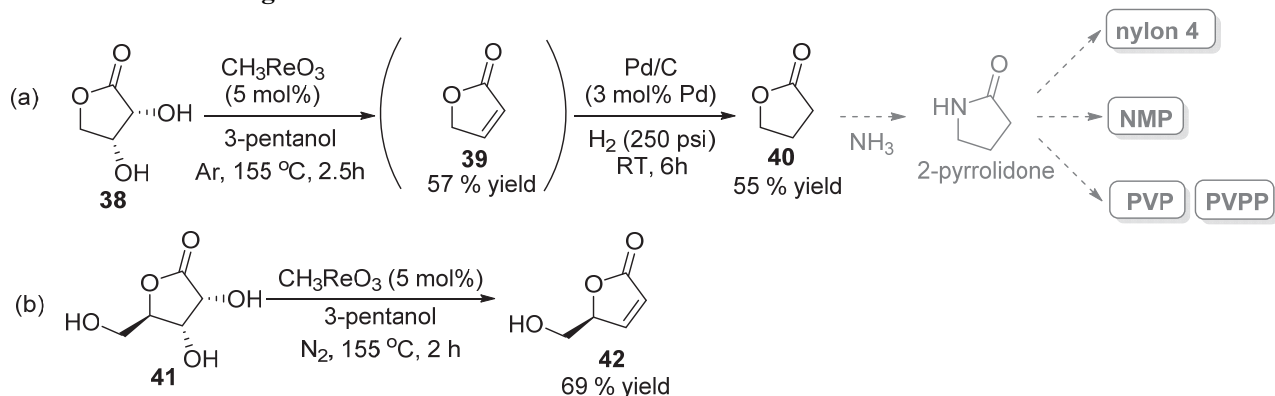
optimal by Abu-Omar et al.) were used. Regarding other C6 aldaric acids, glucaric acid, the oxidized form of glucose, was also investigated but it was not handled as easily as mucic acid. Glucaric acid is commercially available only in its salt form (Na, Ca, K) but these salts were themselves totally unreactive toward DODH. Monopotassium glucarate could be easily derivatized into N,N'-dibenzyl-D-glucaramide (72 % yield)^[45], but this amide also gave no appreciable products. Glucosaminic acid was also unreactive, thus it is possible that nitrogen or any other basic functionality is harmful to the catalysis.^[24c] When monopotassium glucarate was pre-acidified with cation exchange resin, dibutyl muconate was obtained in 25 % yield, with diastereoselectivity of *trans, trans*:*cis, trans*=7:18 (see Appendix for details).



Scheme 15 DODH of gluconic acid with 3-pentanol.



Scheme 16 DODH of gluconic acid with 1-butanol.



Scheme 17 Conversion of D-erythronolactone and D(+)-ribo-1,4-lactone.

Encouraged by the efficient DODH reaction of mucic acid to muconic/adipic acid with the tunability between carboxylic acid and ester products, we also investigated other sugar acids. Considering that adipic acid is the feedstock for nylon 6-6, we first sought to obtain ϵ -caprolactone from C6 aldonic acid for the production of nylon 6. When D-gluconic acid **34** (obtained by the oxidation of D-glucose, supplied as 50 wt % solution in water) was examined, the attempt to preserve the terminal OH group by using the secondary alcohol-CH₃ReO₃

conditions afforded alcohols **35a/35b** in 50 % total yield, with ethers **36a/36b** being the minor products (Scheme 15). In contrast, by using the acidic HReO_4 catalyst, the products converged to (*2E*, *4E*)-ether **37** (Scheme 16). We were delighted to obtain **35-37**, the promising precursor compounds to ϵ -caprolactone: Our preliminary studies, however, found neither forming a seven-membered ring lactone after the hydrogenation of **35a/35b** nor cleaving the ether bond of **37** to be a trivial task. Thus, while our efforts on these downstream conversions are underway, we demonstrated the one-pot two-step conversion of D-erythronolactone (**38**), C4 aldonic acid lactone derivative, to γ -butyrolactone (**40**) via γ -crotonolactone (**39**) (Scheme 17a). Just as ϵ -caprolactone, it is known that treatment of **40** with NH_3 furnishes 2-pyrrolidone,^[46] which can be converted into nylon 4.^[47] 2-Pyrrolidone is also a valuable precursor to *N*-methylpyrrolidone (NMP), polyvinylpyrrolidone (PVP) and polyvinylpolypyrrolidone (PVPP).^[48] Additionally, D-(+)-ribo-1,4-lactone (**41**), a C5 aldonic acid lactone derivative, was also converted to **42** in good yield without optimization (Scheme 17b), confirming that the five-membered ring lactone is relatively rigid (stable toward alcoholysis) and that the ethers obtained in Scheme 15 and 16 were presumably formed via a pentadienyl cation-type intermediate instead of the dehydrative ether formation of the primary alcohol, analogously to C5 sugar alcohols (see Scheme 5). We are currently also exploring the utility of this product **42** in fine chemical applications.

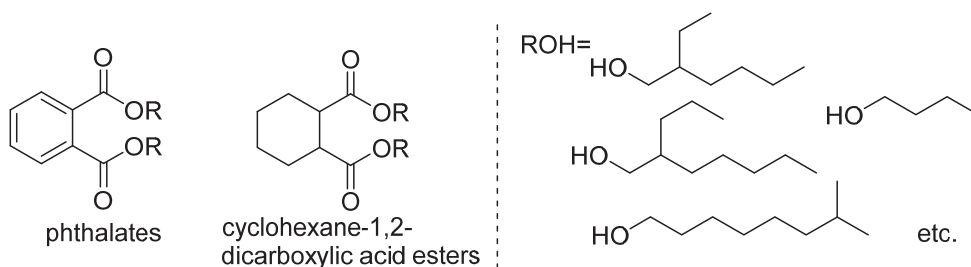
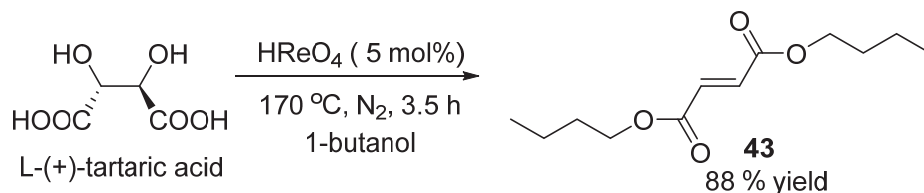
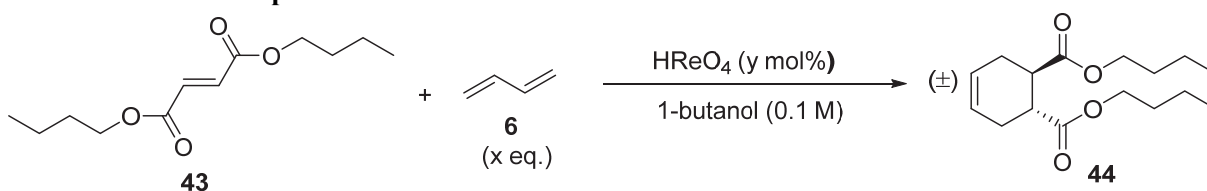


Figure 4 The common plasticizer structures.



Scheme 18 DODH of L-(+)-tartaric acid with 1-butanol.

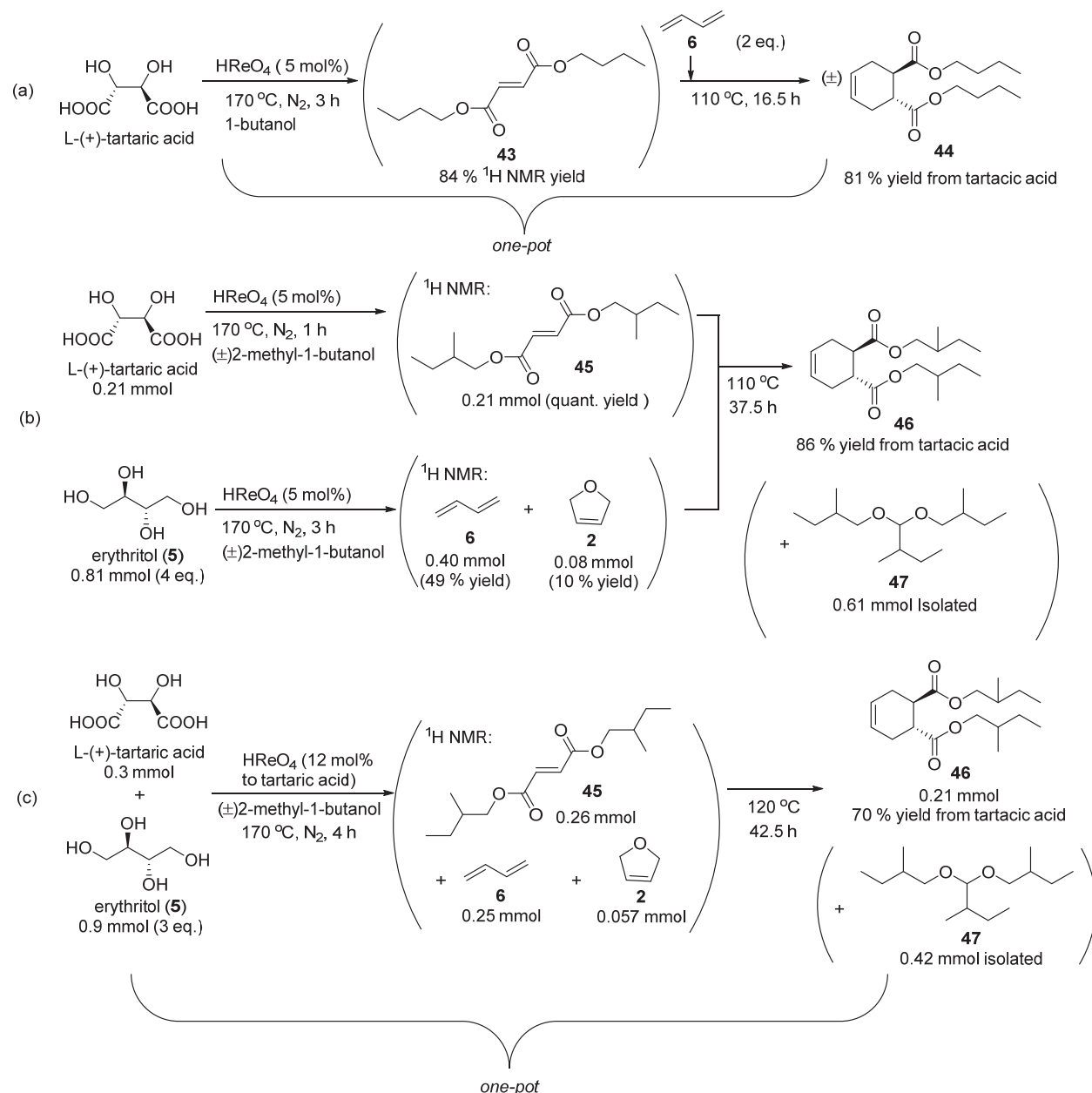
Table 5 The condition optimization for Diels-Alder reaction.

entry	temp. (°C)	time (h)	x (eq.)	y (mol%)	44 yield	43 conv. (%)
1	170	4.5	2.5	5	17	22
2	155	4.5	2.5	5	14	27
3	130	13.5	2.5	5	68	68
4	110	13.5	2.5	5	75	93
5	110	13.5	2.5	10	85	89
6	110	13.5	3.2	5	78	92
7	110	13.5	1.5	5	67	82
8 ^[a]	110	4.5	2.5	5	20	20
9 ^[a]	110	4.5	2.5	0	17	31
10	80	17	2.5	5	39	46
11	RT	17	2.5	5	0	0

[a] In toluene instead of 1-butanol.

Finally, in order to demonstrate the further utility of the DODH reaction in the synthesis of biomass-derived commodity chemicals, we sought to combine a DODH reaction with other reactions, given the unique capability of HReO₄ to act as a DODH/acid dual-catalyst. Noting that plasticizers have a large market in industry and they consist mostly of phthalates and more recently of cyclohexane-1,2-dicarboxylic acid esters (claimed lower toxicity than phthalates)^[49] shown in Figure 4, we aimed to construct the 4-cyclohexene-1,2-dicarboxylic acid ester structure (e.g. **44**) from L-(+)-tartaric acid (naturally abundant C4 aldaric acid) and erythritol (**5**) by combining DODH, esterification and Diels-Alder reaction. The alkene functionality of this compound would serve as a good manipulation handle to either oxidize or disproportionate to phthalates,^[50] or to hydrogenate to cyclohexane-1,2-dicarboxylic acid esters. As the conversion of erythritol to butadiene was established previously (Table 3), we first confirmed the efficiency of L-(+)-tartaric acid DODH. As expected, dibutyl fumarate **43** was isolated in good yield (88 %, Scheme 18). When *meso*-tartaric acid was used instead, dibutyl maleate was isolated in 75 % yield. However, it was soon realized that the Diels-Alder reaction of **43** and butadiene **6** is inefficient at the temperature where DODH is operative (155-170 °C) (Table 5, entries 1 and 2). The decomposition of butadiene prevailed at this temperature after extended reaction times. The optimum temperature was found to be ca. 110 °C (entry 4). Changing the catalyst loading or the amount of butadiene affected the yield of **44** only slightly (entries 5-7) and it was furthermore found that the thermal Diels-Alder reaction also takes place at a similar rate to 5 mol% HReO₄-catalyzed conditions (entries 8 and 9). Therefore, despite the initial inspiration of using HReO₄ as the esterification/DODH/Diels-Alder tri-purpose catalyst, it appears the HReO₄ is not significantly accelerating the Diels-Alder reaction step. Considering the length of the required reaction time, we think that the high steric hindrance around the double bond of moiety **43** is

limiting the reaction rate, while **43** is electronically active enough to undergo the addition to butadiene and to prevent the retro Diels-Alder reaction at this temperature.

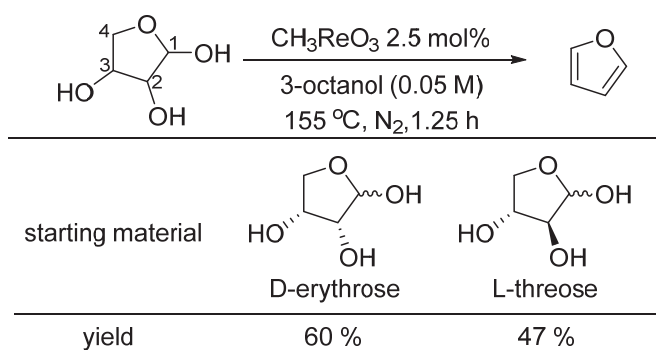


Scheme 19 Conversion of L-(+)-tartaric acid and erythritol to plasticizer precursor **44**, **46**.

The investigation above directed us to the two-step process consisting of (1) DODH reaction at 155-170 °C and (2) Diels-Alder reaction at ca. 110 °C. First, in a one-pot two-step process using butadiene, **44** was isolated in 81 % yield (Scheme 19a). When we subsequently studied the substitution of butadiene with erythritol, we changed the alcohol to 2-methyl-1-butanol, because it features the branched aliphatic chain commonly used in plasticizers. In a two-pot two-step

procedure converting L-(+)-tartaric acid to **45** and erythritol to butadiene separately before combining two streams, **46** was isolated in 86 % yield (Scheme 19b). Finally, in the most operationally straightforward one-pot two-step procedure, DODH of the mixture of L-(+)-tartaric acid and erythritol followed by the Diels-Alder reaction furnished **46** in 70 % yield (Scheme 19c). This reaction combines the total deoxygenation of the sugar alcohol to unsaturated hydrocarbons and the selective deoxygenation of the sugar acid preserving the ester group, and exemplifies the capability of the DODH reaction to construct the structures with very specific functionality from biomass-derived polyols. It also underscores the advantage of the DODH reaction over conventional biomass deoxygenation methods such as hydrogenation and hydrogenolysis, in that the product alkenes are deoxygenated but still synthetically versatile.

Sugars



Scheme 20 Deoxygenation of tetroses.

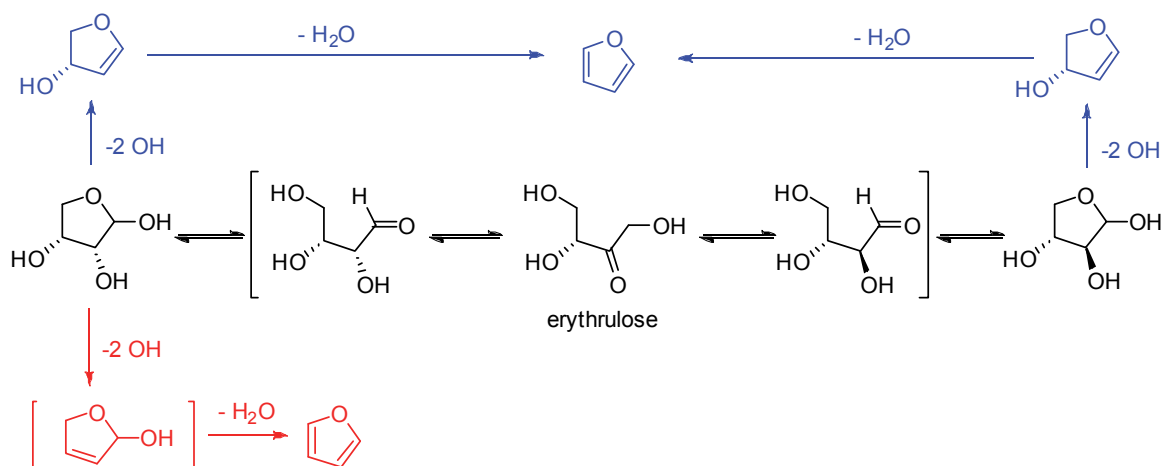
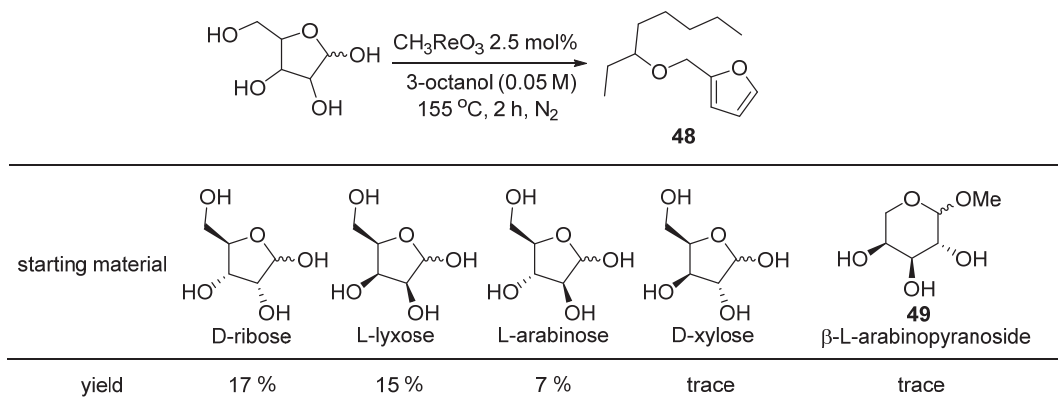


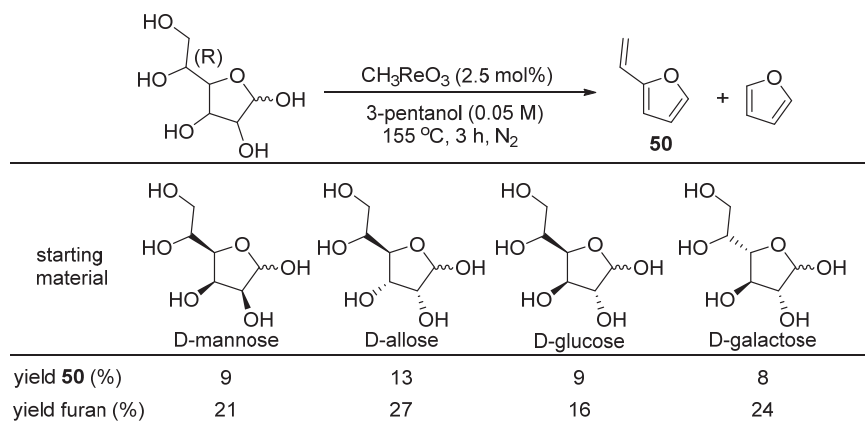
Figure 5 Possible pathways of tetrose DODH.

We are currently investigating the application of this methodology to sugars, the most direct feedstock from biomass but arguably the most challenging substrate due to their thermal instability as well as the complexity associated with the equilibrium between multiple isomeric forms (furanose/pyranose, aldose/ketose, α -isomer/ β -isomer); a critical consideration given the *cis*-diol specificity of oxorhenium-catalyzed DODH reaction. When we first examined tetroses to assess the effect of aldose functionality, both D-erythrose and L-threose afforded furan (via DODH reaction followed by dehydration) in comparable yields (Scheme 20). The high reactivity of threose in our DODH process can have two plausible explanations; (1) DODH of the C-1 and C-2 hydroxyl groups, and (2) the epimerization of the C-2 hydroxyl group via erythrulose (Figure 5). The DODH of internal diol (C2 and C3 hydroxyl groups) in the open-chain form is unlikely because threose would then yield (*E*)-4-hydroxybut-2-enal, which cannot re-cyclize due to the *trans* geometry. While this experiment alone could not specify which pathway was

operative, it suggested that the *cis*-stereochemistry requirement of DODH is not necessarily stringent for sugars when the epimerization on C-1 and C-2 hydroxyl groups can provide access for the substrate to funnel through to the stable, deoxygenated product. Similar to the inositol case, once the first DODH reaction occurs, the resulting alkene directs the dehydration reaction to produce a stable compound (in this case furan) given the appropriate structure. This appears a very effective strategy to achieve a good selectivity in the DODH-based sugar deoxygenation reaction. We also examined HReO_4 as catalyst for sugar substrates, with the hope of promoting the equilibration between isomers as well as the subsequent dehydration by acidity. However, sugars were extremely acid-sensitive at elevated temperatures and the immediate complete decomposition occurred even at a much reduced catalyst loading.



Scheme 21 Deoxygenation of pentoses.



Scheme 22 Deoxygenation of hexoses.

The combination of DODH and aromatization-driven dehydration reaction was also applicable to pentoses and hexoses and our preliminary results are rather promising. For pentoses, the predominant product obtained was ether **48** (Scheme 21). The furfuryl alcohol ethers are relatively stable and high energy content potential biodiesel candidates.^[51] Moieties like **48** are thus conventionally produced via the dehydration of xylose/arabinose to furfural, followed by

hydrogenation and etherification with alcohol.^[52] Although the yields are currently low, it is interesting that the same class of compound was obtained in one-pot from sugars based on the different mechanism, without the addition of external hydrogen. It is reasonable to expect that **48** is derived from furanose form, while the majority of pentoses exist in pyranose form in solutions. The fact that D-ribose and L-lyxose, which possess the *cis*-diol structure on C-2/C-3, were more reactive than L-arabinose and D-xylose does not contradict this hypothesis. It is uncertain whether the pyranose isomer underwent DODH or not. Although 2H-pyran or related structure was not detected, it is possible that the decomposition occurred to those moieties under reaction conditions due to their limited stability compared to **48**. When the isomerization of L-arabinose was prevented by methoxy protection on C-1 position, no appreciable products were obtained from methyl β -L-arabinopyranoside **49**, supporting this hypothesis. However, because the overall efficiency of pentose DODH is still very low, it is safer to wait the detailed discussion on the reactivity until the yields are optimized. Finally, applying the same strategy to hexoses, 2-vinylfuran (**50**), another interesting chemical candidate for material application,^[53] was obtained (Scheme 22). Interestingly, it was accompanied by the significant formation of furan. We propose the retro-aldol reaction of the common intermediate (Figure 6), but due to the volatility, acetaldehyde was not quantified.

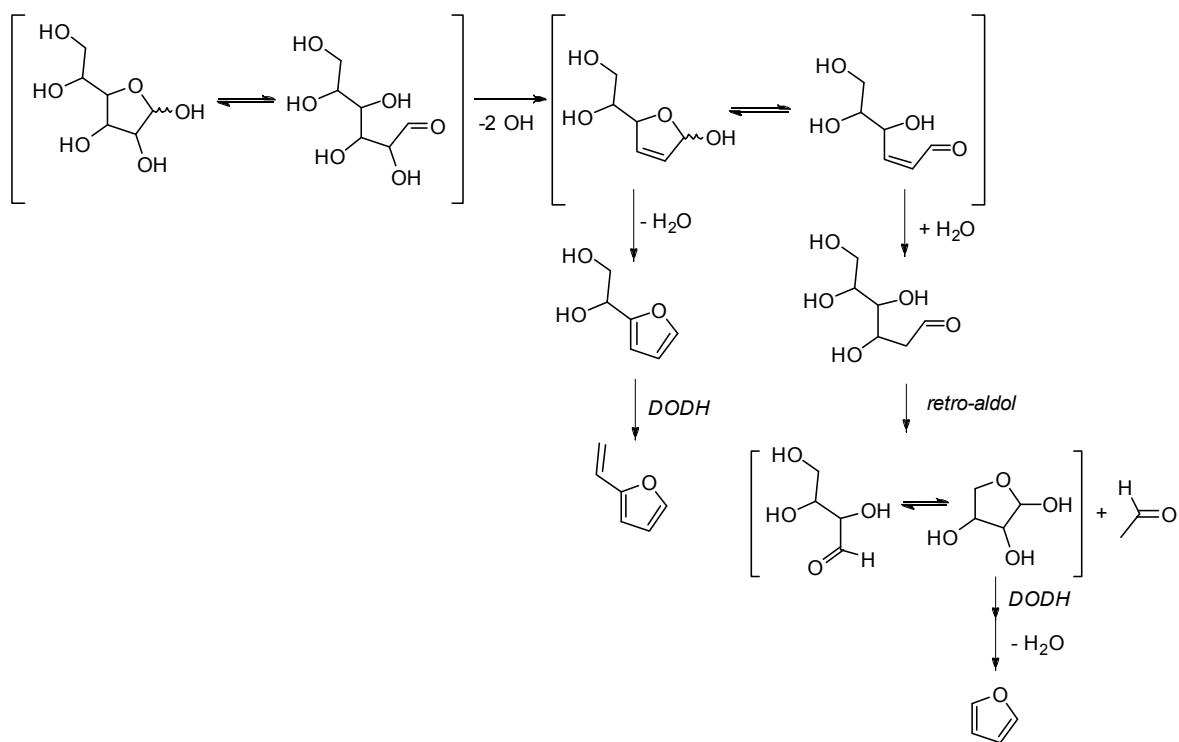


Figure 6 Retro-aldol reaction as a possible mechanism for formation of furan from hexoses.

Conclusion

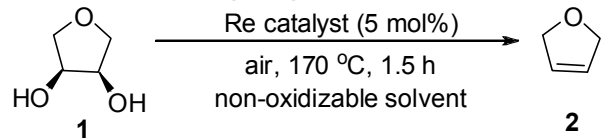
In summary, we have developed an oxorhenium-catalyzed DODH reaction using alcohol as a reductant and successfully achieved the deoxygenation of biomass-derived polyols, namely, sugar alcohols, sugar acids and sugars. CH_3ReO_3 and HReO_4 showed much higher activity than the previously reported rhenium-carbonyl catalysts and enabled the DODH reaction to be applied to those substrates which are challenging in terms of selectivity and thermal stability. We observed a remarkable product selectivity toward total DODH products over partial DODH products; i.e. in most cases only one single product was obtained from the polyol DODH in appreciable yields. Besides the *cis*-diol stereospecificity, one plausible explanation was provided by our finding of the novel modes of DODH on 2-ene-1,4-diols (1,4-DODH) and on 2,4-diene-1,6-diols (1,6-DODH) in addition to the conventional vicinal diol DODH (1,2-DODH). Insights on the DODH mechanism were garnered by studying the proposed catalytic cycle step-wise (1. the reduction of Re^{VII} to Re^{V} by alcohol, 2. Diol coordination to Re^{V} and 3. olefin extrusion) using the isolated Re^{V} species. The viability of the use of bio-derived alcohols such as 1-butanol in the DODH reaction was also established, especially for HReO_4 catalyst. Sugar alcohols yielded linear polyene products, possible feedstock for polyolefin materials and fuels. Sugar acids were converted into correspondent unsaturated acids/esters/lactones, the high-potential building blocks for various commodity chemicals. A benchmark example from this work is the production of adipic acid (for nylon 6,6) from mucic acid (from galactose). Combining DODH with subsequent dehydration reaction, sugars were converted into furan moieties. Despite the currently moderate yields, these are the first examples of direct DODH reaction of sugars and consist a major advantage in the development of DODH-based biomass conversion methodologies. Future work will include increasing the efficiency of sugar DODH, exploring the utility of 1,4- and 1,6-DODH, further substrate scope expansion and investigation on functional group tolerance, application to oligo/polysaccharides and other biomass-based feedstock, immobilization/recycling of the catalyst and designing the suitable continuous flow reactor system.

Appendix

1. Control experiment with no reductant

In 2011, Fernandes et al. reported that the aryl epoxides can be deoxygenated to alkenes with no reductant in the presence of rhenium catalysts. As they proposed the diol resulting from the hydrolytic epoxide ring opening (e.g. 1-phenyl-1,2-ethanediol from styrene oxide) as an intermediate,^[12] we examined if such a reductant-free deoxygenation is indeed responsible for our diol DODH reaction in alcohols. As shown in Table 3, we tested the DODH of **1** without alcohol reductant using DODH-active oxorhenium catalysts (cf. Table 1). When MTO was used as catalyst, **2** was not formed; **1** was unreactive in dioxane or chloroform (entries 1-2) and unknown decomposition occurred in toluene (entries 3 and 4). PPh₃ ligands on ReIO₂(PPh₃)₂ appeared to act as a stoichiometric reducing agent, affording **2** in up to 10 % yield (entries 5 and 6). Also, when 1,2-dodecanediol was heated in refluxing toluene with 10 mol% ReIO₂(PPh₃)₂, no 1-dodecene was detected after 80 min. We thus concluded that the reductant-free DODH does not occur for aliphatic diols.

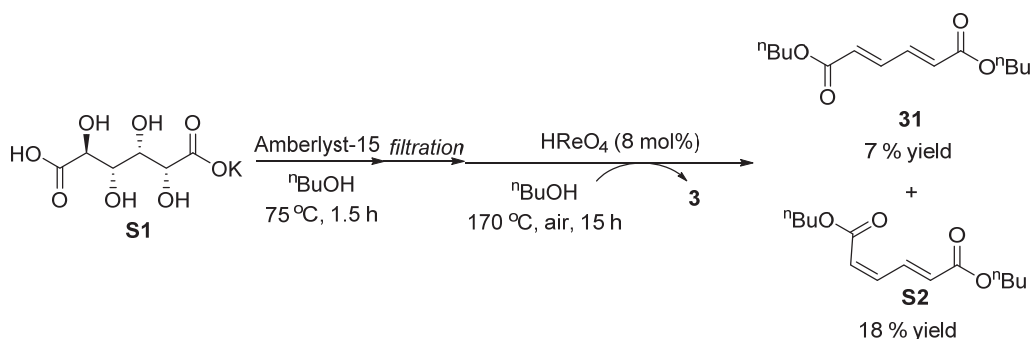
Table 3 Control experiments without reducing reagents.



entry	Re catalyst	solvent	yield (%)	conv. (%)
1	CH ₃ ReO ₃	dioxane	0	4
2	CH ₃ ReO ₃	CDCl ₃	trace	23
3	CH ₃ ReO ₃	toluene-d ₈	1	91
4 ^[a]	CH ₃ ReO ₃	toluene-d ₈	0	85
5	ReIO ₂ (PPh ₃) ₂	toluene-d ₈	10	45
6	ReIO ₂ (PPh ₃) ₂	THF	8	18

[a] 110 °C, 3 h.

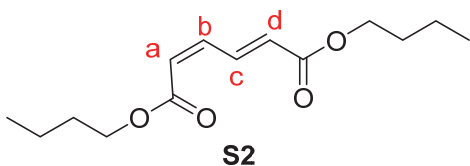
2. Monopotassium D-glucarate (**S1**) to diⁿbutyl muconate (**31** and **S2**)



E. Kiely et al. has described that the acidification of D-saccharic acid potassium salt (**S1**) with cation exchange resin Rexyn 101 or HCl in methanol at room temperature furnishes the mixture of dimethyl D-glucarate, methyl D-glucarate 1,4-lactone and methyl D-glucarate 6,3-lactone.^[45]

Using the similar protocol, monopotassium D-glucarate (**S1**) 249 mg (1.0 mmol), Amberlyst-15 (503 mg, 200 wt%), 1-butanol (2 mL) were charged in a flask equipped with a stir bar, and heated at 75 °C^[54] with magnetic stirring for 1.5 h. During this time, the white suspension above Amberlyst-15 became a clear solution. This mixture was cooled to room temperature and filtered into a Parr stainless-steel reactor vessel (50 mL). The filtered Amberlyst was washed with 18 mL of 1-butanol and combined. HReO₄ (76.5 % in H₂O solution 26.6 mg, 0.080 mmol) was added, the vessel was sealed and heated at 170 °C with mechanical stirring for 15 h. After cooling to room temperature, the dark brown mixture was transferred to a flask, concentrated and purified by flash column chromatography (Hexanes: EtOAc = 40:1 to 17:1) to afford a mixture of **31** and **S2** (64.4 mg, 25 % yield total, **31**:**S2**=7:18 by ¹H NMR) as well as 1,1-dibutoxybutane **3** (87.4 mg, 0.43 mmol, 22 % yield).

S2 was characterized after second flash column chromatography (Hexanes: CH₂Cl₂ = 2:1 to 1:2) to separate **S2** from **31**. ¹H NMR of the alkene region was similar to that of the known *trans*, *cis*-muconic acid dimethyl ester.^[55] ¹H NMR (CDCl₃, 600 MHz): δ8.37 (Hc, dd, 1H, *J*=11.4, 15.6 Hz), 6.63 (Hb, dd (apparent t), 1H, 11.4, 11.4 Hz), 6.10 (Hd, d, 1H, *J*=15.6 Hz), 5.96 (Ha, d, 1H, *J*=11.4 Hz), 4.183 (t, 2H, *J*=6.6 Hz), 4.181 (t, 2H, *J*=6.6 Hz), 1.63-1.70 (m, 4H), 1.36-1.45 (m, 4H), 0.953 (t, 3H, *J*=7.2 Hz), 0.946 (t, 3H, *J*=7.2 Hz). ¹³C NMR (CDCl₃, 150 MHz): δ166.12, 165.41, 140.31(b), 138.47(c), 128.99(d), 124.67(a), 64.62, 64.53, 30.64, 30.58, 19.14, 19.10, 13.67, 13.65. (The proton and carbon assignments of double bond region are based on COSY and HSQC analysis.) EI-HRMS (EI⁺): C₁₄H₂₂O₄ ([M]⁺) calc'd 254.1518, found 254.1518.



In a separate batch, D-saccharic acid potassium salt (**S1**) 500 mg (2.0 mmol), Amberlyst-15 (1.0 g, 200 wt%), 1-butanol (4 mL) were charged in a flask equipped with a stir bar, and heated at 75 °C with magnetic stirring for 3 h. This mixture was cooled to room temperature and filtered into a flask. The filtered Amberlyst was washed with 1-butanol and combined. The filtrate was concentrated under reduced pressure to yield 194.2 mg of pale-brown thick liquid. Its ¹H NMR spectra is shown in Figure 7. Using Dowex 50W-X8 instead of Amberlyst-15 provided the virtually identical result.

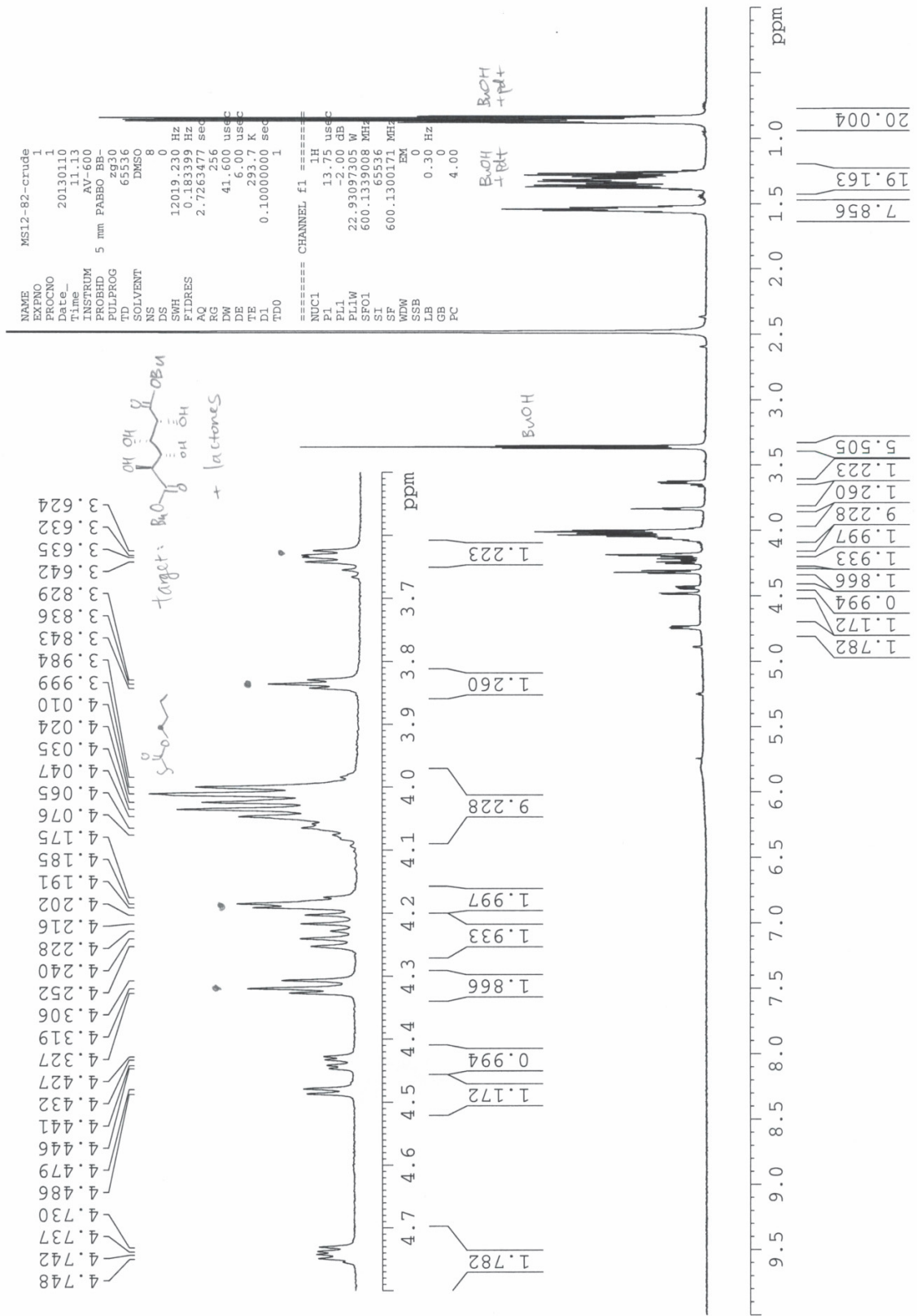
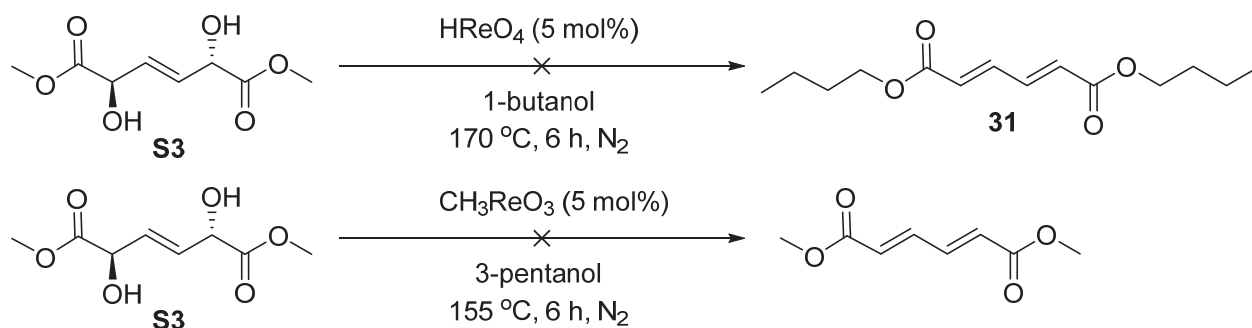


Figure 7 ^1H NMR spectra of monopotassium D-glucarate (S1) acidified in 1-butanol (DMSO- d_6 , 600 MHz).

3. 1,4-DODH of dimethyl (2*R*,5*S*,*E*)-2,5-dihydroxyhex-3-enedioate (**S3**)



Scheme 23 Attempted 1,4-DODH reactions of **S3**.

During the investigation of 1,4-DODH, we realized that the dehydration is a competing pathway (Table 4). In an attempt to avoid this side-reaction, we investigated **S3** as a 2-ene-1,4-diol bearing electron withdrawing groups. However, despite our expectation, no diene products were observed by ^1H NMR under the standard conditions while the starting material (**S3**) was all consumed. We were unable to identify the specific decomposition products. We do not have a clear explanation of the inferior reactivity of **S3** to other 1,4-diols, because **S3** is the substrate most relevant to mucic acid DODH which was indeed very successful (Scheme 14). It is possible that **S3** is too reactive and the milder conditions were needed. The transesterification on both sides also seems to add another layer of complexity. No further studies were conducted on this substrate.

4. X-ray crystal structure of dimethyl (2*R*,5*S*,*E*)-2,5-dihydroxyhex-3-enedioate (**S3**)

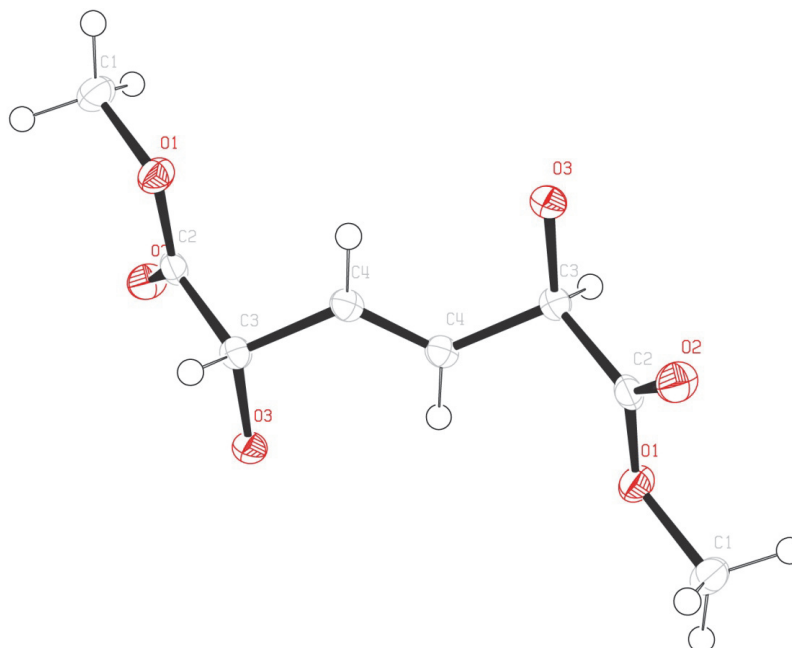


Table A1. Crystal data and structure refinement for **S3**.

Identification code	shelxl	
Empirical formula	C ₈ H ₁₂ O ₆	
Formula weight	204.18	
Temperature	100(2) K	
Wavelength	1.54178 Å	
Crystal system	Monoclinic	
Space group	P2(1)/c	
Unit cell dimensions	a = 7.8708(7) Å	α = 90°.
	b = 4.0736(3) Å	β = 96.925(3)°.
	c = 14.4856(12) Å	γ = 90°.
Volume	461.06(7) Å ³	
Z	2	
Density (calculated)	1.471 Mg/m ³	
Absorption coefficient	1.107 mm ⁻¹	
F(000)	216	
Crystal size	0.10 x 0.05 x 0.05 mm ³	
Theta range for data collection	5.66 to 68.56°.	
Index ranges	-9 ≤ h ≤ 9, -4 ≤ k ≤ 4, -17 ≤ l ≤ 17	
Reflections collected	6452	
Independent reflections	839 [R(int) = 0.0178]	
Completeness to theta = 67.00°	99.8 %	
Absorption correction	Multi_scan	
Max. and min. transmission	0.9467 and 0.8974	
Refinement method	Full-matrix least-squares on F ²	
Data / restraints / parameters	839 / 0 / 66	
Goodness-of-fit on F ²	1.087	
Final R indices [I > 2σ(I)]	R1 = 0.0283, wR2 = 0.0773	
R indices (all data)	R1 = 0.0286, wR2 = 0.0776	
Largest diff. peak and hole	0.284 and -0.191 e.Å ⁻³	

Table A2. Atomic coordinates ($\times 10^4$) and equivalent isotropic displacement parameters ($\text{\AA}^2 \times 10^3$) for **S3**. $U(\text{eq})$ is defined as one third of the trace of the orthogonalized U^{ij} tensor.

	x	y	z	$U(\text{eq})$
O(2)	7674(1)	844(2)	2970(1)	23(1)
O(3)	4354(1)	-180(2)	3268(1)	20(1)
C(1)	10351(1)	-2161(3)	3886(1)	24(1)
C(2)	7399(1)	-1045(3)	3576(1)	17(1)
C(3)	5625(1)	-1871(3)	3844(1)	17(1)
C(4)	5567(1)	-1014(3)	4857(1)	16(1)
O(1)	8615(1)	-2679(2)	4104(1)	20(1)

Table A3. Bond lengths [\AA] and angles [$^\circ$] for **S3**.

O(2)-C(2)	1.2055(13)
O(3)-C(3)	1.4042(13)
O(3)-H(3A)	0.8400
C(1)-O(1)	1.4538(13)
C(1)-H(1A)	0.9800
C(1)-H(1B)	0.9800
C(1)-H(1C)	0.9800
C(2)-O(1)	1.3294(13)
C(2)-C(3)	1.5317(14)
C(3)-C(4)	1.5134(14)
C(3)-H(3)	1.0000
C(4)-C(4)#1	1.319(2)
C(4)-H(4)	0.9500
C(3)-O(3)-H(3A)	109.5
O(1)-C(1)-H(1A)	109.5
O(1)-C(1)-H(1B)	109.5
H(1A)-C(1)-H(1B)	109.5
O(1)-C(1)-H(1C)	109.5

H(1A)-C(1)-H(1C)	109.5
H(1B)-C(1)-H(1C)	109.5
O(2)-C(2)-O(1)	123.93(10)
O(2)-C(2)-C(3)	125.02(10)
O(1)-C(2)-C(3)	111.05(9)
O(3)-C(3)-C(4)	111.13(9)
O(3)-C(3)-C(2)	110.31(9)
C(4)-C(3)-C(2)	109.28(8)
O(3)-C(3)-H(3)	108.7
C(4)-C(3)-H(3)	108.7
C(2)-C(3)-H(3)	108.7
C(4)#1-C(4)-C(3)	123.37(12)
C(4)#1-C(4)-H(4)	118.3
C(3)-C(4)-H(4)	118.3
C(2)-O(1)-C(1)	115.65(8)

Symmetry transformations used to generate equivalent atoms:

#1 -x+1,-y,-z+1

Table A4. Anisotropic displacement parameters ($\text{\AA}^2 \times 10^3$) for **S3**. The anisotropic displacement factor exponent takes the form: $-2 \pi^2 [h^2 a^{*2} U_{11} + \dots + 2 h k a^* b^* U_{12}]$

	U11	U22	U33	U23	U13	U12
O(2)	20(1)	29(1)	19(1)	6(1)	5(1)	0(1)
O(3)	18(1)	25(1)	15(1)	-2(1)	-1(1)	0(1)
C(1)	16(1)	32(1)	25(1)	1(1)	5(1)	3(1)
C(2)	20(1)	18(1)	12(1)	-3(1)	2(1)	0(1)
C(3)	17(1)	19(1)	14(1)	0(1)	2(1)	0(1)
C(4)	16(1)	19(1)	14(1)	2(1)	2(1)	-3(1)
O(1)	17(1)	26(1)	19(1)	3(1)	4(1)	3(1)

Table A5. Hydrogen coordinates ($\times 10^4$) and isotropic displacement parameters ($\text{\AA}^2 \times 10^3$) for **S3**.

	x	y	z	U(eq)
H(3A)	3886	-1463	2860	29
H(1A)	10470	-3106	3275	36
H(1B)	11161	-3228	4359	36
H(1C)	10592	198	3877	36
H(3)	5425	-4283	3762	20
H(4)	6390	-1985	5309	19

Experimental

1. General information

Commercial materials and solvents were reagent grade and used as received. ^1H , ^{13}C NMR spectra were recorded with Bruker AV-300, AVB-400, AVQ-400, DRX-500, and AV-600 spectrometers; chemical shifts are reported in ppm. The proton and carbon assignments were based on COSY, HSQC, splitting patterns and the chemical shifts. EI and ESI MS data were obtained in the QB3 Analytical Facility operated by the College of Chemistry, University of California, Berkeley. GC analysis was carried out using a Varian CP-3800 gas chromatograph equipped with a flame ionization detector coupled to a Varian 320-MS mass spectrometer using a FactoFour capillary column (VF-5 ms, 30 m length, 0.25 mm diameter) coated with a 0.25 mm thick stationary phase (5% phenyl and 95% dimethylpolysiloxane). Thin-layer chromatography (TLC) analysis was performed using Merck silica gel 60 F254 TLC plates, and visualized by UV(254/365 nm) or by staining with *p*-anisaldehyde, cerium ammonium molybdate, phosphomolybdic acid or potassium permanganate. Flash column chromatography was carried out on Merck 60 silica gel (32–63 μm). The reactions under auto-generated pressure (i.e. reaction temperature higher than the boiling point of solvent or product) were carried out either in a Parr4560 mini-reactor (with monitoring and control of the internal temperature and mechanical stirring) or in a Biotage microwave vials (10-20mL, 2-5 mL or 0.5-2 mL) equipped with a magnetic stir bar and fitted with a septum cap.

2. DODH reactions

I. Sugar alcohols, inositols and sugars

a) Representative procedure A: DODH of sorbitol

D-sorbitol (36.4 mg, 0.20 mmol) and CH_3ReO_3 (1.2 mg, 0.0050 mmol) was charged in a Biotage microwave vial (10-20mL) equipped with a magnetic stir bar. The vial was purged with N_2 (vacuum/ N_2 cycles, 3 times) and sealed with a cap with septum. 3-pentanol (4 mL) was added through the septum and the vial was immersed in an oil bath pre-heated to 200 $^\circ\text{C}$. The reaction mixture was stirred at the same temperature for 1 h, during which the suspension became a homogeneous solution. The vial was quickly cooled with an ice bath, mesitylene (16.2 mg, 0.13 mmol) was added as an internal standard and mixed well. An aliquot (~ 0.1 mL) of sample was taken, diluted with CDCl_3 (~ 0.8 mL) and analyzed by ^1H NMR. The product peaks of olefin were used for yield calculation. In some cases, mesitylene was added initially to the reaction mixture before heating starts. Same results were obtained from both procedures.

b) Representative procedure B: DODH of inositols

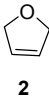
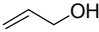
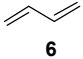
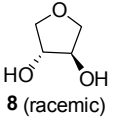
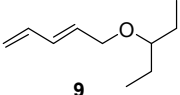
Inositol (9.0 mg, 0.050 mmol) was charged in a Biotage microwave vial (0.5-2 mL) equipped with a magnetic stir bar. The vial was purged with N_2 and sealed. CH_3ReO_3 was added as a 3-pentanol solution (0.00125 mmol/mL, 1 mL). The reaction mixture was immersed to the pre-heated oil bath and heated with magnetic stirring. Upon cooling, mesitylene (internal standard) was added as a 3-pentanol solution (100 μL of 40 mg/mL solution). An aliquot of sample was diluted with CDCl_3 and analyzed by ^1H NMR, GC-FID and GC-MS.

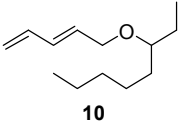
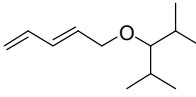
c) Product identification

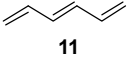
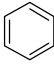
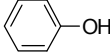
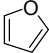
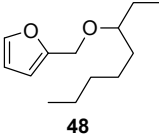
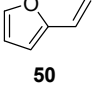
NMR and other compound characterization data are listed below. The product peaks in the olefin region of ^1H NMR spectra were used for yield calculation. ^1H NMR peak of internal standard (mesitylene) (500 MHz, CDCl_3): δ 6.78 (s, 3 H, used for calculation), 2.28 (s, 9H).

Note that the ^1H NMR peaks of phenol were shifted in the reaction mixture from the ones in pure CDCl_3 due to the significant (~10 %) presence of solvent/reductant alcohol. The same shift was observed when a commercial authentic sample of phenol was analyzed by ^1H NMR in the identical solvent mixture (i.e. 10 % 3-octanol or 3-pentanol in CDCl_3).

Table 4 Identification data for DODH products.

entry	product	structure	NMR data	Other Identification
1	2,5-dihydrofuran	 2	^1H NMR (CDCl_3 , 500 MHz): δ 5.87 (s, 2H), 4.62 (s, 4H), ^{13}C NMR (toluene- d_8 , 150 MHz): δ 126.08, 74.86.	A), B)
2	allyl alcohol		^1H NMR (CDCl_3 , 400 MHz): δ 5.99 (m, 1H), 5.27 (d, 1H, $J=17.2$ Hz), 5.13 (d, 1H, $J=10.4$ Hz), 4.14 (d, 2H, $J=4.8$ Hz)	A), B)
3	1,3-butadiene	 6	^1H NMR (CDCl_3 , 500 MHz): δ 6.36 (m, 2H), 5.24 (d, 2H, $J=12.4$ Hz), 5.12 (d, 2H, $J=7.2$ Hz)	A), B)
4	1,4-anhydrothreitol (racemic)	 8 (racemic)	^1H NMR (CDCl_3 , 500 MHz): δ 4.24 (s, 2H), 4.08 (dd, 2H, $J=9.8, 3.8$ Hz), 3.75 (d, 2H, $J=10.0$ Hz)	B)
5	(<i>E</i>)-5-(pentan-3-yloxy)penta-1,3-diene	 9	^1H NMR (CDCl_3 , 500 MHz): δ 6.38 (dt, 1H, $J=17.0, 10.5$ Hz), 6.28 (dd, 1H, $J=15.0, 10.3$ Hz), 5.83 (dt, 1H, $J=15.0, 6.0$ Hz), 5.23 (d, 1H, $J=17.0$ Hz), 5.11 (d, 1H, $J=10.0$ Hz), 4.05 (d, 2H, $J=6.0$ Hz),	D) HRMS (EI) calc'd for $[\text{C}_{10}\text{H}_{18}\text{O}]^+$ 154.1358, found: 154.1363.

			3.26-3.12 (m, 1H), 1.58-1.46 (m, 4H), 0.93 (t, 6H, $J=7.5$ Hz) ^{13}C NMR (CDCl_3 , 125 MHz): δ 136.56, 132.48, 131.16, 117.15, 81.44, 68.98, 25.96, 9.63	
6	(<i>E</i>)-3-(penta-2,4-dienyloxy)octane	 10	^1H NMR (CDCl_3 , 500 MHz): δ 6.40 (dt, 1H, $J=17.0, 10.5$ Hz), 6.30 (dd, 1H, $J=15.0, 10.5$ Hz), 5.84 (dt, 1H, $J=10.0$ Hz), 5.25 (d, 1H, $J=16.5$ Hz), 5.13 (d, 1H, $J=10.0$ Hz), 4.07 (fused multiplet, br, 2H), 3.28 (quintet, 1H, $J=6.0$ Hz), 1.6-1.2 (m, 12H), 0.95 (t, 3H, $J=7.5$ Hz), 0.94 (t, 3H, $J=7.0$ Hz) ^{13}C NMR (CDCl_3 , 150 MHz): δ 136.51, 132.39, 131.13, 117.02, 80.24, 68.90, 33.40, 32.03, 26.37, 25.05, 22.62, 14.03, 9.51	D) HRMS (EI) calc'd for $[\text{C}_{13}\text{H}_{24}\text{O}]^+$ 196.1827, found: 196.1828.
7	(<i>E</i>)-5-(2,4-dimethylpentan-3-yloxy)penta-1,3-diene		^1H NMR (CDCl_3 , 500 MHz): δ 6.36 (dt, 1H, $J=16.5, 10.5$ Hz), 6.27 (dd, 1H, $J=15.0, 11.0$ Hz), 5.83 (dt, 1H, $J=15.0, 6.0$ Hz), 5.21 (d, 1H, $J=16.5$ Hz), 5.09 (d, 1H, $J=9.5$ Hz), 4.12 (d, 2H, $J=5.5$ Hz), 2.72 (t, 1H, $J=5.5$ Hz), 1.83 (dq, 2H, $J=26.3, 6.5$ Hz), 0.94 (t, 12H, $J=6.5$ Hz) ^{13}C NMR (CDCl_3 , 100 MHz): δ 136.66, 132.14, 131.09, 117.04, 90.69, 73.91, 30.81, 20.33, 17.79	D) HRMS (EI) calc'd for $[\text{C}_{12}\text{H}_{22}\text{O}]^+$ 182.1671, found: 182.1669.

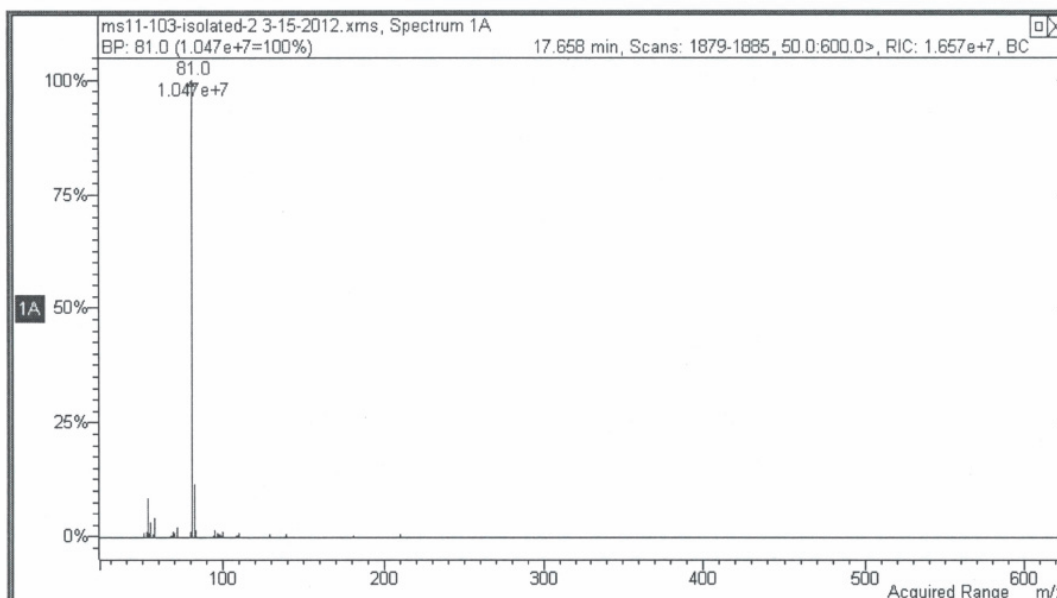
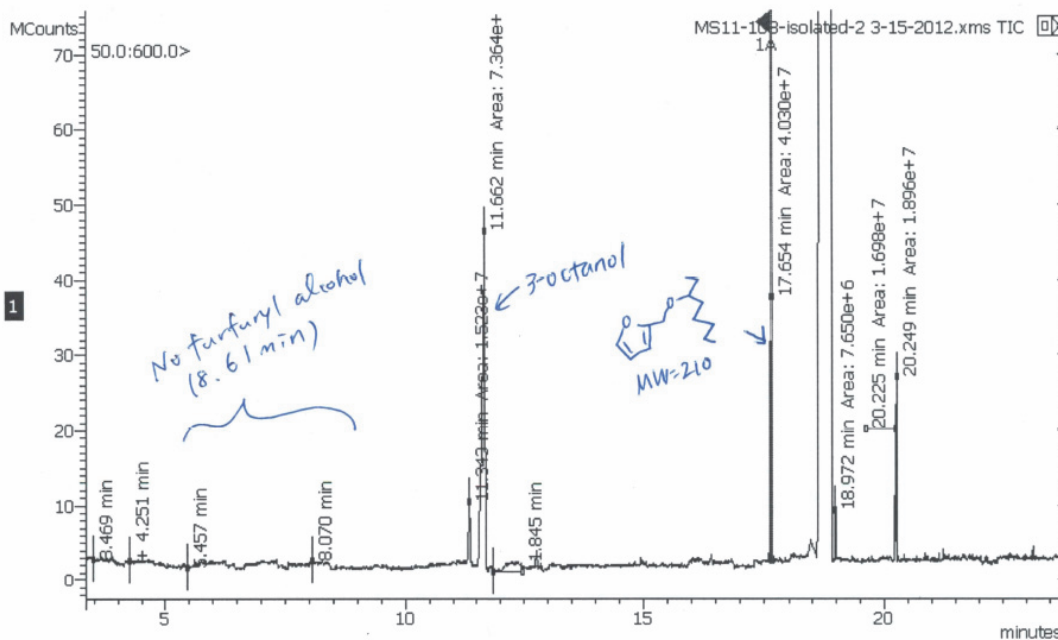
8	(E)-hexatriene		¹ H NMR (CDCl ₃ , 500 MHz): δ6.36-6.44 (2H, m), 6.27 (2H, dd, <i>J</i> =7.0, 3.0 Hz), 5.27 (2H, dd, <i>J</i> =16.7, 1.5 Hz), 5.15 (2H, dd, <i>J</i> =10.0, 1.5 Hz) ¹³ C NMR (CDCl ₃ , 125 MHz): δ136.80, 133.72, 117.85	E)
9	benzene		¹ H NMR (CDCl ₃ , 500 MHz): δ7.37 (s, 6H)	A), B), F)
10	phenol		¹ H NMR (CDCl ₃ , 500 MHz): δ7.22 (t, 2H, <i>J</i> =7.8 Hz), 6.87 (t, 1H, <i>J</i> =7.0 Hz) and 6.84 (d, 2H, <i>J</i> =8.5 Hz) fused (3H total)	A), C), F)
11	furan		¹ H NMR (CDCl ₃ , 500 MHz): δ7.41 (s, 2H), 6.36 (s, 2H)	A), B)
12	2-((octan-3-yloxy)methyl)furan		¹ H NMR (CDCl ₃ , 400 MHz): δ7.41 (fused d (apparent s), 1H), 6.34 (dd, 1H, <i>J</i> =3.2, 2.0 Hz), 6.30 (d, 1H, <i>J</i> =3.2 Hz), 4.47 (d, 2H, <i>J</i> =1.6 Hz), 3.32 (quintet, 1H, <i>J</i> =6.0 Hz), 1.7-1.1 (m, 10 H), 1.1-0.7 (m, 6H)	G)
13	2-vinylfuran		¹ H NMR (CDCl ₃ , 600 MHz): δ7.31 (s, 1H), 6.46 (dd, 1H, <i>J</i> =17.7, 11.4 Hz), 6.32 (apparent s, 1H), 6.21 (d, 1H, <i>J</i> =2.4 Hz), 5.61 (d, 1H, <i>J</i> =18.0 Hz), 5.11 (d, 1H, <i>J</i> =11.4 Hz)	Authentic sample was prepared according to the literature. A), B)

- A) GC MS and GC FID analysis (retention time, spectra) matched with the authentic sample.
 B) The product peaks in ¹H NMR spectra of the reaction mixture were in agreement with the ¹H NMR spectra of the authentic sample taken in CDCl₃ (literature value or sample prepared).
 C) ¹H NMR spectra of the authentic sample in the identical (~10 % 3-octanol or 3-pentanol in CDCl₃) solvent matched with the product peaks in ¹H NMR spectra of the reaction mixture.

- D) Product was somewhat volatile but could be isolated by flash column chromatography on silica gel. (Column packed with hexanes 100%, eluted with hexanes:CH₂Cl₂ = 15:1 to 8:1). It was difficult to separate the product from solvent alcohol on column chromatography and thus often required the second column chromatography purification.
- E) While the closed-system high-temperature reaction gave higher yields (see main text), for the characterization purpose the product was isolated by direct distillative separation from the reaction mixture. The DODH reaction of sorbitol (2.0 mmol scale) was carried out in a 100 mL round-bottom flask equipped with a short-path distillation apparatus at 155 °C in 3-octanol (0.05 M, MTO 2.5 mol %, air). The receiving flask was cooled with acetone/dry ice bath. After 5.5 h, the mixture of octenes and (*E*)-hexatriene (10:1 mol ratio) was collected in the receiving flask (515 mg). The second distillation of this mixture at 90 °C afforded pure (*E*)-hexatriene (8.9 mg, 0.11 mmol). ¹H and ¹³C NMR was correspondent to the literature values.
- F) GC (FID) yield based on the standard curve (internal standard: mesitylene) method matched with the ¹H NMR yield.

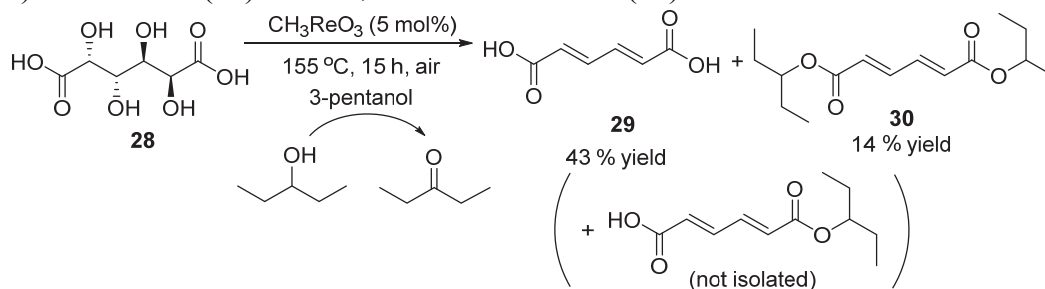
G) Isolation of the product was attempted by flash column chromatography on silica gel (column packed with hexanes 100%, eluted with hexanes:CH₂Cl₂ = 50:1 to 10:1), but it was difficult to totally separate the product from 3-octanol in our hands. GC-MS analysis indicated the ether structure shown, and by TLC and GC-MS analysis comparisons with the authentic sample, furfuryl alcohol was not detected.

GCMS spectra



II. Sugar acids and lactones

a) mucic acid (**28**) to *trans,trans*-muconic acid (**29**)

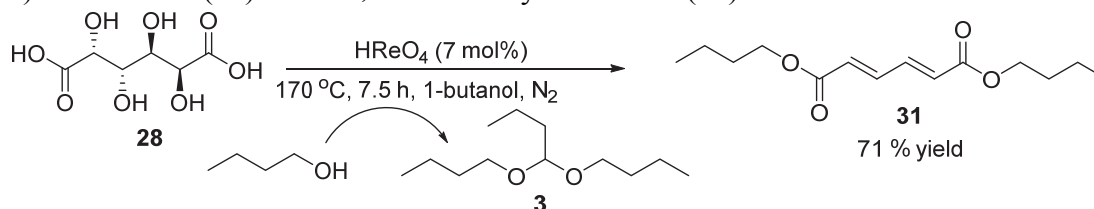


A Parr stainless-steel reactor vessel (50 mL) was charged with mucic acid (**28**) (209 mg, 1.0 mmol), CH_3ReO_3 (12.4 mg, 0.050 mmol) and 3-pentanol (10 mL) and sealed. The vessel was heated at 155 °C with mechanical stirring for 15 h and cooled to room temperature. The content (brown-grey suspension) was transferred to a flask and concentrated under the reduced pressure. The mixture was basified with 1 N NaOH aq. (10 mL) and extracted with CH_2Cl_2 (10 mL x 2). The combined organic phases were dried over MgSO_4 , filtered, concentrated and purified by flash column chromatography (hexanes:EtOAc=20:1) to give **30** (39.3 mg, 0.14 mmol, 14 % yield). The aqueous phase was acidified with 1.5 N HCl to pH=0. The formation of white precipitate was observed. After leaving at 5 °C for 3 h, it was filtered to recover the white solid **29** (60.5 mg, 0.43 mmol, 43 % yield).

29 ^1H and ^{13}C NMR spectra were identical to those of the authentic sample. ^1H NMR (CD_3OD , 600 MHz): δ 7.35 (dd, 2H, $J=7.8, 21.6$ Hz), 6.24 (dd, 2H, $J=8.4, 21.6$ Hz). ^{13}C NMR (CD_3OD , 150 MHz): δ 167.79, 141.09, 128.36.

30 The alkene part of the ^1H NMR spectra corresponded to that of *trans, trans*-muconic acid as well as to that of the known *trans, trans*-muconic acid dimethyl ester.^[56] (*cis, cis*-^[57] isomer has distinctly different chemical shifts.) ^1H NMR (CD_2Cl_2 , 600 MHz): δ 7.32 (dd, 2H, $J=9.0, 21.9$ Hz), 6.22 (dd, 2H, $J=9.0, 22.2$ Hz), 4.83 (fused pentet, 2H, $J=5.4$ Hz), 1.55-1.70 (m, 8H), 0.902 (t, 12H, $J=7.2$ Hz). ^{13}C NMR (CD_2Cl_2 , 150 MHz): δ 165.61, 140.41, 128.65, 77.15, 26.38, 9.28. EI-MS found 253 ($[\text{M}-\text{CH}_2\text{CH}_3]^+$), 195 ($[\text{M}-\text{CH}_3\text{CH}_2\text{C}(\text{H})\text{CH}_2\text{CH}_3]^+$).

b) mucic acid (**28**) to *trans,trans*-dibutyl muconate (**31**)



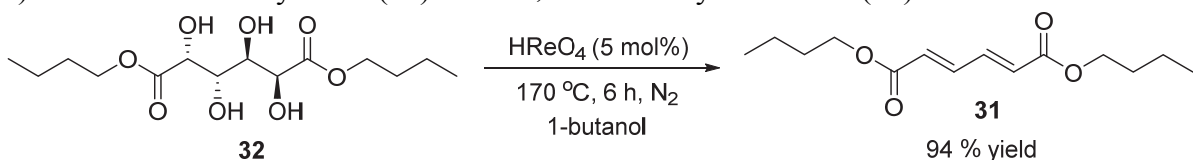
To a Biotage μ W vial (10-20 mL capacity) equipped with a stir bar, mucic acid (**28**) (63.0mg, 0.30 mmol) was added. The vial was purged with N_2 , sealed, a solution of $HReO_4$ (76.5 % in H_2O solution, 6.6 mg, 0.020 mmol) in 1-butanol (6 mL) was added through the septum cap. The vial was immersed in a pre-heated oil bath (170 $^\circ C$), heated at 170 $^\circ C$ with magnetic stirring for 7.5 h and cooled in an ice bath. The resulting pale-yellow clear solution was transferred to a flask and concentrated, and the workup as in a) was conducted. No precipitate was formed from the aqueous phase. The organic layer was purified by flash column chromatography (hexanes: CH_2Cl_2 =2:1 to 1:1) to afford **31** (54.3 mg, 0.21 mmol, 71 % yield).

31 The alkene part of the 1H NMR spectra corresponded to that of the authentic sample of *trans, trans*-muconic acid as well as to that of the known *trans, trans*-muconic acid dimethyl ester.^[56] (*cis, cis*-^[57] isomer has distinctly different chemical shifts.) 1H NMR ($CDCl_3$, 500 MHz): δ 7.33 (2H, dd, $J=3.0, 11.5$ Hz), 6.22 (2H, dd, $J=3.5, 11.5$ Hz), 4.21 (4H, t, $J=7.0$ Hz), 1.69 (4H, apparent pentet, $J=6.5$ Hz), 1.43 (4H, apparent sextet, $J=7.5$ Hz), 0.97 (6H, t, $J=7.5$ Hz). ^{13}C NMR ($CDCl_3$, 125 MHz): δ 166.07, 140.80, 128.43, 64.82, 30.65, 19.16, 13.74. ESI-HRMS (EI^+): $C_{14}H_{22}O_4$ ($[M]^+$) calc'd 254.1518, found 254.1523.

Co-product **3** was always isolated in variable but yet significant amount (30-60 % yield, assuming two butanal molecules are produced from the deoxygenation of one **28**) from the very non-polar fractions of flash column chromatography when the DODH reactions were conducted using the combination of $HReO_4$ and 1-butanol.

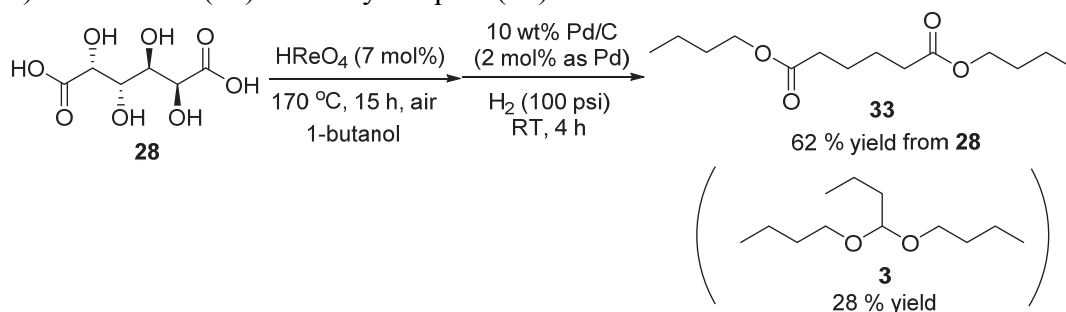
3 1H NMR ($CDCl_3$, 500 MHz): δ 4.50 (t, 1H, $J=6.0$ Hz), 3.60 (dt, 2H, $J=6.5, 9.0$ Hz), 3.43 (dt, 2H, $J=6.5, 9.0$ Hz), 1.53-1.64 (m, 6H), 1.35-1.45 (m, 6H), 0.95 (t, 9H, $J=7.5$ Hz). ^{13}C NMR ($CDCl_3$, 125 MHz): δ 102.93, 65.14, 35.60, 32.03, 19.48, 18.15, 14.02, 13.96. ESI-HRMS (EI^+): $C_{12}H_{25}O_2$ ($[M-H]^+$) calc'd 201.1855, found 201.1853.

c) mucic acid diⁿbutyl ester (**32**) to *trans,trans*- dibutyl muconate (**31**)



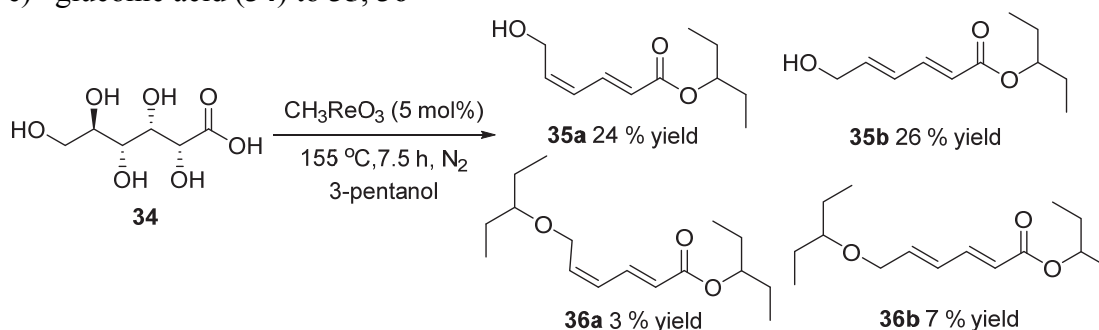
To a Biotage μ W vial (10-20 mL capacity) equipped with a stir bar, mucic acid dibutyl ester (**32**) (97.8 mg, 0.30 mmol) were added. The vial was purged with N_2 , sealed, and a solution of $HReO_4$ (76.5 % in H_2O solution, 4.8 mg, 0.015 mmol) in 1-butanol (6 mL) was added through the septum cap. The vial was immersed in a pre-heated oil bath (170 $^\circ C$), heated at 170 $^\circ C$ with magnetic stirring for 6h and cooled in an ice bath. The resulting brown solution was transferred to a flask and concentrated, and purified by flash column chromatography (hexanes: CH_2Cl_2 =4:1 to 2:1) to afford 71.4 mg of **31** as a pale-yellow crystalline solid (0.28 mmol, 94 % yield).

d) mucic acid (**28**) to dibutyl adipate (**33**)



A Parr stainless-steel reactor vessel (50 mL) was charged with mucic acid (**28**) (210 mg, 1.0 mmol), HReO₄ (76.5 % in H₂O solution, 23.2 mg, 0.07 mmol) and 1-butanol (20 mL) and sealed. The vessel was heated at 170 °C with mechanical stirring for 15 h and cooled to room temperature. The vessel was opened. (At this point, an aliquot of mixture was taken, diluted with DMSO-d₆ and analyzed by ¹H NMR, confirming the formation of **31** and the total consumption of **28**.) To this mixture, palladium on carbon (Aldrich, 10 wt % Pd, 22.4 mg, 0.020 mmol Pd) was added. The vessel was re-sealed, pressurized with H₂ (100 psi) and mechanically stirred at room temperature for 4 h. The mixture was filtered to a flask (solid was washed with CH₂Cl₂ and combined), concentrated, then filtered through silica (eluted with EtOAc), and concentrated to afford 271 mg of colorless oil. To this oil, mesitylene (29.1 mg, 0.24 mmol, internal standard) and CDCl₃ (3 mL) were added and mixed well. An aliquot was drawn, diluted with CDCl₃ and analyzed by ¹H NMR to find this oil to be the mixture of **33** and **3** (mol ratio mesitylene: **33** : **3**=1: 2.51:2.20). ¹H NMR yield **33** (0.60 mmol, 60 %), **3** (0.53 mmol, 26 %); isolated yield (calculated) **33** (160 mg, 0.62 mmol, 62 %), **3** (111 mg, 0.55 mmol, 28 %). GC analysis (retention times and MS spectra) also matched the authentic sample of **33** and the previously isolated **3**. GC yield based on the standard curve method (internal standard=mesitylene): **33** 56 % yield.

e) gluconic acid (**34**) to **35**, **36**



To a Biotage μW vial (10-20 mL capacity) equipped with a stir bar, D-gluconic acid (**34**) (50 % in H₂O, 118 mg, 0.30 mmol) and CH₃ReO₃ (3.4 mg, 0.014 mmol) were added. The vial was purged with N₂, sealed, and 3-pentanol (6 mL) was added through the septum cap. The vial was immersed in a pre-heated oil bath (155 °C), heated at the same temperature with magnetic stirring for 7.5 h and cooled in an ice bath. The resulting pale-yellow clear solution was transferred to a flask (the vial was washed with CH₂Cl₂ and combined) and concentrated

to give a red-brown solution. The TLC of this mixture showed three UV spots, R_f (hexanes:EtOAc=1:1) 0.89 (spot a), 0.51 (spot b), and 0.40 (spot c). The purification by flash column chromatography (hexanes:EtOAc=30:1 to 5:1) afforded three product fractions:

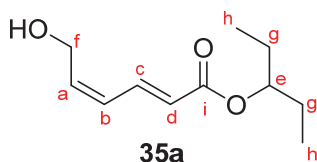
The first fraction (spot a, 7.9 mg, clear colorless liquid) was a mixture of **36a** and **36b** (mol ratio **36a:36b**=0.38:1).

The second fraction (spot b, 10.2 mg, clear colorless liquid) was exclusively **35a**.

The third fraction (spot b and c co-eluted, 20.5 mg, clear colorless liquid) was a mixture of **35a** and **35b** (mol ratio **35a:35b**=0.39:1).

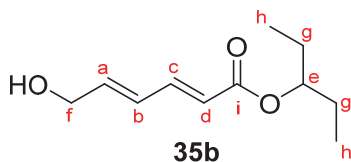
Thus, in total, **35a** (0.072 mmol, 24 % yield), **35b** (0.078 mmol, 26 % yield), **36a** (0.01 mmol, 3 % yield), **36b** (0.02 mmol, 7 % yield) were obtained.

35a



¹H NMR (CD₂Cl₂, 500 MHz): δ7.59 (dd, 1H, H_c, *J*=11.5, 14.8 Hz), 6.25 (dd, 1H, H_b, *J*=11.0, 11.0 Hz), 5.95-6.02 (m, 2H, H_a and H_d), 4.84 (pentet, 1H, H_e, *J*=5.5 Hz), 4.45 (bs, 2H, H_f), 1.61-1.68 (m, 4H, H_g), 0.92 (t, 6H, H_h, *J*=7.5 Hz). ¹³C NMR (CD₂Cl₂, 150 MHz): δ166.43 (i), 137.93 (c), 137.89 (a), 127.48 (b), 123.61 (d), 76.63 (e), 58.75 (f), 26.45 (g), 9.31 (h). The (*2E*, *4Z*) geometry was assigned based on the coupling constants (14.8 Hz between H_c and H_d, 11.0 Hz between H_a and H_b) as well as the observation of NOE between H_c and H_f and lack thereof between H_c and H_a.

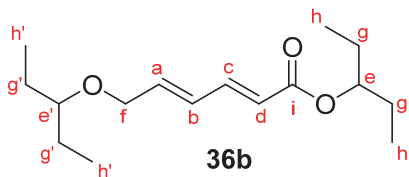
35b



¹H NMR (CD₂Cl₂, 500 MHz): δ7.31 (dd, 1H, H_c, *J*=11.0, 15.3 Hz), 6.45 (dd, 1H, H_b, *J*=11.0 Hz, 13.3 Hz), 6.24-6.29 (m, 1H, H_a), 5.93 (d, 1H, H_d, *J*=15.0 Hz), 4.80-4.85 (m, 1H, H_e), 4.29 (d, 2H, H_f, *J*=4.0 Hz), 1.56-1.67 (m, 4H, H_g), 0.91 (t, 6H, H_h, *J*=7.5 Hz). ¹³C NMR (CD₂Cl₂, 125 MHz): δ166.67 (i), 143.31 (c), 141.25(a), 127.45 (b), 121.76 (d), 76.52 (e), 62.52 (f), 26.41(g), 9.39 (h). The (*2E*, *4E*) geometry was assigned based on the coupling constants (15.0 Hz between H_c and H_d, 13.3 Hz between H_a and H_b) as well as the observation of NOE between H_c and H_a and lack thereof between H_c and H_f.

^1H NMR spectra of **36a**, **36b** were very similar to those of **35a**, **35b**.

36b



^1H NMR (CD_2Cl_2 , 500 MHz): δ 7.30 (dd, 1H, Hc, $J=11.0$, 15.5 Hz), 6.45 (dd, 1H, Hb, $J=11.0$, 13.2 Hz), 6.18-6.25 (m, 1H, Ha), 5.91 (d, 1H, Hd, $J=15.5$ Hz), 4.82 (pentet, 1H, He, $J=5.5$ Hz), 4.11 (d, 2H, Hf, $J=4.0$ Hz), 3.21 (pentet, 1H, He', $J=5.5$ Hz), 1.51-1.64 (m, 8H, Hg and Hg'), 0.90-0.97 (m, 12H, Hh and Hh'). ^{13}C NMR (CD_2Cl_2 , 150 MHz): δ 166.60(i), 143.47(c), 139.86(a), 128.13(b), 121.45 (d), 81.77 (e'), 76.37 (e), 68.20 (f), 26.45, 25.81 (g and g'), 9.31, 9.24 (h and h'). The (2*E*, 4*E*) geometry was assigned based on the coupling constants (15.5 Hz between Hc and Hd, 13.2 Hz between Ha and Hb) and by analogy to **35b**.

It was difficult to fully characterize the NMR spectra of **36a** due to the overlap with **36b**, but several characteristic peaks which resemble **35a** were identified and used for the ratio calculation, such as ^1H NMR (CD_2Cl_2 , 500 MHz): δ 7.61 (dd, 1H, $J=12.5$, 15.0 Hz) and 4.27 (d, 2H, $J=6.5$ Hz).

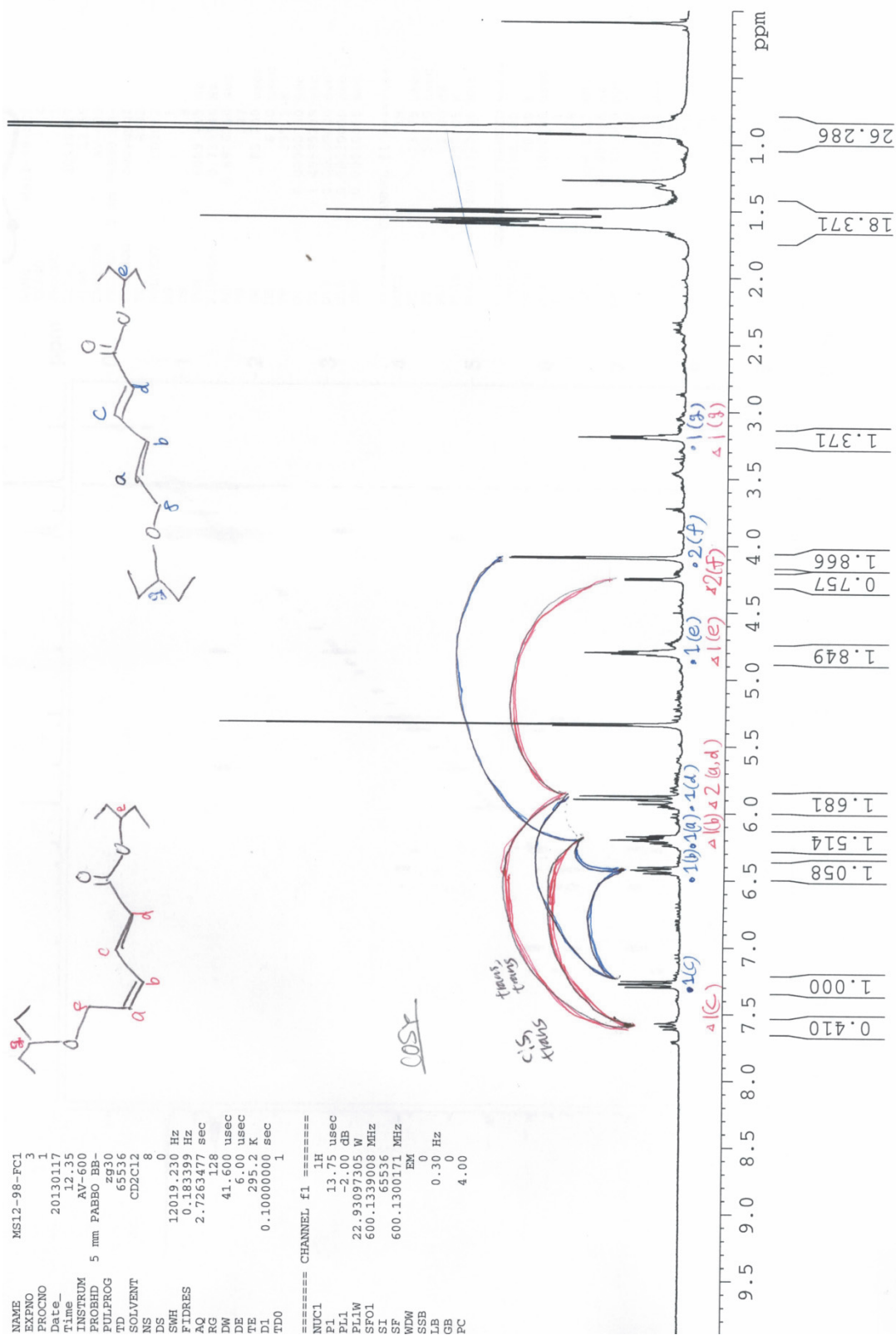


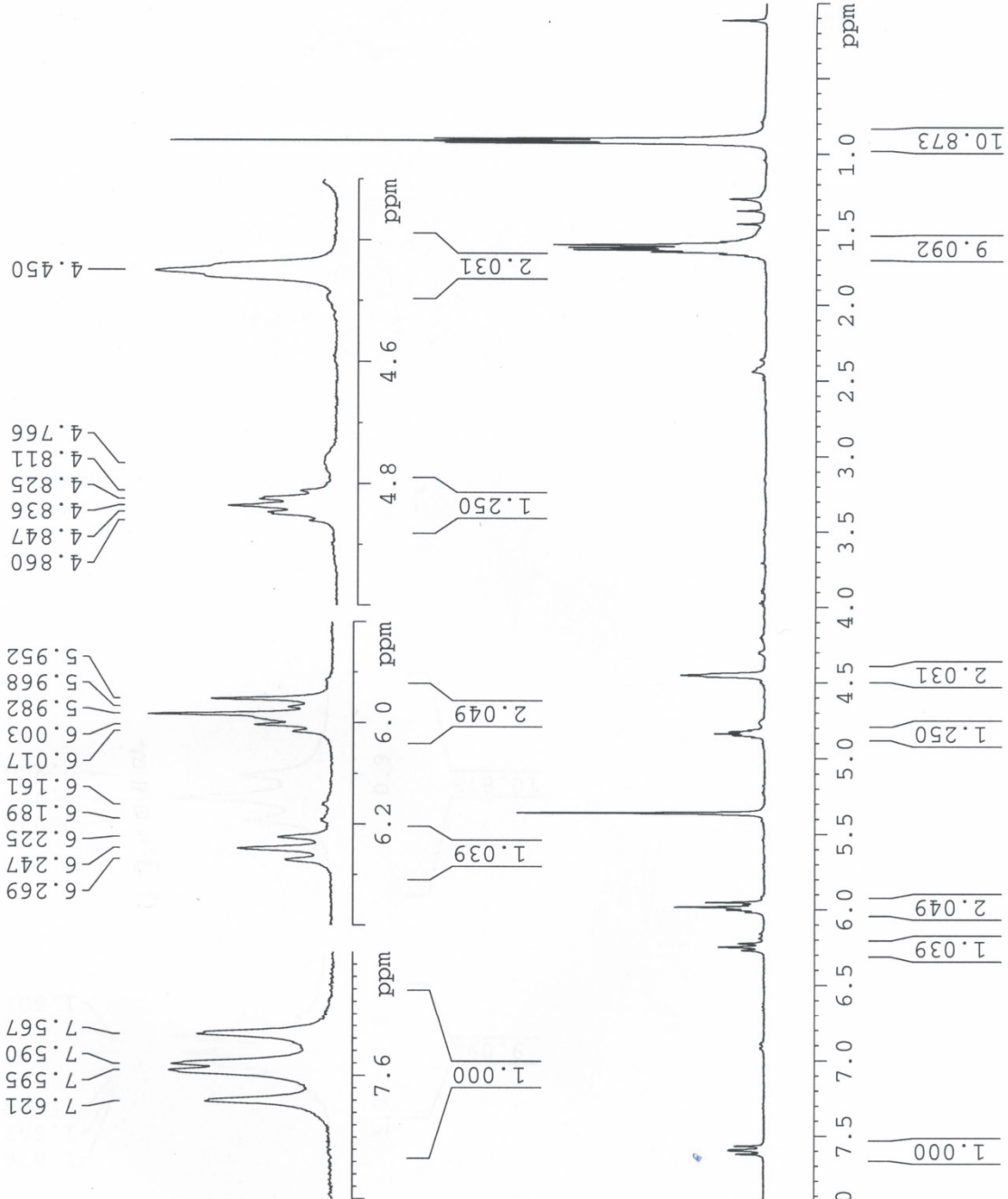
Figure 9 ^1H NMR spectra of fraction 1 (CD_2Cl_2 , 600 MHz).

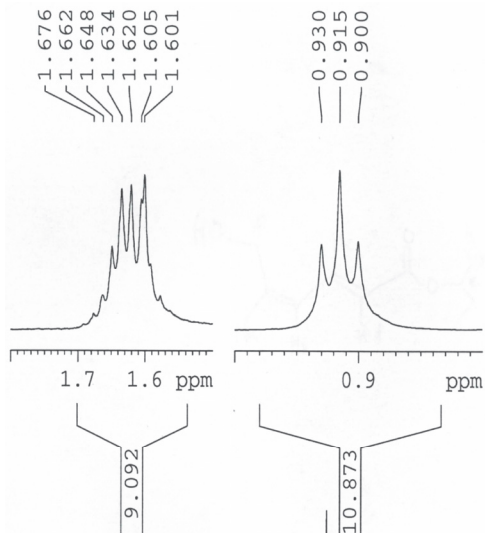
```

NAME MS12-98-FC2
EXPNO 1
PROCNO 1
Date_ 20130116
Time_ 15.50
INSTRUM DRX-500
PROBHD 5 mm BBO BB-1H
PULPROG zg30
TD 65536
SOLVENT CD2Cl2
NS 8
DS 0
SWH 10000.000 Hz
FIDRES 0.152588 Hz
AQ 3.2768500 sec
RG 362
DW 50.000 usec
DE 7.11 usec
TE 292.0 K
D1 1.00000000 sec
TD0 1

===== CHANNEL f1 =====
NUC1 1H
P1 15.00 usec
PL1 -5.00 dB
SFO1 500.1630885 MHz
SI 65536
SF 500.1600000 MHz
WDW EM
SSB 0
LB 0.20 Hz
GB 0
PC 3.00

```





```

NAME      MS12-98-FC2
EXPNO    3
PROCNO   1
Date_    20130117
Time     11.55
INSTRUM  AV-600
PROBHD   5 mm PABBO BB-
PULPROG  zg30
TD        65536
SOLVENT  CD2Cl2
NS        8
DS        0
SWH       12019.230 Hz
FIDRES   0.183399 Hz
AQ        2.7263477 sec
RG        256
DW        41.600 usec
DE        6.00 usec
TE        294.9 K
D1        0.10000000 sec
TDO       1

===== CHANNEL f1 =====
NUC1      1H
P1        13.75 usec
PL1       -2.00 dB
PL1W      22.93097305 W
SFO1      600.1339008 MHz
SI        65536
SF        600.1300171 MHz
WDW       EM
SSB       0
LB        0.30 Hz
GB        0
PC        4.00

```

Cosy

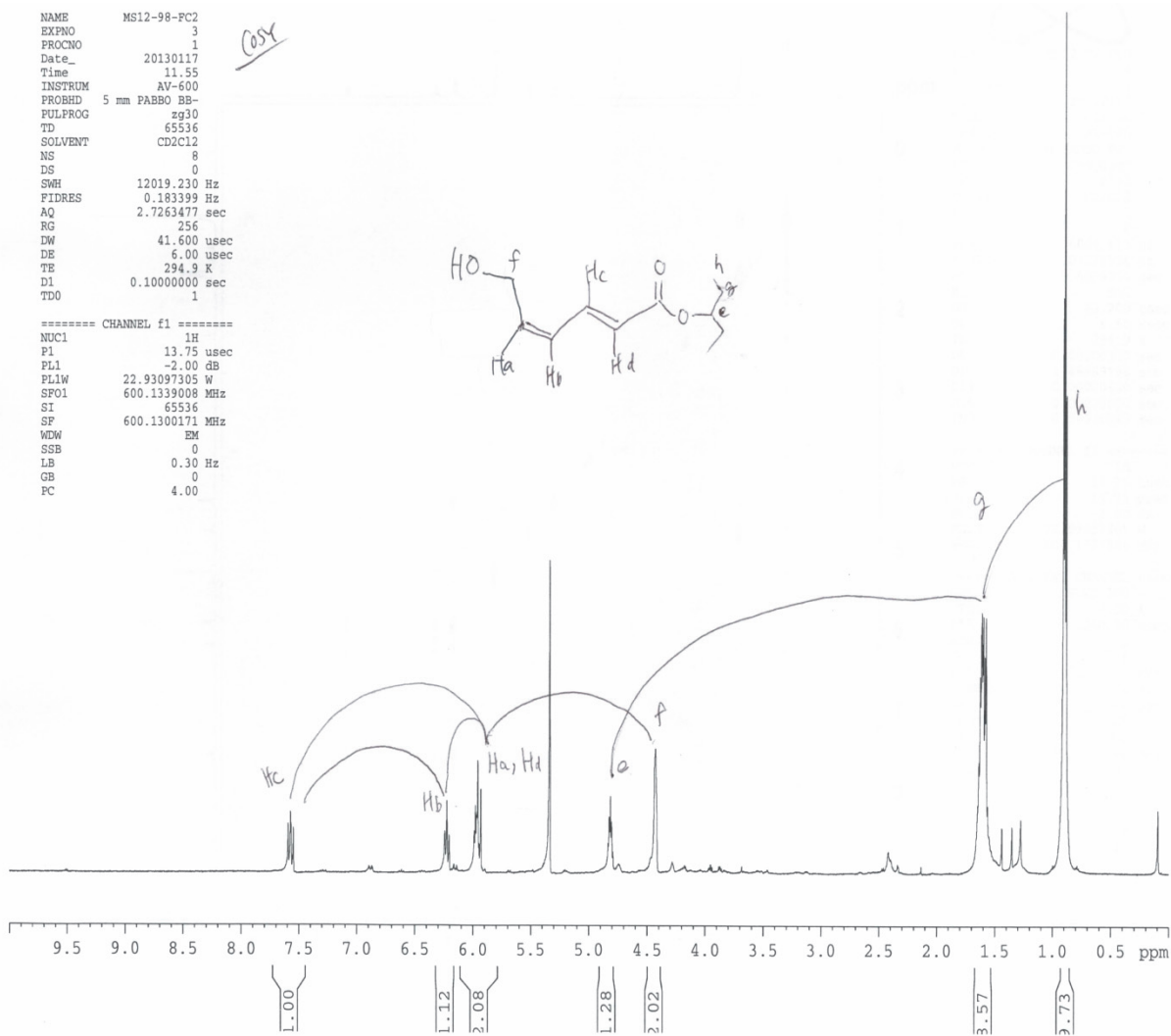
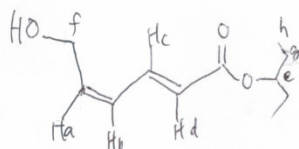
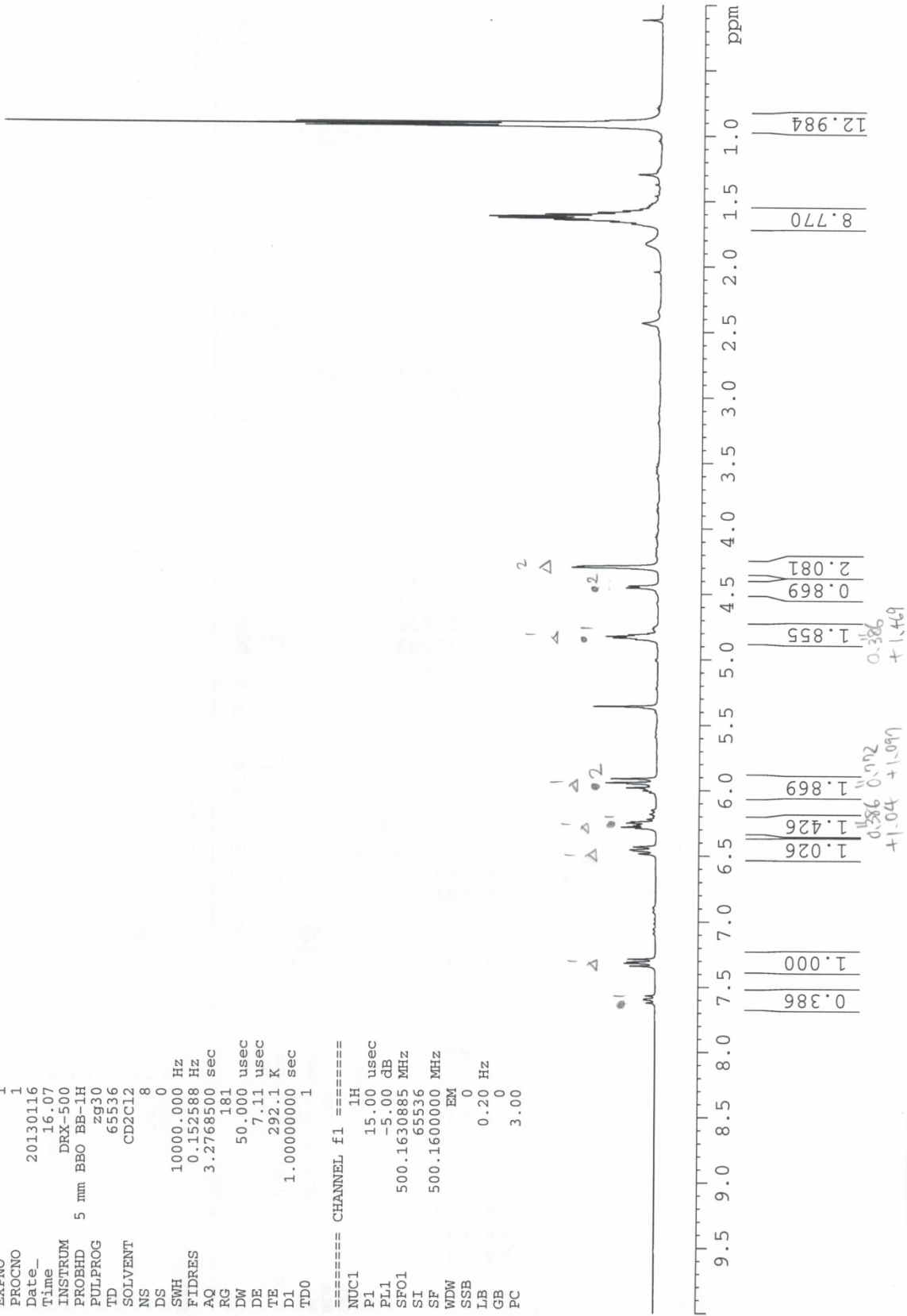


Figure 10 ^1H NMR spectra of fraction 2 (CD_2Cl_2 , 600 MHz).

NAME MS12-98-FC3
 EXPNO 1
 PROCNO 1
 Date_ 20130116
 Time 16.07
 INSTRUM DRX-500
 PROBHD 5 mm BBO BB-1H
 PULPROG zg30
 TD 65536
 SOLVENT CD2Cl2
 NS 8
 DS 0
 SWH 10000.000 Hz
 FIDRES 0.152588 Hz
 AQ 3.2768500 sec
 RG 181
 DW 50.000 usec
 DE 7.11 usec
 TE 292.1 K
 D1 1.00000000 sec
 TD0 1

===== CHANNEL f1 =====
 NUC1 1H
 P1 15.00 usec
 PL1 -5.00 dB
 SF01 500.1630885 MHz
 SI 65536
 SF 500.1600000 MHz
 WDW EM
 SSB 0
 LB 0.20 Hz
 GB 0
 PC 3.00



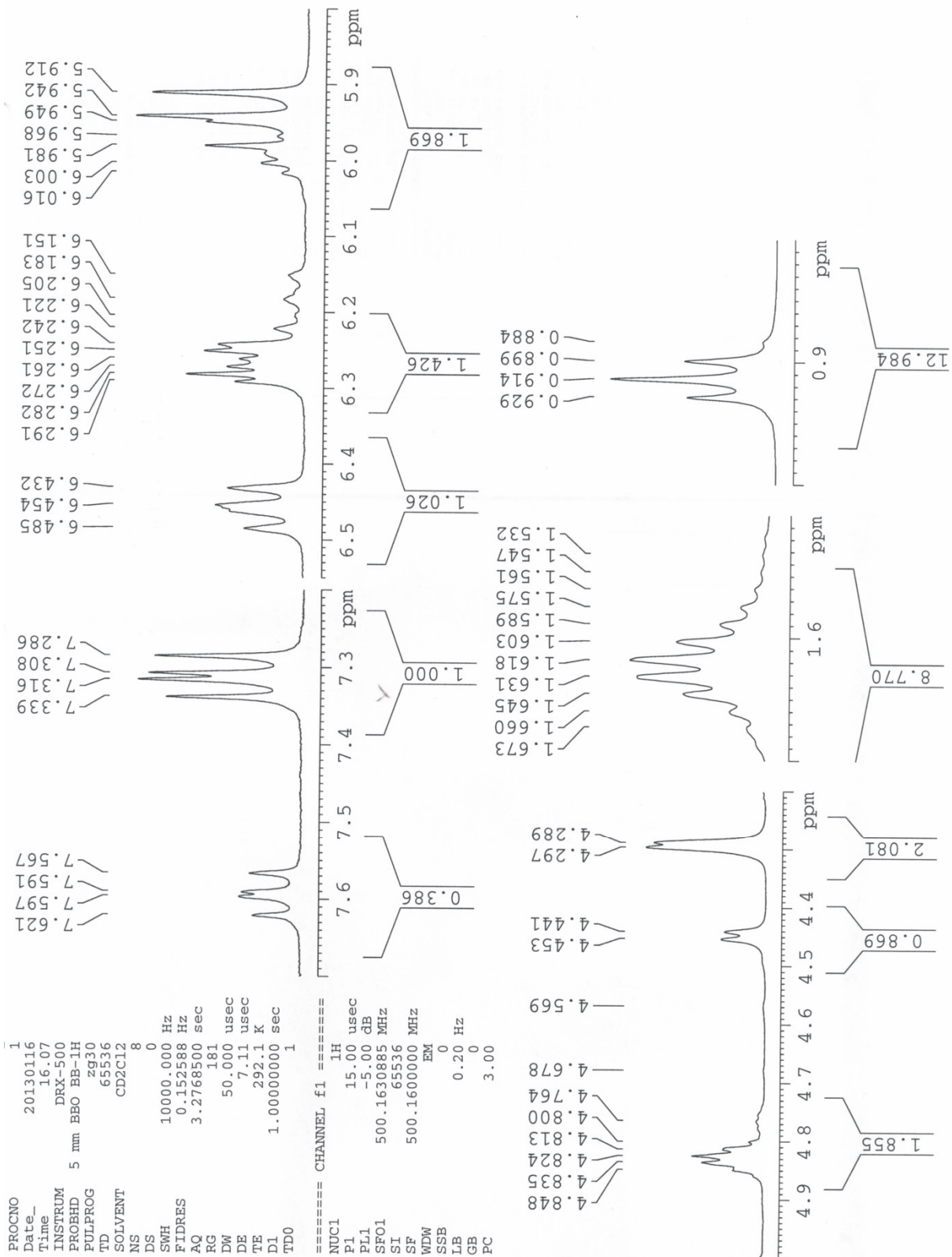
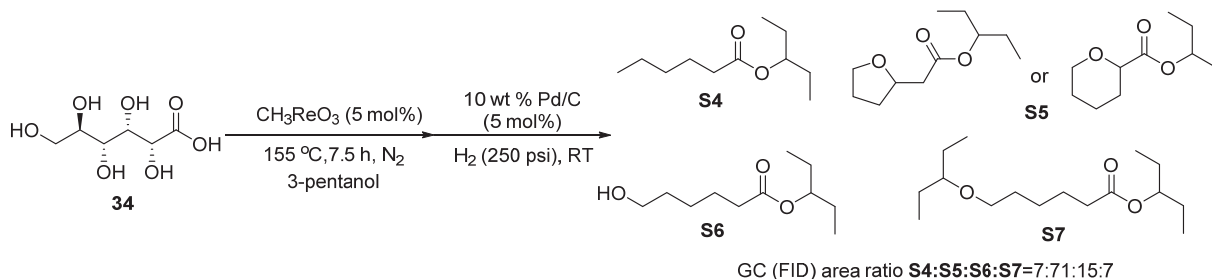
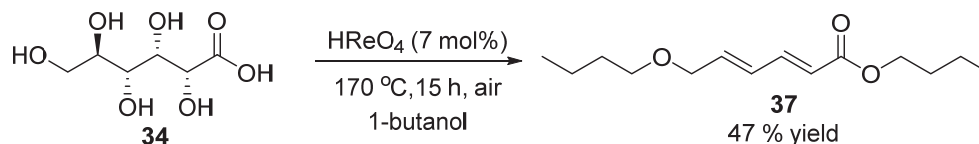


Figure 11 ¹H NMR spectra of fraction 3 (CD₂Cl₂, 500 MHz).

In our preliminary attempt to apply the 1-pot 2-step hydrogenation reaction on **34** using the above DODH conditions, no ϵ -caprolactone was observed and the main products appeared the cyclized ester compounds by GC MS/FID analysis. It suggested that the more forcing hydrogenation catalyst/conditions are necessary.

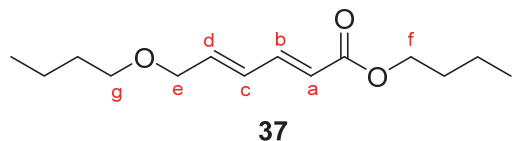


f) gluconic acid (**34**) to **37**



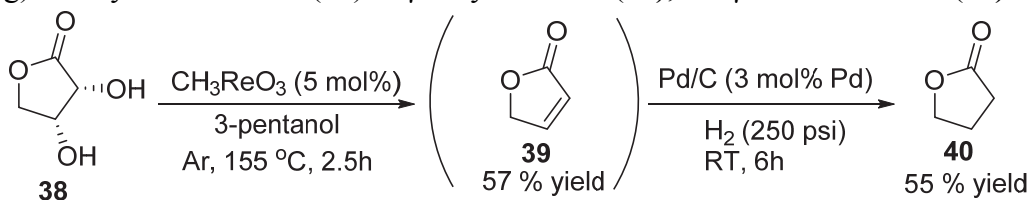
A Parr stainless-steel reactor vessel (50 mL) was charged with gluconic acid (**34**) (50 % in H_2O , 361 mg, 0.92 mmol), HReO_4 (76.5 % in H_2O solution, 22.5 mg, 0.070 mmol) and 1-butanol (20 mL). The vessel was heated at 170 °C with mechanical stirring for 15 h and cooled to room temperature. The mixture (amber solution) was transferred to a flask and concentrated under the reduced pressure. The purification by flash column chromatography (hexanes:EtOAc=40:1) gave 104.1 mg of **37** (yellow oil, 0.43 mmol, 47 % yield) as well as **3** (yellow oil, 185 mg, 0.92 mmol, 50 % yield).

37



The (*2E*, *4E*) geometry was assigned based on the coupling constants (15.0 Hz between Hc and Hd, 15.5 Hz between Ha and Hb) as well as the observation of NOE between Hc and Ha, Hc and He, Hb and Hd. ^1H NMR (CD_2Cl_2 , 500 MHz): δ 7.30 (dd, Hb, 1H, $J=11.5$, 15.3 Hz), 6.43 (dd, Hc, 1H, $J=11.5$, 15.0 Hz), 6.20 (dt, Hd, 1H, $J=5.5$, 15.0 Hz), 5.91 (d, Ha, 1H, $J=15.5$ Hz), 4.15 (t, Hf, 2H, $J=6.5$ Hz), 4.09 (d, 2H, He, $J=5.0$ Hz), 3.47 (t, 2H, Hg, $J=6.5$ Hz), 1.36-1.71 (m, 12H), 0.93-1.00 (m, 6H). ^{13}C NMR (CD_2Cl_2 , 125 MHz): δ 166.80, 143.64, 139.50, 128.40, 121.20, 70.55, 70.11, 64.13, 31.82, 30.75, 19.34, 19.18, 13.69, 13.52. ESI-HRMS (EI^+): $\text{C}_{14}\text{H}_{24}\text{O}_3$ ($[\text{M}]^+$) calc'd 240.1725, found 240.1730.

g) D-erythronolactone (**38**) to γ -butyrolactone (**40**), via γ -crotonolactone (**39**)



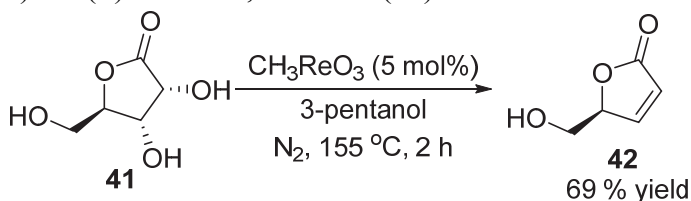
A Parr stainless-steel reactor vessel (20 mL) was charged with D-erythronolactone (**38**) (89.2 mg, 0.75 mmol), CH_3ReO_3 (9.3 mg, 0.038 mmol) and 3-pentanol (7.5 mL). The vessel was purged with Ar, sealed and heated at 155 °C with mechanical stirring for 2.5 h and cooled to room temperature. The vessel was opened, palladium on carbon (Aldrich, 10 wt % Pd, 25.0 mg, 0.023 mmol Pd) was added and the vessel was re-sealed. The vessel was pressurized with H_2 (250 psi) and mechanically stirred at room temperature for 6 h. The mixture was filtered to a flask (solid was washed with CH_2Cl_2 and combined) and concentrated to afford 359 mg of clear colorless liquid. Mestylene (12.2 mg, 0.10 mmol) was added as a NMR internal standard and mixed well. An aliquot of sample was diluted with CDCl_3 and analyzed by ^1H NMR. ^1H NMR yield of **40**: 55 % yield.

40 ^1H NMR (CDCl_3 , 500 MHz): δ 4.38 (t, 2H, $J=7.0$ Hz), 2.52 (t, 2H, $J=8.0$ Hz), 2.29 (tt, apparent pentet, 2H, $J=7.5$ Hz).

The conversion of **38** to γ -crotonolactone (**39**) was confirmed by performing the first DODH step in a separate batch (0.3 mmol scale, Biotage μW vial (2-5 mL capacity), N_2 instead of Ar). After the reaction, the crude mixture was concentrated and purified by flash column chromatography (hexanes: $\text{CH}_2\text{Cl}_2=2:1$ to CH_2Cl_2 100 %) to afford 14.3 mg (0.17 mmol, 57 % yield) of **39**.

39 ^1H NMR (CDCl_3 , 400 MHz): δ 7.59 (dt, 1H, $J=1.6, 6.0$ Hz), 6.18 (dt, 1H, $J=2.0, 6.0$ Hz), 4.92 (dd, 2H, $J=1.6, 2.0$ Hz). ^{13}C NMR (CDCl_3 , 125 MHz): δ 173.70, 152.74, 121.69, 72.13.

h) D-(+)-ribo-1,4-lactone (**41**) to **42**



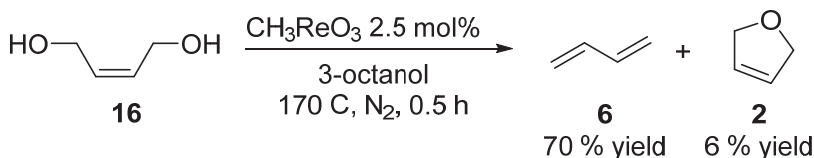
To a Biotage μW vial (2-5 mL capacity) equipped with a stir bar, D-(+)-ribo-1,4-lactone (**41**) (44.5 mg, 0.30 mmol), CH_3ReO_3 (4.0 mg, 0.016 mmol) were added. The vial was

purged with N₂, sealed, and 3-petanol (3 mL) was added through the septum cap. The vial was immersed in a pre-heated oil bath (155 °C), heated at the same temperature with magnetic stirring for 2h and cooled in an ice bath. The resulting black mixture was filtered through celite into a flask. The celite was washed with CH₂Cl₂ and combined. The filtrate (colorless clear solution) was concentrated to give **42** (23.5 mg, 0.21 mmol, 69 % yield) as a clear colorless oil.

42 ¹H NMR (CDCl₃, 500 MHz): δ7.49 (dd, 1H, *J*=1.5, 5.7 Hz), 6.25 (dd, 1H, *J*=2.0, 5.5 Hz), 5.18 (m, 1H), 4.03 (dd, 1H, *J*=3.5, 12.3 Hz), 3.82 (dd, 1H, *J*=5.0, 12.0 Hz). ¹³C NMR (CDCl₃, 125 MHz): δ173.46, 153.87, 122.96, 84.26, 62.23. GC-MS spectra matched with the authentic spectra (found *m/z*=114.0, 83.9, 54.9).

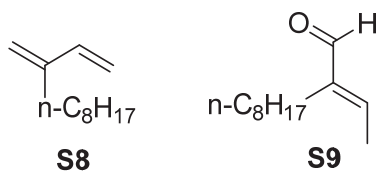
III. 1,4- and 1,6-DODH reactions

A representative procedure: *cis*-but-2-ene-1,4-diol (**16**) to butadiene (**6**) and 2,5-dihydrofuran (**2**)



cis-But-2-ene-1,4-diol (**16**) 26.6 mg (0.30 mmol) was charged in a Biotage μW vial (2-5 mL capacity) equipped with a stir bar. The vial was sealed under N₂. A solution of CH₃ReO₃ (1.8 mg, 0.0075 mmol) in 3-octanol (3 mL) and mesitylene (internal standard, 14.4 mg, 0.12 mmol) was added through the septum cap. The vial was immersed in a pre-heated oil bath (170 °C), heated at 170 °C with magnetic stirring for 0.5 h and cooled in an ice bath. The aliquot (ca. 25 μL) of the resulting dark-colored mixture was taken, diluted with CDCl₃ (ca. 0.7 mL) and analyzed by ¹H NMR. The total consumption of the starting material was observed, and the product peaks matched with those of the authentic sample. GCMS further confirmed the product identification. The yields were determined by ¹H NMR using mesitylene as an internal standard, due to the volatility of the products.

For the conversion of **22**, after determining the ¹H NMR yields using the characteristic alkene and aldehyde peak, the reaction mixture was concentrated and purified by flash column chromatography (hexanes:EtOAc=1:1 to 1:4) for further characterization. Note **S8** was still volatile and evaporated when left under the high-vacuum overnight, and **S9** was rather unstable and decomposed over time when stored at room temperature.

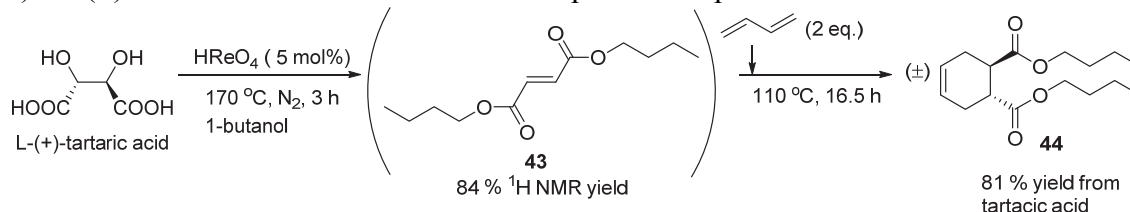


S8 ^1H NMR (CDCl_3 , 500 MHz): δ 6.40 (dd, 1H, $J=11.0$, 18.5 Hz), 5.25 (d, 1H, $J=18.0$ Hz), 5.07 (d, 1H, $J=11.0$ Hz), 5.02 (s, 1H), 5.01 (s, 1H), 2.22 (t, 2H, $J=7.5$ Hz), 1.51 (pentet, 2H, $J=7.5$ Hz), 1.30 (broad m, 10H), 0.91 (t, 3H, $J=7.0$ Hz). ^{13}C NMR (CDCl_3 , 125 MHz): δ 146.66, 139.06, 115.48, 113.06, 31.92, 31.36, 29.66, 29.53, 29.33, 28.18, 22.70, 14.14.

S9 ^1H NMR (CDCl_3 , 500 MHz): δ 9.39 (s, 1H), 6.58 (q, 1H, $J=7.0$ Hz), 2.26 (t, 2H, $J=7.5$ Hz), 2.01 (d, 3H, $J=7.0$ Hz), 1.29 (broad s, 12H), 0.90 (t, 3H, $J=7.0$ Hz). The (*Z*) geometry was assigned based on the observation of NOE between aldehyde H (9.39 ppm) and alkene H (6.58 ppm) and the lack thereof between aldehyde H (9.39 ppm) and the doublet CH_3 (2.01 ppm).

3. Conversion of L-(+)-tartaric acid and erythritol to 4-cyclohexene-1,2-dicarboxylic acid ester

a) L-(+)-tartaric acid and butadiene in one-pot two-step



To a Biotage μ W vial (10-20 mL capacity) equipped with a stir bar, L-(+)-tartaric acid (44.5 mg, 0.30 mmol) was added. The vial was purged with N₂, sealed, and a solution of HReO₄ (76.5 % in H₂O solution, 4.9 mg, 0.015 mmol) in 1-butanol (6 mL) was added through the septum cap. The vial was immersed in a pre-heated oil bath (170 °C), heated at 170 °C with magnetic stirring for 3 h and cooled in an ice bath. Mesitylene 16.2 mg (0.13 mmol) was added as an internal standard and mixed well. An aliquot of this mixture was taken, diluted with CDCl₃ and analyzed by ¹H NMR. ¹H NMR yield of **43**: 0.25 mmol, 84 % yield.

Butadiene (20 wt% solution in toluene 157 mg, 0.58 mmol) was then added under N₂ through the septum cap and the mixture was stirred at 110 °C. The reaction progress was monitored by occasional ¹H NMR analysis of an aliquot diluted with CDCl₃. After 16.5 h, the mixture was concentrated under the reduced pressure and purified by flash column chromatography (hexanes: CH₂Cl₂=6:1 to 1:2) to afford 68.7 mg of **44** (81 % yield from L-(+)-tartaric acid, 96 % for Diels-Alder reaction step) as clear colorless oil.

44 ¹H NMR (CDCl₃, 400 MHz): δ 5.70 (d, 2H, $J=3.0$ Hz), 4.04-4.15 (m, 4H), 2.85-2.87 (m, 2H), 2.41 and 2.46 (two overlapping bs, 2H), 2.14-2.21 (m, 2H), 1.57-1.65 (m, 4H), 1.34-1.43 (m, 4H, or apparent sextet at 1.38 ppm, $J=7.2$ Hz), 0.93 (t, 6H, $J=7.2$ Hz). ¹³C NMR (CDCl₃, 100 MHz): δ 174.89, 124.95, 64.46, 41.26, 30.59, 27.98, 19.06, 13.69.

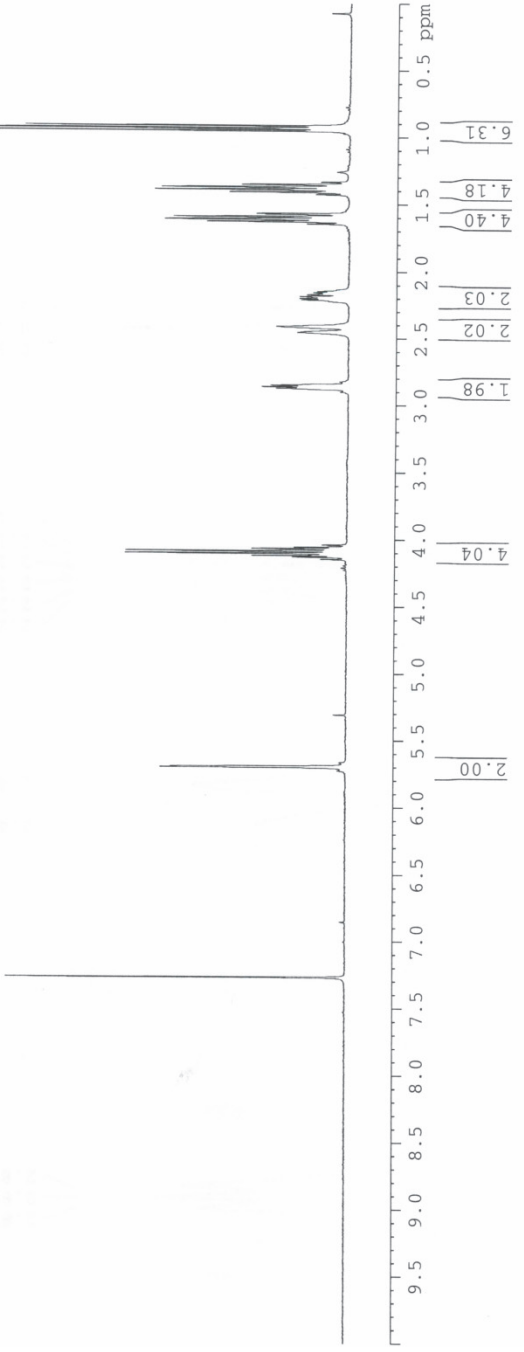
In a separate batch, the reaction was stopped after the first DODH step and the mixture was concentrated and purified by flash column chromatography (hexanes: CH₂Cl₂=4:1 to 2:1) to yield 59.9 mg (0.26 mmol, 88 % yield) of **43** as colorless oil.

43 NMR spectra matched with the authentic sample. ¹H NMR (CDCl₃, 500 MHz): δ 6.87 (s, 2H), 4.23 (t, 4H, $J=7.0$ Hz), 1.69 (apparent pentet, 4H, $J=7.0$ Hz), 1.43 (apparent hextet, 4H, $J=7.5$ Hz), 0.97 (t, 6H, $J=7.5$ Hz). ¹³C NMR (CDCl₃, 125 MHz): δ 165.15, 133.64, 65.25, 30.53, 19.12, 13.71.

1.335
 1.353
 1.371
 1.390
 1.409
 1.427
 1.568
 1.573
 1.591
 1.611
 1.628
 1.645
 2.145
 2.156
 2.171
 2.184
 2.200
 2.210
 2.410
 2.455
 2.850
 2.862
 2.874
 4.039
 4.056
 4.066
 4.083
 4.102
 4.113
 4.119
 4.129
 4.146
 4.210
 5.308
 5.692
 5.698

6.854
 7.268

NAME MS12-146
 EXPNO 1
 PROCNO 1
 Date_ 20130202
 Time 19:34
 INSTRUM AV630
 PROBD 5 mm QNP 1H/13
 PULPROG zg30
 TD 65536
 SOLVENT CDCl3
 NS 8
 DS 0
 SWH 8012.820 Hz
 FIDRES 0.095586 Hz
 AQ 4.0835586 sec
 RG 256
 DW 62.400 usec
 DE 6.00 usec
 TE 293.1 K
 D1 1.00000000 sec
 TD0 1
 ===== CHANNEL f1 =====
 NUC1 1H
 P1 12.80 usec
 PL1 0.00 dB
 PL1W 9.54516888 W
 SFO1 400.1324700 MHz
 SI 65536
 SF 400.1300142 MHz
 EQ
 SSB 0
 LB 0.30 Hz
 GB 0
 PC 4.00



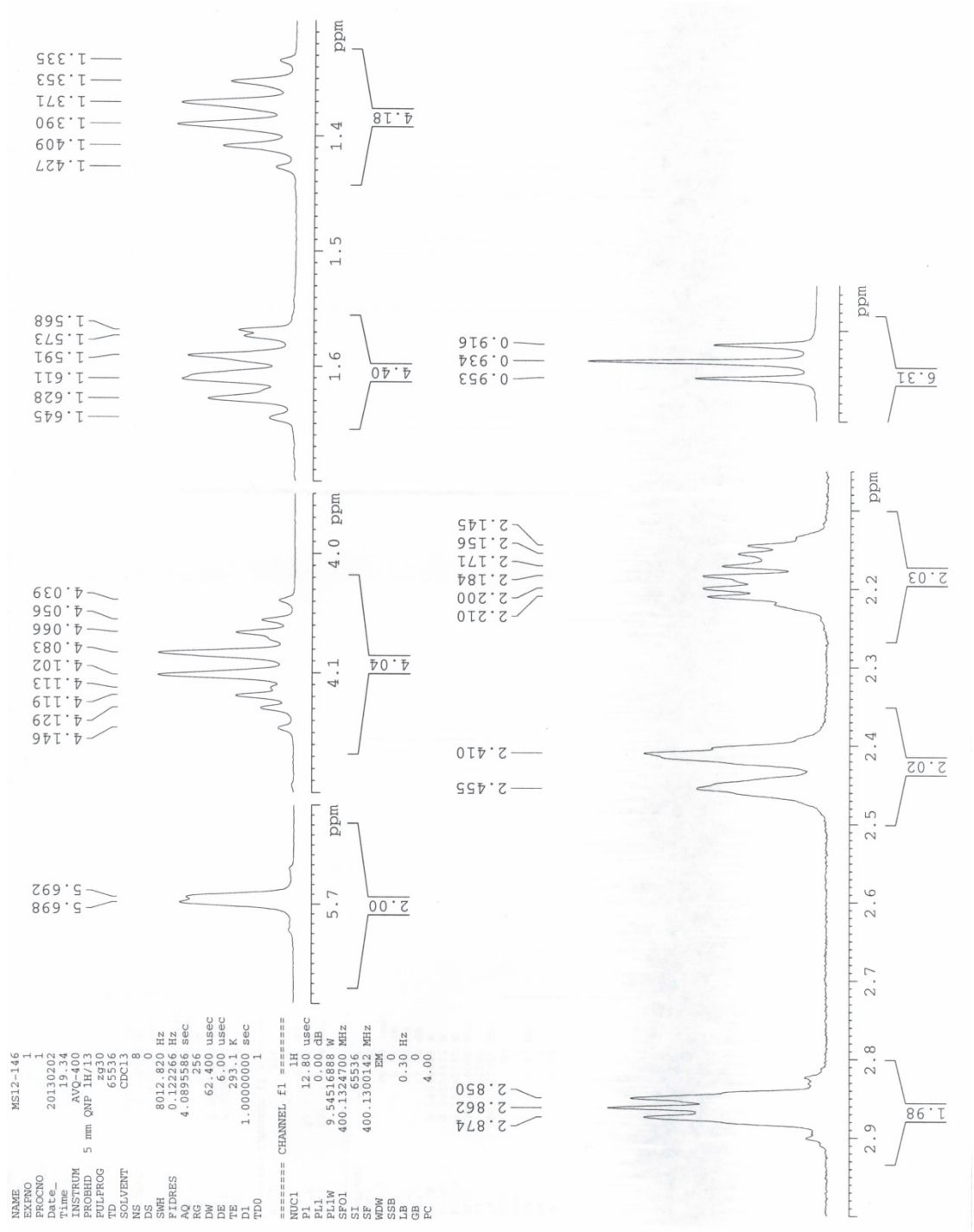
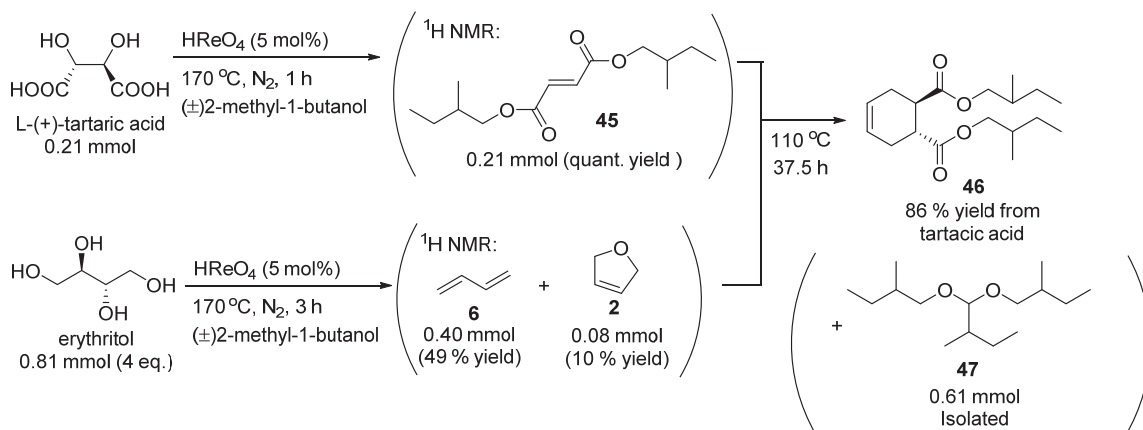


Figure 12 ^1H NMR spectra of diesel 44 (CDCl_3 , 400 MHz).

b) L-(+)-tartaric acid and erythritol in two-pot two-step



To a Biotage μ W vial (2-5 mL capacity) equipped with a stir bar, L-(+)-tartaric acid (30.8 mg, 0.21 mmol) was added. The vial was purged with N₂, sealed, a solution of HReO₄ (76.5 % in H₂O solution 3.7 mg, 0.011 mmol) in (±)2-methyl-1-butanol (2 mL) and mesitylene (internal standard, 15.5 mg, 0.13 mmol) were added through the septum cap. The vial was immersed in a pre-heated oil bath (170 °C), heated at 170 °C with magnetic stirring for 1 h and cooled in an ice bath. An aliquot of this mixture was drawn, diluted with CDCl₃ and analyzed by ¹H NMR. ¹H NMR yield of **45**: 0.21 mmol, quantitative yield.

In a separate Biotage μ W vial (10-20 mL capacity) equipped with a stir bar, erythritol (98.8 mg, 0.81 mmol) was added. The vial was purged with N₂, sealed, a solution of HReO₄ (76.5 % in H₂O solution, 13.9 mg, 0.042 mmol) in (±)2-methyl-1-butanol (3 mL) and mesitylene (internal standard, 12.6 mg, 0.11 mmol) were added through the septum cap. The vial was immersed in a pre-heated oil bath (170 °C), heated at 170 °C with magnetic stirring for 3 h and cooled in an ice bath. An aliquot of this mixture was drawn, diluted with CDCl₃ and analyzed by ¹H NMR. ¹H NMR yield of butadiene: 0.40 mmol, 49 % yield. The dehydration+DODH product 2,5-dihydrofuran 0.081 mmol (10 % yield) was also observed.

This mixture containing butadiene was cooled to -78 °C, and the mixture containing **45** was added through the septum cap. The vial was washed with 1 mL of (±)2-methyl-1-butanol and combined. The combined mixture was heated at 110 °C with magnetic stirring. The reaction progress was monitored by occasional ¹H NMR analysis of an aliquot diluted with CDCl₃. After 37.5 h, ¹H NMR analysis using mesitylene (12.6 mg + 15.5 mg=28.1 mg=0.23 mmol, the sample loss due to the ¹H NMR monitoring was ignored) indicated that the mixture contained **45** 0.037 mmol (18 % yield), butadiene 0.18 mmol, 2,5-dihydrofuran 0.072 mmol, and **46** 0.17 mmol (83 % yield). At this point, the mixture was concentrated under the reduced pressure and purified by flash column chromatography (hexanes: CH₂Cl₂=5:1 to 3:1) to afford **46** as clear colorless oil (54.6 mg, 0.18 mmol, 86 % yield). **47** was also isolated from the non-polar fractions (clear colorless oil, 149 mg, 0.61 mmol).

Based on the well-established Diels-Alder reaction mechanism, the product **46** should have an anti stereochemistry for the two ester groups. The endo isomer and the exo isomer would be a pair of enantiomers if a nonchiral alcohol was used (e.g. **44**). However, because racemic 2-methyl-1-butanol was used in this case, **46** consists of four diastereomers due to the two stereocenters of the alkyl chain. Likewise, **46** consists of multiple diastereomers due to three stereocenters. However, they were not separable by chromatography and we did not distinguish those isomers for the purpose of this study.

46 EI-HRMS (EI^+): $\text{C}_{18}\text{H}_{30}\text{O}_4$ ($[\text{M}]^+$) calc'd 310.2144, found 310.2142.

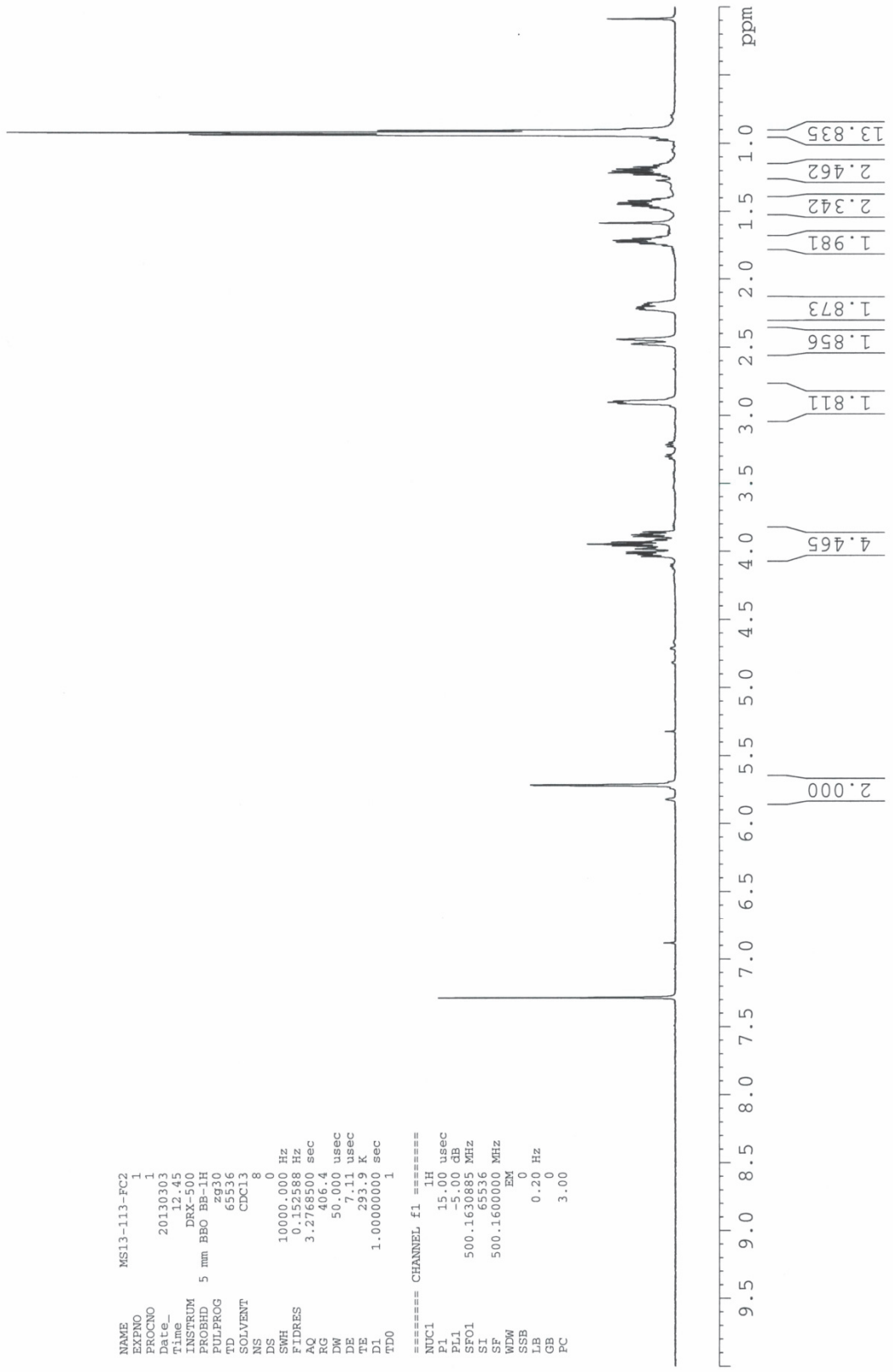
47 EI-HRMS (EI^+): $\text{C}_{15}\text{H}_{31}\text{O}_2$ ($[\text{M}-\text{H}]^+$) calc'd 243.2324, found 243.2320.

```

NAME MS13-113-FC2
EXPNO 1
PROCNO 1
Date_ 20130303
Time 12.45
INSTRUM DRX-500
PROBHD 5 mm BBO BB-1H
PULPROG zg30
TD 65536
SOLVENT CDCl3
NS 8
DS 0
SWH 10000.000 Hz
FIDRES 0.152588 Hz
AQ 3.2768500 sec
RG 406.4
DW 50.000 usec
DE 27.11 usec
TE 293.2 K
D1 1.00000000 sec
TD0 1

===== CHANNEL f1 =====
NUC1 1H
P1 15.00 usec
PL1 -5.00 dB
SF01 500.1630885 MHz
SI 65536
SF 500.1600000 MHz
WDW EM
SSB 0
LB 0.20 Hz
GB 0
PC 3.00

```



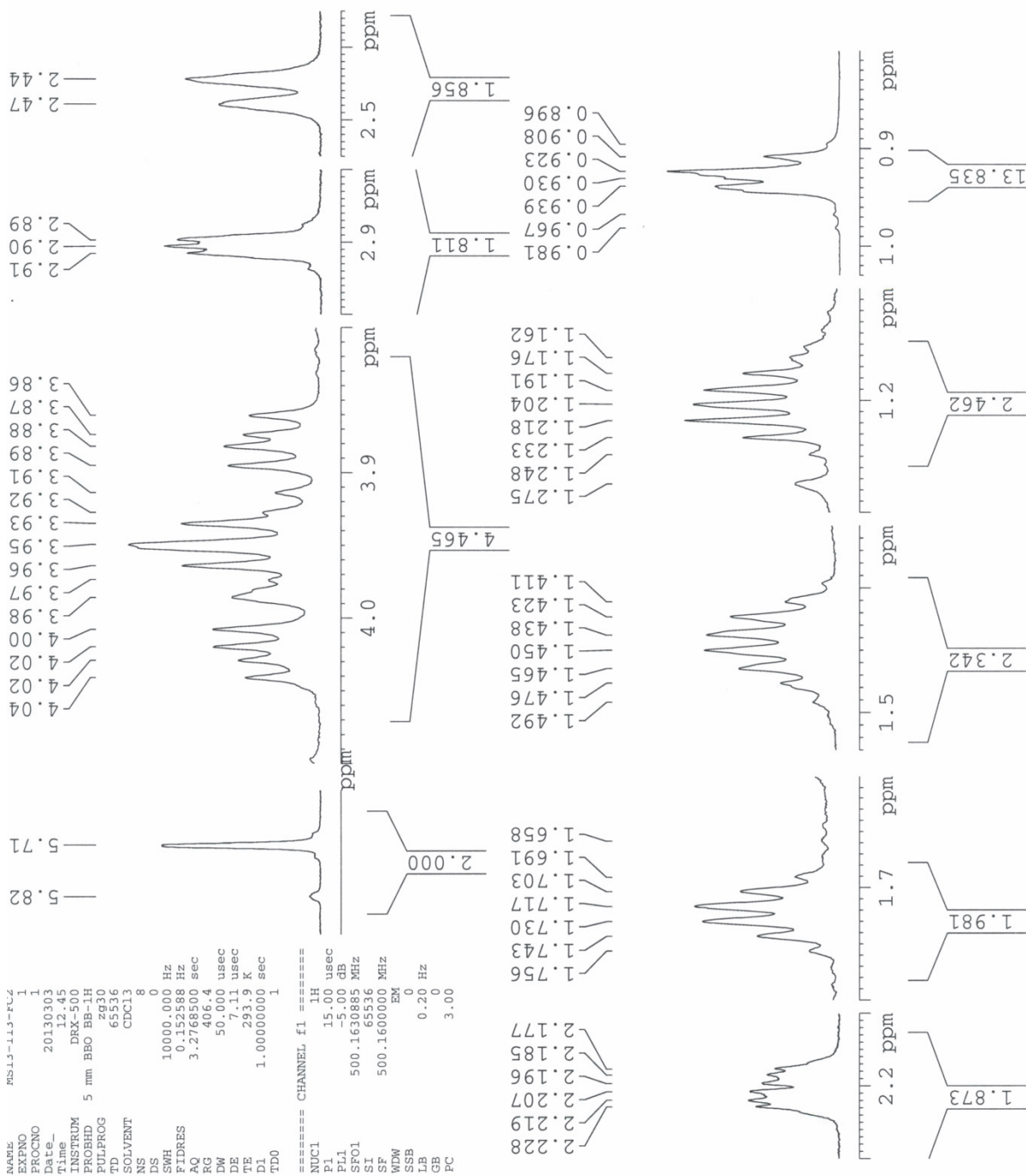


Figure 13 ^1H NMR spectra of compound 46 (CDCl_3 , 500 MHz).

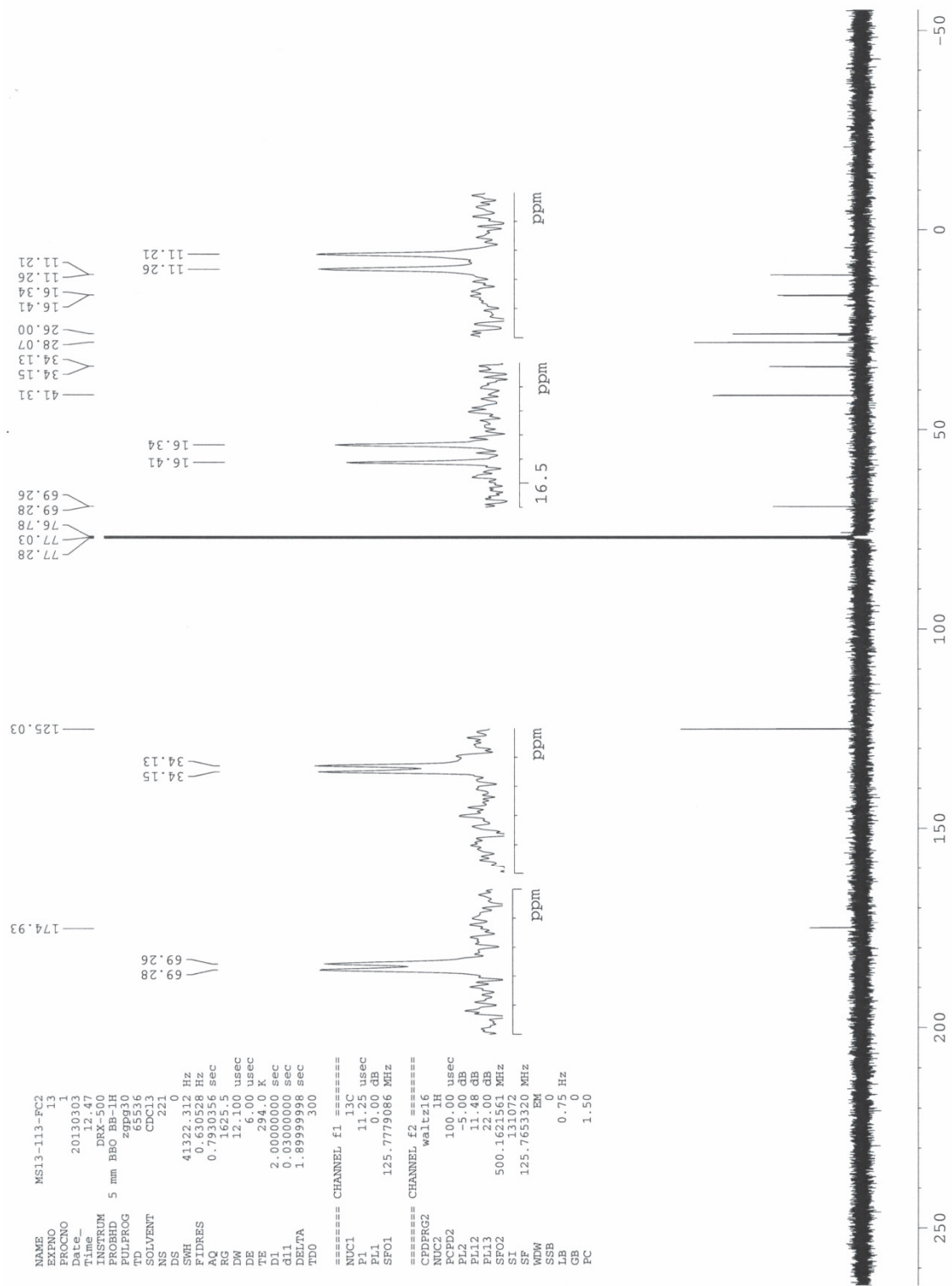
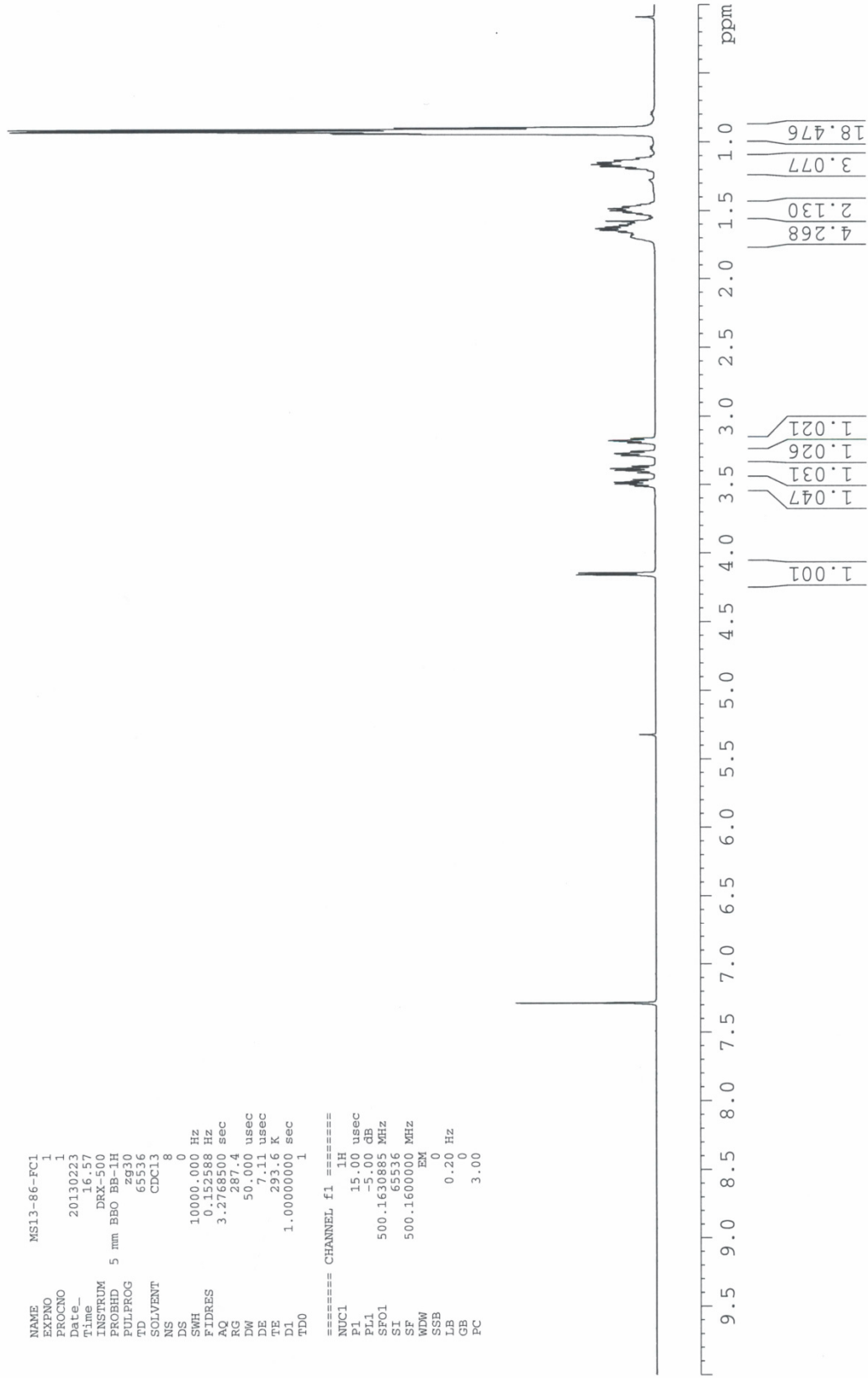


Figure 14 ^{13}C NMR spectra of compound 46 (CDCl_3 , 125 MHz).

NAME MS13-86-FC1
 EXPNO 1
 PROCNO 1
 Date_ 20130223
 Time_ 16.57
 INSTRUM DRX-500
 PROBHD 5 mm BBO BB-1H
 PULPROG zg30
 TD 65536
 SOLVENT CDCl3
 NS 8
 DS 0
 SWH 10000.000 Hz
 FIDRES 0.152588 Hz
 AQ 3.2768500 sec
 RG 287.4
 DW 50.000 usec
 DE 7.11 usec
 TE 293.6 K
 D1 1.00000000 sec
 TDO 1

===== CHANNEL f1 =====
 NUC1 1H
 P1 15.00 usec
 PL1 -5.00 dB
 SFO1 500.1630885 MHz
 SI 65536
 SF 500.1600000 MHz
 WDW EM
 SSB 0
 LB 0.20 Hz
 GB 0
 PC 3.00



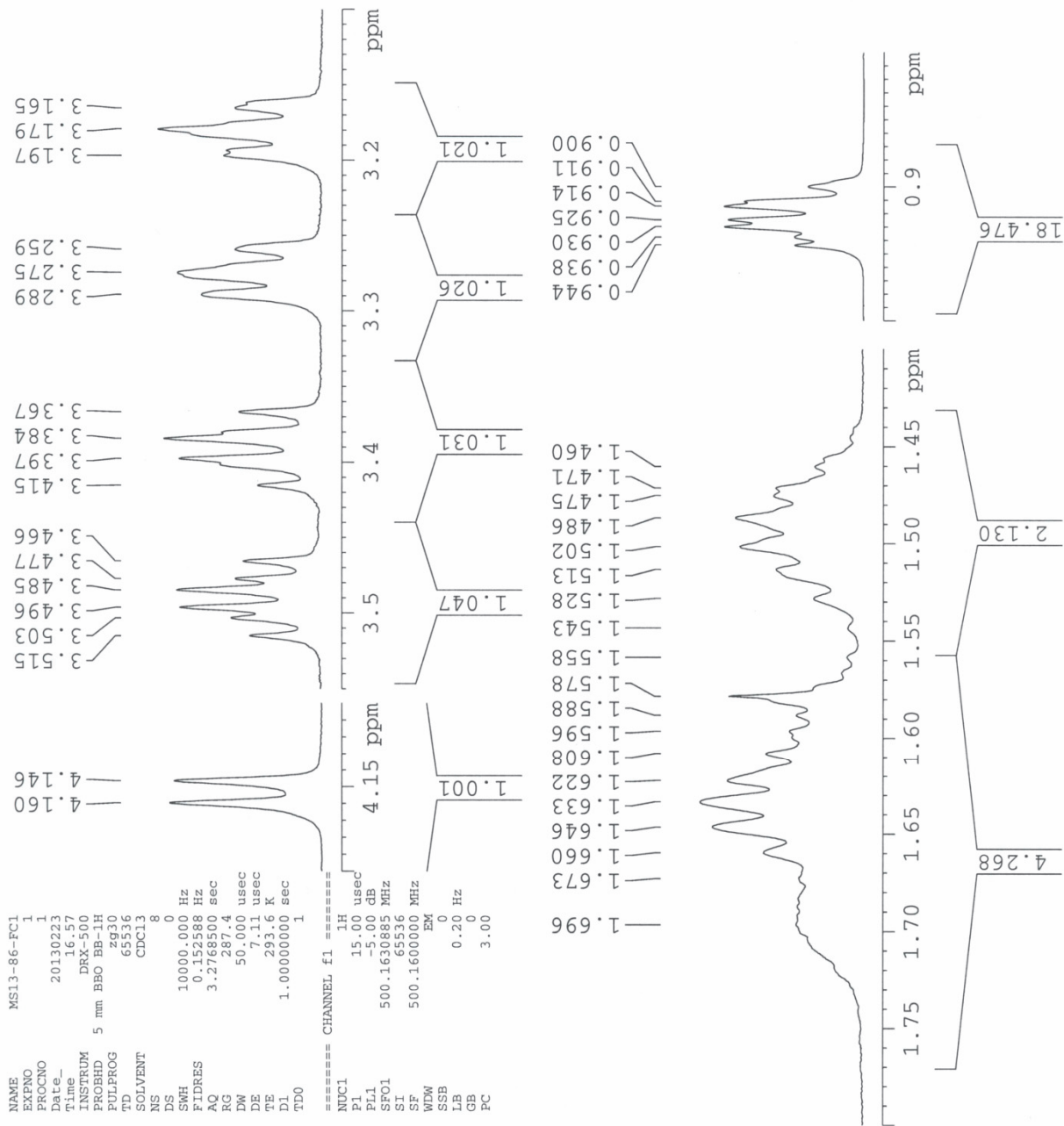


Figure 15 ^1H NMR spectra of compound 47 (CDCl_3 , 500 MHz).

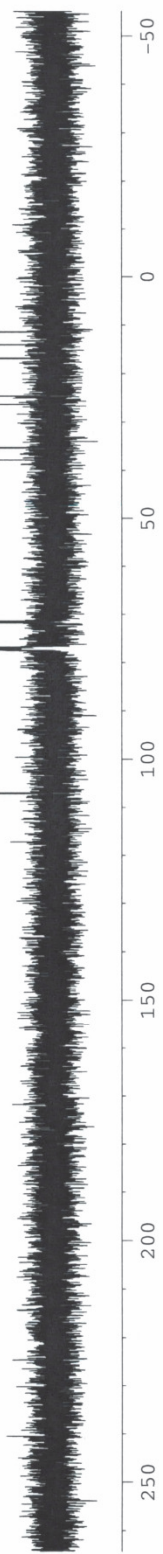
11.35
 11.38
 11.41
 11.43
 13.98
 16.72
 16.73
 16.85
 16.86
 24.59
 26.29
 26.32
 26.34
 35.22
 35.23
 35.31
 37.72
 37.75
 71.29
 71.32
 71.45
 71.47
 71.58
 71.60
 71.71
 76.78
 77.03
 77.28
 77.49
 106.94
 107.03
 107.12

```

NAME MS13-86-FC1
PRCNO 1
Date_ 20130223
Time_ 16.59
INSTRUM DRX-500
PROBHD 5 mm BBO BB-1H
PULPROG zgpg30
TD 65536
SOLVENT CDC13
NS 183
DS 0
SWH 41322.312 Hz
FIDRES 0.630528 Hz
AQ 0.7930356 sec
RG 8182
DE 12.100 usec
TE 293.6 K
D1 2.0000000 sec
d11 0.03000000 sec
DELTA 1.89999998 sec
TD0 300

===== CHANNEL f1 =====
NUC1 13C
P1 11.25 usec
PL1 0.00 dB
SFO1 125.7779086 MHz

===== CHANNEL f2 =====
CPDPRG2 waltz16
NUC2 1H
PCPD2 100.00 usec
PL2 3.00 dB
PL12 13.00 dB
PL13 22.00 dB
SFO2 500.1621561 MHz
SI 131072
SF 125.7653320 MHz
WDW EM
SSB 0
LB 0.75 Hz
GB 0
PC 1.20
  
```



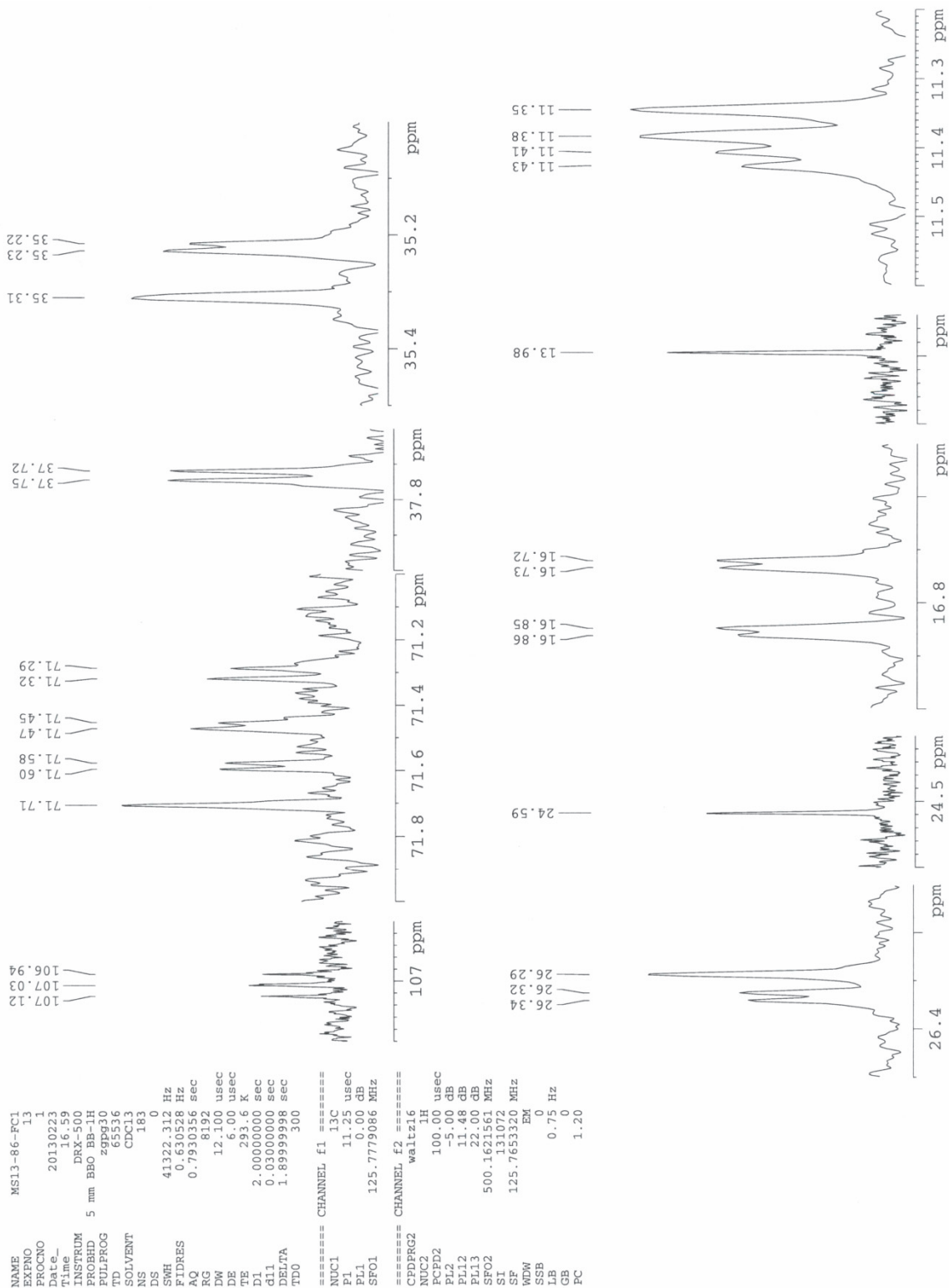


Figure 16 ^{13}C NMR spectra of compound 47 (CDCl_3 , 125 MHz).

In a separate batch, the DODH reaction of L-(+)-tartaric acid in (±)2-methyl-1-butanol was conducted in 0.3 mmol scale following the procedure described above. The reaction mixture was concentrated and purified by flash column chromatography (hexanes: CH₂Cl₂=4:1 to 3:1). 72.4 mg (0.28 mmol, 94 % yield) of **45** was isolated as clear colorless oil. The two isomers due to the two stereocenters of alkyl chain were not distinguishable.

45 ¹H NMR (CDCl₃, 500 MHz): δ6.88 (s, 2H), 4.11 (dd, 2H, *J*=6.0, 10.5 Hz), 4.03 (dd, 2H, *J*=6.5, 10.8 Hz), 1.76-1.83 (m, 2H), 1.44-1.52 (m, 2H), 1.21-1.29 (m, 2H), 0.97 (d, 6H, *J*=6.5 Hz), 0.95 (t, 6H, *J*=7.5 Hz). ¹³C NMR (CDCl₃, 125 MHz): δ165.18, 133.62, 69.97, 34.10, 25.99, 16.37, 11.22. EI-HRMS (EI⁺): C₁₄H₂₅O₄ ([M+H]⁺) calc'd 257.1753, found 257.1758.

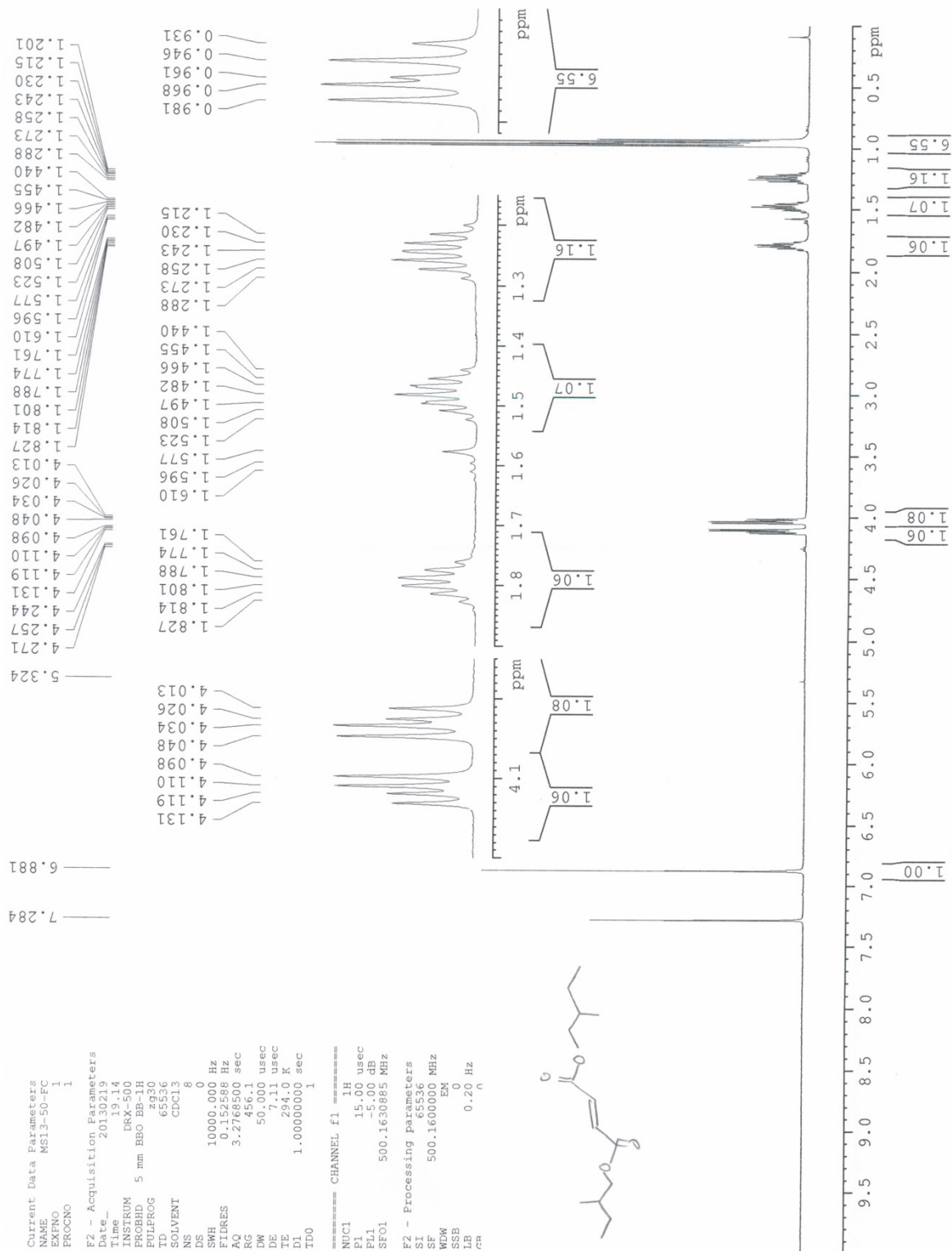


Figure 17 ^1H NMR spectra of diester 45 (CDCl_3 , 500 MHz).

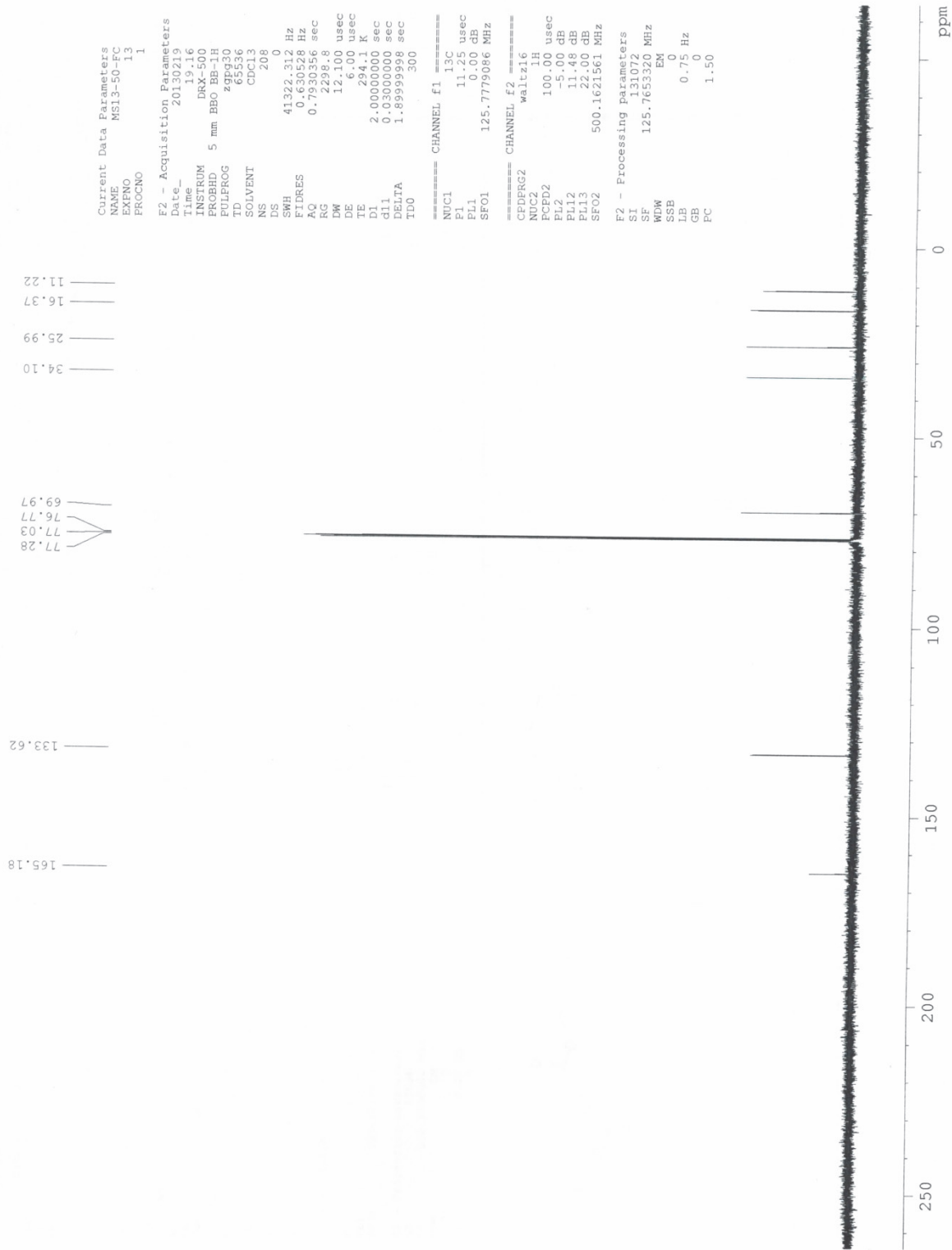
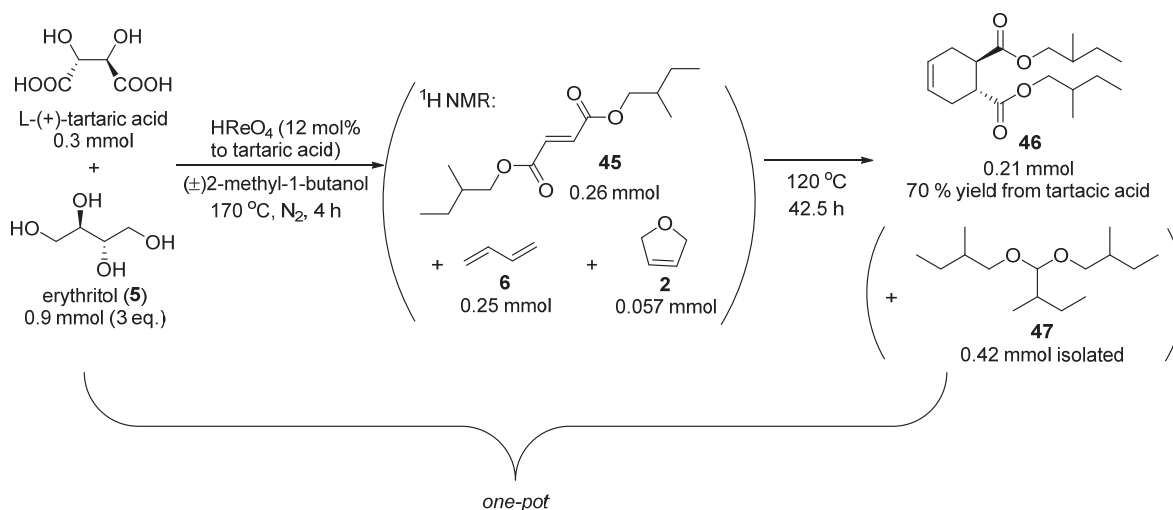


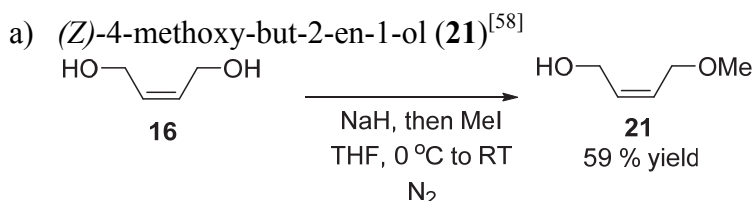
Figure 18 ¹³C NMR spectra of diester 45 (CDCl₃, 125 MHz).

c) L-(+)-tartaric acid and erythritol in one-pot two-step

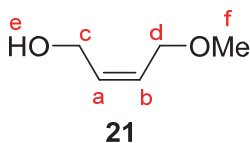


In a Biotage μ W vial (10-20 mL capacity) equipped with a stir bar, erythritol (110 mg, 0.90 mmol) and L-(+)-tartaric acid (45.0 mg, 0.30 mmol) were added. The vial was purged with N₂, sealed, a solution of HReO₄ (76.5 % in H₂O solution, 12.3 mg, 0.037 mmol) in (±)2-methyl-1-butanol (9 mL) and mesitylene (internal standard, 12.7 mg, 0.11 mmol) were added through the septum cap. The vial was immersed in a pre-heated oil bath (170 °C), heated at 170 °C with magnetic stirring for 4 h and cooled in an ice bath. An aliquot of this mixture was drawn, diluted with CDCl₃ and analyzed by ¹H NMR. ¹H NMR showed the presence of **45**: 0.26 mmol (87 % yield), butadiene (**6**): 0.25 mmol, 2,5-dihydrofuran (**2**) (dehydration+DODH product) 0.057 mmol. This mixture was then heated at 120 °C with stirring. The reaction progress was monitored by occasional ¹H NMR analysis of an aliquot. After 42.5 h, ¹H NMR analysis using mesitylene as internal standard (the sample loss due to the ¹H NMR monitoring was ignored) indicated that the mixture contained **45** 0.083 mmol (28 % yield), butadiene 0.060 mmol, 2,5-dihydrofuran 0.049 mmol, and **46** 0.21 mmol (70 % yield). At this point, the mixture was concentrated under the reduced pressure and purified by flash column chromatography (hexanes: CH₂Cl₂=5:1 to 2:1) to afford **46** as clear colorless oil (65.6 mg, 0.21 mmol, 70 % yield). **47** was also isolated from the non-polar fractions (clear colorless oil, 102 mg, 0.42 mmol).

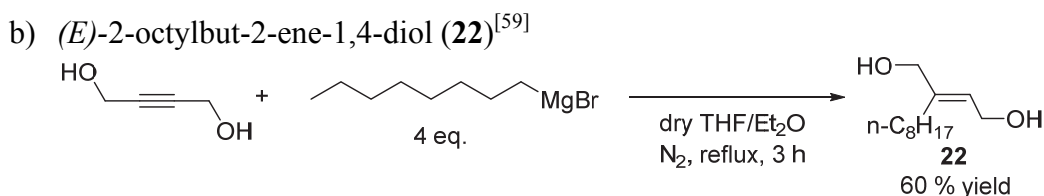
4. Synthesis



To a 250 mL round-bottom flask equipped with a stir bar under N₂, NaH (dry, 316 mg, 13 mmol) and 40 mL of anhydrous THF were added. *cis*-Butene-1,4-diol (**16**, 2.65 g, 30 mmol) was slowly added while stirring the solution at 0 °C. The reaction mixture was warmed to room temperature and stirred for 0.5 h. The mixture was cooled to 0 °C again and MeI (0.81 mL, 13 mmol) was slowly added over 10 min. The mixture was stirred for 2.5 h at 0 °C, and then for 6 h at room temperature. The resulting yellow homogeneous solution was quenched with saturated NH₄Cl aq. (40 mL), extracted with EtOAc x3, the combined organic phase was dried over Na₂SO₄ and concentrated under reduced pressure to afford yellow oil. The product (**21**) was well separated on TLC from the remaining **16** (**21**: R_f=0.34, **16**: R_f=0.11, hexanes:EtOAc=1:1). The crude product was purified by flash column chromatography (hexanes: EtOAc=2:1 to 1:1) and 778 mg of **21** was obtained as yellow oil (7.62 mmol, 59 % yield).



21 ¹H NMR (CDCl₃, 500 MHz): δ5.83-5.88 (m, 1H, Ha), 5.70-5.75 (m, 1H, Hb), 4.24 (bs, 2H, Hc), 4.04 (d, 2H, Hd, *J*=6.0 Hz), 3.38 (s, 3H, Hf), 1.88 (bs, 1H, He). ¹³C NMR (CDCl₃, 125 MHz): δ132.28, 128.35, 68.20, 58.86, 58.24. NOE was observed between Hb and Ha but not between Hb and Hc.

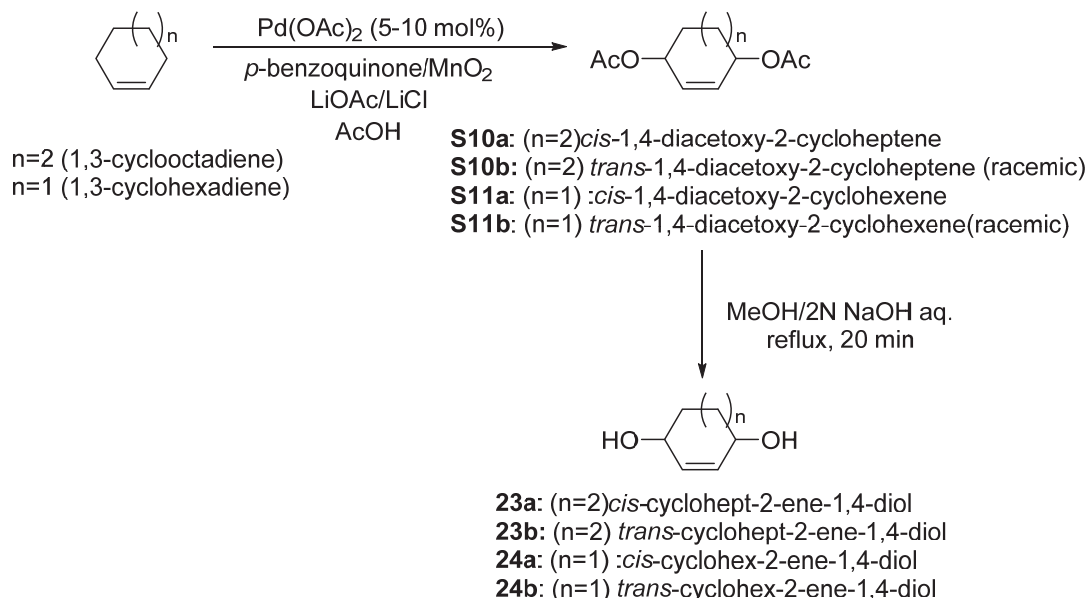


Octylmagnesium bromide (2M in Et₂O) 12 mL (24 mmol) was placed in a N₂-purged 3-neck 250 mL round-bottom flask equipped with a stir bar and a reflux condenser. Additional anhydrous Et₂O (90 mL) was added. While stirring, a solution of 2-butyn-1,4-diol (517.3 mg, 6.0 mmol) in anhydrous THF (12.3 mL) was added dropwise over 15 min. The reaction mixture was stirred at room temperature for 0.5 h, and then refluxed for 3 h. After cooling to 0 °C, it was quenched with saturated NH₄Cl aq. (70 mL) and the organic layer was separated. Aqueous layer was washed with Et₂O (x2), and the combined organic layer was washed with brine (x1), dried over Na₂SO₄ and concentrated under reduced pressure. This crude mixture was purified by flash column

chromatography (hexanes: EtOAc=4:1 to 1:1. TLC: Rf=0.29 at hexanes:EtOAc=1:1) and 719 mg of **22** was obtained as white powder (3.6 mmol, 60 % yield).

22 ¹H NMR (CDCl₃, 500 MHz): δ5.69 (t, 1H, *J*=6.5 Hz), 4.25 (t, 2H, *J*=6.0 Hz), 4.11 (d, 2H, *J*=6.5 Hz), 2.13 (t, 2H, *J*=7.5 Hz), 1.30 (bs, 12H), 0.90 (t, 3H, *J*=7.0 Hz). ¹³C NMR (CDCl₃, 125 MHz): δ142.54, 123.70, 65.86, 58.71, 31.88, 29.74, 29.46, 29.29, 28.99, 28.28, 22.66, 14.10.

- c) *cis*-cyclohept-2-ene-1,4-diol (**23a**), *trans*-cyclohept-2-ene-1,4-diol (racemic) (**23b**), *cis*-cyclohex-2-ene-1,4-diol (**24a**), *trans*-cyclohex-2-ene-1,4-diol (racemic) (**24b**)



1,4-diacetoxy-2-cycloheptene (**S10a**, **S10b**) and 1,4-diacetoxy-2-cyclohexene (**S11a**, **S11b**) were prepared according to the literature^[60]. The reactions were conducted under inert atmosphere.

S10a

To a mixture of Li₂PdCl₄ (50.3 mg, 0.192 mmol), LiOAc·2H₂O (1.60 g, 15.7 mmol) and *p*-benzoquinone (482 mg, 4.4 mmol) in AcOH (8 mL). 1,3-cycloheptadiene (199 mg, 2.11 mmol) was added over 2 h at room temperature. After stirring at room temperature for another 25 h, the mixture was filtered, diluted with brine, extracted with CH₂Cl₂ (x2). The combined organic phases was washed with water (x1), 2N NaOH (x3), brine (x1), dried over Na₂SO₄, filtered and concentrated. The crude mixture was purified by flash column chromatography (hexanes:EtOAc=6:1 to 4:1) to afford 264.5 mg of white powder. 1.25 mmol, 59 % yield, exclusively *cis* (**S10a**).

S10b

To a mixture of Pd(OAc)₂ (73.6 mg, 0.328 mmol) and *p*-benzoquinone (689 mg, 6.38 mmol) in AcOH (10.6 mL). 1,3-cycloheptadiene (278 mg, 2.95 mmol) was added over 1 h at room temperature. After stirring at 40 °C for another 23.5 h, the mixture was filtered, diluted with brine, extracted with CH₂Cl₂ (x2). The combined organic phases was washed with water (x1), 2N NaOH (x3), brine (x1), dried over Na₂SO₄, filtered and concentrated. The crude mixture was purified by flash column chromatography (hexanes:EtOAc=8:1 to 6:1) to afford 483 mg of yellow oil. 2.27 mmol, 77 % total yield, a mixture of **S10a/S10b**; 42 % *cis* (**S10a**), 58% *trans* (**S10b**).

S11a

To a mixture of Pd(OAc)₂ (140 mg, 0.625 mmol), LiCl (106 mg, 2.50 mmol), LiOAc•2H₂O (4.31 g, 42.2 mmol) and *p*-benzoquinone (327.1 mg, 3 mmol) in AcOH (20 mL), MnO₂ (1.30 g, 15.0 mmol) was added while stirring. The solution of 1,3-cyclohexadiene (1.10 mg, 13.7 mmol) in pentane (40 mL) was then added and the resulting bi-phase mixture was stirred at room temperature for 18 h. The pentane phase was separated. The AcOH phase was diluted with brine, filtered, extracted with Et₂O (x3). The combined organic phase was washed with water (x1), 2N NaOH (x3), brine (x1), dried over Na₂SO₄, filtered and concentrated. The crude mixture was purified by flash column chromatography (hexanes:EtOAc=8:1) to afford 1.66 g of yellow oil. 8.38 mmol, 61 % total yield, a mixture of **S11a/S11b**; 90 % *cis* (**S11a**), 10 % *trans* (**S11b**).

S11b

To a mixture of Pd(OAc)₂ (141 mg, 0.628 mmol), LiOAc•2H₂O (1.35 g, 13.4 mmol) and *p*-benzoquinone (380 mg, 3.50 mmol) in AcOH (20 mL), MnO₂ (1.31 g, 15.0 mmol) was added while stirring. The solution of 1,3-cyclohexadiene (1.01 mg, 12.6 mmol) in pentane (40 mL) was then added and the resulting biphasic mixture was stirred at room temperature for 16.5 h. The pentane phase was separated. The AcOH phase was diluted with brine, filtered, extracted with Et₂O (x3). The combined organic phase was washed with water (x1), 2N NaOH (x3), brine (x1), dried over Na₂SO₄, filtered and concentrated. The crude mixture was purified by flash column chromatography (hexanes:EtOAc=8:1 to 6:1) to afford 1.48 g of white powder. 7.5 mmol, 59 % total yield, a mixture of **S11a/S11b**; 10 % *cis* (**S11a**), 90 % *trans* (**S11b**).

A representative procedure for the hydrolysis of **S10**, **S11** to **23**, **24** was as follows:

To a solution of a mixture of **S11a/S11b** (**S11a:S11b**=90:10) (493 mg, 2.5 mmol) in methanol (12 mL), 2N NaOH aq. (3 mL) was added. The mixture was stirred at reflux for 20 min. After cooling to room temperature, it was concentrated under the reduced pressure and extracted with EtOAc (x3). The combined organic layer was dried over Na₂SO₄, filtered and concentrated under the reduced pressure. The crude product was purified and isomers were separated by flash column chromatography (Unlike the

diacetoxy derivative, the diol isomers were separable on flash column chromatography) to isolate **24a**.

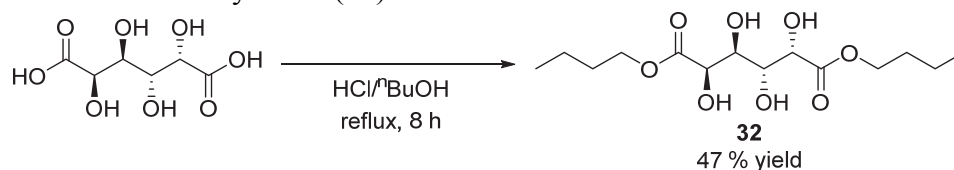
23a White powder. Quantitative yield for the hydrolysis step from **S10a**. ^1H NMR (CDCl_3 , 500 MHz): δ 5.75 (s, 2H), 4.30 (d, 2H, $J=8.0$ Hz), 2.02-2.08 (m, 1H), 1.78-1.83 (m, 2H), 1.75 (br, 1H), 1.56-1.72 (m, 4H). ^{13}C NMR (CDCl_3 , 125 MHz): δ 135.72, 71.44, 36.05, 23.09. EI-HRMS (EI^+): $\text{C}_7\text{H}_{11}\text{O}_2$ ($[\text{M}-\text{H}]^+$) calc'd 127.0759, found 127.0760. TLC: $R_f=0.44$ (EtOAc 100 %, visualized by PMA)

23b Colorless oil. 14 % yield for the hydrolysis step from the **S10a/S10b** mixture (**S10a:S10b**=42:58). The significant loss of yield was due to the co-elusion of **23a** and **23b** in the flash column chromatography purification. ^1H NMR (CDCl_3 , 600 MHz): δ 5.79 (s, 2H), 4.43 (broad d, 2H, $J=4.4$ Hz), 1.70-1.89 (m, 6H), 1.47 (bs, 2H). ^{13}C NMR (CDCl_3 , 125 MHz): δ 135.51, 69.47, 35.31, 19.49. TLC: $R_f=0.34$ (EtOAc 100 %, visualized by PMA)

24a Colorless crystalline solid. 73 % yield for the hydrolysis step from the **S11a/S11b** mixture (**S11a:S11b**=90:10). ^1H NMR ($\text{DMSO}-d_6$, 500 MHz): δ 5.63 (s, alkene H, 2H), 4.69 (d, 2H, $-\text{OH}$, $J=5.0$ Hz), 3.90 (bs, $\text{CH}(\text{OH})$, 2H), 1.56-1.62 (broad m, 4H). ^{13}C NMR ($\text{DMSO}-d_6$, 125 MHz): δ 132.62, 64.08, 28.55.

24b White powder. 59 % yield for the hydrolysis step from the **S11a/S11b** mixture (**S11a:S11b**=10:90). ^1H NMR ($\text{DMSO}-d_6$, 500 MHz): δ 5.58 (s, alkene H, 2H), 4.71 (d, 2H, $-\text{OH}$, $J=4.5$ Hz), 4.01 (bs, $\text{CH}(\text{OH})$, 2H), 1.85-1.94 (m, 2H), 1.26-1.35 (m, 2H). ^{13}C NMR ($\text{DMSO}-d_6$, 125 MHz): δ 133.21, 65.49, 31.31.

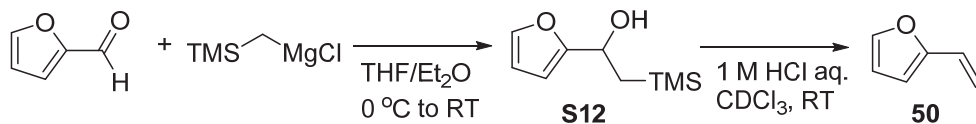
d) mucic acid diⁿbutyl ester (**32**)^[61]



Mucic acid (4.21 g, 20.0 mmol) was added to mixture of 1-butanol (100 mL) and conc. HCl (4 mL) and refluxed while stirring. After 8 h, the mixture was filtered while hot. The filtrate was left for 2 days at room temperature. **32** precipitated as white crystalline solid and it was recovered by filtration, washed with THF (25 mL) and air-dried. **32** 3.02 g (47 % yield).

32 ^1H NMR spectra was similar to that of the known mucic acid dimethyl ester.^[61] ^1H NMR ($\text{DMSO}-d_6$, 500 MHz): δ 4.86 (dd, 2H, $J=8.0$, 15.5 Hz), 4.73-4.80 (m, 2H), 4.30 (d, 2H, $J=7.5$ Hz), 4.03-4.11 (m, 4H), 3.78 (br, 2H), 1.57 (apparent pentet, 4H, $J=7.5$ Hz), 1.34 (apparent sextet, 4H, $J=7.5$ Hz), 0.90 (t, 6H, $J=7.5$ Hz). ^{13}C NMR ($\text{DMSO}-d_6$, 125 MHz): δ 174.19, 71.79, 70.62, 64.24, 30.74, 19.05, 14.07.

e) 2-vinylfuran (**50**): preparation of the authentic sample^[62]



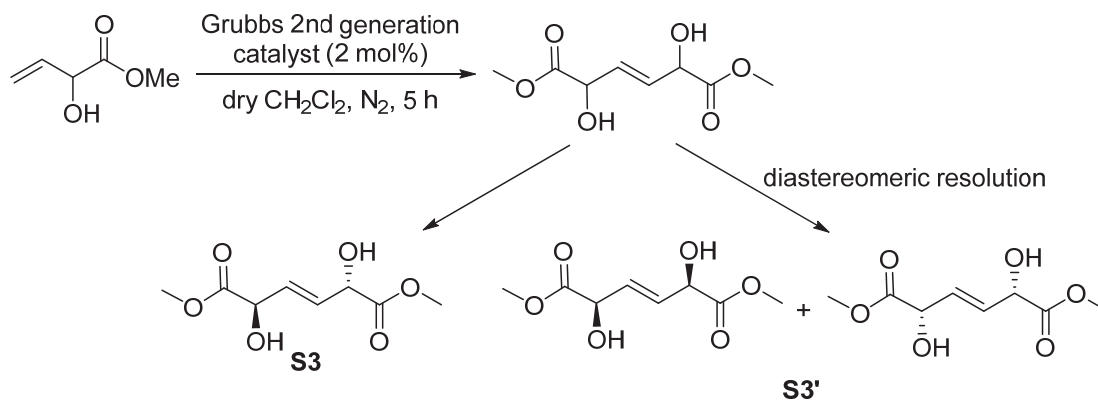
6.0 mmol of TMSCH₂MgCl (1.3 M solution in THF, commercial, 4.6 mL) was placed in a dry 100 mL round-bottom flask equipped with a stir bar under N₂. While stirring at 0 °C, the solution of furfural (503 mg, 5.2 mmol) in dry Et₂O (5.2 mL) was added over 10 min. The mixture was stirred at 0 °C for 8 h, gradually warmed to room temperature and stirred overnight (11 h). The reaction was quenched with sat. NH₄Cl aq. (5 mL) at 0 °C, extracted with Et₂O (30 mL × 3). The combined organic phases were washed with sat. NaHCO₃ aq. (30 mL) and with brine (30 mL), dried over Na₂SO₄ and concentrated under reduced pressure. Sufficiently pure 1-(2-furyl)-2-(trimethylsilyl)ethanol (**S12**) was obtained (699 mg, 3.8 mmol, 73 % yield).

S12: ¹H NMR (CDCl₃, 400 MHz): δ 7.36 (s, 1H), 6.32 (s, 1H), 6.21 (d, 1H, *J*=2.8 Hz), 4.85 (t, 1H, *J*=8.0 Hz), 1.89 (bs, 1H), 1.30 (dd, 2H, *J*=18.2, 8.4 Hz), -0.05 (s, 9H); ¹³C NMR (CDCl₃, 100 MHz): δ 157.68, 141.65, 110.11, 105.47, 65.63, 24.73, -1.41.

50.0 mg (0.27 mmol) of **S12** was dissolved in CDCl₃ (1 mL) in a 4 mL screw-top vial equipped with a stir bar. 1 N HCl (1 mL) was added and the biphasic mixture was stirred at RT overnight. The organic phase contained 2-vinylfuran (**50**) as a major product after 9 h. (The minor by-products were bis-trimethylsilyl ether and the Diels-Alder reaction product trimethyl(phenoxy)silane, detected by GC-MS. **50** was not isolated from the CDCl₃ solution due to the volatility.)

50: ¹H NMR (CDCl₃, 500 MHz): δ 7.38 (d, 1H, *J*=1.5 Hz), 6.54 (dd, 1H, *J*=17.5, 11.0 Hz), 6.40 (dd, 1H, *J*=3.2, 1.5 Hz), 6.29 (d, 1H, *J*=3.0 Hz), 5.69 (dd, 1H, *J*=17.5, 0.5 Hz), 5.19 (dd, 1H, *J*=11.0, 1.0 Hz), 5.19 (dd, 1H, *J*=11.0, 1.0 Hz). ¹³C NMR (CDCl₃, 100 MHz): δ 153.21, 141.98, 125.04, 112.22, 111.21, 107.97.

f) dimethyl (2R,5S,E)-2,5-dihydroxyhex-3-enedioate (**S3**)



100 mg (0.120 mmol) of the commercial Grubbs 2nd generation catalyst was added to a 50 mL 3-neck round bottom flask equipped with a stir bar and a reflux condenser and purged with N₂. A solution of methyl DL-2-hydroxy-3-butenate (693 mg, 6.00 mmol) in dry CH₂Cl₂ (8 mL) was added to the flask and the resulting brown solution was refluxed for 5 h. The solvent was evaporated and the crude mixture was purified by flash column chromatography (hexanes:EtOAc=2:1 to 1:4, TLC: visualized by KMnO₄, R_f=0.48 with EtOAc 100 %, R_f=0.16 with hexanes:EtOAc=1:1) to afford 583 mg (2.9 mmol, 48 % yield) of white powder. ¹H and ¹³C NMR indicated that this was the approximately 1:1 mixture of two isomers, which were tentatively called **S3** and **S3'**. It was realized that **S3'** was much more soluble in EtOAc than **S3**. Therefore, when small amount of EtOAc was added to the above 1:1 mixture, white powder was left at the bottom of the yellow solution. It was decanted, each phase was dried and analyzed by ¹H and ¹³C NMR. The white solid portion (**P1**) was **S3**:**S3'**=0.74 : 0.26 and the solution phase (**P2**) was **S3**:**S3'**=0.22: 0.78. 229.2 mg of dried **P1** was washed again with 2 mL of EtOAc and filtered. The recovered white solid (**P3**) was a pure isomer **S3** (158 mg, 0.77 mmol).

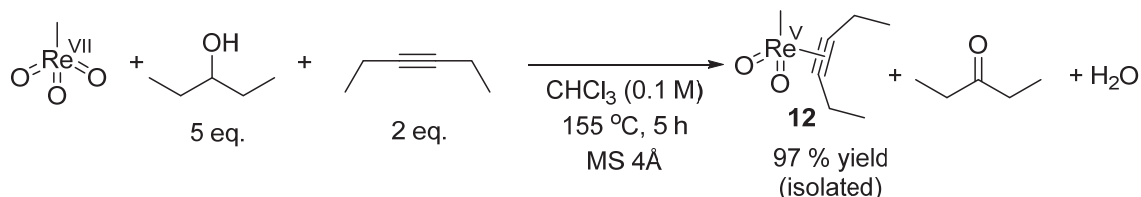
S3 was further recrystallized from EtOAc. X-ray crystallography data confirmed that this is an (*E*)-alkene, and the diol stereochemistry is (2R, 5S) (see Appendix section). Based on the extreme similarity of ¹H and ¹³C NMR spectra as well as the known general selectivity of Grubbs catalyst to prefer (*E*)-alkenes over (*Z*)-alkenes, we assume **S3'** to be an (*E*)-alkene bearing (2R, 5R) and (2S, 5S) diol stereochemistry. We attempted the second diastereomeric resolution of **P2** using EtOAc to obtain pure **S3'**: that is, **P2** was concentrated to give a brown powder, and a small amount of EtOAc was added to this powder. The insoluble white powder was filtered and filtrate was concentrated to give brown solid (**P4**). However, this could not totally remove **S3** and **P4** was **S3**:**S3'**=0.12: 0.88. Thus, it was difficult to obtain pure **S3'** with this strategy and **S3'** was not isolated in pure form to confirm the absolute stereochemistry by X-ray crystal structure.

S3: ¹H NMR (CDCl₃, 500 MHz):δ 6.10 (d, *J*=2.0 Hz), 4.75 (bs, 2H), 3.84 (s, 3H), 2.99 (br, 2H). ¹³C NMR (CDCl₃, 125 MHz):δ 164.56, 128.30, 70.36, 53.11. HR-ESI (ESI⁺): C₈H₁₂O₆Na ([M+Na]⁺) calc'd 227.0526, found 227.0524.

S3': ¹H NMR (CDCl₃, 500 MHz):δ 6.08 (d, 2H, *J*=2.0 Hz), 4.77 (bs, 2H), 3.84 (s, 6H), 2.99 (br, 2H). ¹³C NMR (CDCl₃, 125 MHz):δ 164.56, 128.44, 70.40, 53.11. HR-ESI (ESI⁺): C₈H₁₂O₆Na ([M+Na]⁺) calc'd 227.0526, found 227.0524.

5. Study of Re(V) compound

a) Synthesis of rhenium(V) compound **12**^[33]



CH_3ReO_3 (37.8 mg, 0.15 mmol) and MS 4Å powder (118 mg) were charged in a heavy-wall glass vial (Biotage microwave vial, 2-5 mL) equipped with a magnetic stir bar. The vial was purged with N_2 and sealed. A solution of 3-pentanol (64.8 mg, 0.74 mmol) and 3-hexyne (25.0 mg, 0.30 mmol) in CHCl_3 (1.5 mL) was added by syringe, and the mixture was stirred at $155\text{ }^\circ\text{C}$ in a oil bath for 5 h. Upon cooling, an aliquot of sample was taken, diluted with CDCl_3 , filtered and analyzed by ^1H NMR. The complete consumption of CH_3ReO_3 was confirmed (3-pentanol: 3-hexyne: 3-pentanone: CH_3ReO_3 = 4.22 : 0.68 : 0.95 : 1, by ^1H NMR). The mixture was filtered through celite and all volatiles were removed under reduced pressure. **12** was obtained as yellow solid, 45.7 mg (0.15 mmol, 97 % yield).

For the larger scale synthesis, the reaction was conducted on 0.50 mmol scale under air using a Biotage microwave vial (10-20 mL). Yield of **12**: 84 %.

12: ^1H NMR (CDCl_3 , 500 MHz): δ 3.25 (q, 2H, $J=7.5$ Hz), 3.06 (q, 2H, $J=7.5$ Hz), 2.53 (s, 3H), 1.46 (t, 3H, $J=7.5$ Hz), 1.40 (t, 3H, $J=7.5$ Hz). ^{13}C NMR (CDCl_3 , 100 MHz): δ 140.99, 136.25, 21.96, 18.24, 14.00, 13.74, 4.20.

The NMR peaks shifted depending on the solvent. ^1H NMR (C_6D_6 , 400 MHz): δ 2.55 (q, 2H, $J=7.6$ Hz), 2.22 (q, 2H, $J=7.6$ Hz), 2.19 (s, 3H), 0.92 (t, 3H, $J=7.6$ Hz), 0.85 (t, 3H, $J=7.6$ Hz). ^{13}C NMR (C_6D_6 , 150 MHz): δ 140.54, 135.25, 21.27, 17.62, 13.32, 13.26, 2.16.

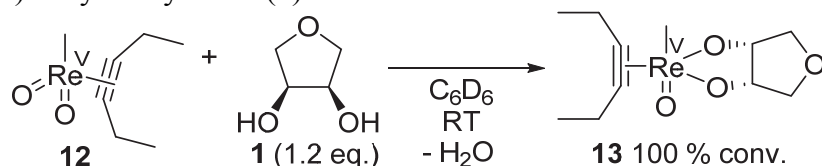
HRMS (EI) calc'd for $[\text{C}_7\text{H}_{13}\text{O}_2\text{Re}]^+$ 314.0445 (^{185}Re) and 316.0473 (^{187}Re), found: 314.0444 and 316.0477.

IR (neat, cm^{-1}) 968, 928.

b) Complexation of diol to rhenium(V) compound **12**

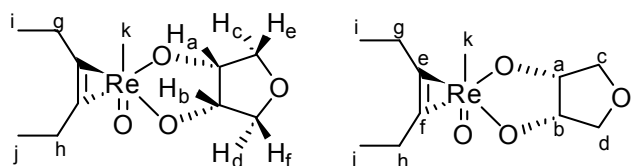
The diol (1.0-1.2 eq.) was placed in a 4 mL screw-top vial. The solution of **12** (0.025-0.050 mmol) in C₆D₆ or toluene-d₈ (0.6 mL) was added and mixed well at room temperature. The solution was then transferred to a NMR tube and analyzed by ¹H and ¹³C NMR. Assignment was given based on COSY and HSQC analyses.

i) anhydroerythritol (**1**)



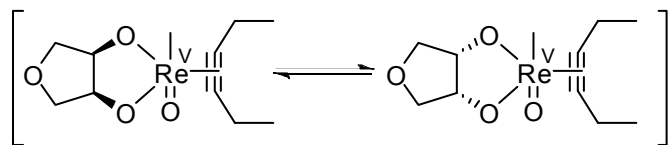
Proton assignment

Carbon assignment



Although the attempt to crystallize **13** was not successful in our hand, a proposed structure consistent with the NMR analyses is shown above. In solution, **13** was not *C_s* symmetric based on ¹H and ¹³C NMR spectra. NOE experiments suggested that 3-hexyne is tilted so that one ethyl group (g, i) is closer to CH₃-Re than the other (h, j). The diol side may be also tilted, but it was difficult to obtain its evidence by NMR methods due to the overlap of correspondent ¹H NMR peaks. Because NOE was observed between H_a, H_b and CH₃-Re, these hydrogens seem to face the same side as CH₃-Re, presumably to avoid the steric interaction between CH₃-Re and the THF ring.

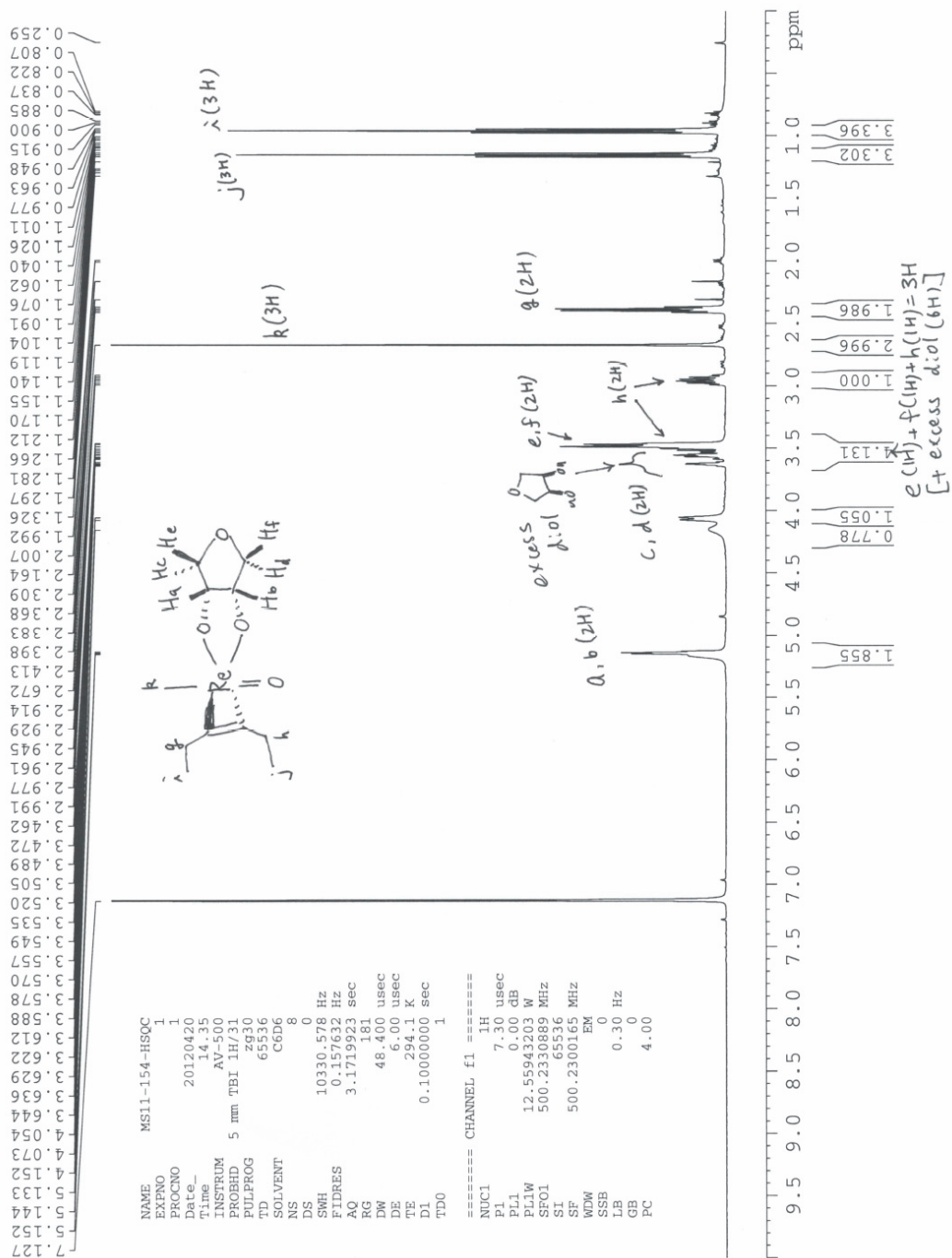
In NOE experiments, some negative peaks were observed at ppm different from the irradiated proton peak. Also, ¹H NMR peaks at 5.16 and 4.15 ppm were broad at room temperature, but sharpened when the solution of **13** in toluene-d₈ was heated (up to 100 °C). These observations are likely due to the equilibrium between two closely related isomers such as conformers (e.g. different tilt angle for anhydroerythritol), or the fast exchange of diol stereochemistry as shown below.

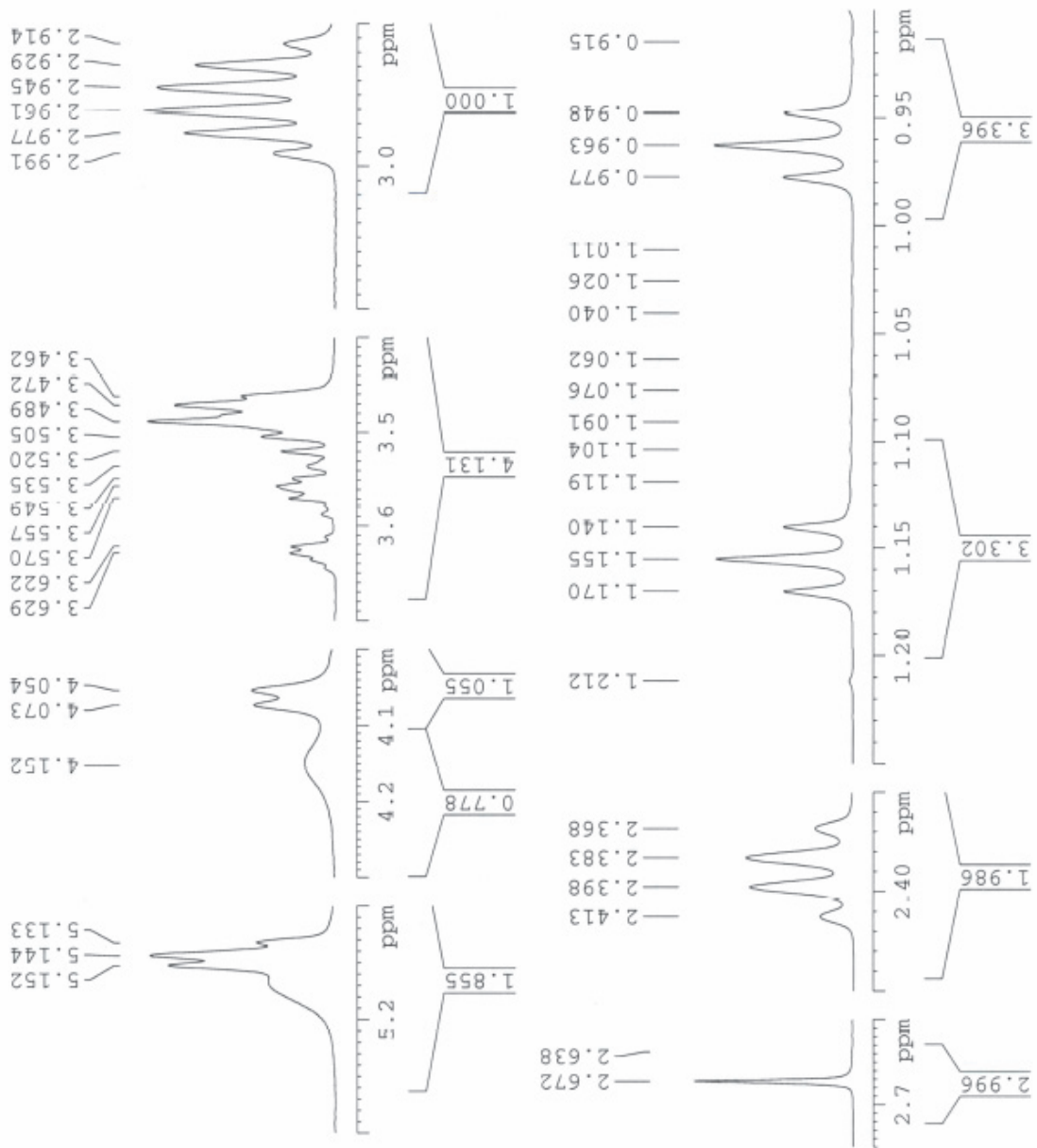


13: HRMS (EI) calc'd for [C₁₁H₁₉O₄Re]⁺ 400.0813 (¹⁸⁵Re) and 402.0841 (¹⁸⁷Re), found: 400.0805 and 402.0837. IR (neat, cm⁻¹) 1112, 1063, 1035, 992, 932, 907, 851.

^1H NMR (C_6D_6 , 500 MHz)

AV-500 new TBI (HXP) probe
1D ^1H starting parameters





¹³C NMR (C₆D₆, 100 MHz)

AVB-400 ZBO Carbon Starting parameters 6/11/03 RN

```

NAME MS11-154
EXPNO 213
PROCNO 1
Date_ 20120418
Time 20.23
INSTRUM AVB-400
PROBHD 5 mm PABBO BB-
PULPROG zgpg30
TD 65536
SOLVENT C6D6
NS 706
DS 0
SWH 23980.814 Hz
FIDRES 0.365518 Hz
AQ 1.3664756 sec
RG 327.5
DM 20.850 usec
DE 6.00 usec
TE 297.3 K
D1 1.50000000 sec
D11 0.03000000 sec
TD0 100

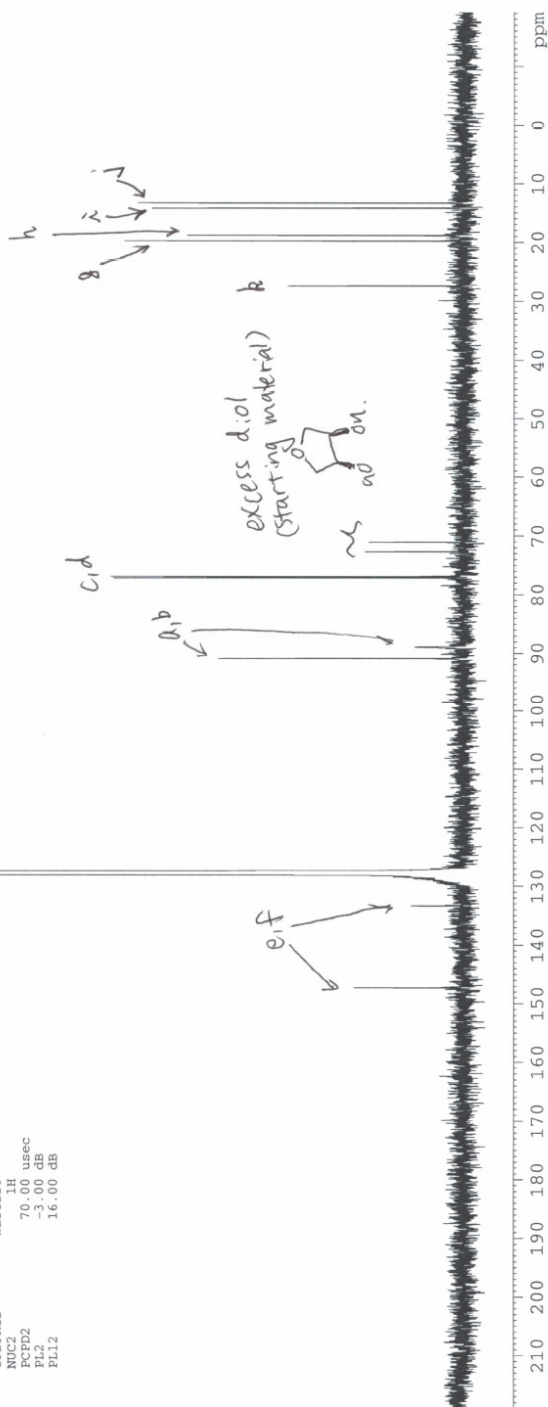
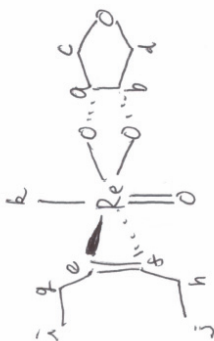
===== CHANNEL f1 =====
NUC1 13C
P1 8.50 usec
PL1 -2.00 dB
PL1W 47.77286148 W
SFO1 100.6228298 MHz

===== CHANNEL f2 =====
CPDPRG2 waltz16
NUC2 1H
PCPD2 70.00 usec
PL2 -3.00 dB
PL12 16.00 dB
    
```

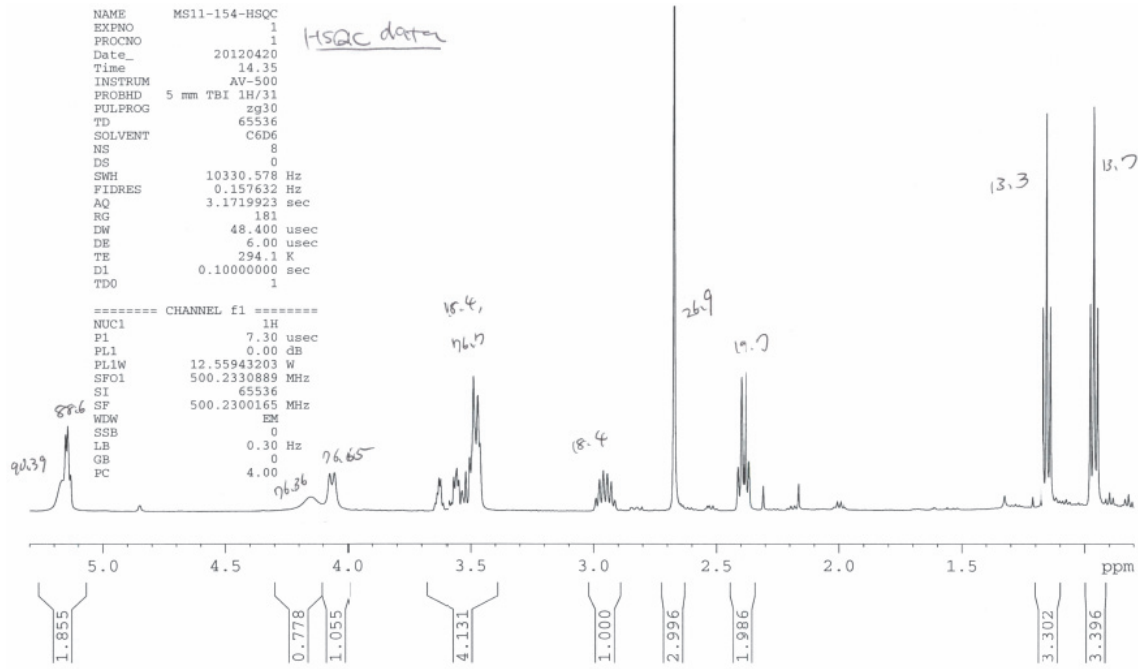
147.24
133.31
127.92
127.68
127.44

90.96
88.87

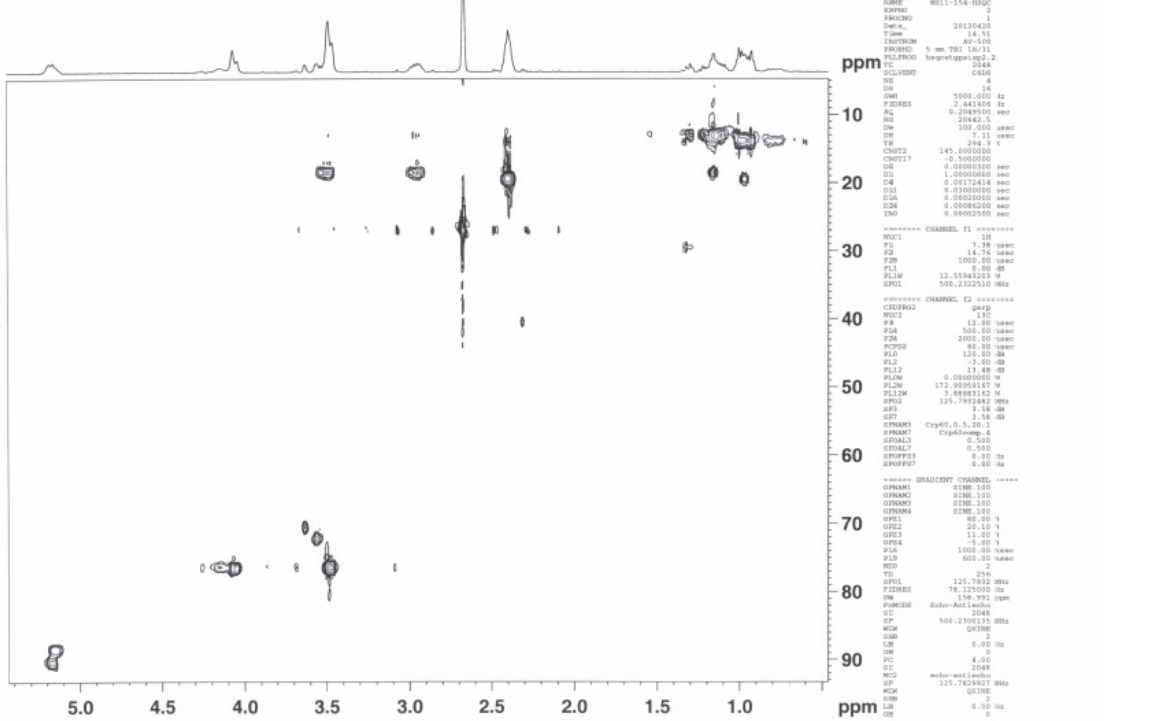
77.09
76.85
72.66
71.04
27.38
19.75
18.79
14.20
13.30



HSQC

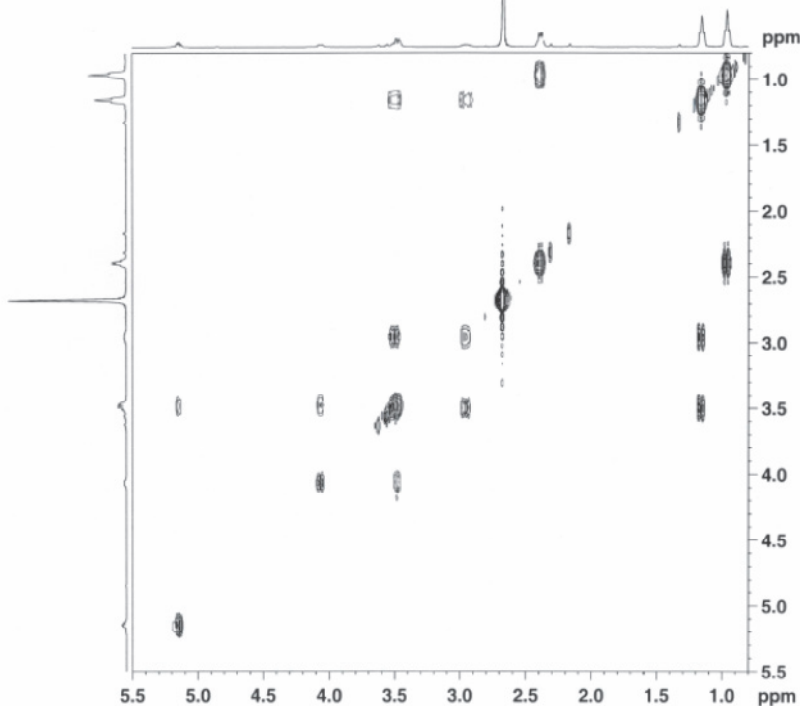


AV-500 new TBI(HXP) probe
 2D (1H,13C) HSQC (starting parameters)
 128 exp., 4 scans each (total time 11min)
 J set to 145
 edte 300K (at 1070 1/h)



COSY

2D gCOSY (magnitude-mode)
 128 exp., 1 scan each, total acq time 5 min 30 sec
 ####remember to use GPRO (or calibrate 90deg 1H pulse
 on your sample; then enter it as pl under ASED)####



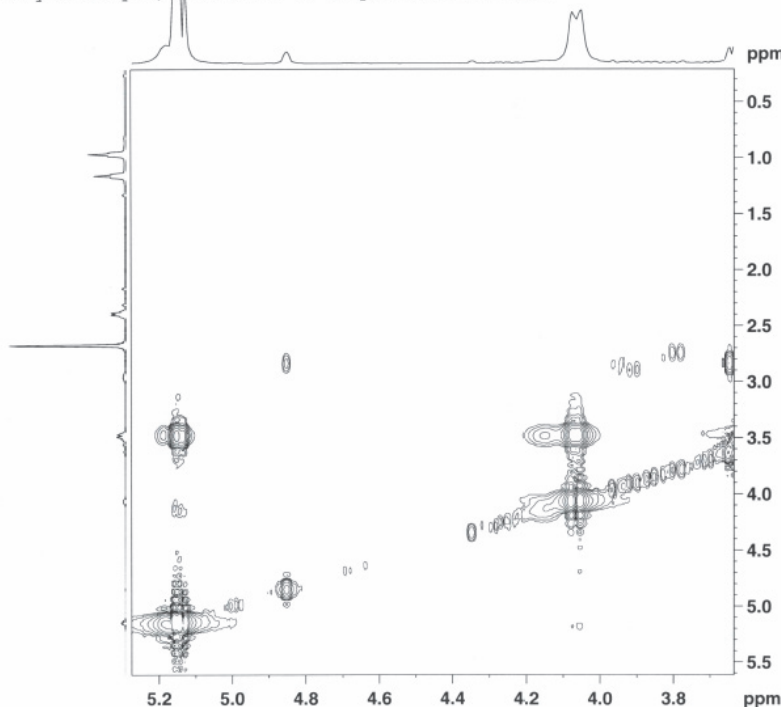
```

NAME MS11-154-COSY
EXPNO 1
PROCNO 1
Date_ 20120420
Time 15.26
INSTRUM AV-500
PROBHD 5 mm TBI LH/31
PULPROG cosygpcqf
TD 2048
SOLVENT C6D6
NS 1
DS 16
SWH 4495.403 Hz
FIDRES 2.195509 Hz
AQ 0.227898 sec
RG 128
DW 111.200 usec
DE 6.00 usec
TE 294.5 K
DO 0.00000300 sec
D1 2.00000000 sec
D13 0.00000400 sec
D16 0.00000000 sec
IN0 0.00022240 sec

===== CHANNEL f1 =====
NUC1 1H
P0 7.38 usec
P1 7.38 usec
PL1 0.00 dB
PL1W 12.55943203 W
SFO1 500.2322510 MHz

===== GRADIENT CHANNEL =====
GPNAM1 SINE.100
GP21 10.00 %
P16 1000.00 usec
ND0 1
TD 128
SFO1 500.2323 MHz
FIDRES 35.128010 Hz
SW 8.989 ppm
F0MODE QF
SI 2048
SF 500.2300155 MHz
W0W SINE
SSB 0
LB 0.00 Hz
GB 0
PC 4.00
SI 2048
MC2 QF
SF 500.2300158 MHz
W0W SINE
SSB 0
LB 0.00 Hz
GB 0
  
```

2D gCOSY (magnitude-mode)
 128 exp., 1 scan each, total acq time 5 min 30 sec
 ####remember to use GPRO (or calibrate 90deg 1H pulse
 on your sample; then enter it as pl under ASED)####



```

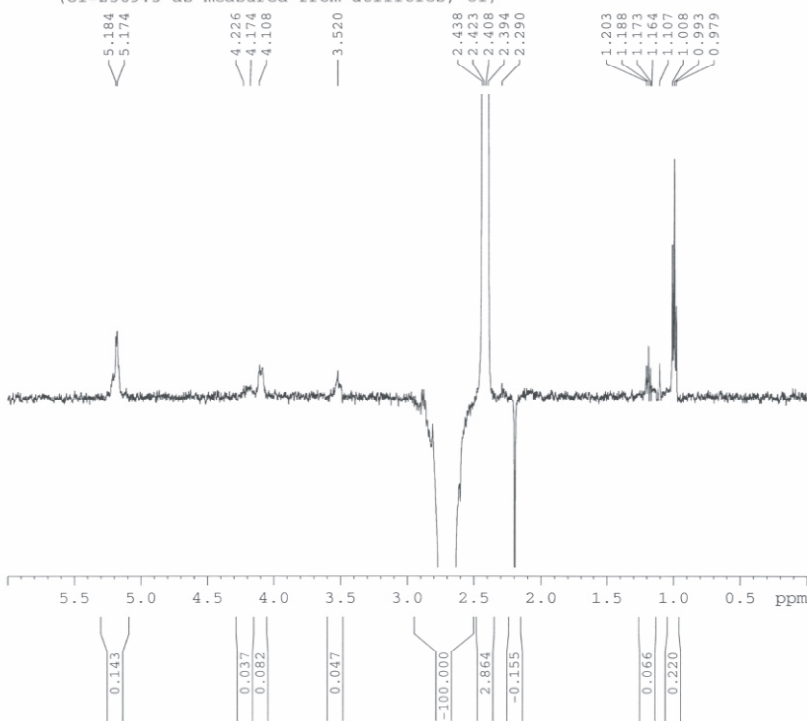
NAME MS11-154-COSY
EXPNO 1
PROCNO 1
Date_ 20120420
Time 15.26
INSTRUM AV-500
PROBHD 5 mm TBI LH/31
PULPROG cosygpcqf
TD 2048
SOLVENT C6D6
NS 1
DS 16
SWH 4496.403 Hz
FIDRES 2.195509 Hz
AQ 0.227898 sec
RG 128
DW 111.200 usec
DE 6.00 usec
TE 294.5 K
DO 0.00000300 sec
D1 2.00000000 sec
D13 0.00000400 sec
D16 0.00000000 sec
IN0 0.00022240 sec

===== CHANNEL f1 =====
NUC1 1H
P0 7.38 usec
P1 7.38 usec
PL1 0.00 dB
PL1W 12.55943203 W
SFO1 500.2322510 MHz

===== GRADIENT CHANNEL =====
GPNAM1 SINE.100
GP21 10.00 %
P16 1000.00 usec
ND0 1
TD 128
SFO1 500.2323 MHz
FIDRES 35.128010 Hz
SW 8.989 ppm
F0MODE QF
SI 2048
SF 500.2300155 MHz
W0W SINE
SSB 0
LB 0.00 Hz
GB 0
PC 4.00
SI 2048
MC2 QF
SF 500.2300158 MHz
W0W SINE
SSB 0
LB 0.00 Hz
GB 0
  
```

1D-NOE

active gNOESY starting parameters (on deoxytrehalose
(ol=2569.3 as measured from utilities, ol)

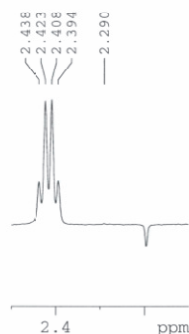


```

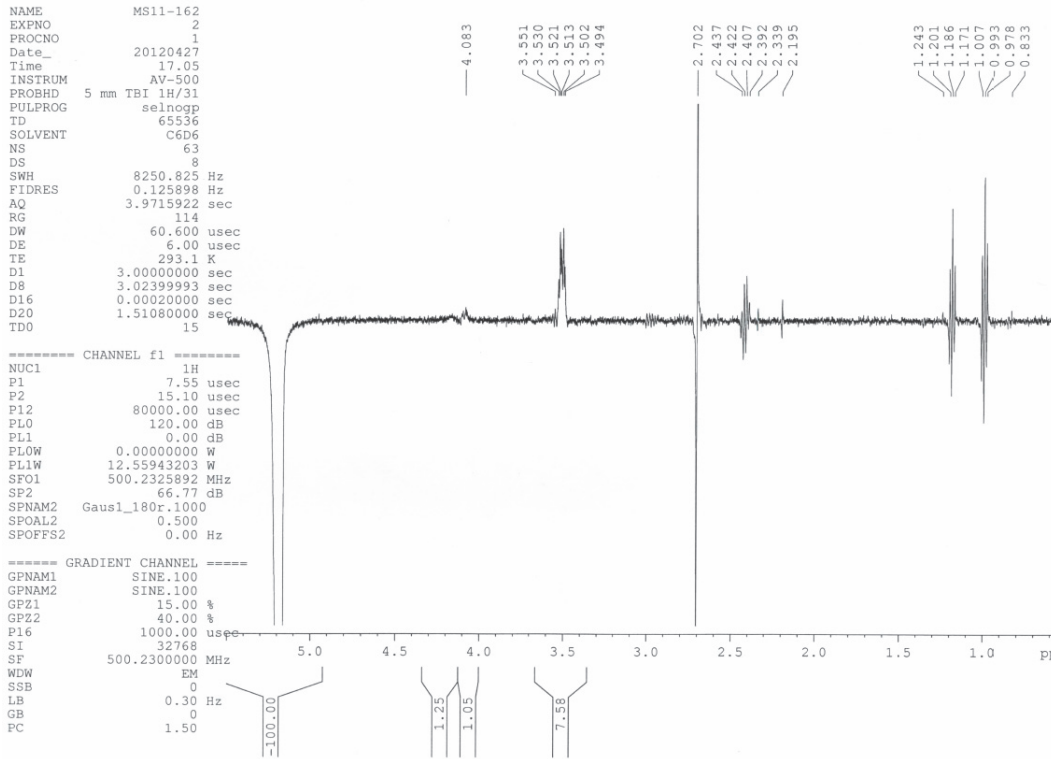
NAME      MS11-161
EXPNO     11
PROCNO    1
Date_     20120426
Time      14.31
INSTRUM   AV-500
PROBHD    5 mm TBI 1H/31
PULPROG   zgpg30
TD         65536
SOLVENT   C6D6
NS         120
DS         8
SWH        8250.825 Hz
FIDRES     0.125898 Hz
AQ         3.9715316 sec
RG         256
DW         50.600 usec
DE         6.00 usec
TE         293.3 K
D1         4.00000000 sec
D8         1.29999995 sec
D16        0.00020000 sec
D50        0.64880002 sec
TD0        15
    
```

```

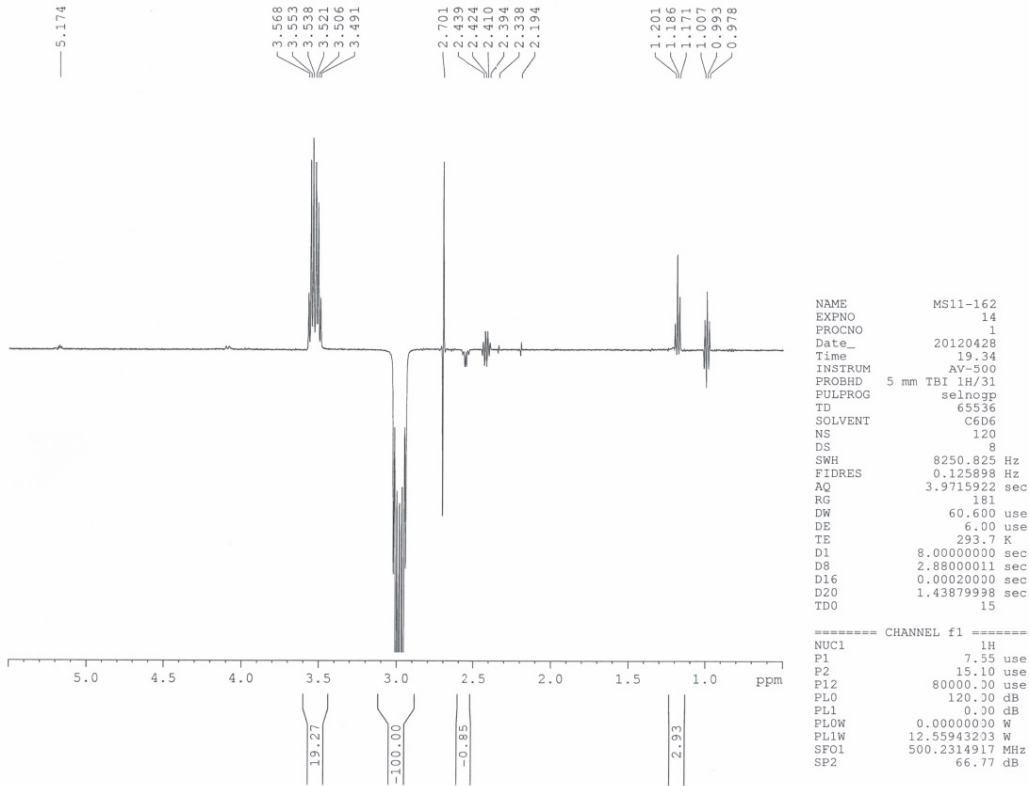
===== CHANNEL f1 =====
NUC1      1H
P1         7.30 usec
P2         14.60 usec
PI2        50000.00 usec
PL0        120.00 dB
PL1         0.00 dB
PL0W       0.00000000 W
PL1W       12.55943203 W
SFO1      500.2313535 MHz
SP2        62.98 dB
    
```



selective gNOESY starting parameters (on deoxytreh
(ol=2569.3 as measured from utilities, ol)



selective gNOESY starting parameters (on deoxytreh
(ol=2569.3 as measured from utilities, ol)



```

NAME      MS11-162
EXPNO     15
PROCNO    1
Date_     20120428
Time      20.08
INSTRUM   AV-500
PROBHD    5 mm TBI 1H/31
PULPROG   selnoggp
TD         65536
SOLVENT   CDCl3
NS         120
DS         8
SWH        8250.825 Hz
FIDRES     0.125898 Hz
AQ         3.9715922 sec
RG         181
DM         60.600 usec
DE         6.00 usec
TE         293.7 K
D1         5.00000000 sec
D8         2.16000009 sec
D16        0.00020000 sec
D20        1.07879996 sec
TD0        15

```

selective gNOESY starting parameters (on deoxytreh
(ol=2569.3 as measured from utilities, ol)

```

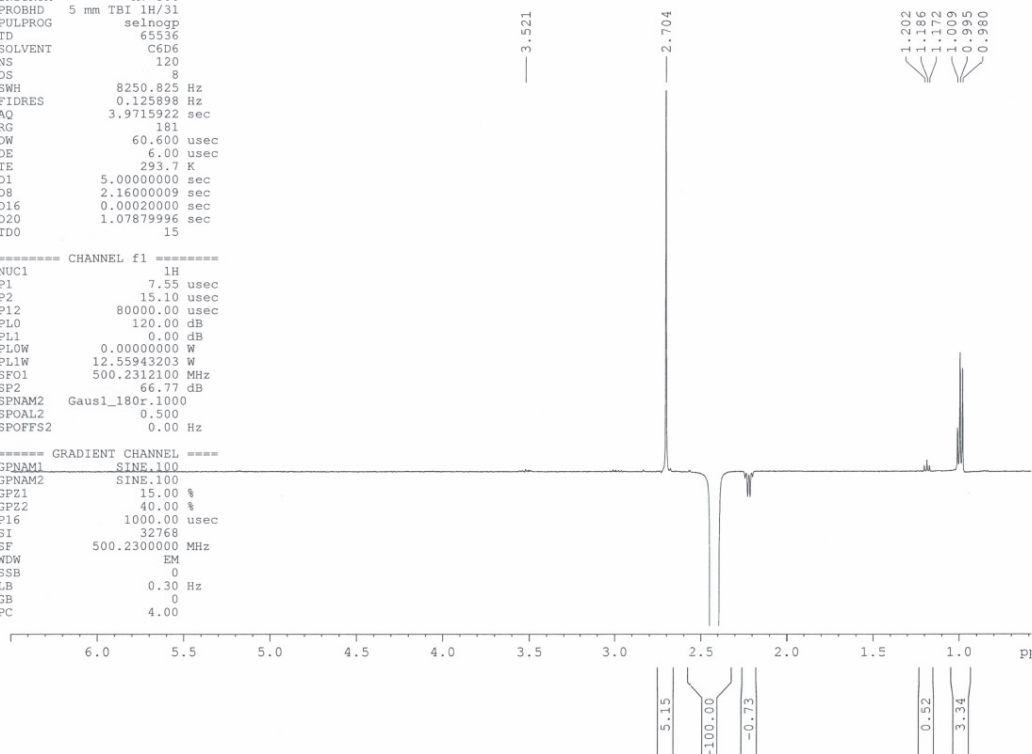
===== CHANNEL f1 =====
NUC1       1H
P1         7.55 usec
P2         15.10 usec
P12        80000.00 usec
PL0        120.00 dB
PL1        0.00 dB
PLOW       0.00000000 W
PL1W       12.55943203 W
SF01       500.2312100 MHz
SP2        66.77 dB
SPNAM2     Gaus1_180r_1000
SFOAL2     0.500
SPOFFS2    0.00 Hz

```

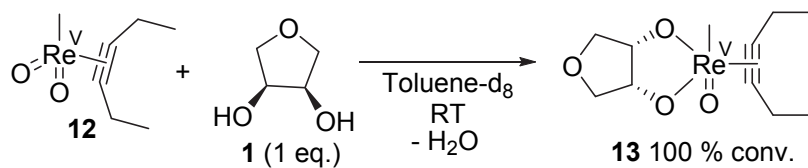
```

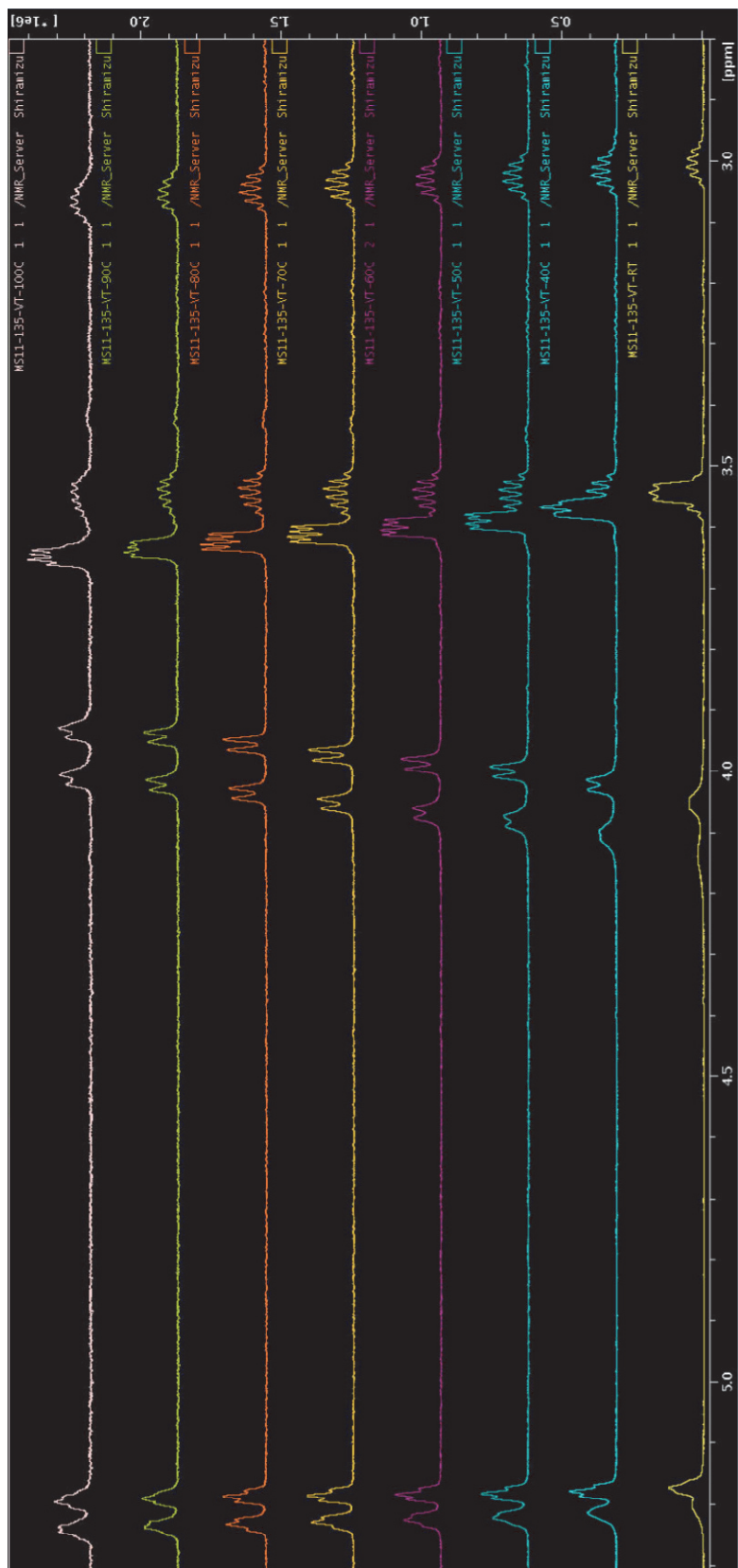
===== GRADIENT CHANNEL =====
GPNAM1     SINE_100
GPNAM2     SINE_100
GP21       15.00 %
GP22       40.00 %
P16        1000.00 usec
SI         32768
SF         500.2300000 MHz
WDW        EM
SSB        0
LB         0.30 Hz
GB         0
PC         4.00

```

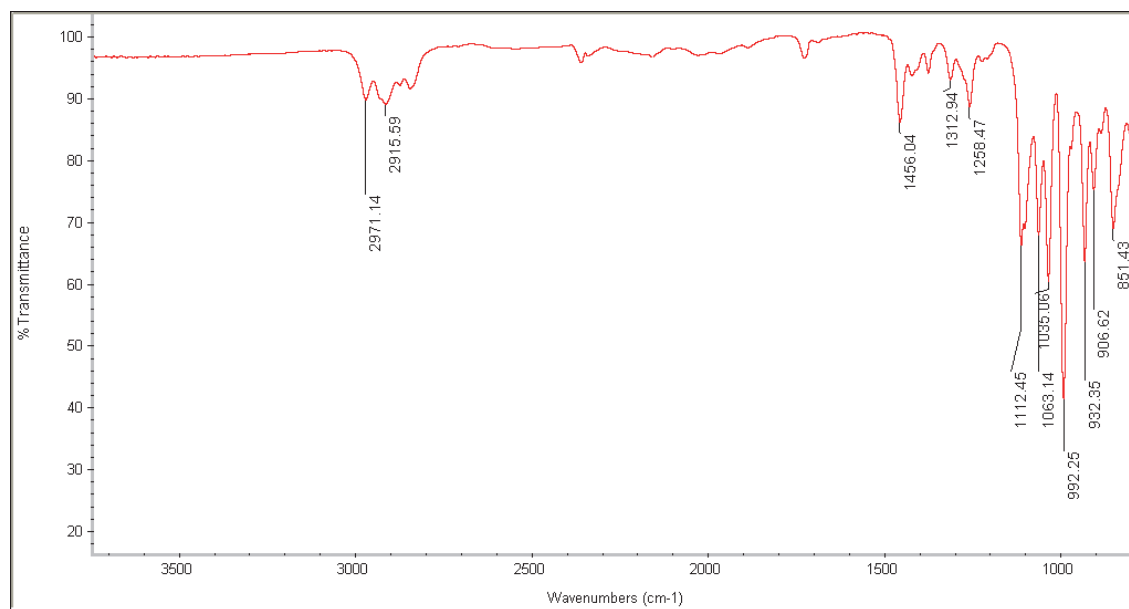


VT-NMR (^1H NMR, toluene- d_8 , 600 MHz) of compound **13**: RT (bottom) to 100 $^\circ\text{C}$ (top)

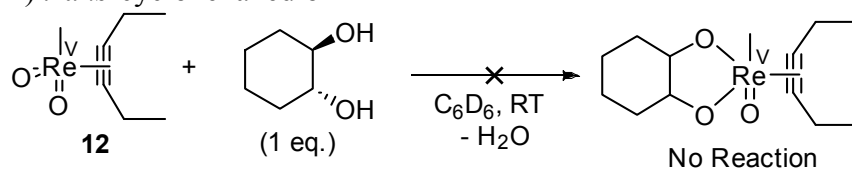




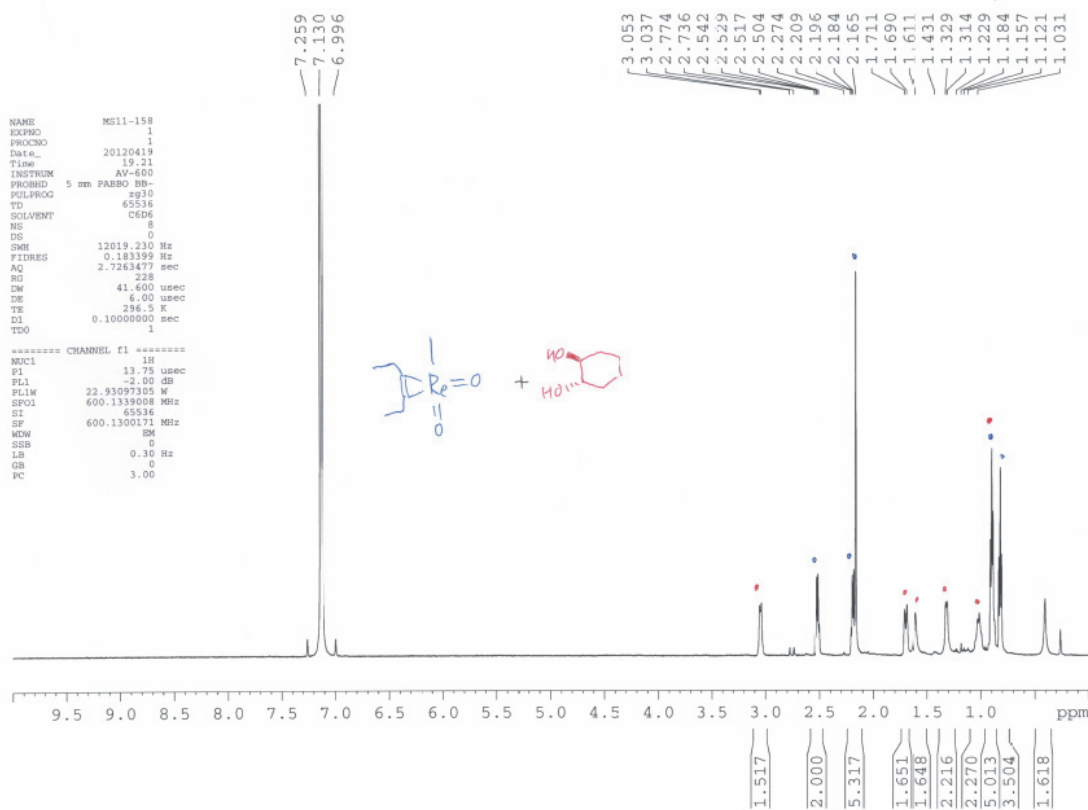
IR (neat)



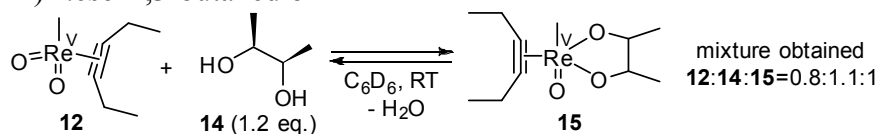
ii) *trans*-cyclohexanediol



^1H NMR (C_6D_6 , 600 MHz)

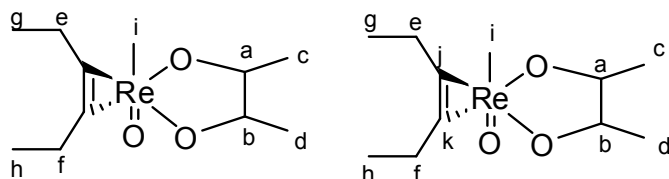


iii) *meso*-2,3-butanediol



Proton assignment

Carbon assignment

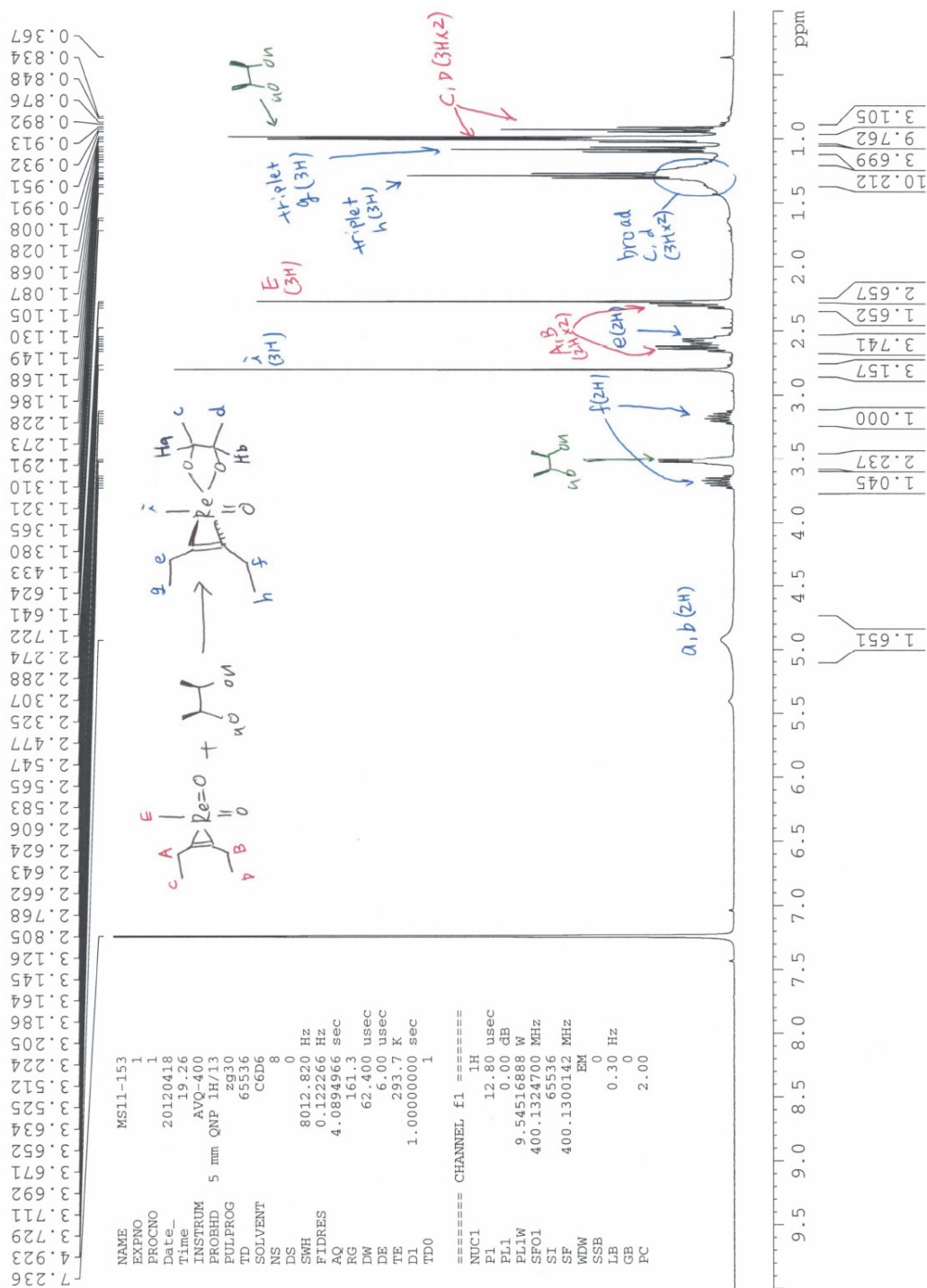


Even when the equivalent of **14** was increased (up to 5 eq.), the conversion did not reach 100 % and a mixture of **12**, **14** and **15** was always obtained. **15** was not *C_s* symmetric and NOE experiments suggested the tilt of 3-hexyne, similar to **13**. However, because no NOE was observed between CH₃-Re and H_a, H_b, H_c, H_d, the stereochemistry on carbon a, b was not determined.

15: HRMS (EI) observed [M-H]⁺ and [M+H]⁺ peaks superimposed due to two Re isotopes (¹⁸⁵Re and ¹⁸⁷Re). Calc'd for [C₁₁H₂₀O₃¹⁸⁵Re]⁺ ([M-H]⁺) 385.0942, found 385.0945. Calc'd for [C₁₁H₂₂O₃¹⁸⁷Re]⁺ ([M+H]⁺) 389.1127, found 389.1136.

$^1\text{H NMR}$ (C_6D_6 , 400 MHz)

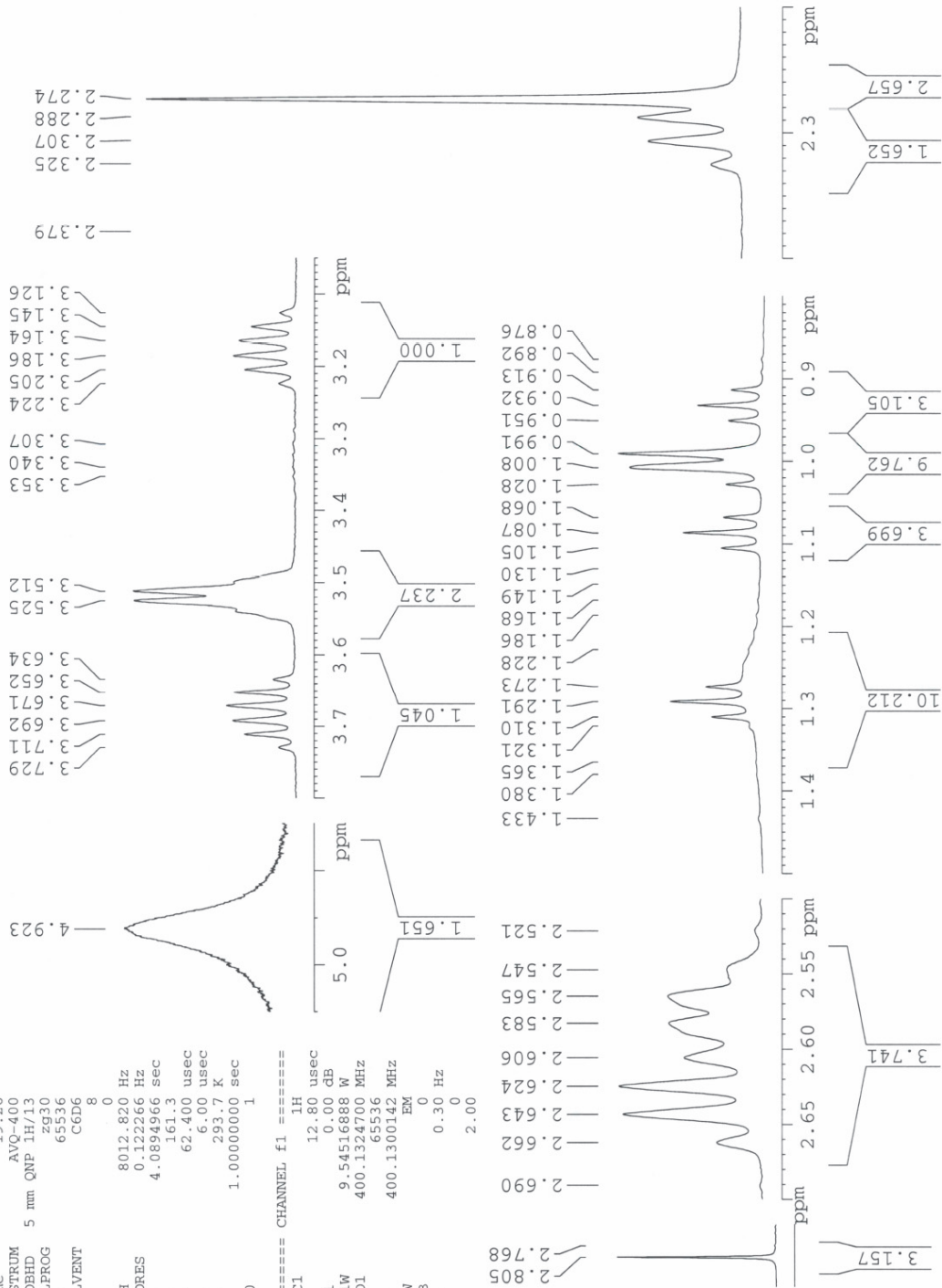
AVQ-400 QNP Proton starting parameters. 7/16/03. Revised 7/22/03 RN



MS11-153
 AVQ-400 QNP Proton starting parameters. 7/16/03. Revised 7/22/03 RN

```

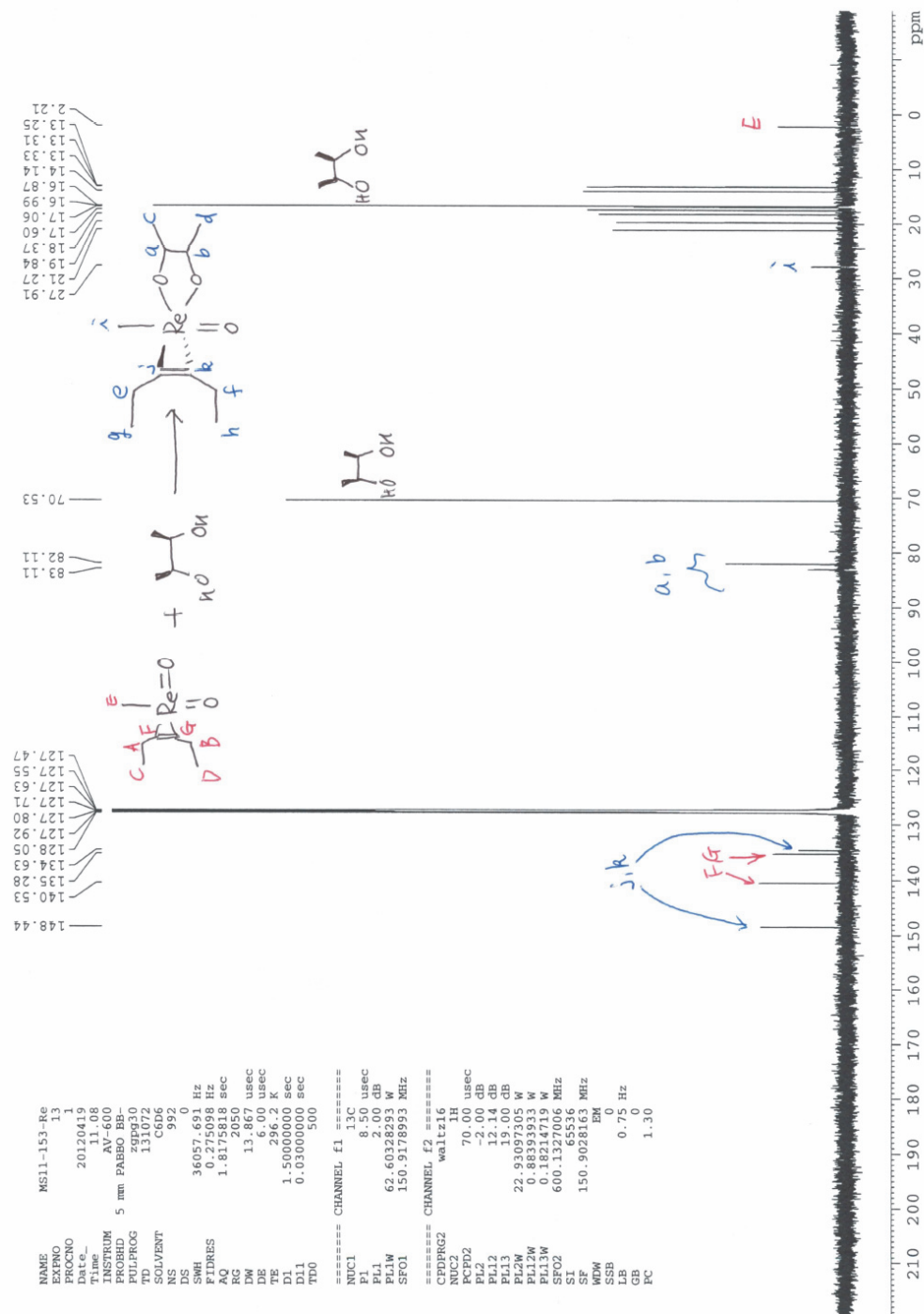
NAME          MS11-153
EXPNO         1
PROCNO        1
Date_         20120418
Time_         19_26
INSTRUM       AVQ-400
PROBHD        5 mm QNP 1H/13
PULPROG       zg30
TD            65536
SOLVENT       C6D6
NS            8
DS            0
SWH           8012.820 Hz
AQ            0.122266 Hz
RG            4.0894966 sec
RG            161.3
DM            62.400 usec
DE            6.00 usec
TE            293.7 K
D1            1.00000000 sec
TD0           1
===== CHANNEL f1 =====
NUC1          1H
P1            12.80 usec
PL1          0.00 dB
PL1W         9.54516888 W
SFO1         400.1324700 MHz
SI           65536
SF           400.1300142 MHz
WDW          EM
SSB          0
LB           0.30 Hz
GB           0
PC           2.00
  
```



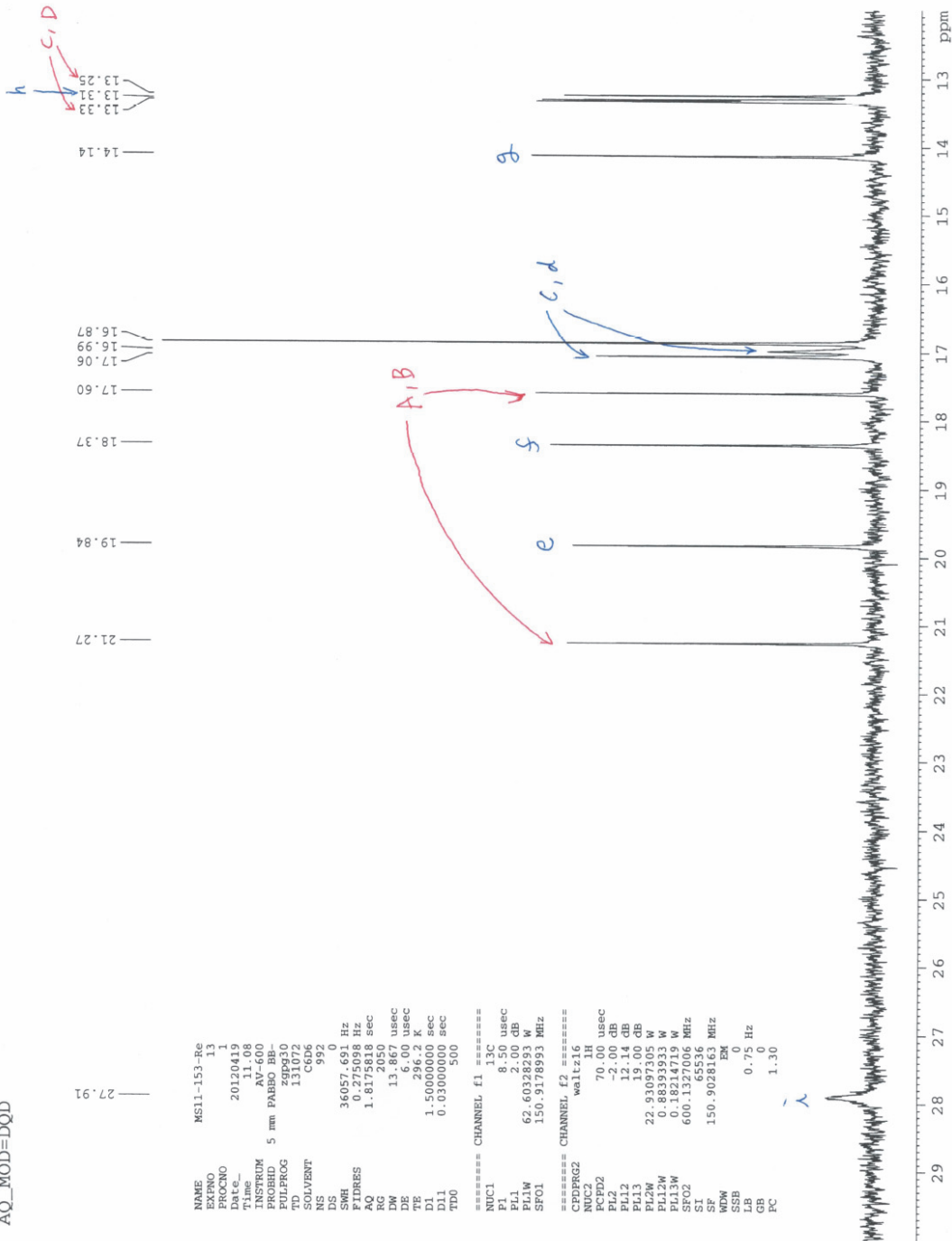
The broadening of H_a, H_b, H_c, H_d peaks of **15** is likely due to the equilibrium between two isomers similar to the case of **13**.

¹³C NMR (C₆D₆, 150 MHz)

12/21/10 CC AV-600 ZBO carbon starting parameters
AQ_MOD=DQD



12/21/10 CC AV-600 ZBO carbon starting parameters
AQ_MOD=DQD

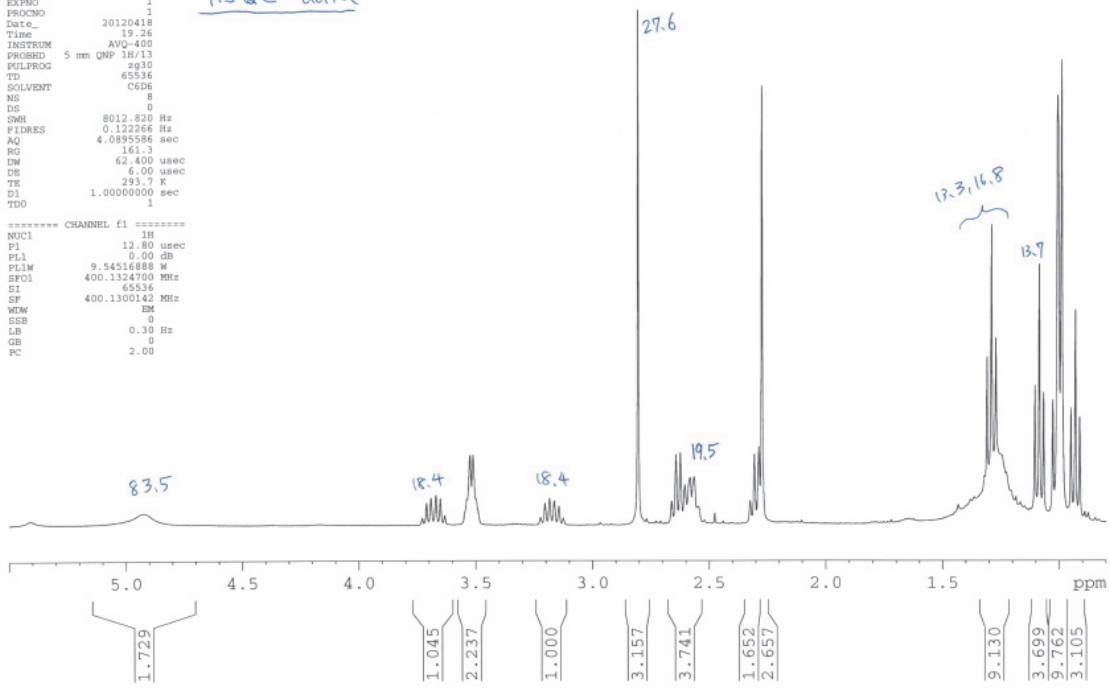


HSQC

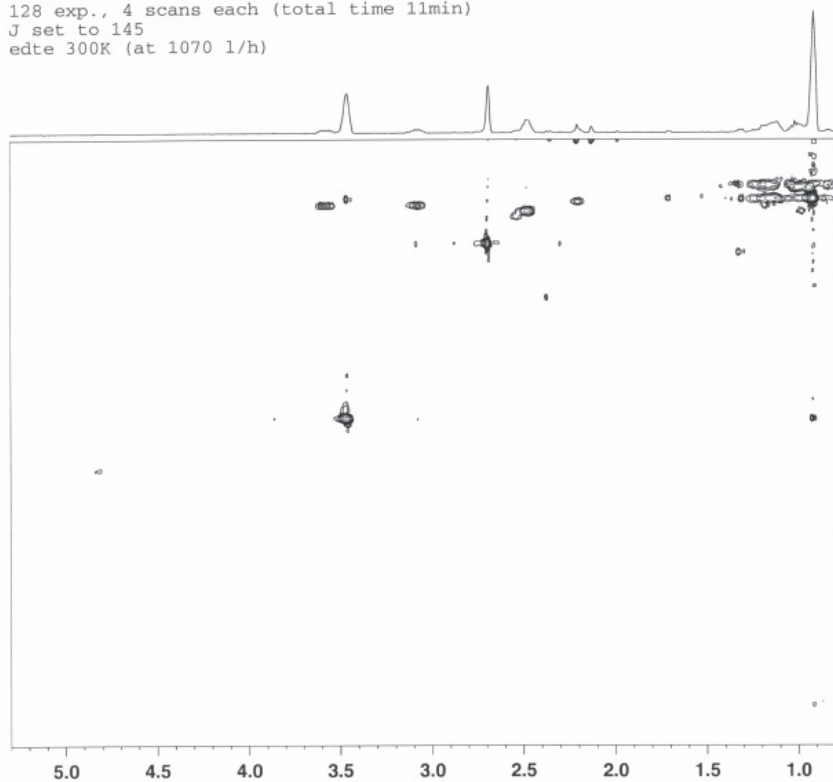
```

NAME      MS11-153
EXPNO    1
PROCNO   1
Date_    20120418
Time     19.26
INSTRUM  AVQ-400
PROBHD   5 mm QNP 1H/13
PULPROG  zgpg30
TD        65536
SOLVENT  C6D6
NS        8
DS        0
SWH       8012.820 Hz
FIDRES   0.122266 Hz
AQ        4.0895586 sec
RG        161.3
DW        62.400 usec
DE        6.00 usec
TE        293.7 K
D1        1.0000000 sec
TDO       1
  
```

HSQC data



AV-500 new TBI(HXP) probe
 2D (1H,13C) HSQC (starting parameters)
 128 exp., 4 scans each (total time 11min)
 J set to 145
 edte 300K (at 1070 1/h)

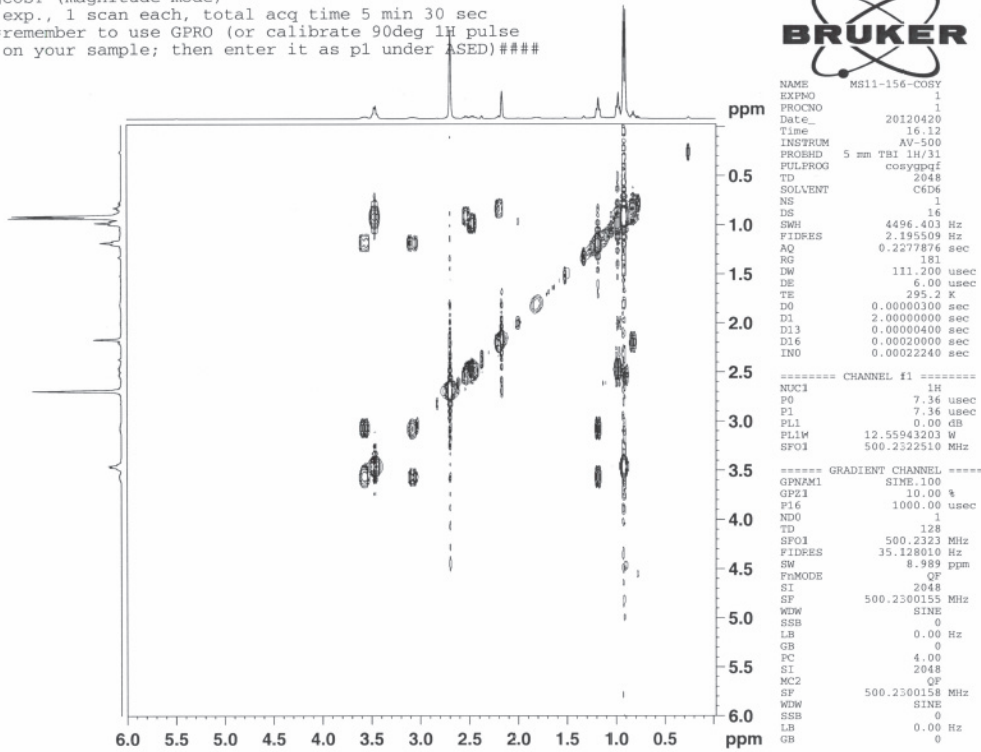


```

NAME      MS11-156-HSQC
EXPNO    1
PROCNO   1
Date_    20120418
Time     19.46
INSTRUM  AVQ-500
PROBHD   5 mm TBI 1H/13
PULPROG  zgpg30
TD        2648
SOLVENT  CDCl3
NS        8
DS        0
SWH       5000.080 Hz
FIDRES   0.2481049 Hz
AQ        0.2049540 sec
RG        1.0364
DW        100.080 usec
DE        1.11 usec
TE        294.2 K
D1        145.0000000 sec
D11       0.5000000 sec
D12       1.0000000 sec
D13       0.00174214 sec
D14       0.0000000 sec
D15       0.0000000 sec
D16       0.0000000 sec
D17       0.0000000 sec
D18       0.0000000 sec
D19       0.0000000 sec
D20       0.0000000 sec
D21       0.0000000 sec
D22       0.0000000 sec
D23       0.0000000 sec
D24       0.0000000 sec
D25       0.0000000 sec
D26       0.0000000 sec
D27       0.0000000 sec
D28       0.0000000 sec
D29       0.0000000 sec
D30       0.0000000 sec
D31       0.0000000 sec
D32       0.0000000 sec
D33       0.0000000 sec
D34       0.0000000 sec
D35       0.0000000 sec
D36       0.0000000 sec
D37       0.0000000 sec
D38       0.0000000 sec
D39       0.0000000 sec
D40       0.0000000 sec
D41       0.0000000 sec
D42       0.0000000 sec
D43       0.0000000 sec
D44       0.0000000 sec
D45       0.0000000 sec
D46       0.0000000 sec
D47       0.0000000 sec
D48       0.0000000 sec
D49       0.0000000 sec
D50       0.0000000 sec
D51       0.0000000 sec
D52       0.0000000 sec
D53       0.0000000 sec
D54       0.0000000 sec
D55       0.0000000 sec
D56       0.0000000 sec
D57       0.0000000 sec
D58       0.0000000 sec
D59       0.0000000 sec
D60       0.0000000 sec
D61       0.0000000 sec
D62       0.0000000 sec
D63       0.0000000 sec
D64       0.0000000 sec
D65       0.0000000 sec
D66       0.0000000 sec
D67       0.0000000 sec
D68       0.0000000 sec
D69       0.0000000 sec
D70       0.0000000 sec
D71       0.0000000 sec
D72       0.0000000 sec
D73       0.0000000 sec
D74       0.0000000 sec
D75       0.0000000 sec
D76       0.0000000 sec
D77       0.0000000 sec
D78       0.0000000 sec
D79       0.0000000 sec
D80       0.0000000 sec
D81       0.0000000 sec
D82       0.0000000 sec
D83       0.0000000 sec
D84       0.0000000 sec
D85       0.0000000 sec
D86       0.0000000 sec
D87       0.0000000 sec
D88       0.0000000 sec
D89       0.0000000 sec
D90       0.0000000 sec
D91       0.0000000 sec
D92       0.0000000 sec
D93       0.0000000 sec
D94       0.0000000 sec
D95       0.0000000 sec
D96       0.0000000 sec
D97       0.0000000 sec
D98       0.0000000 sec
D99       0.0000000 sec
D100      0.0000000 sec
  
```

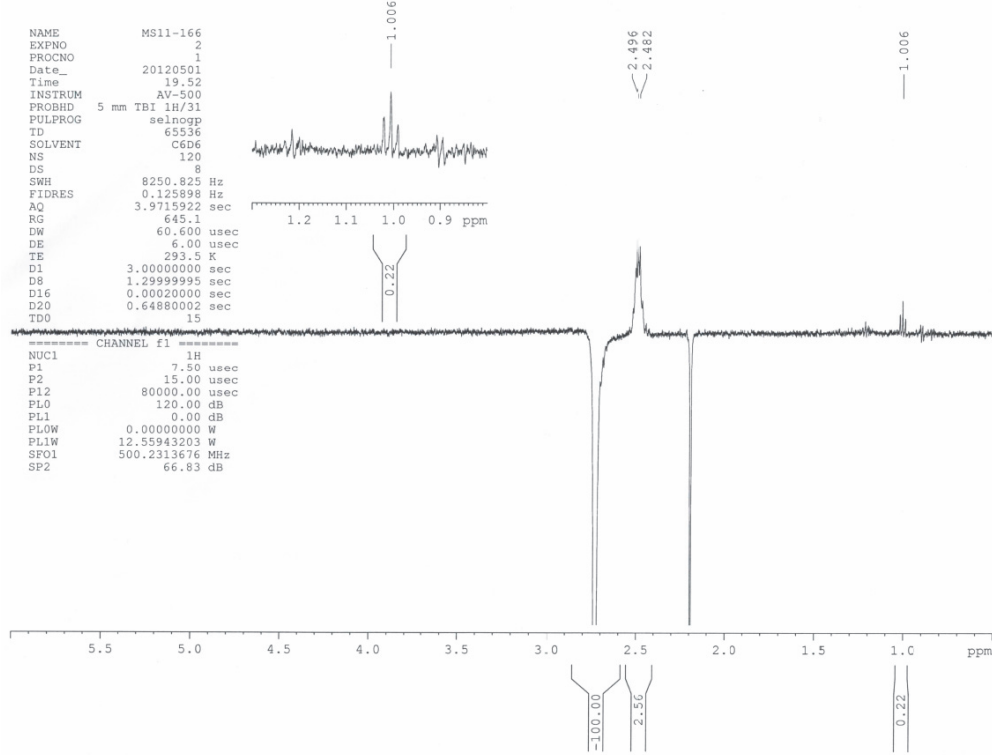
COSY

2D gCOSY (magnitude-mode)
128 exp., 1 scan each, total acq time 5 min 30 sec
###remember to use GPRO (or calibrate 90deg 1H pulse
on your sample; then enter it as pl under ASED)###

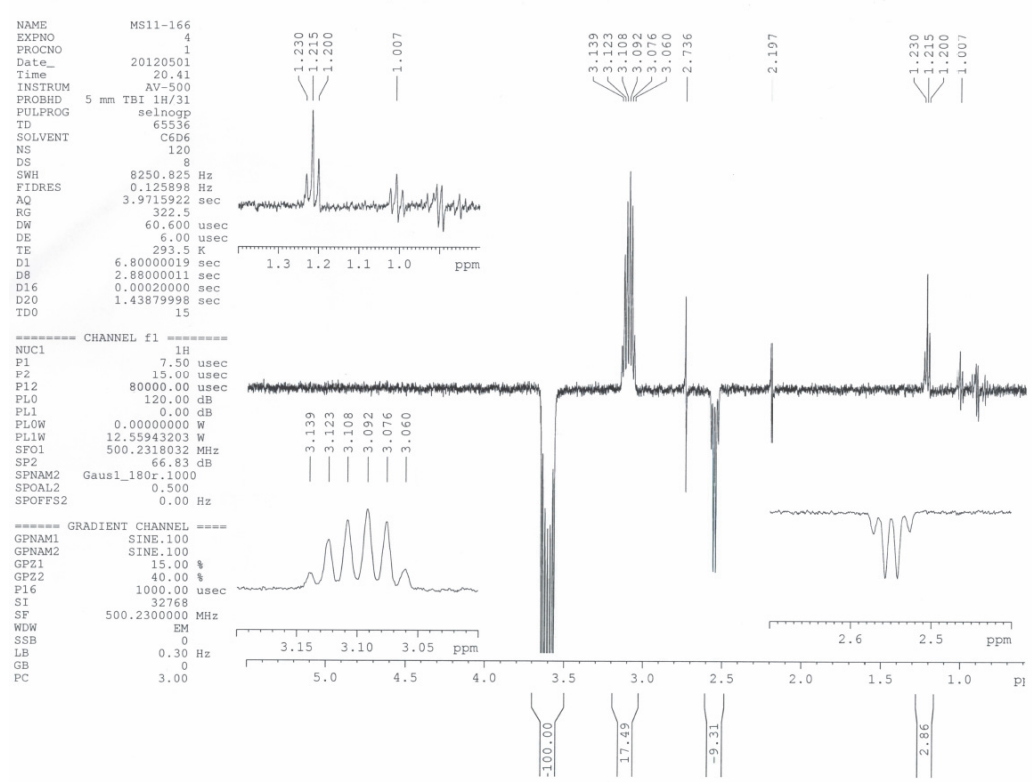


1D-NOE

selective gNOESY starting parameters (on ceoxytrehaloses)
(ol=2569.3 as measured from utilities, ol)

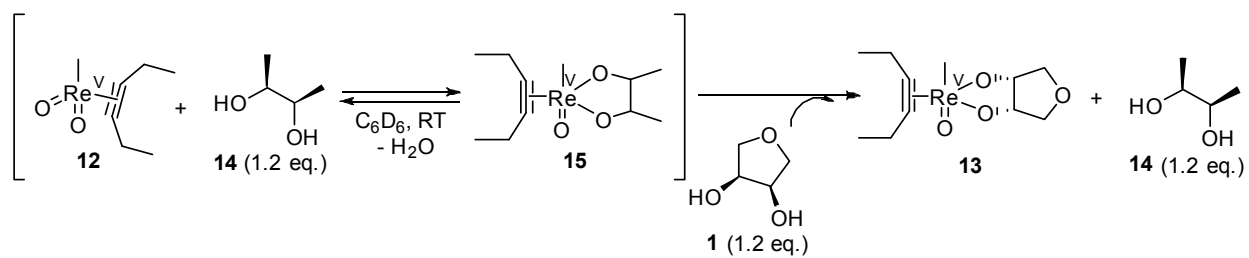


selective gNOESY starting parameters (on deoxytreh)
(ol=2569.3 as measured from utilities, ol)



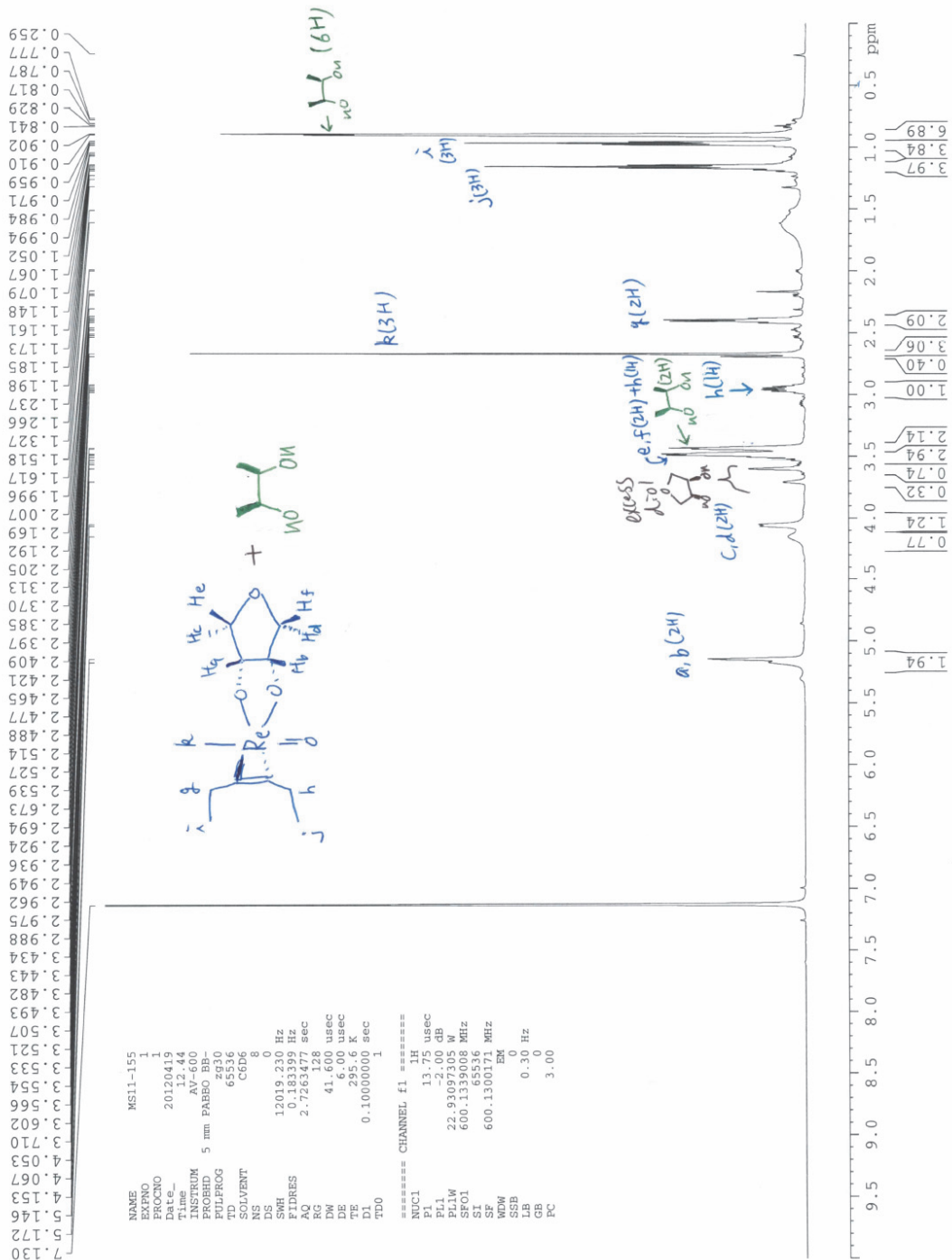
iv) Diol exchange from *meso*-2,3-butanediol to anhydroerythritol

To the mixture described in iii) (mol ratio **12**:**14**:**15**=0.8 : 1.1 : 1), **1** (1.2 eq.) was added and mixed well at room temperature. ^1H and ^{13}C NMR (see below) indicated that both **12** and **15** disappeared and the solution contained only **13**, **14** and **1** (excess amount). (**13**:**14**:**1**=1: 1.2 : 0.2).



¹H NMR (600 MHz, C₆D₆)

AV-600 ZBO proton starting parameters 11/16/08 RN



References and Notes

- [1] a) Q. Zhang, J. Chang, T. Wang, Y. Xu, *Energy Convers. Manage.* **2007**, *48*, 87-92; b) D. Mohan, C. U. Pittman, P. H. Steele, *Energy & Fuels* **2006**, *20*, 848-889.
- [2] a) F. Jin, H. Enomoto, *Energy Environ. Sci.* **2011**, *4*, 382-397; b) X. Tong, Y. Ma, Y. Li, *Appl. Catal., A* **2010**, *385*, 1-13; c) R. Rinaldi, F. Schuth, *Energy Environ. Sci.* **2009**, *2*, 610-626.
- [3] A. Corma, S. Iborra, A. Velty, *Chem. Rev.* **2007**, *107*, 2411-2502.
- [4] a) S. Dutta, *ChemSusChem* **2012**, *5*, 2125-2127; b) J. O. Metzger, *ChemCatChem* **2013**, *5*, 680-682.
- [5] a) S. Stanowski, K. M. Nicholas, R. S. Srivastava, *Organometallics* **2012**, *31*, 515-518; b) S. Murru, K. M. Nicholas, R. S. Srivastava, *J. Mol. Catal. A: Chem.* **2012**, *363-364*, 460-464.
- [6] G. Chapman, K. M. Nicholas, *Chem. Commun.* **2013**, *49*, 8199-8201.
- [7] L. Hills, R. Moyano, F. Montilla, A. Pastor, A. Galindo, E. Álvarez, F. Marchetti, C. Pettinari, *Eur. J. Inorg. Chem.* **2013**, *2013*, 3352-3361.
- [8] a) G. K. Cook, M. A. Andrews, *J. Am. Chem. Soc.* **1996**, *118*, 9448-9449; b) S. Raju, J. T. B. H. Jastrzebski, M. Lutz, R. J. M. Klein Gebbink, *ChemSusChem* **2013**, doi: 10.1002/cssc.201300364.
- [9] J. E. Ziegler, M. J. Zdilla, A. J. Evans, M. M. Abu-Omar, *Inorg. Chem.* **2009**, *48*, 9998-10000.
- [10] a) P. Liu, K. M. Nicholas, *Organometallics* **2013**, *32*, 1821-1831; b) I. Ahmad, G. Chapman, K. M. Nicholas, *Organometallics* **2011**, *30*, 2810-2818; c) S. Vkuturi, G. Chapman, I. Ahmad, K. M. Nicholas, *Inorg. Chem.* **2010**, *49*, 4744-4746.
- [11] A. L. Denning, H. Dang, Z. Liu, K. M. Nicholas, F. C. Jentoft, *ChemCatChem* **2013**, doi: 10.1002/cctc.201300545.
- [12] S. C. A. Sousa, A. C. Fernandes, *Tet. Lett.* **2011**, *52*, 6960-6962.
- [13] E. Arceo, J. A. Ellman, R. G. Bergman, *J. Am. Chem. Soc.* **2010**, *132*, 11408-11409.
- [14] T. Strassner, in *Computational Modeling of Homogeneous Catalysis, Vol. 25* (Eds.: F. Maseras, A. Lledós), Springer US, **2002**, pp. 253-268.
- [15] M. Shiramizu, F. D. Toste, *Angew. Chem. Int. Ed.* **2012**, *51*, 8082-8086.
- [16] S. Qu, Y. Dang, M. Wen, Z.-X. Wang, *Chem. Eur. J.* **2013**, *19*, 3827-3832.
- [17] S. Liu, A. Senocak, J. L. Smeltz, L. Yang, B. Wegenhart, J. Yi, H. I. Kenttämä, E. A. Ison, M. M. Abu-Omar, *Organometallics* **2013**, *32*, 3210-3219.
- [18] J. Yi, S. Liu, M. M. Abu-Omar, *ChemSusChem* **2012**, *5*, 1401-1404.
- [19] C. Boucher-Jacobs, K. M. Nicholas, *ChemSusChem* **2013**, *6*, 597-599.
- [20] a) J. J. Kennedy-Smith, K. A. Nolin, H. P. Gunterman, F. D. Toste, *J. Am. Chem. Soc.* **2003**, *125*, 4056-4057; b) K. A. Nolin, R. W. Ahn, F. D. Toste, *J. Am. Chem. Soc.* **2005**, *127*, 12462-12463; c) K. A. Nolin, J. R. Krumper, M. D. Pluth, R. G. Bergman, F. D. Toste, *J. Am. Chem. Soc.* **2007**, *129*, 14684-14696; d) K. A. Nolin, R. W. Ahn, Y. Kobayashi, J. J. Kennedy-Smith, F. D. Toste, *Chem. Eur. J.* **2010**, *16*, 9555-9562.
- [21] a) B. G. Harvey, H. A. Meylemans, *J. Chem. Technol. Biotechnol.* **2011**, *86*, 2-9; b) M. Kumar, K. Gayen, *Appl. Energy* **2011**, *88*, 1999-2012.
- [22] A. Cann, J. Liao, *Appl. Microbiol. Biotechnol.* **2010**, *85*, 893-899.
- [23] Water is produced from DODH reaction itself and the reaction was tolerant to moisture in the air. However, note the reaction is inhibited when very significant amount of water is initially present: For example, no reaction was observed in 3-octanol:H₂O=5:1 (biphasic),

- 1-butanol:H₂O=10:1 (biphasic), 1-propanol:H₂O=10:1 (one-phase) under Table 3, condition I.
- [24] a) T. J. Korstanje, E. F. de Waard, J. T. B. H. Jastrzebski, R. J. M. Klein Gebbink, *ACS Catal.* **2012**, *2*, 2173-2181; b) T. J. Korstanje, J. T. B. H. Jastrzebski, R. J. M. Klein Gebbink, *ChemSusChem* **2010**, *3*, 695-697; c) T. J. Korstanje, J. T. B. H. Jastrzebski, R. J. M. Klein Gebbink, *Chem. Eur. J.* **2013**, doi: 10.1002/chem.201300209.
- [25] a) B. Katryniok, S. Paul, V. Belliere-Baca, P. Rey, F. Dumeignil, *Green Chem.* **2010**, *12*, 2079-2098; b) J. J. Bozell, G. R. Petersen, *Green Chem.* **2010**, *12*, 539-554; c) M. Pagliaro, R. Ciriminna, H. Kimura, M. Rossi, C. Della Pina, *Angew. Chem. Int. Ed.* **2007**, *46*, 4434-4440.
- [26] E.-S. Koh, T.-H. Lee, D.-Y. Lee, H.-J. Kim, Y.-W. Ryu, J.-H. Seo, *Biotechnol. Lett* **2003**, *25*, 2103-2105.
- [27] R. N. Monrad, R. Madsen, *J. Org. Chem.* **2007**, *72*, 9782-9785.
- [28] V. L. Bell, *J. Polym. Sci. A* **1964**, *2*, 5291-5303.
- [29] a) E. Arceo, J. A. Ellman, R. G. Bergman, *ChemSusChem* **2010**, *3*, 811-813; b) E. Arceo, P. Marsden, R. G. Bergman, J. A. Ellman, *Chem. Commun.* **2009**, 3357-3359.
- [30] (Pentan-3-yloxy)benzene, hydroquinone and catechol were detected by GC-MS but yields were insignificant (¹H NMR, GC-FID analysis).
- [31] A. T. Herrmann, T. Saito, C. E. Stivala, J. Tom, A. Zakarian, *J. Am. Chem. Soc.* **2010**, *132*, 5962-5963.
- [32] a) K. P. Gable, F. A. Zhuravlev, *J. Am. Chem. Soc.* **2002**, *124*, 3970-3979; b) K. P. Gable, A. AbuBaker, K. Zientara, A. M. Wainwright, *Organometallics* **1998**, *18*, 173-179; c) K. P. Gable, J. J. Juliette, *J. Am. Chem. Soc.* **1996**, *118*, 2625-2633; d) K. P. Gable, *Organometallics* **1994**, *13*, 2486-2488; e) K. P. Gable, T. N. Phan, *J. Am. Chem. Soc.* **1994**, *116*, 833-839.
- [33] J. K. Felixberger, J. G. Kuchler, E. Herdtweck, R. A. Paciello, W. A. Herrmann, *Angew. Chem. Int. Ed.* **1988**, *27*, 946-948.
- [34] M. M. Abu-Omar, E. H. Appelman, J. H. Espenson, *Inorg. Chem.* **1996**, *35*, 7751-7757.
- [35] The VT-NMR experiment was conducted only up to 100 °C limited by the boiling point of solvent (toluene-d₆). The temperature between 100 °C and 155 °C was not studied.
- [36] S. Liu, A. Senocak, J. L. Smeltz, L. Yang, B. Wegenhart, J. Yi, H. I. Kenttämaa, E. A. Ison, M. M. Abu-Omar, *Organometallics* **2013**.
- [37] The concept of synthesizing adipic acid from glucose via DODH was touched on by Metzger in his mini-review on biomass deoxygenation (reference 4b), but no specific pathway of such a reaction has been described.
- [38] a) Amyris, Inc.; D. Schweitzer, WO2012/82725 A1, 2012. b) Amyris, Inc.; J. W. Frost, A. Miermont, D. Schweitzer, V. Bui, US 20100314243 A1, 2010.
- [39] Amyris, Inc.; V. Bui, J. W. Frost, WO2012/141993 A1, 2012.
- [40] G. Gunbas, S. Sreekumar, K. Goulas and F. D. Toste, unpublished results.
- [41] a) W. Niu, K. M. Draths, J. W. Frost, *Biotechnol. Progr.* **2002**, *18*, 201-211; b) K. M. Draths, J. W. Frost, *J. Am. Chem. Soc.* **1994**, *116*, 399-400.
- [42] The corresponding monoester was not isolated.
- [43] **29** was not produced in isolable amount. Monoester was not observable on TLC.
- [44] a) H. C. Lo, H. Han, L. J. D'Souza, S. C. Sinha, E. Keinan, *J. Am. Chem. Soc.* **2007**, *129*, 1246-1253; b) R. Umeda, T. Nishimura, K. Kaiba, T. Tanaka, Y. Takahashi, Y. Nishiyama, *Tetrahedron* **2011**, *67*, 7217-7221.

- [45] a) A. Viswanathan, D. E. Kiely, *J. Carbohydr. Chem.* **2003**, *22*, 903-918; b) D. E. Kiely, L. Chen, T. H. Lin, *J. Am. Chem. Soc.* **1994**, *116*, 571-578; c) L. Chen, D. E. Kiely, *J. Carbohydr. Chem.* **1994**, *13*, 585-601.
- [46] a) Dairen Chemical Corporation; S.-C. Chen, J.-M. Lin, C.-L. Tsai, F.-S. Lin, L.-A. Hsu, US6350883 B1, 2002. b) ISP Investments Inc.; F. B. Minnock, P. D. Taylor, US5393888, 1995. c) BASF Aktiengesellschaft; M. Rudloff, P. Stops, E. Henkes, H. Schmidtke, R.-H. Fischer, M. Julius, R. Lebkuecher, K.-H. Ross, WO 2003022811, 2003.
- [47] C. E. Barnes, *Lenzinger Ber.* **1987**, *62*, 62-66.
- [48] A. L. Harreus, R. Backes, J. O. Eichler, R. Feuerhake, C. Jäkel, U. Mahn, R. Pinkos, R. Vogelsang, in *Ullmann's Encyclopedia of Industrial Chemistry*, Wiley-VCH Verlag GmbH & Co. KGaA, **2000**.
- [49] BASF Aktiengesellschaft; M. Brunner, A. Bottcher, B. Breitscheidel, K. Halbritter, J. Henkelmann, L. Thil, R. Pinkos, US6284917 B1, 2001.
- [50] a) C. M. Buchan, J. I. G. Cadogan, I. Gosney, B. J. Hamill, S. F. Newlands, D. A. Whan, *J. Chem. Soc., Chem. Commun.* **1983**, 725-726; b) X. Zhang, L. Xu, X. Wang, N. Ma, F. Sun, *Chin. J. Chem.* **2012**, *30*, 1525-1530.
- [51] G. J. M. Gruter, EP 2487170 A1, 2012.
- [52] a) E.-J. Ras, S. Maisuls, P. Haesackers, G.-J. Gruter, G. Rothenberg, *Adv. Synth. Catal.* **2009**, *351*, 3175-3185; b) M. Mascal, E. B. Nikitin, *Angew. Chem.* **2008**, *120*, 8042-8044; c) M. Balakrishnan, E. R. Sacia, A. T. Bell, *Green Chem.* **2012**, *14*, 1626-1634.
- [53] a) A. Gandini, *Vol. 25*, Springer Berlin / Heidelberg, **1977**, pp. 47-96; b) S. Höhne, S. Spange, *Macromol. Chem. Phys.* **2003**, *204*, 841-849.
- [54] At room temperature, esterification in 1-butanol was very slow.
- [55] M.-E. Martin, D. Planchenault, F. Huet, *Tetrahedron* **1995**, *51*, 4985-4990.
- [56] L. Boisvert, F. Beaumier, C. Spino, *Org. Lett.* **2007**, *9*, 5361-5363.
- [57] S. K. Bagal, S. G. Davies, J. A. Lee, P. M. Roberts, A. J. Russell, P. M. Scott, J. E. Thomson, *Org. Lett.* **2009**, *12*, 136-139.
- [58] E. Tayama, S. Otoyama, W. Isaka, *Chem. Commun.* **2008**, *0*, 4216-4218.
- [59] Y. Ishino, K. Wakamoto, T. Hirashima, *Chem. Lett.* **1984**, *13*, 765-768.
- [60] a) J. E. Baeckvall, S. E. Bystroem, R. E. Nordberg, *J. Org. Chem.* **1984**, *49*, 4619-4631; b) J. E. Baeckvall, R. E. Nordberg, *J. Am. Chem. Soc.* **1981**, *103*, 4959-4960.
- [61] S. Amslinger, A. Hirsch, F. Hampel, *Tetrahedron* **2004**, *60*, 11565-11569.
- [62] a) M. L. Bushey, M. H. Haukaas, G. A. O'Doherty, *J. Org. Chem.* **1999**, *64*, 2984-2985; b) J. Waser, B. Gaspar, H. Nambu, E. M. Carreira, *J. Am. Chem. Soc.* **2006**, *128*, 11693-11712.